NGT-21-002-080
NGT-80001

AAE

AERONAUTICAL AND ASTRONAUTICAL ENGINEERING DEPARTMENT

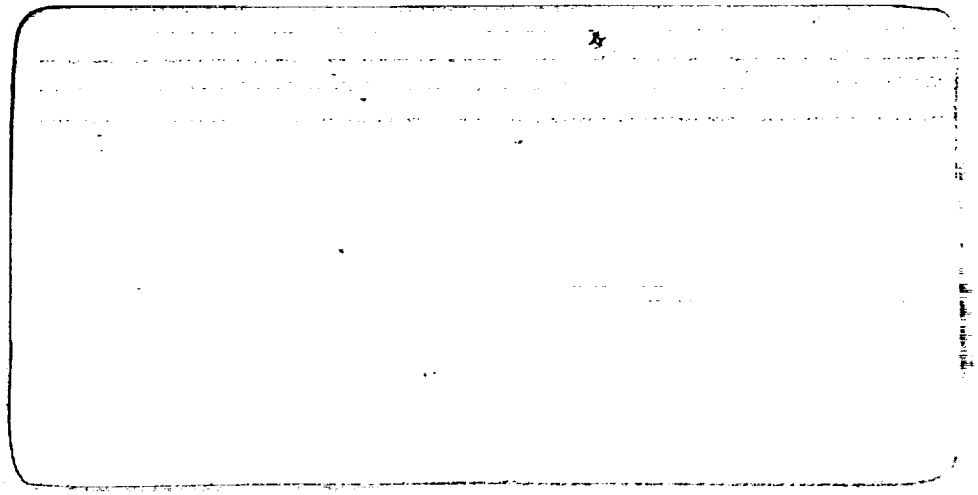

ENGINEERING EXPERIMENT STATION, COLLEGE OF ENGINEERING, UNIVERSITY OF ILLINOIS, URBANA

University of Illinois
at
Urbana-Champaign
Aeronautical and Astronautical Engineering

AAE 241
Aerospace Vehicle Design, Spacecraft Section
Final Project Reports

Volume II
Aircraft Section Groups 5 through 8

May 1988

<100
KRS

MARS AIRCRAFT

GROUP 5 PROPOSAL

BILL WOODRUFF - AERODYNAMICS
RON GOLEMBIEWSKI - PERFORMANCE
SCOTT HILDRETH - POWER AND PROPULSION
PAUL BECKWITH - STABILITY AND CONTROL
BRUCE ZIMMERMAN - STRUCTURES
RON CIHAK - SURFACE OPERATIONS
TERRI PULSFORD - WEIGHTS AND BALANCES

Introduction

William H. Woodruff

Abstract

The next major step in the evolution of the space program is the exploration of the planet Mars. In preparation of this, much research is needed on the problem of surveying the planet surface. An aircraft appears to be a viable solution because it can carry men and equipment large distances in a short period of time as compared with ground transportation. The purpose of this report is to examine the problems and design of an aircraft which would be able to survey the planet Mars.

Overview

This overview section will begin by defining the design requirements of the aircraft. Next it will look at the aircraft presented in this report and how it meets the requirements. Finally, it will briefly discuss some of the problems associated with the design of a mars aircraft.

The basic requirements of the aircraft were as follows:

Be able to fly on Mars
Support a payload of 1200 N on Mars
Have an endurance of 8 hours

In addition to these constraints, the design group added several more:

Be able to fly at low airspeeds
Offer as high a safety factor as possible
Be able to take off and land vertically

In order to satisfy the constraints, the aircraft has a number of unusual features. The requirements of supporting a large payload and being able to fly at low airspeeds, dictated that the aircraft must be able to produce a large amount of lift at low airspeeds. Unfortunately since the atmosphere of Mars is so thin, this is very hard to do and requires a very large wing area. On the other hand, the required endurance forces the aircraft to have a low drag or the fuel weight becomes too high. The two needs of large wing area and low drag are rather contradictory since the larger the wing area is the higher the drag is. The aircraft employs a joined wing in an attempt to compromise these two factors because it allows a lighter wing structure while producing lower drag than a comparable cantilevered wing. Another problem is the landing and takeoff on the planet surface. As outlined later in the paper, the surface of the planet is littered with boulders which would destroy an aircraft attempting to roll on the ground. It was given that the aircraft could take-off and land from a prepared field at the main base. But this imposes serious limitations on the flexibility of the aircraft since it would not be able to land and investigate the surface of the planet anywhere except the landing strip. In addition, if the engine failed the pilot would be killed during the landing. To solve these serious problems, it was decided that the aircraft should be able to take-off and land vertically. It was also required that the aircraft fly slowly. This was done because it will have to make accurate measurements of physical quantities of the planet and it is advantageous to be moving slowly. Also, if the pilot should have to make a crash landing, his chances of survival increase the slower he would impact the surface.

The rest of the report is organized by technical sections. Each section will discuss the current design in detail and outline any unusual problems encountered.

AAE 241
Spring 1988
INITIAL SIZING DATA SUMMARY

Gross Weight: 3494 N

Wing Loading: 3.92 N/m^2

Fuel Weight: 690 N

Useful Load Fraction: 0.52

Maximum Take-off Power 12.9 kw

Power Loading: 144.9 N/kw

Fuel Fraction: 0.198

Geometry

Ref. Wing Area = 842 m^2

AR = 25

Propulsion

Engine/Motor Type: CO-O_2 DIESEL

No. of Engines/Motors = 1

$P_{o_{max}}$ /engine = 24.1 kw

c_p at cruise = 1.91 $\frac{kg_m}{kw\text{-}hr}$

Aerodynamics

Cruise; C_{D_o} = 0.029

e_o = 0.80

C_L = 1.1

$(\frac{L}{D})_{max}$ = 8.94

Cruise Performance

h = 1.5 km

V = 45 m/s

Take-off; C_L = 1.36

$C_{L_{max}}$ = 1.64

Landing; C_L = 1.33

$C_{l_{max}}$ = 1.60

AAE 241
Spring 1988
DESIGN DATA SUMMARY

Gross Weight: 6000 N
Wing Loading: 20.06 N/m²
Maximum Fuel Weight: 864 N
Useful Load Fraction: 0.344

Maximum Take-off Power VTOL 8896 N THI
Power Loading: 222 N/kw
Fuel Fraction: 0.144

Geometry

Ref. Wing Area = 299 m²
AR = 16.38
Λ_{LE} = 12.07°
λ = .3
t/c = .157

Propulsion

Engine Description: Electric D.C. moto
Number of Engines = 1
$P_{0_{max}}$ /Engine = 27 kw
Weight/Engine = 93 N
c_p at Cruise = .11
Prop. Diam. = 5 m
No. of Blades = 3
Blade Cruise R_e = 1.51×10^5

Performance

Cruise R_e = 1.15×10^5
Cruise h = 1500 m
Cruise M = .311
Cruise V = 70 m/s
Take-off Field Length = N/A
Take-off Speed = N/A
Landing Field Length = 951 m (EMERGENCY)
Landing Speed = 44 m/s "
Maximum Landing Weight = 6000 N
OEI Climb Gradient (%): = N/A
2nd Segment = N/A
Missed Approach = N/A
Sea Level $(R/C)_{max}$ = 2.17 m/s

Aerodynamics

Airfoil: GA203A
High Lift System: —

Cruise; C_{D_o} = .01423 !
e_o = 1.356
C_L = .576
(L/D_{max}) = 32.6
Take-off; C_L = N/A
$C_{L_{max}}$ = N/A
Landing; C_L = N/A
$C_{L_{max}}$ = N/A

Stability and Control

Static Margin Range = .469 − .1
Acceptable C.G. Range = 6.2 to 6.87
Actual C.G. Range = 6.57 to 6.59 (1 Pilot)
6.13 to 6.15 (2 Pilot)

ORIGINAL PAGE IS
OF POOR QUALITY

THREE-VIEW

FRONT 1/8" = 1 METER

FOLDOUT FRAME

TOP 1/8" = 1 METER

SIDE 1/2" = 1 METER

ORIGINAL PAGE IS
OF POOR QUALITY

FOLDOUT FRAME

AERODYNAMICS

William H. Woodruff

Introduction

As a brief introduction, the basic goal of the aerodynamic design was to provide a slow moving surveillance aircraft which could carry a 1200N payload and have a large cruise speed stall speed separation for pilot safety. With respect to these goals, it was decided the cruise speed would be in the neighborhood of 50 to 100 m/s with the stall speed not more than 60% of the cruise speed. The reason so much attention was placed on the stall speed was twofold. First of all, practical experience has shown that it is very easy for a pilot to accidentally roll into a steep bank, a pitch high attitude, or a combination of both. This is particularly true when the pilot's attention is frequently diverted from flying the aircraft as it will be on the mars aircraft to run the on - board experiments. Second, the surface of Mars is very rough as shown in the planet profile. In the event that a vertical landing is not possible and the aircraft must crash land, the slower it is moving on impact, the greater the chances of pilot survival.

The report format will attempt to follow the design process as much as possible with some exception due to its iterative nature. It will begin with the airfoil selection, followed by the wing design and the complete configuration, continuing with the drag analysis, and finished by looking at the effects of scaling the aircraft. In addition, any notable design philosophy will be discussed.

Airfoil selection

The airfoil selection was difficult because of the very low Reynolds number the aircraft must fly at. The average Reynolds number (R_e) of the wing is 1.15×10^5 at 70 m/s. The amount of

information about low Reynolds number airfoils is relatively limited. Nonetheless, the LA203A airfoil was selected. The airfoil was chosen primarily because it had a high maximum coefficient of lift, $C_{l\ max}$, of 1.70 and it was designed to operate at a Reynolds number of 2.5×10^5. The design Reynolds number is very important because the airfoil section properties change drastically with Reynolds number. Typically, as is true with the LA203A, the coefficient of drag increases and the $C_{l\ max}$ decreases with decreasing Reynolds number. In addition, the drag estimation techniques are not very accurate for Reynolds numbers far from the design point. The airfoil cross sectional view and graphs of sectional properties are given in Figures 1-2, 3, 4, and 5.

Wing design

A joined wing design was chosen for the aircraft. The joined wing boasts many advantages over a conventional design as described in Ref. 2. A pertinent list is lower induced drag, light weight, and high strength. The spanwise efficiency (e) of a joined wing is dependant on the vertical separation of the two wing roots (h) divided by the tip- to- tip span (b) of the aircraft. The dependance of e on h/b is given in Fig 1-6. Preliminary drag calculations showed that using a lower h/b ratio was advantageous because the increase in parasitic drag from the larger structures necessary with the larger vertical separations was not offset by the corresponding increase in e. The aircraft has a h/b of 0.171. From information in Ref. 11, a taper ratio (λ) of 0.3 was selected because it corresponds to the highest spanwise efficiency. The spanwise efficiencies of the joined wing given in Fig. 1-6 are based on a λ of 0.5 (Ref. 12) A correction factor was necessary to account for the different taper ratios. Again from Ref. 11, the value of e for an ideal cantilevered wing with a taper ratio of 0.3 was divided by the e for one with a taper ratio of 0.5. The e values given in Fig. 1-6 were then multiplied by this factor. The e for the aircraft was 1.356. The joined wing configuration offers another distinct advantage in that the downwash of the

front wing tends to reduce the angle of attack of the rear wing. As a result, the front wing stalls before the rear wing and longitudinal control can be maintained during stall without requiring twist in the wing. Consequently, the wings were designed to operate at a constant coefficient of lift. Because of this, the wing coefficient of lift, C_L , is equal to the sectional coefficient of lift, C_l, and the wing coefficient of pitching moment, C_M, is equal to the sectional coefficient of pitching moment C_m. At this point it was necessary to specify the cruise velocity. The cruise velocity was set at 70 m/s because it was a good trade between speed and efficiency. In addition, the powerplant could not produce enough power to maneuver the aircraft at a higher cruise speed. With the cruise velocity, the variables of wing area (s), aspect ratio (AR), and stall speed were optimized. The result was s = 299 m^2, AR = 16.38, and stall speed = 41 m/s. It was desired that the stall speed be lower, but the necessary wing area caused the drag at cruise to become too high for the available power. The aspect ratio was set at 16.38 because drag increased substantially for lower values and higher values increased the wing span. The downwash on the rear wing was calculated as per Ref. 4 and it was found that the rear wing root needs an additional 1.28 deg. angle of incidence with a -1.8×10^{-3} deg./m twist out to the tips relative to the front wing to maintain a constant C_L at cruise. When the downwash was calculated at stall, it was found to decrease the angle of attack by an additional 1.5 deg. at the root of the rear wing which will be adequate for stall stability. The wing loading was determined using a Schrenk approximation and is given in Figure 5-1. Thus, the wing geometry is complete and is given in Fig. 1-1 and the aircraft views.

Final configuration

The complete design saw the addition of winglets and the fuselage. The reason for the addition of winglets is illustrated in Figure 1-6. The maximum e for a joined wing without winglets is about 1.1 while the maximum e for one with winglets is as high as

1.5. In the case of this aircraft, the winglets caused a reduction in induced drag that was twice the increase in parasitic drag. As a matter of interest, in configurations with a larger h/b ratio the increase in parasitic drag from full size winglets was greater than the decrease in induced drag. The winglet on the aircraft operates at a Reynolds number of 0.75×10^5. It was assumed that the LA203A airfoil would operate at this Reynolds number. Certainly this is a questionable assumption and more testing of the airfoil is required to determine if it will be satisfactory for the winglet. The actual geometry of the winglet was specified in Ref. 12 and it was applied directly to the aircraft with one exception. The winglet used has a taper ratio of 0.3 instead of 0.5 to take advantage of the lower induced drag. It was assumed this reduction was taken into account by the span efficiency correction factor previously discussed. The tip geometry is given in Figure 1-1 as well as the aircraft views. There is still a fair amount of information unknown concerning the winglets. Most notably, the required angle of attack is unknown. The winglets will require more research before they can be considered optimized to any degree. The fuselage was modeled after common sailplane designs. The pilot area was sized based on the volume necessary to hold two pilots, landing gear, electronics, and fuel. A boom was extended from the rear of the main pod to the vertical fin which tied into the rear wing root. The boom was sized based on the requirement that the fuel cells fit inside it and the vertical fin was sized based on an area requirement given by stability and control. The front wing is mounted at an angle of incidence of -1.0 deg. and the rear wing root at an angle of 0.28 deg. A graph of C_L vs. α of the aircraft is given in Fig. 1-7. The complete geometry is given in the aircraft views.

Drag calculation

With the complete configuration, it was possible to estimate the drag of the aircraft. The drag estimation is based on Methods of Estimating Drag Polars of Subsonic Aircraft, by Jan Roskam (Ref.

3). The calculation consisted of breaking the aircraft into five parts the fuselage pod, boom, fin, wing, and winglets. The coefficient of skin friction was based on the assumption that the flow was everywhere laminar. This is a good assumption considering the highest Reynolds number encountered on the aircraft is 4.8×10^5 on the boom. The induced drag was calculated for the wing and fuselage along with the interference drag between the wing and fuselage. The drag was estimated through out the flight regime and the results are are tabulated in Fig. 1 - 8 thru 14. It is important to note that the drag was estimated at 40 m/s as if the plane was still in flight even though it would have stalled at 41 m/s. This was done to help describe the nature of the drag curve in the stall region.

Scaling

The final section of the aerodynamics report is dedicated to the effects of scaling the aircraft. At this point, a pertinent question is, "Why is the aircraft so large?" There are several major factors which cause this problem. In the first place, the atmosphere is very thin as evidenced by the extremely low Reynolds numbers at which the aircraft must fly. Consequently, a large planform area is needed to generate any appreciable lift. Second, the aircraft must carry all its fuel on - board unlike aircraft on earth which fly in one of its fuel reactants. Last, the fuel cells used to generate power are extremely heavy compared with their power output. The net result of all these factors is to push the gross weight up and consequently the size of the aircraft. Another problem which arises is that the structural weight of the aircraft really begins to increase rapidly as the wing span gets large. This is due to the fact that the structure itself becomes so long it needs a large amount of additional strength to support itself and counteract the moments exerted through the long lever arms. The current payload of the aircraft is 1200 N and the gross weight is 6000 N. This gives a useful load fraction of 20%. Looking at some comparable examples of earth aircraft: a Mooney

205 which is an aluminum four place aircraft has a useful load fraction of 39%, and an Aero Mirage which is an all composite four place aircraft has a useful load fraction of 44%. Even granted the adverse flight conditions on Mars, it still seems unreasonable that the design would have a useful load less that half of its counterpart on Earth. It was thought that possibly an aircraft might exist with a useful load fraction on the order of 25 to 35%. With a very simple computer program, the size of the current design was scaled smaller with the restriction the cruise and stall speeds must remain relatively constant. The results were very interesting. In graphic form, the general nature of the curve of average aircraft density vs. size is as follows:

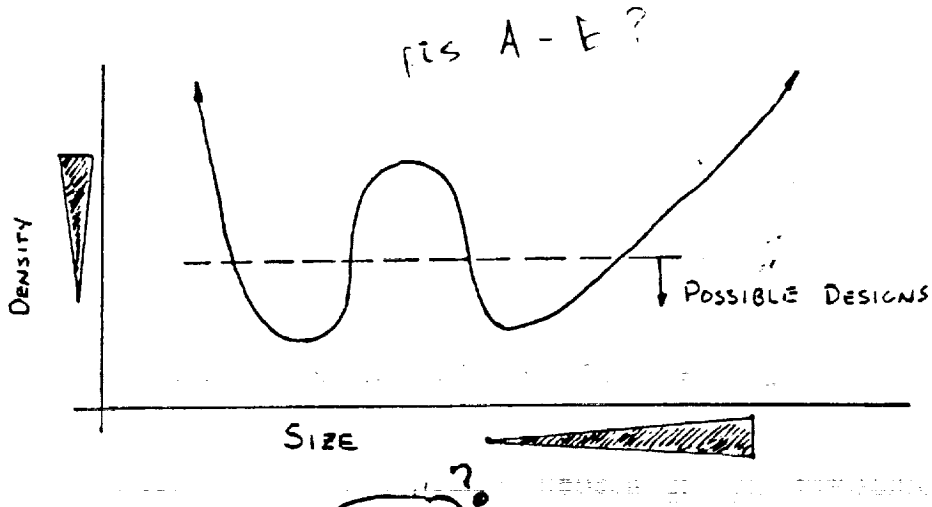

The region A represents the point at which the aircraft is too small to support the required payload. Region E represents the point at which the aircraft is so large that it becomes too heavy from structural weight. The features B, C, and D are the ones of interest. Point D represents the position of the current design with a 70 m wing and three fuel cells, it is a relative density minimum but it is not the minimum aircraft size. Point B represents another density minimum as well as the overall size minimum. The computer data indicates that the aircraft at point B has approximately a 30 - 40 m wingspan and it requires two fuel cells for power. The point C is the critical point at which the increased aircraft drag requires another fuel cell and therefore a large increase in gross weight. It appears the deciding

factor between the two aircraft is careful optimization of the drag so that it requires only two fuel cells. The group looked at a design with a 35 meter wing span and 4000 N gross weight. The drag of this aircraft was a little too high. At that point it was decided to use the current configuration. But there is strong evidence to suggest that an optimum does exist at a wingspan of approximately 40 m and a gross weight of approximately 4500 N.

Conclusion

It is apparent that the overall size of the current aircraft is too large in a practical sense. From the scaling data it seems that the basic configuration is sound. It is strongly recommended that future work is done on scaling this aircraft particularly in the range of 35 - 45 m wingspan and 4000 - 4500 N gross weight. Also, if technology can increase the efficiency and decrease the weight of the fuel cells, there may be an optimum design with a still smaller overall size.

References

1. Liebeck, R. H. and Camacho, P. P., "Airfoil Design at Low Reynolds Numbers with Constrained Pitching Moment," Proceedings of the on Low Reynolds Number Aerodynamics, University of Notre Dame UNDAS - CP - 77B123, June 1985.

2. Wolkovitch, J. Principles of the Joined Wing, Engel Engineering Company Report no. 80-1, Dec 3, 1980.

3. Roskam, J., Methods for Estimating Drag Polars of Subsonic Aircraft, Professor of Aerospace Engineering, The University of Kansas, Lawrence, Kansas.

4. Sivier, K., "AAE 316 lecture Notes," Department of Aeronautical Engineering, University of Illinois, Champaign-Urbana Il, Fall 1987.

5. Wolkovitch, J. " The Joined Wing: An Overview," J. Aircraft, March 1986 pp. 160 - 178.

6. Reid, E. G., Applied Wing Theory, McGraw - Hill, 1932.

7. Durand, W. F., Aerodynamic Theory, 1936; reprinted by Dover Press, New York, 1963 (Section by L. V. Kerber).

8. Glauert, H., The Elements of Aerofoil and Airscrew Theory, Cambridge University Press, England, 1926.

9. Laitone, E. R., "Positive Tail Loads for Minimum Induced Drag of Subsonic Aircraft," J. Aircraft, Vol. 15, Dec. 1978, pp. 837 - 842.

10. Roskam, J., Airplane Flight Dynamics and Automatic Controls, Parts I & II. Roskam Aviation and Engineering Corporation. 1979.

11. McCormick, Barns W., Aeronautics, Astronautics, and Flight Mechanics., John Wiley and Sons, Inc. 1979.

12 Wolkovitch, Julian and Lund, David., Application of the Joined Wing to Turboprop Transport Aircraft, NASA Contract NAS2 - 11255.

FIG 1-1

AIRCRAFT DATA

Gross Weight = 6000 N
Cruise Speed = 70 m/s
Stall Velocity = 41 m/s
Span = 70 m
Height = 11.97 m
length = 15 m
S = 299 m^2
e = 1.356
AR = 16.33
λ Front = 0.3
Rear = 0.3
Λ Front = 12.07°
Rear = -12.07°
Twist Front = 0
Rear = -1.8×10^{-3} DEG/m

Chord Root = 3.23 m
Tip = 0.93 m
Airfoil = LA203A

WINGLET DATA

Airfoil = LA203A
Chord Root = 1.97 m
Tip = 0.59 m
λ = 0.3
Λ = 30°
S = 15.34 m^2

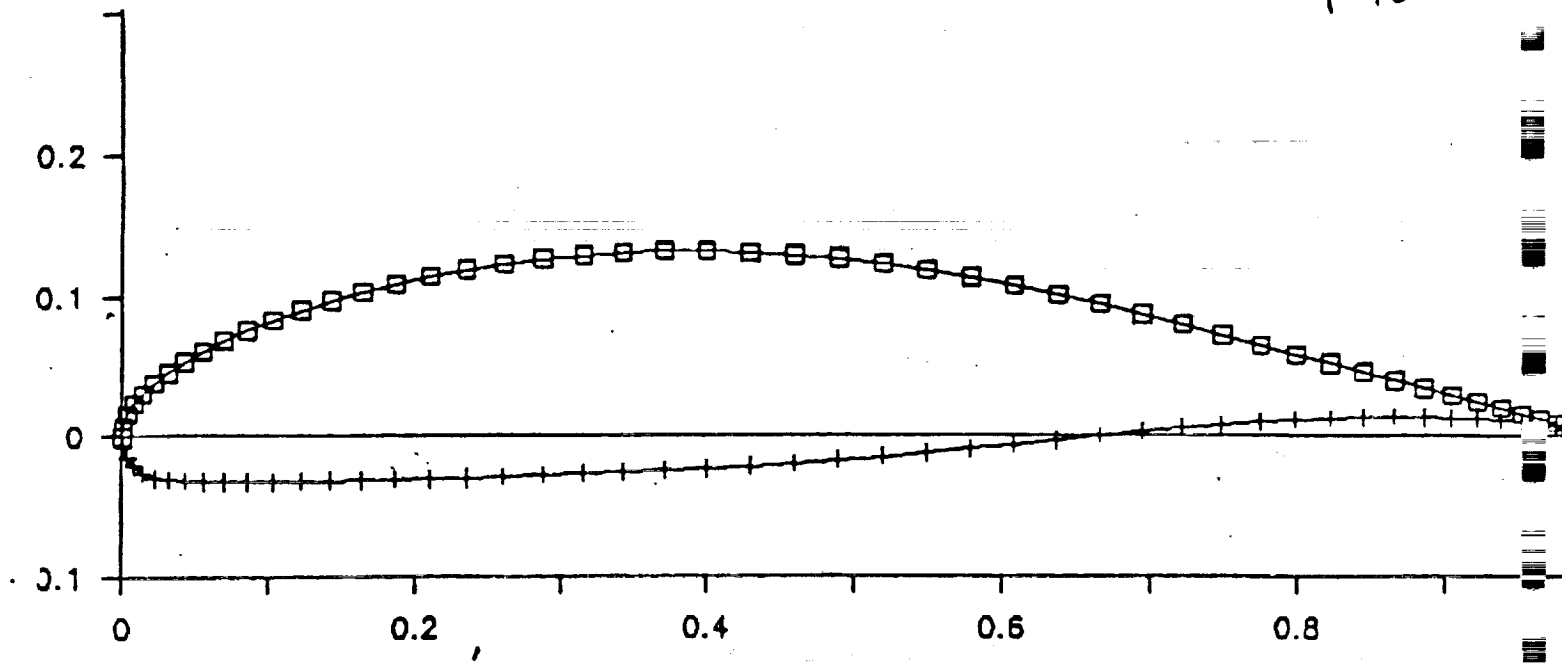

FIG 1-2

AIRFOIL PERFORMANCE CURVE(S)

Sym	Airfoil	$R_n(10^6)$	Transition
□	LNV109A	0.375	Free
○	LA203A	0.375	Free

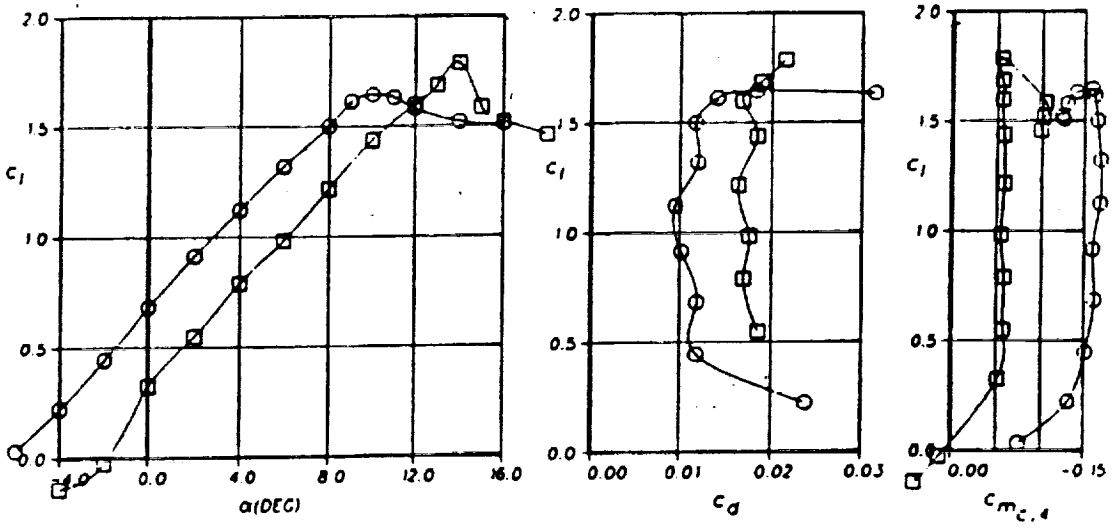

FIG. 1-3 FIG. 1-4 FIG. 1-5

LA 203A
AIRFOIL

FIGURE 13. CALCULATED SPAN-EFFICIENCY FACTOR FOR JOINED WING WITH SYMMETRIC INCLINED WINGLETS ("CARPET" PLOT)

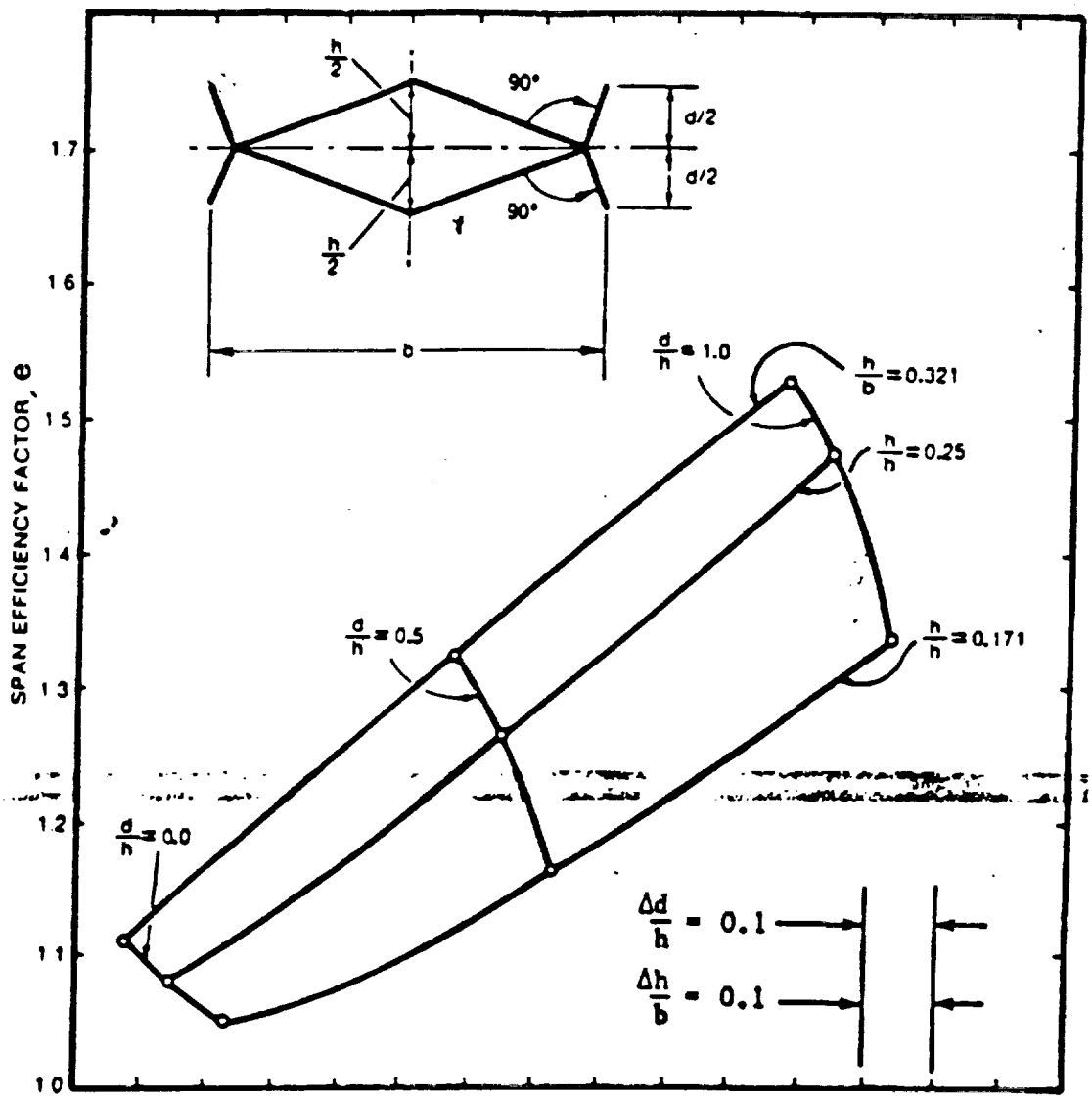

FIG 1-6 (REF. 2)

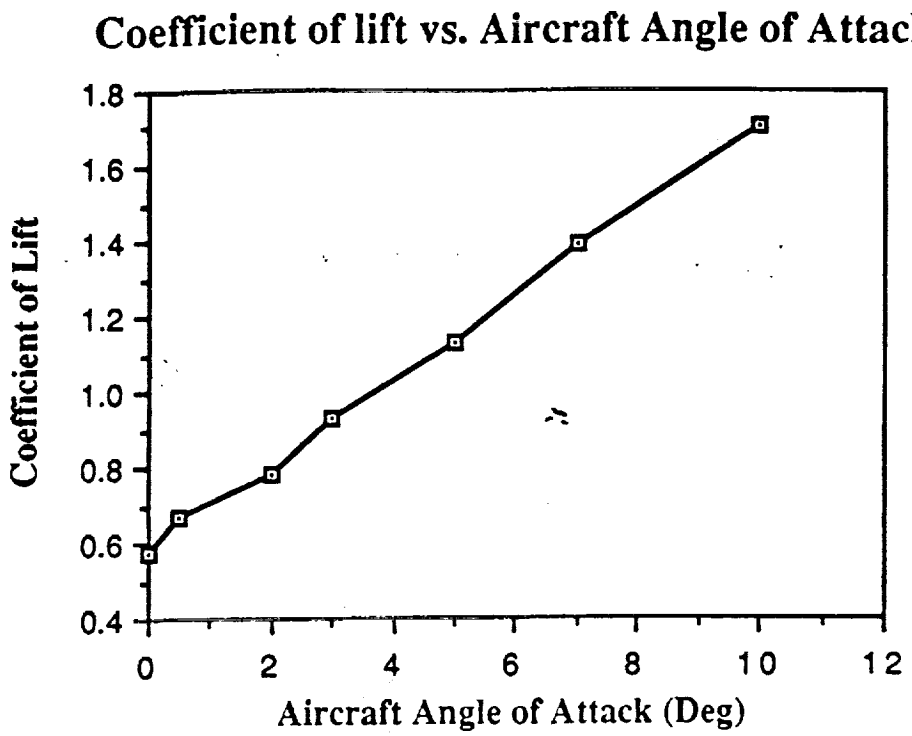
Coefficient of lift vs. Aircraft Angle of Attack
Coefficient of Lift
1.8
1.6
1.4
1.2
1.0
0.8
0.6
0.4
0
2
4
6
8
10
12
Aircraft Angle of Attack (Deg)

FIG. 1-7

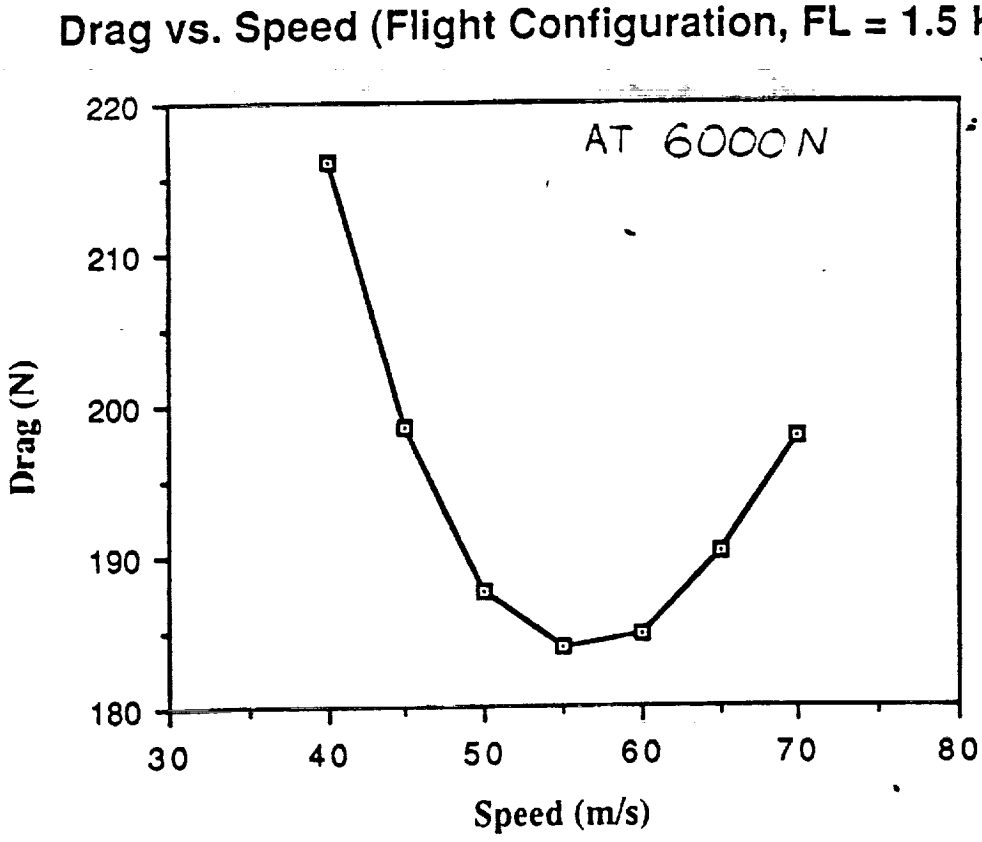
Drag vs. Speed (Flight Configuration, FL = 1.5 Km)
AT 6000 N
Drag (N)
220
210
200
190
180
30
40
50
60
70
80
Speed (m/s)

FIG. 1-8

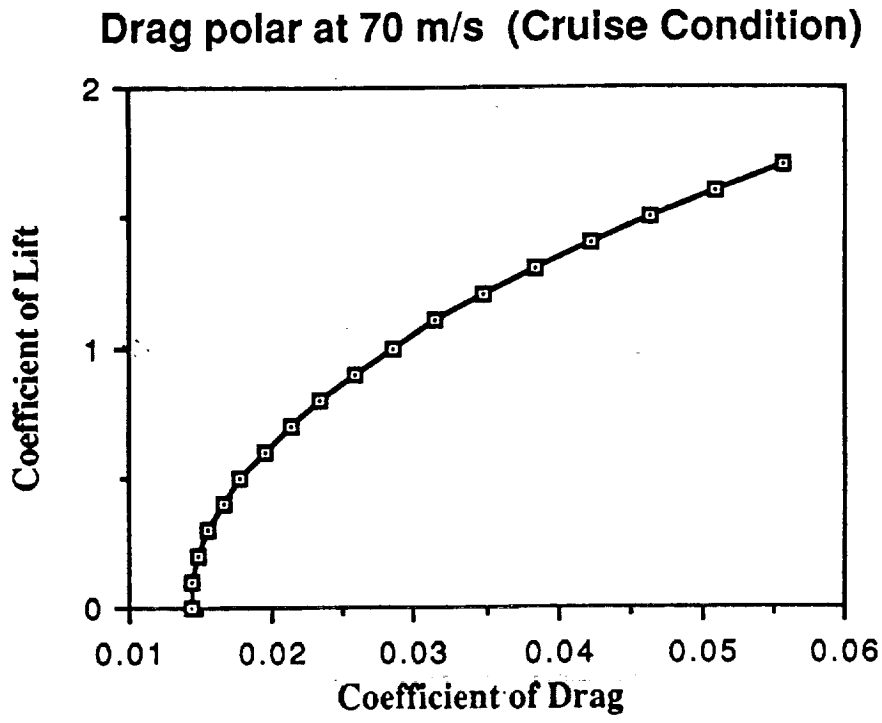

FIG 1-9

CRUISE VELOCITY = 70 m/s		
COMPONENT	PARASITIC	INDUCED
WING AND FUSELAGE	.01232	$.0143(C_L)^2$
BOOM	SMALL	SMALL
FIN	.00043	SMALL
WINGLETS	.00147	IN WING TERM
POLAR EQ. = $.01423 + .0143(C_L)^2$		

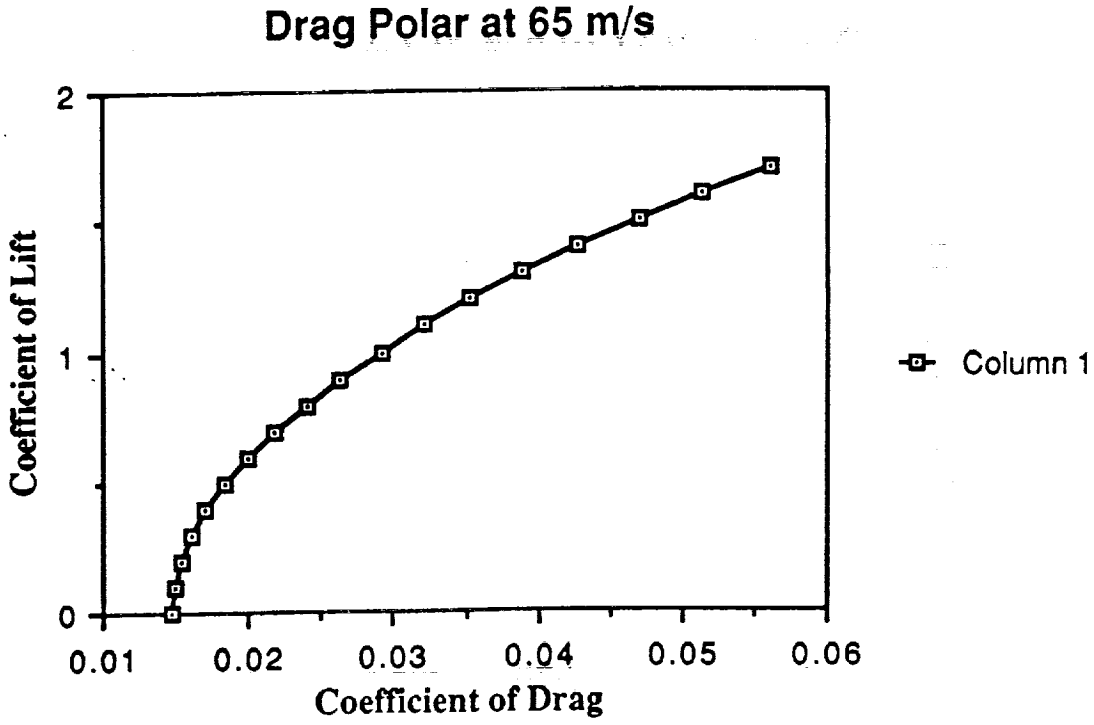

FIG 1-10

CRUISE VELOCITY = 65 m/s		
COMPONENT	PARASITIC	INDUCED
WING AND FUSELAGE	.01279	$.01433(C_L)^2$
BOOM	SMALL	SMALL
FIN	.00045	SMALL
WINGLETS	.00153	IN WING TERM
POLAR EQ. = .01477 + $.01433(C_L)^2$		

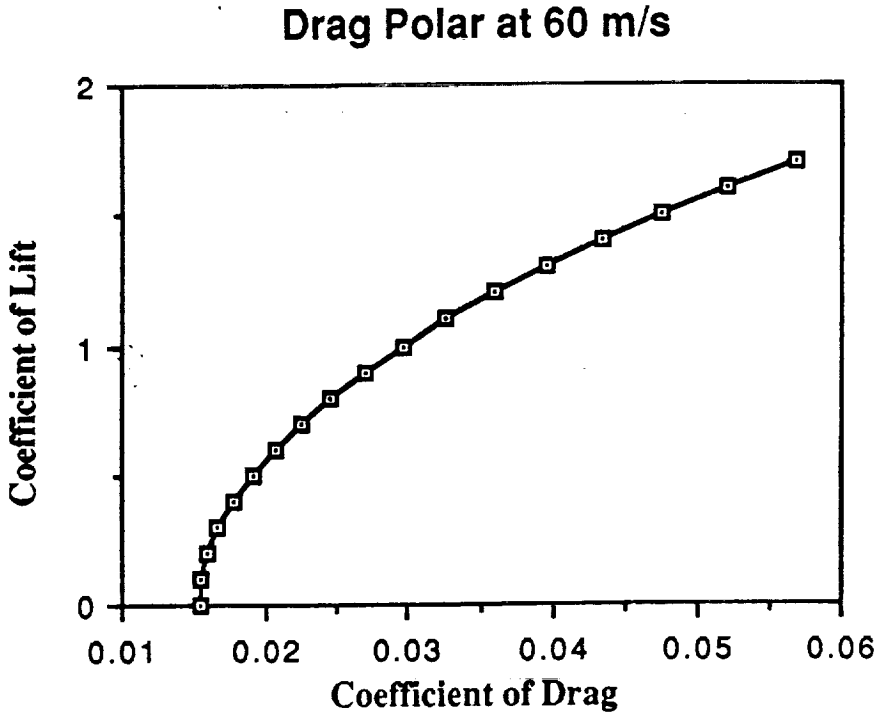

FIG 1-11

CRUISE VELOCITY = 60 m/s		
COMPONENT	PARASITIC	INDUCED
WING AND FUSELAGE	.01331	.00001 + .01433$(C_L)^2$
BOOM	SMALL	SMALL
FIN	.00047	SMALL
WINGLETS	.00159	IN WING TERM
POLAR EQ. = .01538 + .01433$(C_L)^2$		

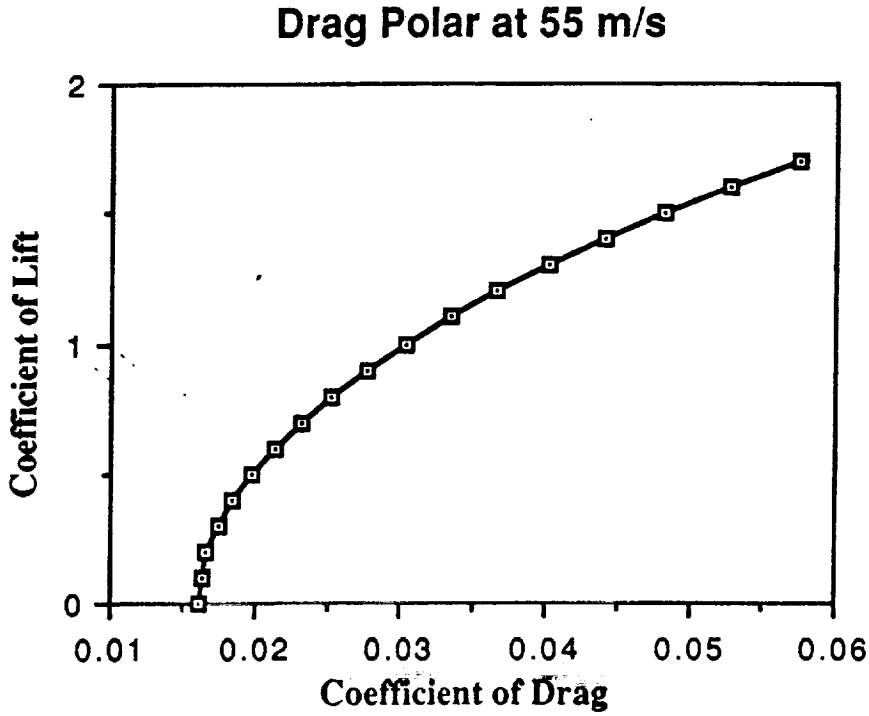

FIG 1-12

CRUISE VELOCITY = 55 m/s		
COMPONENT	PARASITIC	INDUCED
WING AND FUSELAGE	.01390	$.00004 + .01433(C_L)^2$
BOOM	SMALL	SMALL
FIN	.00049	SMALL
WINGLETS	.00166	IN WING TERM
POLAR EQ. = $.01609 + .01433(C_L)^2$		

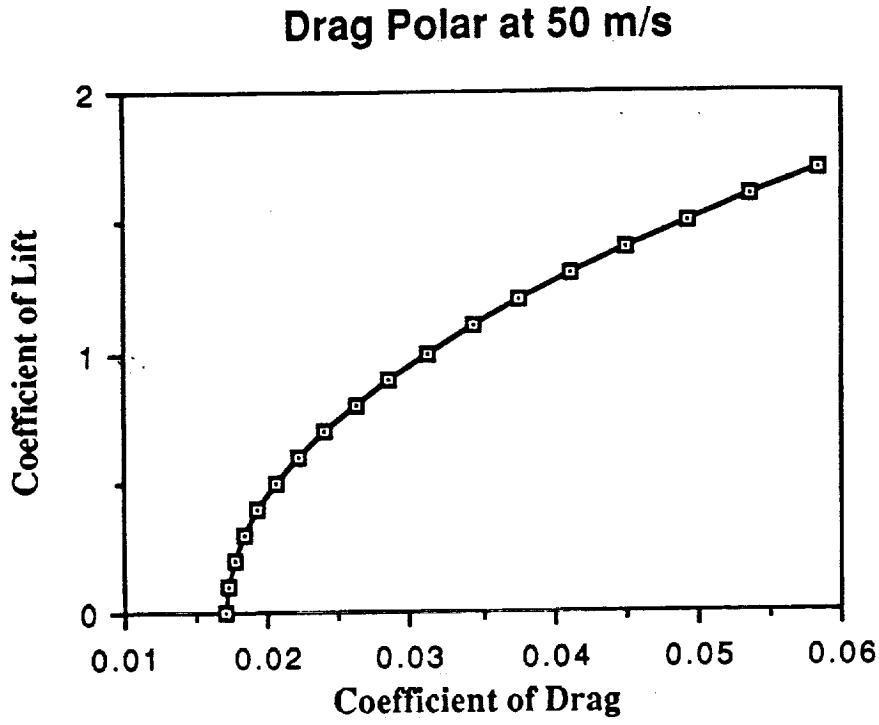

FIG 1-13

CRUISE VELOCITY = 50 m/s		
COMPONENT	PARASITIC	INDUCED
WING AND FUSELAGE	.01458	$.00020 + .01433(C_L)^2$
BOOM	SMALL	SMALL
FIN	.00051	SMALL
WINGLETS	.00174	IN WING TERM
POLAR EQ. = $.01704 + .01433(C_L)^2$		

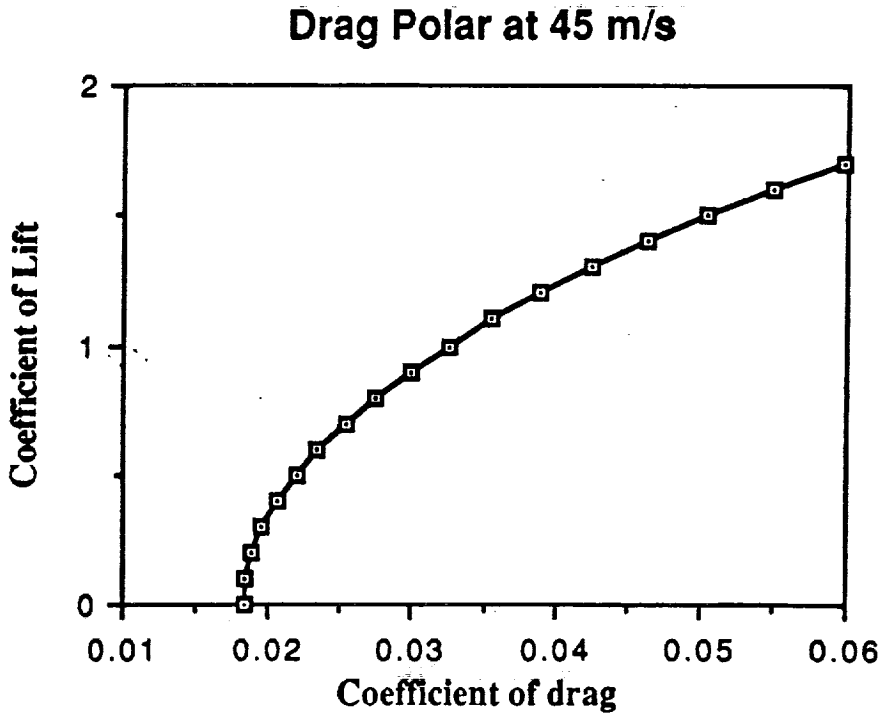

FIG 1-14

CRUISE VELOCITY = 45 m/s		
COMPONENT	PARASITIC	INDUCED
WING AND FUSELAGE	.01537	.00055 + .01433$(C_L)^2$
BOOM	SMALL	SMALL
FIN	.00054	SMALL
WINGLETS	.00183	IN WING TERM
POLAR EQ. = .01830 + .01433$(C_L)^2$		

Performance

Ron Golembiewski

The nagging question of "what if..." seems inevitable. People are always asking what's in store for the future? A mission to mars maybe? Since the space shuttle has been in operation a mission to mars does not seem out of reach for the years to come. In fact a reconnaissance mission that would be based on the surface of mars would also be a reasonable extension of the mission. The idea of a mars airplane with a joined wing configuration, eight hour endurance and a vertical take off and landing has been investigated. The performance of the mars plane can be broken into three areas, climb form 16.5 m to 1500 m, cruise at a constant 1500m and descent from 1500 m to 16.5 m .

CLIMB

In order to evaluate performance characteristics of climb the power available, which is the power that the propulsion system is able to produce given a specific altitude, must be known. If the propulsion system is propellor driven, the the power available will be dependent on the altitude. In other words, the power available is a function of altitude.

However, if the rpm were regulated for different altitudes the power available could be assumed constant. Therefore, power and propulsion states a constant power available of 26.85 kW. From this information and knowing the power required to climb, the knowledge to determine actual flight is acquired. Using the power required curves (Fig. 2-1 and Fig. 2-2) the maximum rate of climb was calculated at different altitudes and velocities. According to Fig. 2-4 (R/C)max is 3.09 m/s with a corresponding power required to climb of 32.39 kW. However, the available power supplied by the propulsion system is 26.85 kW. Obviously the power available must

be greater than the power required to climb and also to cruise. The power required to climb is the sum of the power required at level cruise plus the rate of increase in potential energy. Using the power required to climb as 26.85 kW, the maximum rate of climb is 2.17 m/s.

The choice was made not to climb at (R/C)max, but instead to climb at 1.5 m/s since this would require only 22.85 kW instead of 26.85 kW. Using a slower rate of 1.5 m/s, 4 kW was saved for the regulation of rpm needed for heavy wind gusts, etc. From a performance standpoint, if (R/C)max was chosen the fuel rate increases to .0126 kg/s using 12.16 kg of fuel and taking 11.41 min. to climb from 16.5 m to 1500 m. Comparing this to R/C of 1.5 m/s the fuel rate is .0107 kg/s using 10.58 kg of fuel, taking 16.5 min. to climb with a range of 66.83 km. The differences are small, but as a group it was chosen not to fly at (R/C)max due to wind gusts and safety factors. From a performance outlook (R/C)max seems to be the better choice.

It is interesting to note how the density on mars has such a small effect on the power required curves Fig. 2-1 and Fig. 2-2. As you can see the maximum variation of the Preq. from zero altitude to 1500 m was .6 kW. As a result of this it was difficult to find the absolute altitude which is 6.5 km with a corresponding velocity of 67.5 m/s, Fig.2-3. The method used was to construct an altitude vs. (R/C)max curve at a constant velocity of 45 m/s Fig. 2-4 and to follow the line to were R/C is zero. The results seem alarming and questionable.

CRUISE

It is important to realize what the propulsion system entails and how it effects the cruise characteristics. For example, the Mars plane has an electric engine powered by fuel cells. These cells consist of fuel and an oxidizer. The production of power results in a by-product, water. The choice is simple: either to discharge the water into the atmosphere or to store the water on board. The choice was made to keep the water on board. This was decided on the basis

that the weight of the fuel used is approximately the same as the weight of the water being created. This causes a constant level flight cruise configuration. Therefore a constant cruise velocity was chosen at 70 m/s at the required altitude of 1500 m. The constant velocity of 70 m/s was made by the restrictions of the aerodynamics which requires a power of 13.85 kW. As a result the cruise characteristics are: a range of 1,887.4 km, time and fuel used of 7.45 hours and 204.26 kg, respectively. Once again, since the assumptions of constant weight and constant velocity were made, the initial velocity and altitude, 70 m/s and 1500 m , the final velocity and altitude remain the same during cruise.

DESCENT

The descent was designed with a 18% power-off condition mainly to keep a uniform descent and climb. Therefore the power available becomes 22 kW and the rate of sink is 1.5 m/s with an initial and final altitude of 1500 m to 16.5 m at a speed of 45 m/s. The descent characteristics include range, time, fuel used of 66.83 km, 16.5 min., 10.18 kg.

COMPLETE MISSION PROFILE

The first stage consists of a vertical take-off. At the time equal to zero the rockets are fired, after engine run up, and the plane is put in a flat configuration. In the first second, the plane is at 5 m at a stall configuration, and the propellor of the main engine is started. The final stage of the VTO is at 11 seconds, velocity of 45 m/s, range of 210 m, final altitude of 16.5, using 27 kg of fuel and 100% propellor power while remaining in a stall configuration.

After the VTO has been completed the mars plane is completely propelled by the main engine, climbing at a rate of 1.5 m/s from 16.5 m to 1500 m, with a time, range, fuel used of 16.5 min., 82.1 km, 10.58 kg, respectively.

Once the plane has reached the required altitude of 1500 m at 70 m/s the time, range, fuel used are, 7.45 hours, 1887.4 km, 204.26 kg.

The plane is then taken from 1500 m back to 16.5 m. The time, range, fuel used are, 16.5 min., 82.1 km, 10.18 kg. Once 16.5 m is reached a vertical landing is enacted having a time, range, and fuel used, of 11 seconds, 204 m, 31 kg.

CONCLUSION

For the eight hour endurance required, the total range is 2011.46 km, approximately 1250 miles, with a total fuel consumption of 283 kgm. To improve on the overall performance of the mars plane, the drag would need to be reduced, thus decreasing the overall power required. A reduction of Preq. would filter throughout the subsections, mainly to the power and propulsion section. Power and propulsion would then be able to scale down the propulsion system resulting in a lighter plane and thus helping other sections such as aerodynamics, surface operations, weights and balances.

SUMMARY OF PERFORMANCE CHARACTERISTIC

R/C = 1.5 m/s
(R/C)max = 2.17 m/s
Habs = 65.5 km
Velocity at (R/C)max = 67.5 m/s
Preq. at climb = 22.85 km
Preq. at cruise = 13.85 kW
Preq. at descent = 22 kW
power-off percentage = 18%
Pavail. = 26.85 kW
cruise velocity = 70 m/s
stall velocity = 40 m/s
weight = 6000 N
fuel rate during climb = .0107 kgm/s
fuel rate during descent = .0103 kgm/s

wing area = 299 m^2
Clmax =1.75
density = .015 - 4.667E-07
cruise altitude = 1500 m
total range = 2011.46 km
required endurance = 8 hrs.
total fuel consumption = 283 kgm

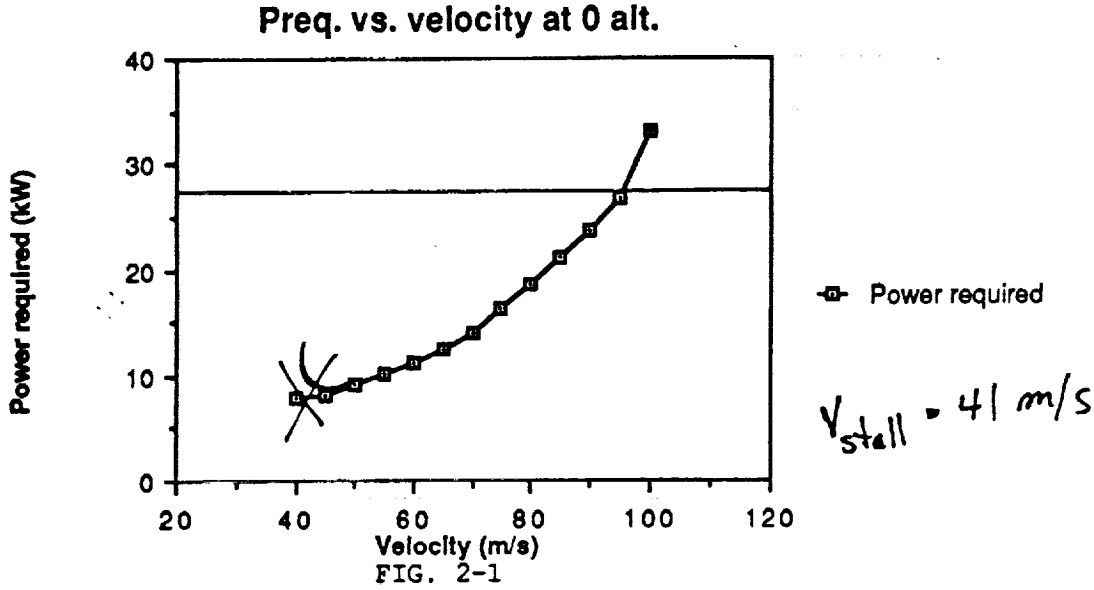

$V_{stall} = 41$ m/s

FIG. 2-1

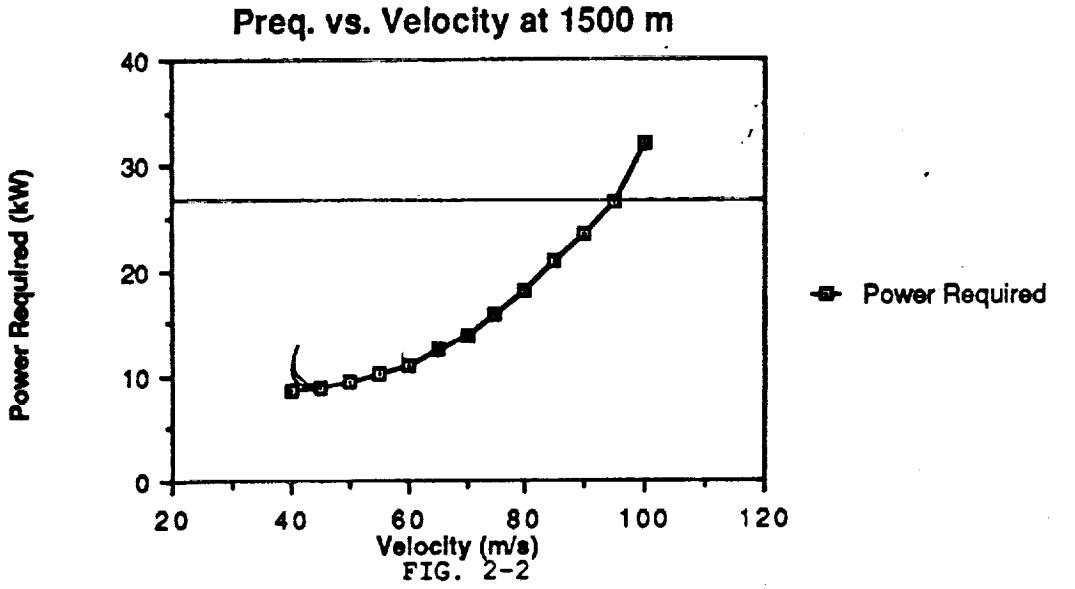

FIG. 2-2

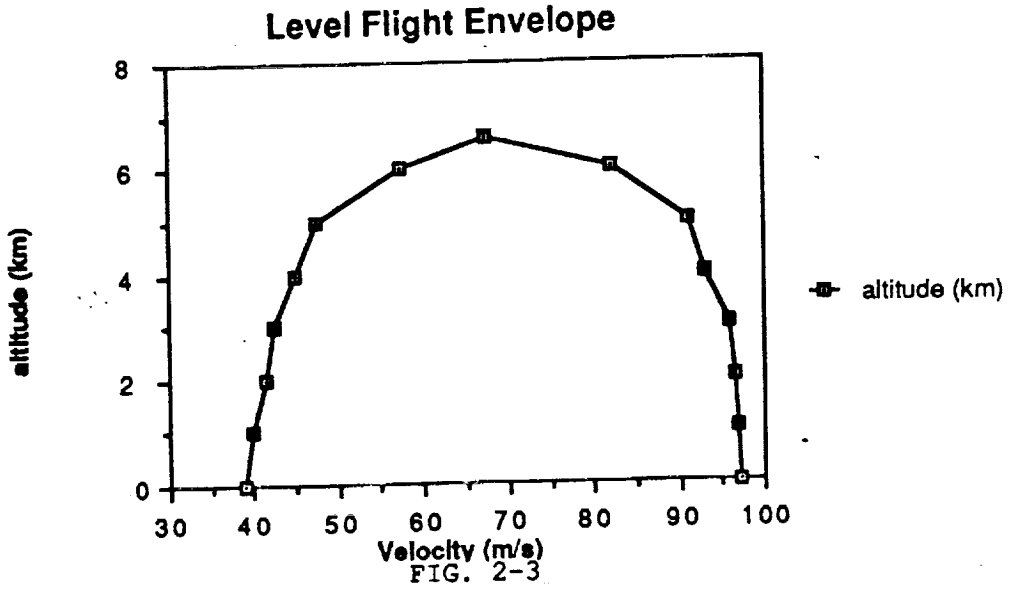
Level Flight Envelope
altitude (km)
8
6
4
2
0
30
40
50
60
70
80
90
100
Velocity (m/s)
altitude (km)

FIG. 2-3

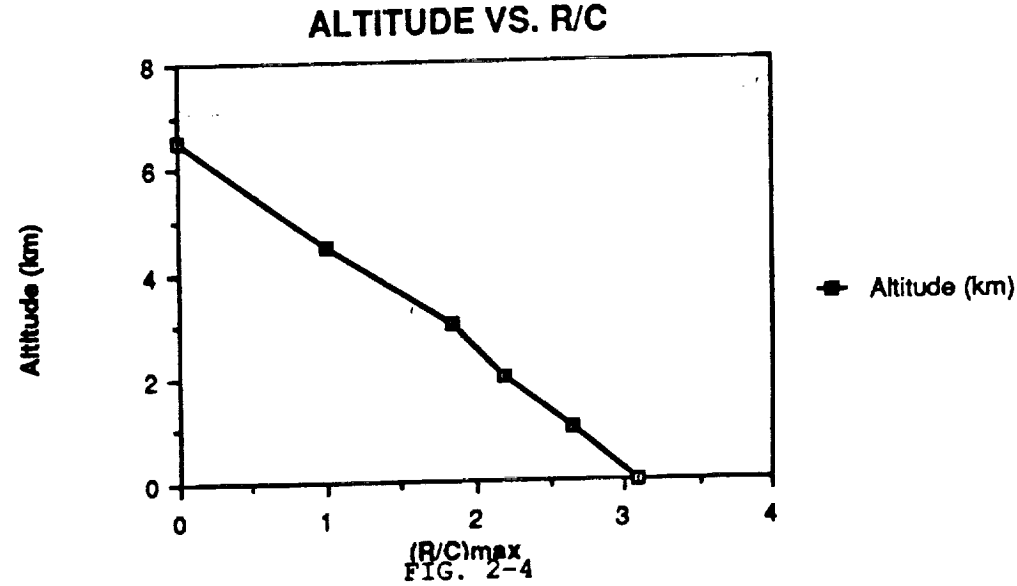
ALTITUDE VS. R/C
Altitude (km)
8
6
4
2
0
0
1
2
3
4
(R/C)max
Altitude (km)

FIG. 2-4

POWER AND PROPULSIONS

Scott Hildreth

SIGNIFICANT DATA

EFFICIENCIES

FUEL CELL - 70%
MOTOR/CONTROLLER - 90%
PROPELLER - 91.8%
GEARBOX - 97%
PROPULSION SYSTEM - 56.1%

MASS AMOUNTS OF FUEL

OXIDIZER (O^2) - 193 kg
FUEL (H^2) - 32 kg

POWER REQUIRED

CLIMB - 19.12 kW
CRUISE - 13.853 kW

TANK VOLUMES

OXIDIZER - .169 m^3
FUEL - .452 m^3
RECLAMATION (m^3)

TOTAL POWER REQUIRED

CLIMB - 23.9 kW
CRUISE - 17.3 kW
ELECTRONICS - 2 kW

PROPELLER

BLADE PITCH ANGLE - 35^0
POWER COEFFICIENT - .11
ADVANCE RATIO - 1.6
DIAMETER - 5.0 m
CLIMB - 970 rpm
CRUISE - 871 rpm

FUEL REQUIRED

CLIMB - 40.0 kg
CRUISE - 185 kg
CAPACITY - 225 kg

FUEL DATA

MASS MIXING RATIO - 6:1
ENERGY AVAILABLE - 3800 kj/kg

Introduction.

The requirements for a manned Mars aircraft design dictated that an energy system which could supply both power for the onboard electronics equipment and propulsion system be as simple and as compact as possible. These requirements were further complicated by the lack of an oxidizer in the Martian atmosphere, thus requiring that the aircraft carry the oxidizer as well as the fuel for the power system. Taking these needs into consideration, it was concluded that a system utilizing an H_2/O_2 fuel cell power plant would be used. This system has the advantage of compact size and high- energy conversion efficiency along with high- energy output, these facts coupled with the ability to carry and deliver the oxidizer and fuel in an efficient form (liquid) were the primary reasons that this system was chosen. The motor chosen to drive the propeller had to be light and efficient while at the same time provide sufficient power to propel the aircraft. After examining these needs an electric motor utilizing rare earth magnets (samarium- cobalt) was chosen. Each of the separate propulsion system components will now be discussed in further detail.

Fuel Cell Power Plant.

The fuel cell power plant that was selected as a model is the unit that is currently being used on the Space Shuttle. Each fuel cell power plant provides 7 kW average power with a peak power output of 12 kW, [1] at an energy conversion efficiency of approximately 70%. This efficiency was used along with the fact that 3800 kj/kg of energy is available from the H_2/O_2 reaction, to obtain a total fuel requirement of 225 kg for the entire 8-hour mission. The maximum amount of energy required from the fuel cells is during climb configuration (24 kW) this would just allow for the use of 2 fuel cell power plants, but since this leaves no margin of safety if more power were required the decision was made to use 3 fuel cells. The penalty paid for this margin of safety is that during cruise only 17.3 kW are needed so the aircraft has an extra 91 kg of mass (the weight of one fuel cell) that is not required, thus increasing the total amount of fuel required for the mission. To make maximum use of space in the aircraft, the fuel cells will have to be manufactured in a cylindrical shape instead of the rectangular shape used on the Shuttle. These

will be coupled in series and then slid, as one package, into the tail boom of the aircraft which will allow easy access for fuel cell maintenance. (Figure 3-3)

← this should be Fig 3-1.

Motor/Controller.

A motor with variable rpm was required so that the propeller would operate at the best rpm for whichever flight configuration the aircraft was in. The type of electric motor chosen was a brushless DC motor with rare earth magnets (samarium-cobalt). These motors provide significantly more power over ferrite magnet DC motors but at a lower motor weight. Based on a Sundstrand preliminary design, the motor/controller combination, linearly scaled for a power output of 27 kW, would have a mass of approximately 25 kg and operate at an efficiency of 90%. [2] This design power output was chosen so that the motor would be able to provide the amount of power that might be required during extreme situations.

Gearbox.

The gearbox data which are also based on a Sundstrand design [2] and scaled linearly with shaft power output at cruise (14.0 kW), would have a mass of 14.0 kg and operate at an efficiency of 97%. This gearbox may be too small to handle the required power output during climb. If so, it could be scaled up to meet these requirements, thus having a mass of 24.0 kg and an efficiency of approximately 95%. For this report 14.0 kg and 97% efficiency have been used.

Propeller.

Based on data for a 3 bladed, 80 activity factor, .500 integrated design C_L,[3] a propeller with a diameter of 5.0 m was chosen operating between 871- 970 rpm for cruise and climb, respectively. This design was calculated for best efficiency at cruise since most of the mission will be spent in this configuration. The variables used were: blade pitch angle of 35 degrees, power coefficient of .11, efficiency of 91.8%, and an advance ratio of 1.6. Fuel consumption and rpm versus velocity were computed for this design, resulting in figures 3-1, and 3-2. These data were used because a suitable propeller design algorithm could not be obtained.

Fuel System.

The fuel system will consist of cryogenically stored O_2 and H_2, along with a reclamation tank to store the water that is produced during fuel consumption. The reclamation system was included in this design, in an effort to conserve water, because it has yet to be discovered in large quantities on the planet. The fuel will be stored in individual tanks in the lower rear of the fuselage, the reclamation tank will positioned above these tanks (figure 3-3) in the forward part of the boom so that no significant distribution of weight will occur during the flight. This configuration was reached in conjunction with the Weights group. Current fuel volume estimates are; LOX - .169 m^3 , LH_2 - .452 m^3 , H_2O - .225 m^3. The oxidizer and fuel tanks will both be spherical in shape and have radius's of .375 m and .625 m, respectively. The water reclamation tank will be cylindrical in shape and have a diameter of .32 m and a length of 3.0 m. The water return lines will be heated to prevent freezing and reclamation tank heating will be an option. The total weight for all of the tanks is estimated at 50 kg.

Conclusion.

During the design of this aircraft the propulsion system was always the limiting factor in how light the aircraft could be built, so any reduction in the propulsion system weight would benefit the overall design of the aircraft. Unfortunately, information concerning fuel cell research and expected advances could not be obtained until after the design freeze date. At the time of this writing, data were found on fuel cell research conducted by General Electric.[4] The fuel cell GE was working on would weigh about 4.55 kg/kW and operate at an efficiency of approximately 90%.

Using these numbers, along with the power requirements used in this report, the fuel cell mass would be reduced by 109.2 kg and the overall fuel mass would be reduced by 50 kg. These two combined mass reductions would amount to almost 10% of the total mass of the aircraft.

Technological improvements, such as this, are needed in the area of propulsions to make building and flying this aircraft possible. As the design now stands, the propulsion system contributes approximately one-third of the total aircraft weight, thus making it difficult to build an aircraft that is light and also structurally sound. By reducing the propulsion system weight, it would be possible to add that extra weight in areas where it is needed.

REFERENCES

(1) Linden, David: Handbook of Batteries and Fuel Cells. McGraw - Hill,1984.

(2) Hall, D.W., Fortenbach, C.D., Dimicel, E.V., Parks, R.W.: A Preliminary Study of Solar Powered Aircraft and Associated Power Trains. NASA CR - 3699, Dec. 1983.

(3) Generalized Method for Propeller Perfomance Estimation. Hamilton - Standard. revised ed., Oct. 1974.

(4) Shoji, J. M.: Final Report Low-Thrust Chemical Rocket Engine Study. NASA CR - 165275, Nov. 1980.

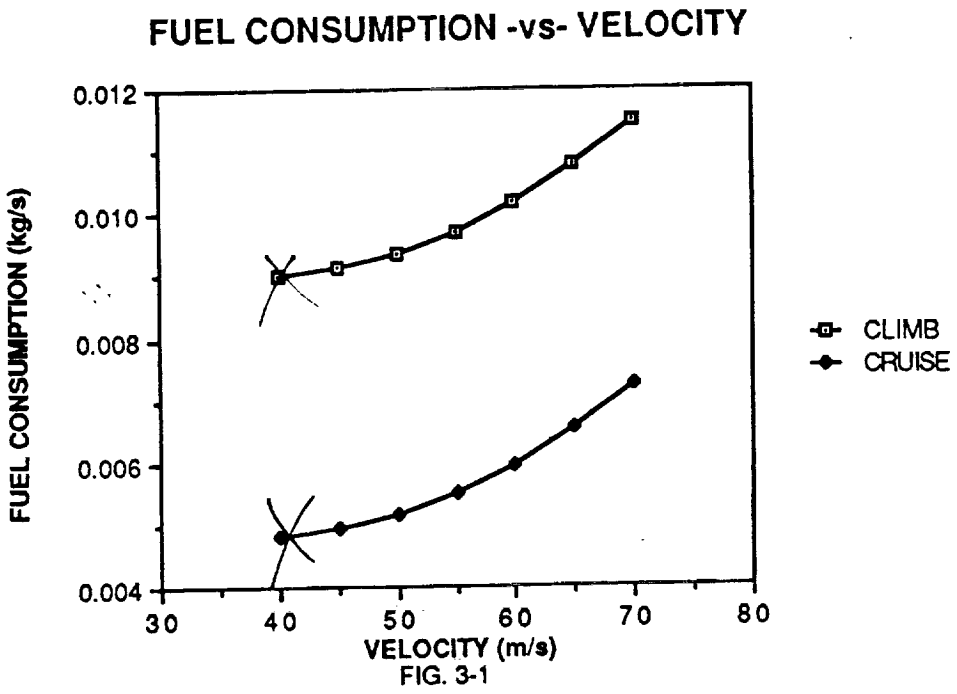
FUEL CONSUMPTION -vs- VELOCITY
FUEL CONSUMPTION (kg/s)
0.012
0.010
0.008
0.006
0.004
30
40
50
60
70
80
VELOCITY (m/s)
CLIMB
CRUISE

FIG. 3-1

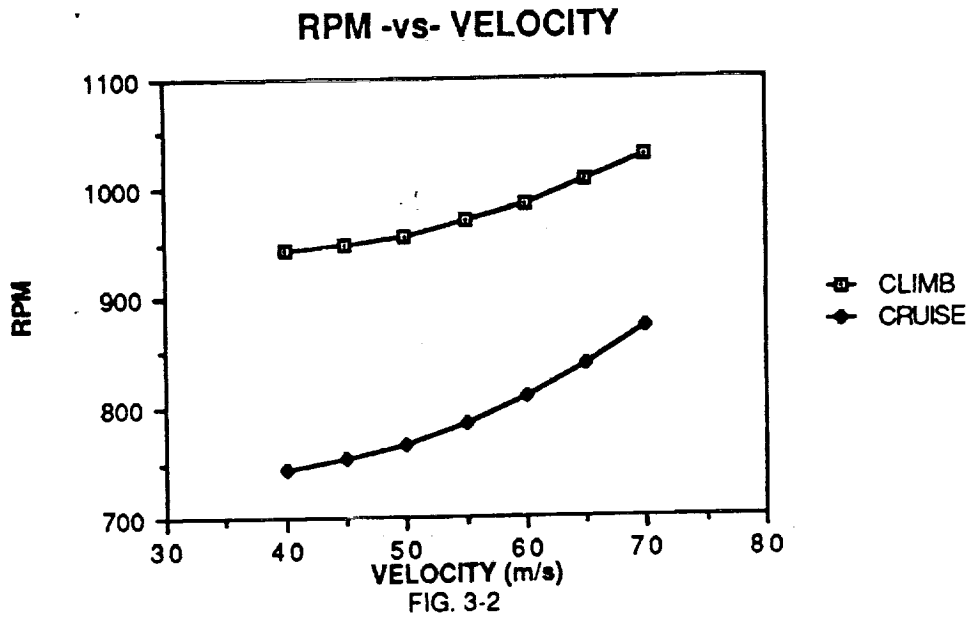
RPM -vs- VELOCITY
RPM
1100
1000
900
800
700
30
40
50
60
70
80
VELOCITY (m/s)
CLIMB
CRUISE

FIG. 3-2

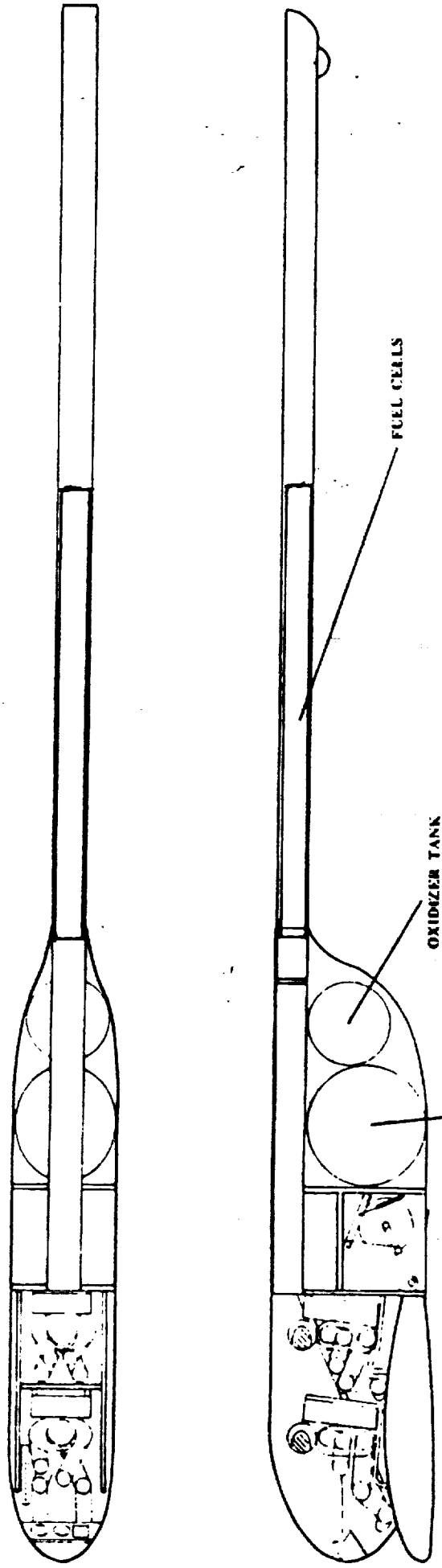

FIG. 3-3

STABILITY AND CONTROL

PAUL BECKWITH

For the plane to fly sufficient stability and control has to exist in three areas. These areas are longitudinal, directional and lateral stability and control.

A joined wing configuration was chosen because it best met the aerodynamic and structural needs defined by the mars atmosphere. The joined wing lessons the effect of downwash on the tail because the tail is swept up, away from the downwash. One control surface is located on each half of each wing (figure 4-1). These control surfaces perform the same functions as the ailerons, elevators, flaps and rudder do for a conventional plane. A rudder is not needed for a joined wing because the control surfaces are arranged with both a sweep angle and a dihedral. Thus a deflection of one surface causes roll, yaw and pitch.

Because the joined wing's geometry and control surface angles are so unusual, straight forward methods for determining longitudinal, directional and lateral stability and control could not be found. Therefore, conventional methods were used. These conventional methods required that the joined wing be treated as a conventional tail aft plane. This method also required that the control surfaces be used as elevators, ailerons, a rudder and flaps separately. This differed in that before a control surface acted as a combination them.

GEOMETRY

In determining the geometry of the plane the aerodynamicist chose the tail to be identical to the wing. Weights and balances determined that the center of gravity (c.g.) location was constant

for all flight configurations (i.e. takeoff, cruise and landing). After wing and tail aerodynamic centers were calculated the neutral point (n.p.) was located. This location was not totally accurate due to the thrust causing a negative change in moment with lift thus increasing the static margin (s.m.) and pushing the n.p. back a short distance. Taking this into consideration the final n.p. location was found and s.m. determined (s.m.= n.p.-c.g.). The n.p. location turned out to be similar to those found in Wolkovitch's readings (ref 1) on joined wings. The locations of the points mentioned can be found in figure 4-1. Their values are listed in table 4-2.

LONGITUDINAL

As shown in figure 4-1 the n.p. is located behind the c.g. causing the desired positive stability. The exact s.m. is listed in table 4-2. As one can see it is greater than the .1 minimum requirement. Because of the vertical take off no flaps were required. The change in moment with positive elevator deflection turned out to be negative which is common for conventional planes. Some of the values associated with the elevator size are listed in table 4-2. The elevator location can be seen in figure 5-9. Because the engine was so high up on the vertical tail, (figure 5-9) a large negative moment resulted due to the thrust. This moment was countered by increasing the lift of the wing (increasing wing incidence angle) and deflecting the elevator a small amount. The elevator deflection angle needed to trim at cruise is listed in table 4-2. The incident angles of the wing and tail could have been adjusted to allow the plane to be trimmed at cruise without elevator deflection. This was not done because the aerodynamicist wanted the wing and tail loading to be as close as possible. In the future improvements could be made by moving the engine down the vertical tail to a point below the vertical c.g., thus lessoning the s.m. and making the net moment less negative, eliminating the need for elevator deflection at cruise.

DIRECTIONAL

A vertical tail was designed. The size and dimensions were given by the aerodynamicist (figure 4-3). A section was found and a rudder size determined. The section chosen was a NACA 009 symmetrical wing section. The values associated with the section and rudder are listed in table 4-2. The derivatives associated with directional stability and control are also listed in 4-2. The change in yaw moment with positive sideslip angle turned out to be positive which satisfies the stability criterion. The other values were reasonable also.

LATERAL

Ailerons were designed. There locations are shown in figure 5-9. Values associated with their size are listed in 4-2. A number of the lateral stability derivatives are also listed in 4-2. The change in rolling moment coefficient with positive aileron deflection turned out to be negative which is correct for positive deflection defined as right aileron down.

For proper stability and control to exist a number of ~~criterion~~ criteria have to be met at take off, cruise and landing. Surface operations chose to have a vertical take off and landing. Therefore criterion for take off were not tested. Criterion for landing were still tested because of the necessity to be able to emergency land conventionally. Propulsion chose to use one engine, therefore engine out criteria was not tested.

CRUISE: BANKED TURN

When the ailerons are deflected and counter deflected the plane is left at a constant roll angle. Therefore additional lift needs to be generated to hold the plane at constant altitude and speed. The power needed to generate this additional lift turned out to be

fourteen kilowatts. The maximum power available as given by power and propulsion is twenty seven kilowatts. More then enough power is available to handle this maneuver.

CRUISE: ROLL RESPONSE

Next it had to be shown that the plane could attain a roll angle of thirty degrees in two seconds with a step aileron deflection and counter deflection. This was satisfied with an eight degree right aileron up deflection and an eight degree left aileron down deflection (vice versa for counter deflection). The ailerons were deflected in these directions because the change in rolling moment with aileron was negative. Therefore, a negative aileron deflection was needed to create a positive roll angle.

LANDING: STALL

When landing it was desired to be able to trim the plane at its maximum lift coefficient (CL/MAX) thus allowing for minimum speed. Being able to trim depends on where the c.g. is located. As the c.g. moves farther forward more and more elevator deflection is needed to trim the plane. Therefore, to be sure the plane will trim at CL/MAX for all c.g. locations only the most forward c.g. has to be tested. The most forward c.g. turned out to be six meters from the front of the plane and an elevator deflection of twenty nine degrees trimmed the plane at CL/MAX.

LANDING: ROLL RESPONSE

This criterion is the same as that for cruise roll response. An angle of fifteen degrees was needed to cause a thirty degree roll angle in two seconds. This increase seems reasonable because when landing the speed is slower and therefore the response would seem to be slower.

LANDING: CROSSWIND

When landing in a crosswind (sideslip angle) a yawing moment is induced which is related to the sideslip angle. This moment makes the plane want to turn to decrease the sideslip angle. Therefore, in order to fly at a constant side slip a rudder moment is needed to counter this moment. To hold a constant sideslip of ten degrees a rudder deflection of eleven degrees was needed. This rudder deflection was much less then the maximum rudder deflection.

LANDING: FULL RUDDER SIDESLIP

When landing at a sideslip angle it is desired to be able to hold the plane level and still have some control power available. It was required to show that the plane could maintain zero roll angle with seventy five percent control power at a maximum sideslip angle (28 degrees). Positive sideslip tends to make the plane roll in the negative direction while negative aileron deflection tends to make the plane roll positive. At seventy five percent aileron deflection (-23.5 degrees) and maximum sideslip, just enough aileron roll moment was created to counter the sideslip roll moment. Therefore the plane can be held level at maximum sideslip and still have some lateral control.

Overall the plane satisfied all the criterion reasonably. If the above results are some what accurate despite the assumptions made, this plane should be longitudinally, laterally and directionally stable and controllable.

REFERENCES

Reference 1, Application of the Joined Wing to Turboprop Transport Aircraft, Julian Wolkovitch and David Lund, NASA Contract NAS2-11255.

Reference 2, Aerodynamics, Aeronautics and Flight Mechanics, Barnes W. McCormick, 1979

Reference 3, Methods For Estimating Stability and Control Derivatives of Conventional Subsonic Airplanes, Jan Roskam, University of Kansas, 1977.

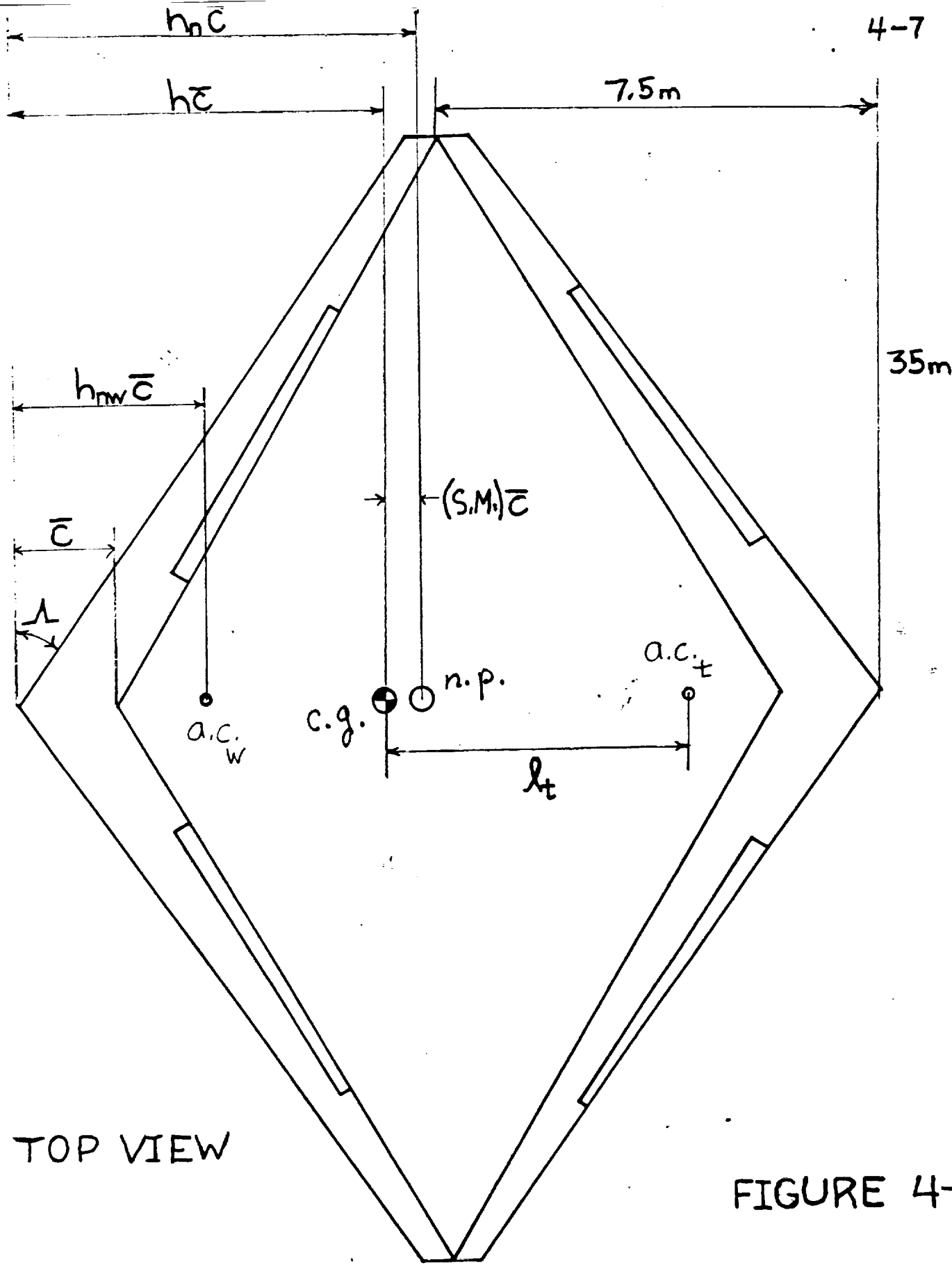

TOP VIEW

FIGURE 4-1

GEOMETRY

$S_w = S_t = 149\ m^2$
$h\bar{c} = 6.57\ m$
$h_{nw}\bar{c} = 3.32\ m$
$h_{nt}\bar{c} = 11.25\ m$
$\Delta S.M._{thrust} = .027$
$h_n\bar{c} = 7.2\ m$
$b = 70\ m$
$\Lambda = 12.07°$
$\Gamma = 17.96°$
$C_o = 3.28\ m$
$\lambda = .3$
$C_t = .98\ m$
$\bar{C}_{mean} = 2.13\ m$
$AR = 32.8$
$t/c = .15$

LONGITUDINAL

$S.M. = -dC_M/dC_L = .29$
$C_{m_\delta} = -3.40$
$\eta_{elevator} = .5$
$C_e/C = .25$
$\delta_{e_{min}} = -30°$
$\delta_{e_{trim/cruise}} = -4.5°$
$i_w = -.75°$
$i_t = -1.25°$
$C_{L_{w/cruise}} = .62472$
$C_{L_{t/cruise}} = .52644$
$C_{L_{max/w}} = 1.75$
$C_{L_{max_t}} = 1.59$
$C_{m_{ac.w}} = C_{m_{ac_t}} = -.17$
$C_{m_{thrust}} = -.113$
$C_{l_{\alpha w}} = C_{l_{\alpha_t}} = 6.44$
$C_{h_{\delta_e}} = 11.62$

DIRECTIONAL

$b_{vertical\ tail} = 10.47\ m$
$S_v = 10.47\ m$
$A_v = 10.47$
$R = 3 \times 10^6$
$(t/c)_v = .1$
$C_{l_{\alpha_v}} = 6.44$
$\eta_{tail} = 1.0$
$C_R/C = .5$
$C_{n_\beta} = .011$
$C_{n_{\delta R}} = -.01$
$\delta_{r_{max}} = 25°$
$C_{n_{\delta A}} \approx 0$

LATERAL

$\eta_{ailerons} = .25$
$c_a/C = .25$

stall:
$C_{l_{\delta A}} = -1.092$
$C_{l_{\delta P}} = -1.2715$
$C_{l_{\delta B}} = -1.248$

cruise:
$C_{l_{\delta A}} = -1.1645$
$C_{l_{\delta P}} = -1.2715$
$C_{l_{\delta B}} = -.795$

TABLE 4-2

FIGURE 4-3

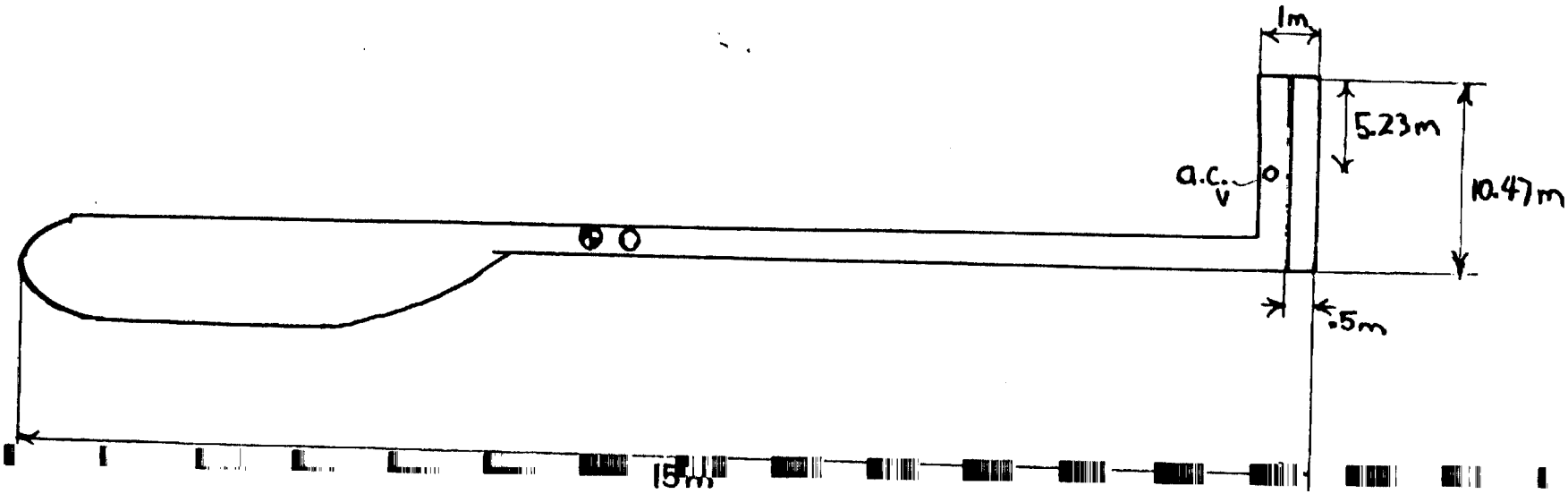

Structures

Bruce Zimmerman

Introduction

Throughout the structural design process, two objectives were considered: (1) safety and (2) performance. Maintaining a reasonable safety factor included using additional supports in high stress areas and maintaining a wing skin thickness which met the stringent shear stress requirements. However, meeting safety factors comes in direct conflict with aircraft performance. Increasing structural support adds weight which influences lift and power requirements. Thus, a method was created for representing typical loading effects upon the aircraft. Discussion of loading, shear, moment, and moment about the aerodynamic center is followed by graphical representations. 1-G FLIGHT and ON-THE-RAMP configurations are considered. Then a method of wing skin thickness analysis is described followed by material selection and a description of the aircraft structure.

Loading-Shear-Moment

Schrenk

Figure 5-1 represents the wing loading during 1-G flight. The loads include the lift (Shrink approximation), wing weight, VSTOL rocket weight, winglet weight, and winglet loading. Shear which results from these loads is represented by Figure 5-2. Maximum shear of 1900 newtons occurs at the wing root. Moment, represented by Figure 5-3, obtains an absolute maximum of 25,000 newton-meters at the root.

A second configuration, on the ramp loading conditions, was also examined. The loading from this configuration, represented by Figure 5-4, includes wing weight, VSTOL rocket weight, and landing gear effects. Shear and moment on the wing are shown by Figures 5-5 and 5-6 with maximum shear of 720 newtons at the wing tip

(resulting from the gear), and an absolute maximum moment of 14,700 newton-meters at the root.

Finally, a diagram representing moment about the aerodynamic center is given in Figure 5-7. This diagram represents only aerodynamic effects due to the fact that all structural components in the wing have negligible influence. Further, due to the joined-wing concept, this moment is insignificant when compared to torsional stiffness.

Figure 5-8 assists in illustrating the method used in determining accurate lift values. The lift component used is that component which is perpendicular to the line joining the root chords of the aircraft.

Skin Thickness

Referring again to Figure 5-8, the method used for determining skin thickness can be described. The cross-sectional area of the wings are concentrated into four areas, A. After finding d, the minimum required areas are found using the equation:

$$4A = \frac{M_y}{\sigma_{yield} \cdot d^2}$$

Once the areas are found the minimum required skin thickness can be determined by dividing the total area by the local perimeter length of the airfoil. Due to high shear strength materials, the minimum required skin thickness is approximately 0.0001 meters.

Structural Design

Figure 5-9 illustrates the internal structural layout of the Mars Plane.[1] The fuselage, represented in detail by Figure 5-10, is attached to the wing using adhesives and small plates with titanium screws. A spar runs through the vertical tail and the boom connecting the two. The top of the cockpit lifts backwards on hinges attached to the bulkhead. This portion of the cockpit has an antennae imbedded to assist the avionics. Landing gear is stored behind and attached to this same bulkhead and the next bulkhead. Fuel tanks

are stored in the back compartment and are strapped to the boom. Beneath the fuselage, small generators bleed off small amounts of fuel used to produce air pressure in the wings, assisting in resisting buckling. Next, in the boom, fuel cells are stored and may be accessed by a rear latch which slides the cells out of the boom. Finally, all control surfaces are controlled by electric motors which have fly-by-wire wiring systems that lead from the cockpit.

Figure 5-11 focuses on the structural layout of one section of the wing and Figure 5-12 represents a cross-sectional view of the wing at the 13 meter station which corresponds to the location of the VSTOL rockets. All other structural supports and instrumentation can be observed in Figure 5-9.

Material Selection

The majority of the aircraft (wing, fuselage, and supports) is constructed using Graphite-Epoxy. With a transverse yield stress of approximately 5×10^8 N/M^2 and a longitudinal yield stress of 2×10^9 N/M^2, the wings can account for the loads applied. Due to the fact that graphite positively expands and epoxy negatively expands in cold temperatures, these materials counteract each other resulting in low expansion and low internal stress in extreme cold. Further, Graphite-Epoxy is highly resistant to fatigue which is important when considering wing flutter. Fuel tanks are constructed of similar graphite-epoxy but include a coating of ceramic on the inside to resist leakage and temperature fluctuations. In addition, insulation and cryogenic polycrystalline wiring is used to protect the avionics systems. Finally, as suggested by surface operations, landing gear cross members will be constructed of composites.[2,3]

Conclusion

To conclude, the following discussion will make suggestions for structural improvements that could be made to complete a successful mission. First, Figure 5-13 has a comparison of current wing skin thickness, minimum required thickness (based on previously

discussed method), and what would be considered a structurally feasible skin thickness. This safe value is based on a .1mm/ply thickness and a $0^{o}/45^{o}/90^{o}/135^{o}$ four ply matrix stacking arrangement of graphite epoxy. So, by looking at the graph, the aircraft does meet the stress requirements. However, it falls significantly short of the safe skin thickness.

To bring the current thickness up to the safe region, a combination of stronger and lighter materials would be required. In addition, because skin thickness varies directly with moment, relocating weight (fuel cells, engines, etc.) into the wings would counteract the enormous lifting moment, making thin wing skins feasible.

It should be noted that placing the engines and/or fuel cells in the wings was considered but was found to be impractical due to the fuel cell dimensions and fuel piping systems that would be required. Thus, given expected improvements in material strength, this structural design is safe and negligibly limits performance.

References

1. Roskam, Jan. Airplane Design Part III: Layout Design of Cockpit, Fuselage,Wing, and Empennage: Cutaways and Inboard Profiles. Published by Roskam Aviation and Engineering Corp. . 1986.

2. Nicolai, Leland M. . Aircraft Design. Published by Mets, Inc. . 1975.

3. Reed, R.P. . Materials at Low Temperatures. American Society for Metals. 1983.

Fig. 5-1

Fig. 5-2

Fig. 5-3

FOLDOUT FRAME 2

Fig. 5-4

Fig. 5-5

Fig. 5-6

EOLDOUT FRAME

EOLDOUT FRAME

ORIGINAL PAGE IS
OF POOR QUALITY

Fig. 5-7

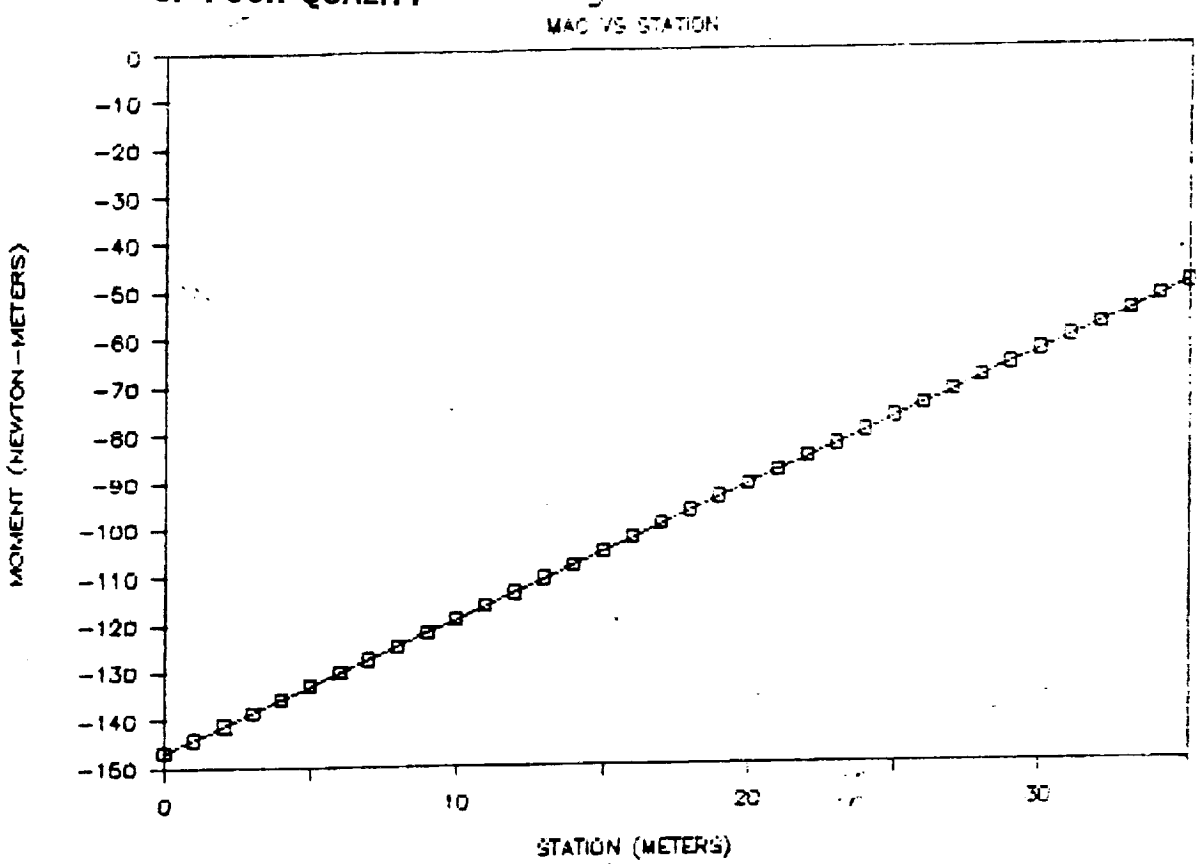

Fig. 5-8

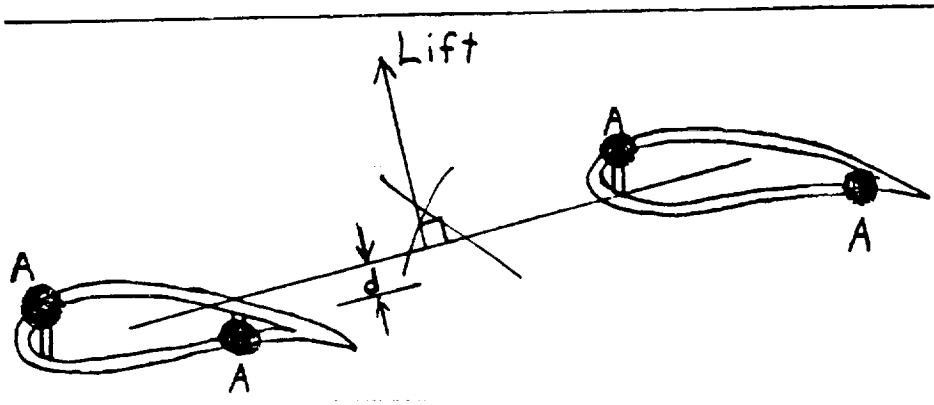

Fig. 5-10

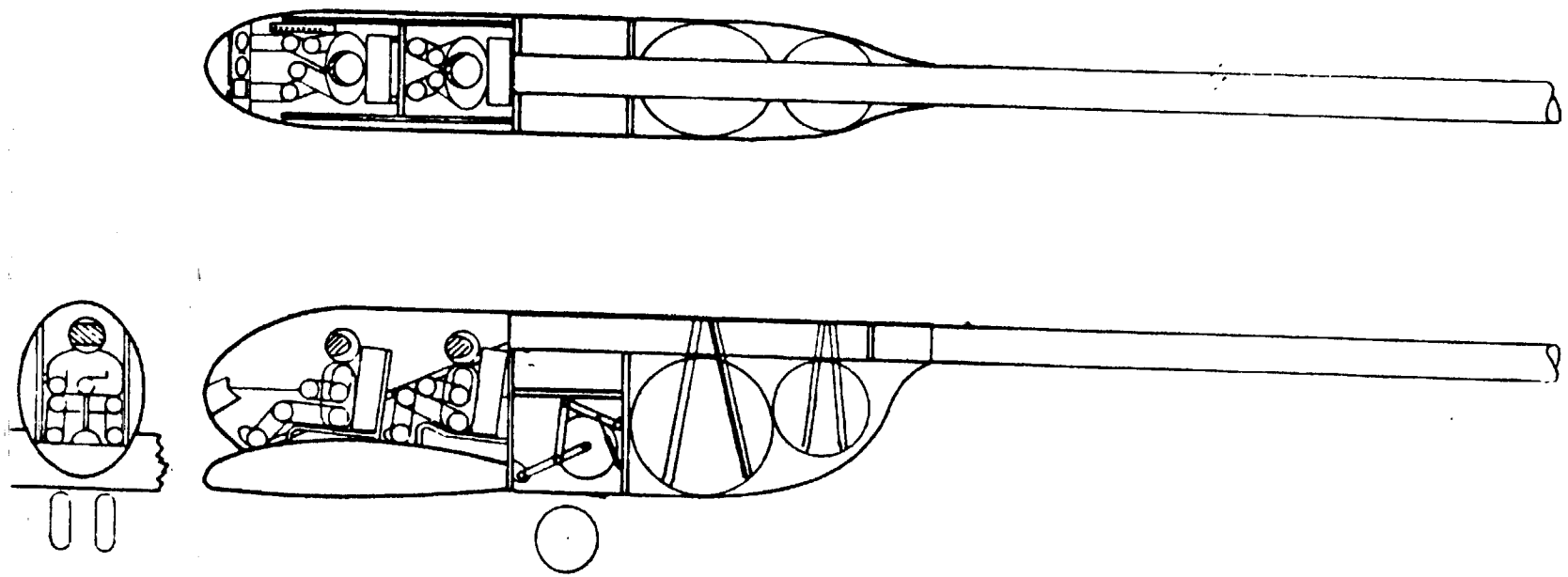

INBOARD PROFILE

Fig. 5-11

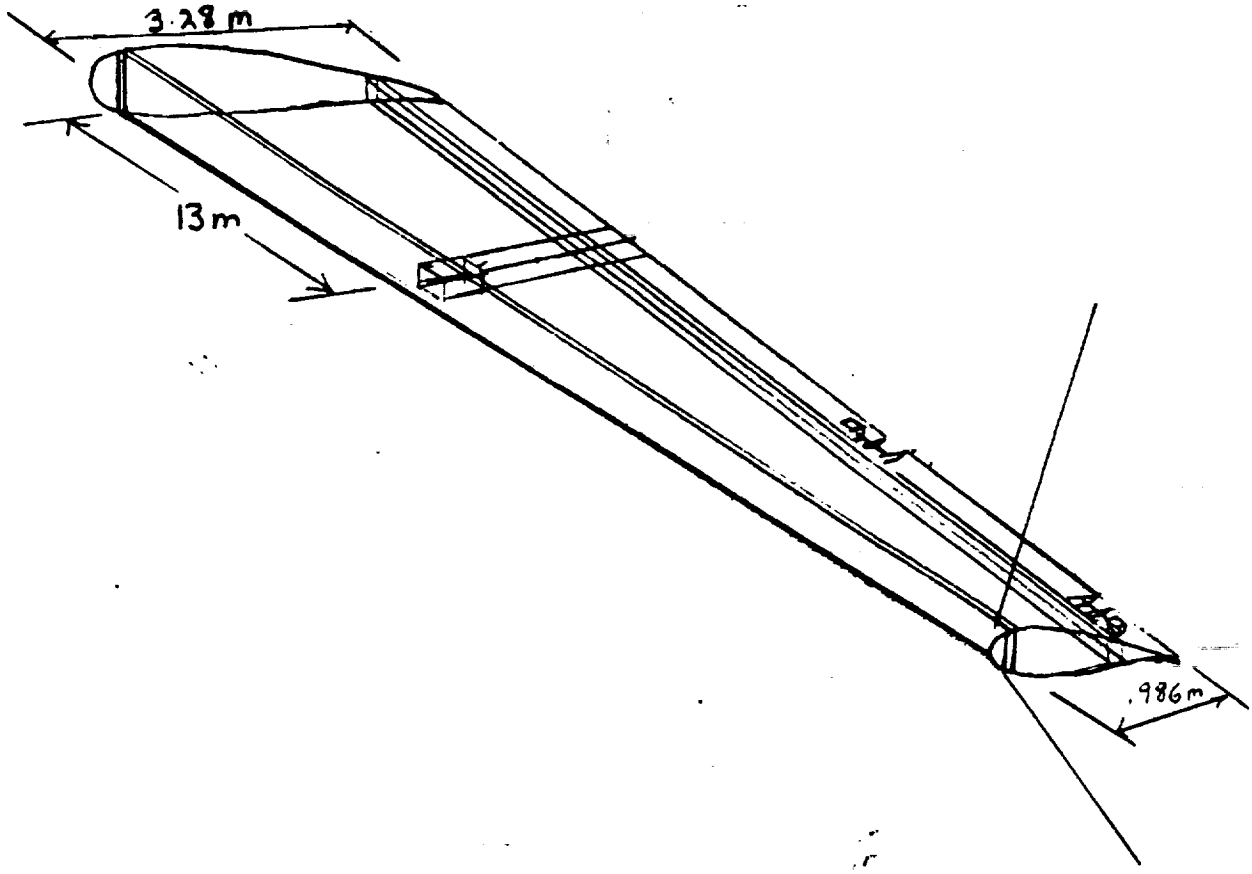

Fig. 5-12

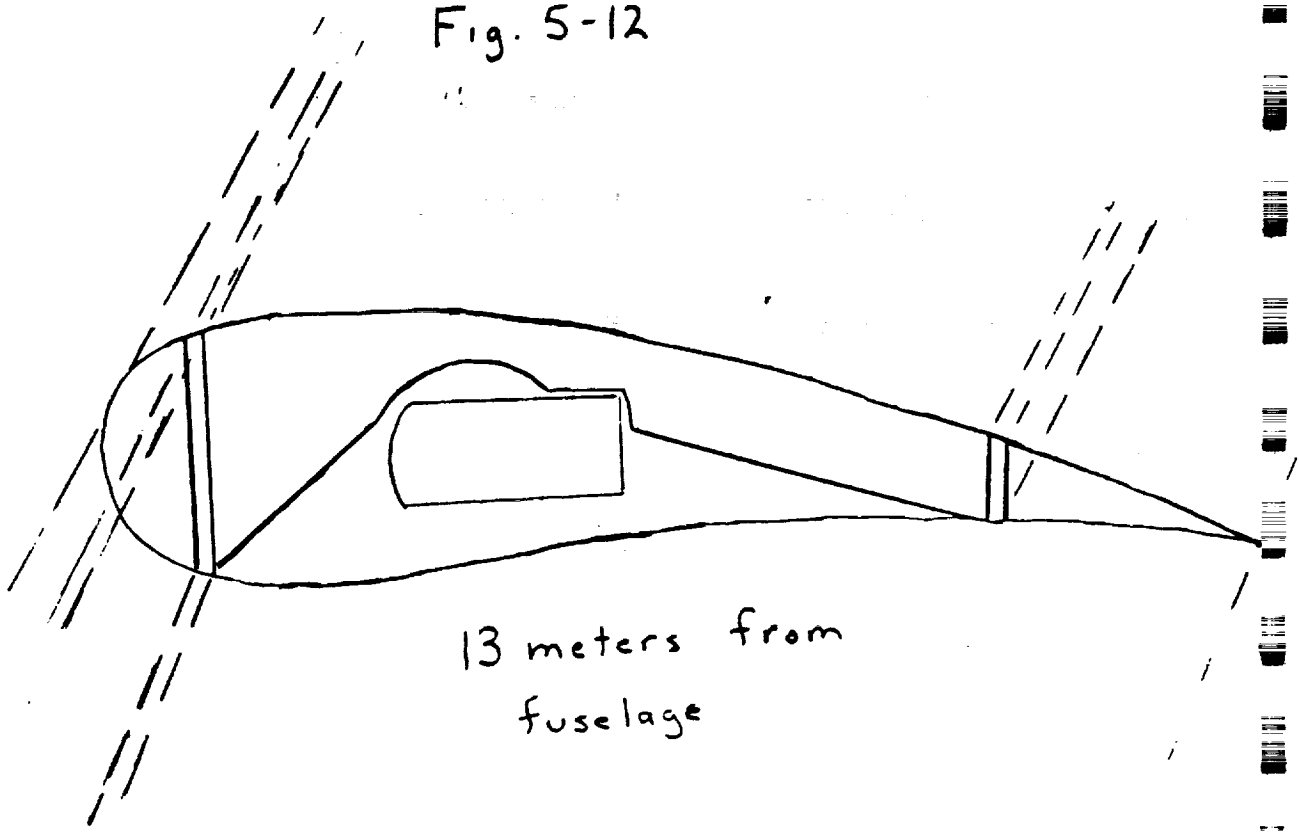

ORIGINAL PAGE IS
OF POOR QUALITY

Fig. 5—13

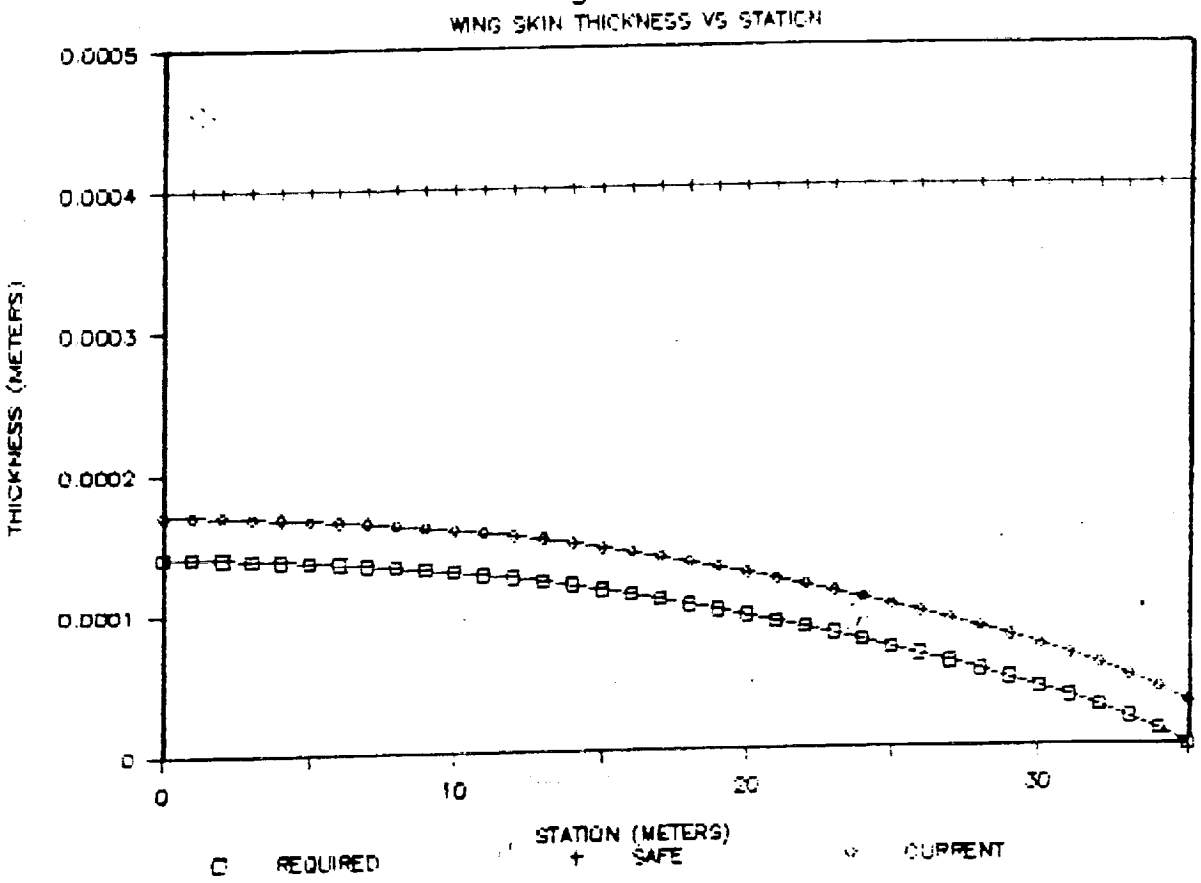

SURFACE OPERATIONS

Ronald L. Cihak

Tables should not be first

Table 6.1 (VTOL) Vertical Take-Off and Landing engine design parameters, derived from tables in,"NASA Final Report Low- Thrust Chemical Rocket Engine Study".

Cooling	Regenerative cooled
Maximum Thrust	2224.1 N
Area Ratio	200.0
Axial Engine Length	56.6 cm
Chamber Pressure	689.5 N/cm^2
Maximum Engine Diameter	20.0 cm
Engine Mass	19.0 kg
Specific Impulse	3625.0 N-s/kg

Table 6.2 (VTOL) Vertical Take-Off and Landing System estimated mass summary for a 1611 kg plane. Data are based on a 1979 technology level.

ITEM	MASS,kg	
PROPULSION SYSTEM (LCH_4-LOX,DRY)		101
Propellant Tanks and Feeds	15	
Main Engines (4)	76	
Vectoring Mechanisms (4)	10	
ONE CYCLE PROPELLANT (LCH_4-LOX)		58
Take-Off Fuel	5.7	
Take-Off Oxidizer	21.3	
Landing Fuel	6.6	
Landing Oxidizer	20.6	
TOTAL MASS BEFORE TAKE-OFF		159
TOTAL AFTER TAKE-OFF		132

Table 6.3 (VTOL) Vertical Take-Off and Landing system estimated mass summary for a 1611 kg plane. Data are based on a 1979 technology level, adjusted for proposed use of composite materials to reduce engine weight by 40%.

ITEM		MASS,kg
PROPULSION SYSTEM {LCH_4-LOX,DRY}		69
	Propellant Tanks and Feeds	11
	Main Engines (4)	48
	Vectoring Mechanisms (4)	10
ONE CYCLE PROPELLANT {LCH_4-LOX}		58
	Take-Off Fuel	5.7
	Take-Off Oxidizer	21.3
	Landing Fuel	6.6
	Landing Oxidizer	20.6
TOTAL MASS BEFORE TAKE-OFF		127
TOTAL AFTER TAKE-OFF		100

Table 6.4 Estimated diameters of fuel and oxidizer tanks capable of carrying enough LCH_4 and LOX for 2.5 (VTOL) cycles. The insulation is included in these calculations.

ITEM	DIAMETER,cm
LCH_4 Tank	34.5
LOX Tank	38.0

Table 6.5 Conventional landing parameters. Landing is to be accomplished on a 1000 m soft field with a 15 m obstacle at the end.

Approach Velocity	44	m/s
Approach Angle	7	deg.
Approach Distance	105	m
Flare Distance	145	m
Ground Roll	701	m
Total Landing Distance	951	m

Table 6.6 Estimated mass of landing gear.

ITEM	MASS,kg
Main Gear Assembly	14.6
Tail Wheel	4.1
Wing-tip Rollers 2@ 4.1	8.2
TOTAL MASS	26.9

Table 6.7 Estimated loading on landing gear when stationary on ground.

ITEM	LOADING, N
Main Gear	4357
Tail Wheel	1643
Wing-tip Rollers	INDETERMINATE
TOTAL	6000

Definitions

VTOL Cycle : In this paper a VTOL cycle is defined as one complete lift-off and landing.

Introduction

The vertical take-off and landing (VTOL) Mars atmospheric plane is proposed as an alternative to a conventional (TOL) configuration. The system proposed would comprise approximately 7.8% by mass, of a 1611 kg plane. This mass would be offset by the reduction in the main propulsion system weight that would be required for a conventional take-off. This concept is seen as an attractive approach because it would allow the plane to operate to and from virtually unprepared facilities. For scientific missions this is an important parameter. Most missions necessitating a manned presence would require an ability to land at remote locations away from the base. These missions could involve the implant and extraction of scientific instrumentation, sample collection and the ability to rescue personnel marooned away from the base. Missions which would not require an ability to land away from the main facility, like photographic, radar or infrared mapping, could be completed more efficiently and with less danger to valuable personnel, by remotely piloted or drone vehicles. Another advantage to the VTOL system is that the cost of construction and maintenance of an airfield on Mars could be greatly reduced, and this monetary savings could be diverted into the aircraft.

The low gravity and atmospheric pressures on Mars allow for rocket powered operations with reasonable fuel mass requirements.[4] Fuel selection has many considerations. Liquid carbon monoxide and liquid oxygen could be produced from the CO_2 rich atmosphere on the red planet.[1] It has been proposed that a LCO-LOX rocket engine could yield specific impulse values (I_{sp}), as high as 2940 N-s/kg.[2] This value is much lower than I_{sp} values for hydrogen based fuels . As future advances in rocket technology are made, LOX-LCO engines could be a feasible substitution.

For this design an assumption was made that hydrogen and a methane production facility are available. Methane was chosen due to its high energy density, and the ease of storage. It is further assumed that the craft in question will have a fly-by-wire computer capable of handling the additional tasks of throttling, and vectoring the four (VTOL) rocket engines during the take-off and landing exercises. It is also assumed that the technological advances of the future will make up for the safety factors ignored herein.

VTOL System Initial Sizing

The initial allowable mass of the (VTOL) system was arrived at after considerations of various parameters. The major limiting factor was that the (VTOL) system mass could at no time be greater than the additional mass required for a conventional (TOL) propulsion system. Acceleration also had to be kept to a reasonable level. There had to be enough reserve thrust to begin horizontal acceleration early enough to gain lift quickly, thereby minimizing fuel consumption. As a result of these considerations a total wet system mass of 130 kg , and a maximum acceleration of 4.5 m/s^2 were decided upon.

VTOL System Description

The VTOL system would be comprised of four LOX-Methane rocket engines, each throttleable and capable of developing 2224 N of thrust, and equipped with a vectoring servo motor. The engine descriptions are given in Table 6.1. These data, based on a 1979 technology level, would yield a operational system as described in Table 6.2, having a wet operational mass of 159 kg. This mass was unacceptably high. After assuming a 37% engine and fuel tank mass reduction due to the predicted use of composites and ceramics in the future, the system mass was reduced to an acceptable level of 127 kg wet. The system data, including computer estimated fuel masses, for this advanced system are shown in Table 6.3.

Each rocket engine would fit inside a cylinder 56.6 cm long and 20 cm in diameter. One engine would be placed in each wing, 12.85 m port and starboard of the fuselage axis. At this distance from the fuselage, the chord of the wing was calculated to be 2.43 m and would easily accommodate an engine of these dimensions, while allowing for the adequate vectorability as shown in Figure 6.1. The engines themselves

will be isolated from the fuel tanks and wing interior by an engine compartment as shown in Figures 6.1 and 6.2.

The engine's center of gravity would be placed 0.81 m back from the leading edge. With this geometry the engine thrust could be vectored 71 degrees forward or 81 degrees aft (Fig. 6.1). Ground clearance for the front forward engine nozzles would never be less than 2.5 m, and for the aft engine nozzles the clearance would never be less than 9 m. Pivoting of the engines would occur about their centers of gravity, and their thrust line would pass through the pivotal axis, which would minimize the torque needed to vector the engines.

The fuel, oxidizer and control lines, which would require a rotatable coupling to allow free movement, would be contained within the vectoring axle. Fuel and oxidizer tanks would be capable of holding 2.5 VTOL cycles of fuel and have diameters as shown in Table 6.4. Location of these tanks would be along the pivotal axis and as close as possible to the engine to minimize mass. The total mass of the fuel/oxidizer tanks and feeds is 11 kg.

The engine layouts are approximately the same for both fore and aft engines. The front starboard engine layout as seen from above is shown in Figure 6.2.

Vertical Take-Off Scenario

The take-off will be a slow transition from vertical take-off to conventional flight. The engines would first be rotated so that the thrust axis for each is perpendicular to the ground. After a short low power engine run-up, the pilot would decide whether to commit to a launch, or to abort. In the event of a commit decision, the pilot would transfer complete vehicle control to the onboard computer. At this point the main engine would be brought to full power. The computer would raise the craft vertically to a transition height of 5 m by firing the rockets, which would take approximately 2 seconds. The excess thrust not needed for the levitation of the plane would then be vectored aft to aid in horizontal acceleration. At approximately 11 seconds after commit, the aircraft would be delivered in stall configuration 209 m down field, altitude of 16 m and a velocity of 45 m/s. At this point the pilot would shut down the engines and stow them. It was numerically calculated that this mission segment would require 27 kg of fuel and oxidizer.

Vertical Landing Scenario

The landing scenario is basically the same procedure in reverse. All calculations for landing were done on the worst case assumption that a landing was needed immediately after launch. The pilot would make a level approach toward the landing site at an altitude of 16 m and a velocity of 45 m/s. At a distance of 500 m from the landing zone, the pilot would rotate all four engines full forward. At 300 m from the landing zone the pilot would commit or abort. In the event of a commit the main gear would be lowered and the engines would be run-up. At 254 m the engines would be fired and the main engine reversed. As lift is lost the engines would be vectored down to maintain an altitude of 3 m. When the landing zone is reached the engine thrust would be reduced until the main gear touched ground. At this point the front engines are cut, and throttle down of the rear engines would continue until the tail wheel touched ground. All systems would then be shut down.

Conventional Landing Scenario

The airbag landing gear system of earlier designs was replaced with a wheel system to facilitate ground handling and a conventional landing either at a prepared runway or in the case of an emergency landing. The runway length required would be 951 m after crossing a 15 m obstacle. Approach velocity for the landing would be 44 m/s. The aircraft would land on the main gear first. The tail gear would follow, and finally when the wings touched due to sag, the rollers on the winglets would prevent damage. Other pertinent landing information is shown in Table 6.5.

Ingress and Egress Procedures

Ingress and egress of the cockpit is a simple matter. The canopy would be hinged along the rear edge to the first fuselage bulkhead. When open, the entire forward area of the fuselage is exposed and easily accessible.

Is the surface strong enough?

The passenger and pilot would step up onto the port front wing from the aft side, open the canopy, step in then close and latch it. Egress procedures are basically the reverse.

Take-Off and Landing Gear Design

Landing gear was designed to be incorporated with already existing structure and to minimize aerodynamic drag. Estimated masses and loadings for the different gear are given in Tables 6.6 and 6.7. The main gear is retractable because it had to be much larger, and have more travel to absorb impact upon landing, than the tail gear (Fig. 6.5). The main gear is stowed by first releasing a solenoid latch which locks it in the deployed position and then pressurizing a small piston with stored CO_2 to push the landing gear up into the fuselage. In the event of a power failure, a solenoid valve which is normally open would open and release the gas. Gravity would then pull the main gear down into the locked position. The landing gear doors would be pulled up by small cables attaches to both the doors and the landing gear.

The tail and winglet wheels as seen in Figures 6.3 and 6.4 respectively are non-pivoting. This reduces the likelihood of cartwheeling due to the aft center of gravity and the torque produced when the wingtip gear hits the ground during a conventional landing. This gear would require an accurate runway approach and a relatively flat runway about 100 meters wide for a conventional landing. Since the wingtip gear would not hit the ground until the later part of the ground roll and it would not be carrying a heavy load, a runway of a much smaller width could be made to accommodate the main gear and tail gear. The later half of the runway could be cleared of big rocks 50 m to each side.

The requirements for a VTOL facility are much simpler. Any flat area with a diameter of 80 m, and nothing higher than 4 m for a 400 meter radius would be acceptable for a landing or take off zone.

Ground Handling & Servicing

Due to the large size of the aircraft, a hanger is not a viable option. The craft will be tied down at the landing gear with the tail pointed into the wind. In the event of strong winds, it may need to be repositioned.

To move the plane a dolly would be placed under the tail and the craft could be towed.

Fueling for the main propulsion system would occur through an access panel at the rear of the fuselage. Fueling of the VTOL tanks could be performed through access panels above the tanks. To get to the aft VTOL engine tanks, existing ladders or scaffolding could be used.

Conclusion

The use of VTOL technology in a manned Mars aircraft is a viable approach to the large problem of getting airborne on the thin atmosphere on Mars. The system design developed in this paper may be optimistic, but for a slight reduction in payload capability, the system could be built now. Besides being an effective method, VTOL operations make possible new missions which otherwise would be impossible.

References

1. Frisbee, R. H., Mass and Power Estimates for a Martian In-Situ Propellant Production System.,JPL D-3648, Jet Propulsion Laboratory, Pasadena, California, October 1986.

2. Clapp,W. M., Propellant Performance of Mars-Produced Carbon Monoxide.,USAF ForeignTechnology Division, Wright-Patterson AFB, OH, June 1986.

3. Shoji, Final Report, Low Thrust Chemical Rocket Engines., Rocketdyne for NASA, Lewis Research Center, June 1980.

4. Sercel J.C., Wood K. L. The Ballistic Mars Hopper: An Alternative Mars Mobility Concept., California Institute of Technology,June 1987.

5. Melchior A.,Thermostructural Composite Materials for Liquid Propellant Rocket engines.,Societe Europeenne de Propulsion, France, June 1987

FIG. 1 BASIC ENGINE DIMENSIONS AND VECTORING GEOMETRY.

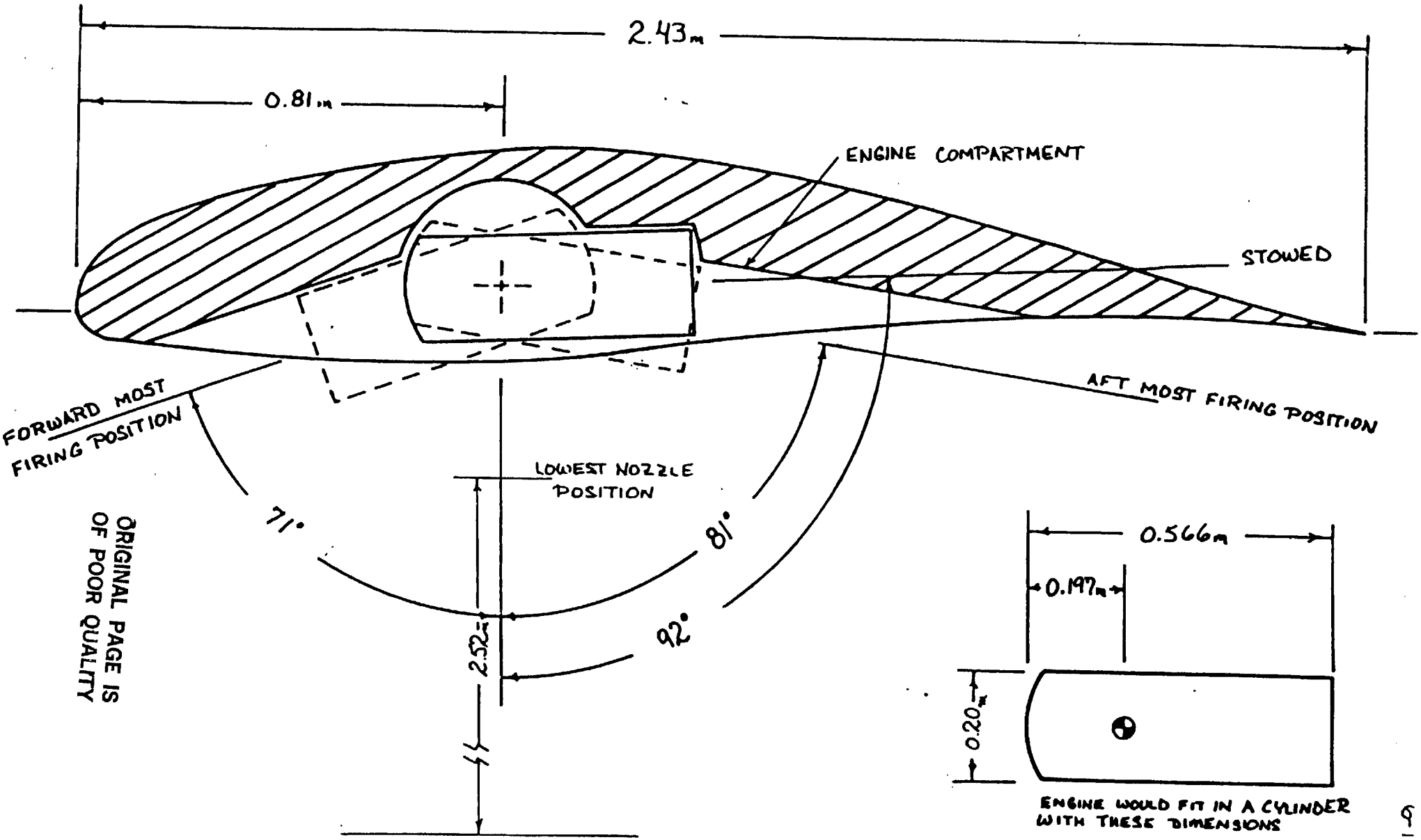

FIG. 2 FRONT STARBOARD VTOL ENGINE LAYOUT SEEN FROM TOP

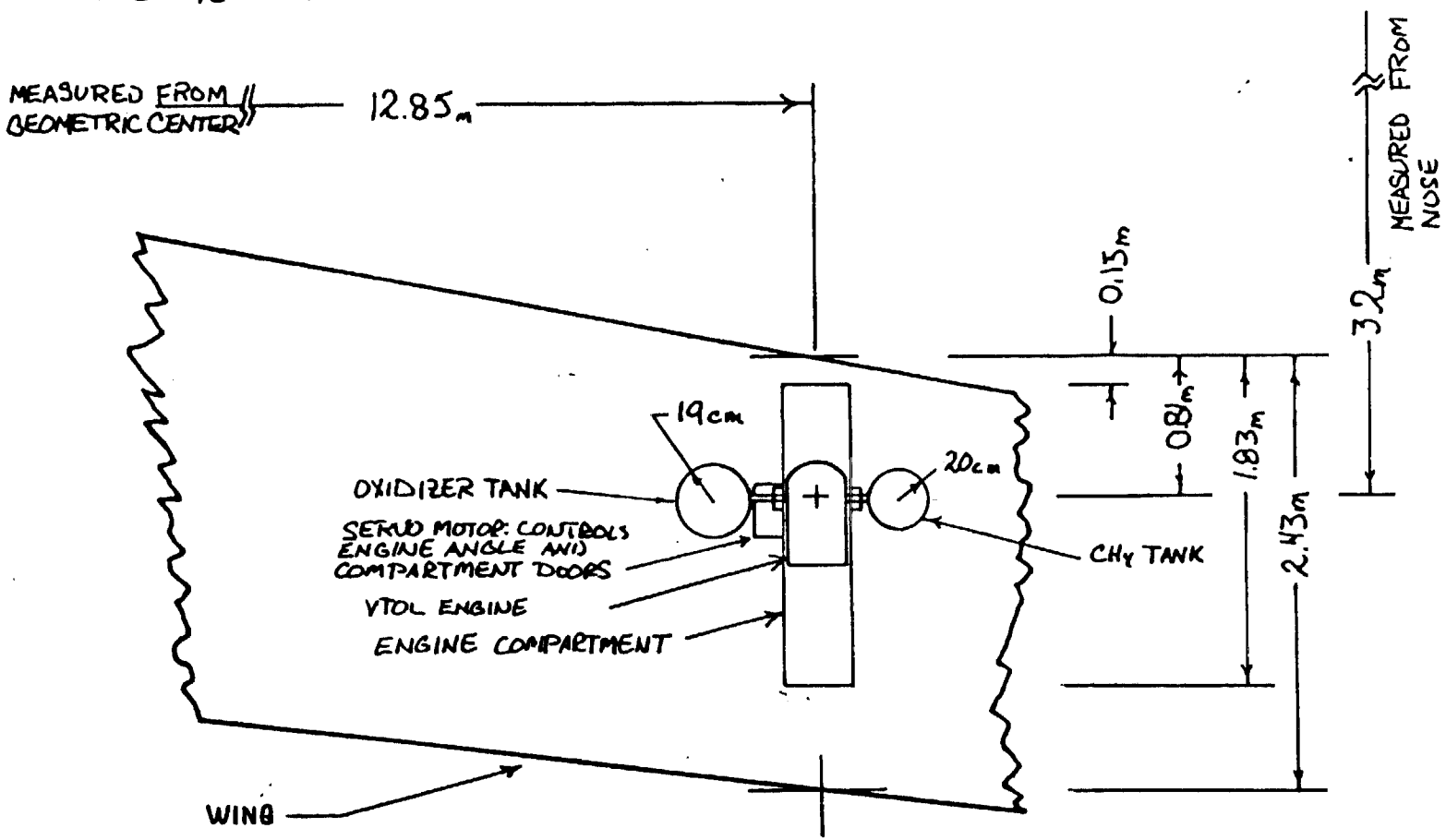

WEIGHTS AND BALANCES

Terri Pulsford

TABLE 7-1
Detailed Group Weight Breakdown
Airplane Type: Joined-wing

Component	W (N)	% of Gross	MA (m)	WxMA (N-m)
AIRFRAME STRUCTURE				
Wing Group (front)	603	10.05	4.68	2822
(rear)	603	10.05	11.50	6934
Winglets (left)	208	3.47	9.09	1891
(right)	208	3.47	9.09	1891
Fuselage	358	5.97	2.70	967
Tail	62	1.03	14.42	894
Tail Boom	46	0.77	9.20	423
Bulkheads (front)	15	0.25	2.50	38
(rear)	14	0.23	3.50	52
Landing Group (main)	54	0.90	3.00	162
(winglet-right)	15	0.25	12.50	188
(winglet-left)	15	0.25	12.50	188
(tail)	15	0.25	14.50	218
Surface Controls	Neg.			
TOTAL	**2216**	**36.94%**		**16,668**
PROPULSION				
Flight:				
Motor & Controller	93	1.55	14.50	1348
Fuel Cells	1007	16.78	8.20	8257
Fuel Tank & Pump	84	1.40	4.12	346
Oxidizer Tank & Pump	18	0.30	5.06	91
Water Storage Tank	84	1.40	4.12	346
Propeller	120	2.00	15.00	1800

FIG. 6.3 TAIL WHEEL

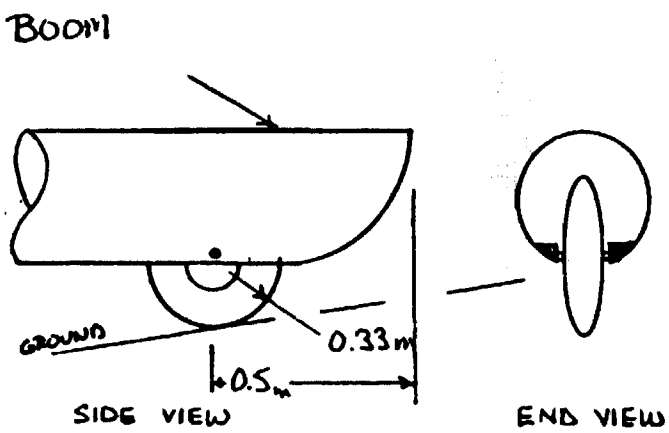

FIG. 6.4 WING TIP ROLLERS

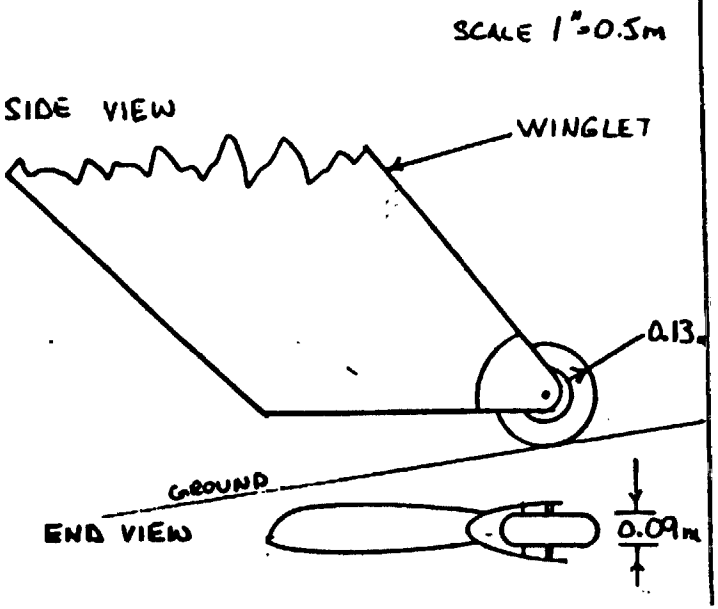

FIG. 6.5 MAIN GEAR LAYOUT

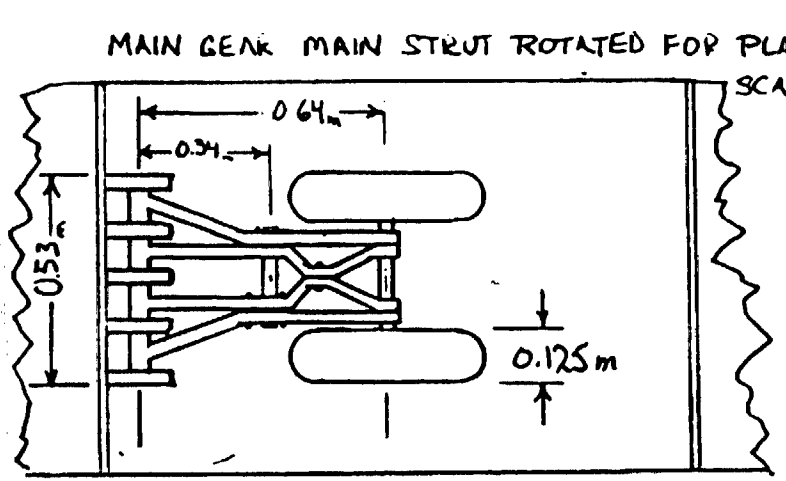

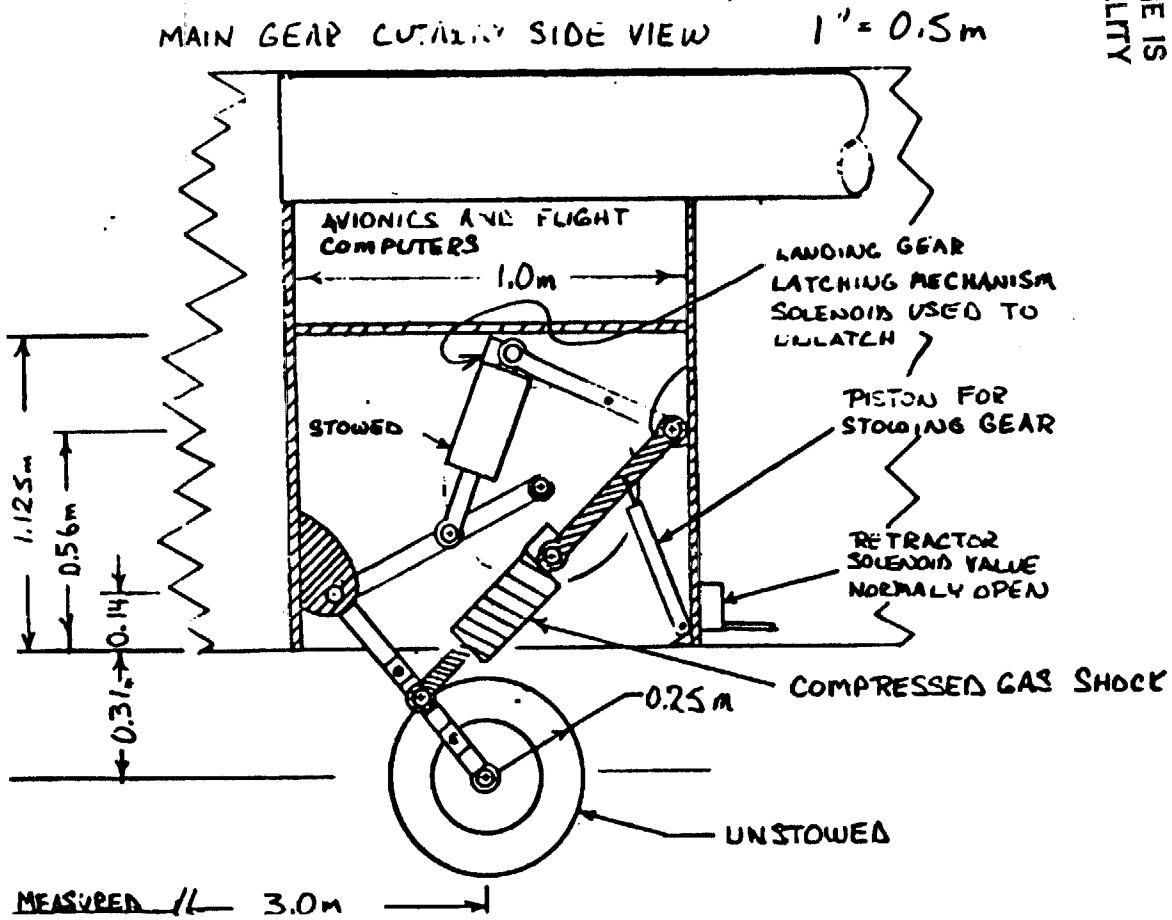

ORIGINAL PAGE IS
OF POOR QUALITY

Component	W (N)	% of Gross	MA (m)	WxMA (N-m)
PROPULSION (continued)				
Take-off & Landing (TOL):				
Engines & Fuel Tanks				
(front)	127	2.12	3.20	406
(rear)	127	2.12	10.99	1396
TOTAL	**1660**	**27.67%**		**13,990**
AIRFRAME SERVICE & EQUIPMENT				
Avionics & Electronics	20	0.33	0.75	15
Furnishings	40	0.67	1.62	65
TOTAL	**60**	**1.00%**		**80**
OPERATIONAL EMPTY WEIGHT	**3936**			**30,738**
PAYLOAD	600	10.00	1.12	672
	600	10.00	2.12	1272
TOTAL	**1200**	**20.00%**		**1944**
MAXIMUM ZERO FUEL WEIGHT	**5136**			**32,682**
FUEL				
Flight:	650	10.83	4.12	2678
TOL (front)	107	1.78	3.20	342
(rear)	107	1.78	10.99	1176
TOTAL	**864**	**14.39%**		**4196**
GROSS WEIGHT	**6000 N**			**36,878 N-m**

CENTER-OF-GRAVITY LOCATION = 36,878 N-m/6000 N
= **6.15** meters back from the nose of the aircraft

In the above table,

W = weight
% = percent
MA = moment arm
N = Newton (all Newtons herein are assumed to be Mars Newtons)
m = meter
Neg. = Negligible

Introduction

As more information about the design of the aircraft was obtained, it was apparent that this design would require a large wing surface area. This large surface area would result in increased weight of the wing, and a component weight estimation would be needed that would minimize the weight magnitudes for the large structural components. Also, an advanced aircraft structural material would have to be used to reduce the overall weight of the aircraft. After some consideration, it was decided that graphite-epoxy composites would provide the necessary weight savings.

Final Weight Breakdown

The final weight breakdown detailed in Table 7-1 was determined using an initial estimated gross weight of 6000 Newtons. Some of the values were estimated by various members of the design group using the design requirements stated for the aircraft as guidelines. In calculating the values for the weights of the larger structural components (i.e. wings, fuselage, tail, tail boom), weight estimation equations were used. [1,2] These values, which were for aluminum parts, were then multiplied by a factor of 0.75 to obtain the reduced weights due to the weight savings of graphite/epoxy, the material used for these components. [3]

The gross weight for this aircraft was calculated to be 6000 Newtons. This value agreed with the initial estimated gross weight. In determining the gross weight, the known or estimated weights of the structural components and the propulsion system were added to the payload and fuel weights. This value was then subtracted from the initial estimated gross weight to determine the weight available for avionics, electronics, and furnishings.

It was assumed that the required payload weight would be equally divided between the two pilots, giving a payload weight of 600 Newtons for a single-pilot mission. It was also assumed that any crew provisions or safety equipment was included in the payload.

It was determined by Power and Propulsion that the water produced while burning fuel should be kept onboard the aircraft, resulting in the assumption that the fuel and the water would essentially weigh an equal amount. Also, the weight of residual fuel was assumed to be negligible compared to the overall weight of the aircraft.

Summary of Weight Breakdown

A short summary of pertinent weight values was tabulated as shown in Table 7-2. Comparable initial sizing data was also listed in this table. The maximum landing weight (W_{LA}) given was calculated by subtracting the weight of the fuel needed to take off, 100 Newtons, from the maximum take-off weight. This value of 5900 Newtons for W_{LA} was also determined to be the weight of the aircraft at cruise due to the weight of the fuel used for flight remaining essentially constant.

Center-of-Gravity Range

In Table 7-1, the center-of-gravity at take-off was shown to be 6.15 meters back from the nose of the aircraft. The center-of-gravity for a variety of configurations was calculated as shown in Table 7-3. From these configurations, center-of-gravity travel diagrams were made as shown in Figure 7-1 and Figure 7-2.

In Table 7-3, the post-flight configuration weights were determined by subtracting the weight of the take-off and landing (TOL) fuel from the weight of the aircraft for pre-flight considerations. It was also determined that for the ground configurations of C, D, E, and F, the aircraft would remain stable on the ground due to landing gear located at 3.00 meters, 12.50 meters, and 14.50 meters aft of the nose.

Examining the flight configurations of A and B, it was determined that the center-of-gravity did not change appreciably during take-off and landing (a maximum of two centimeters). This was due to the symmetrical placement of TOL engines and fuel tanks and strategic burning of TOL fuel.

Comparing the center-of-gravity travel ranges obtained to the acceptable Stability and Control ranges, it was noted that, for configuration A, the Weights and Balances center-of-gravity range of 6.11 - 6.15 meters aft fell within the Stability and Control range of 6.10 - 6.98 meters aft. Similarly, it was also noted that the configuration B range of 6.57 - 6.59 meters aft fell within the acceptable range of 6.21 - 6.98 meters aft from Stability and Control.

Weight History

In arriving at the final design, several other designs were considered and subsequently dismissed. Originally, a joined-wing design was not considered. A conventional aircraft was analyzed, and it was found that the component weights, when summed, resulted in a gross weight much higher than the initial estimated gross weight decided upon. As more analysis was performed, the magnitude of the initial estimated gross weight increased due to the desire for the aircraft to meet certain specifications. It was finally decided that a joined-wing configuration would best serve the purpose.

The joined-wing was decided upon just prior to the midterm report. For that report, a gross weight of 6061 Newtons was calculated. This value was 61 Newtons greater in magnitude than the initial estimated gross weight of 6000 Newtons. After the

midterm report, a wing weight estimation equation for joined-wing aircraft was developed for the class by teaching assistant John Henderson. Upon using this equation, a wing weight savings of approximately 600 Newtons was noted. This excess weight was divided and used for other components of the aircraft. The final design was essentially reached.

Comparing the values for initial sizing and final design in Table 7-2, a large discrepancy was noted. This was due to the increasing magnitude of the gross weight as the final design was developed. In the initial sizing data, the maximum fuel fraction was greater than that for the final design. This difference was due to an initial low estimate for structural weight and overall aircraft weight. Also, the useful load fraction, which is actually a function of fuel and payload weights, was initially estimated to be much higher than the final design result. This was another example of underestimation of structural and overall weights.

Conclusion

In designing this aircraft, it was concluded that a lighter-weight airplane could be developed in the future. With advances in aircraft structural materials, especially composites, an aircraft of the future made almost entirely of composite materials would be practically commonplace. A greater weight savings, for large structural parts in particular, would result. Using this assumption, some of the component weights for this report were estimated to be lower than they might actually be at present. However, since present-day equations [4,5] were used to arrive at the weights for nearly all of the structural components, these weights represent high estimates when considering the future.

In conclusion, since the gross weight of this aircraft could be lower, performance characteristics in the future would improve accordingly. These results would also affect other aspects of the aircraft, resulting in a more efficient design in the future.

References

1 Roskam, Dr. J., Airplane Design: Part V - Component Weight Estimation. Copyrighted by Roskam Aviation and Engineering Corporation, 1985.

2 Lecture Material, AAE 241. John Henderson, 1988.

3 Nicolai, Leland N., Fundamentals of Aircraft Design. METS, Inc. 1975.

4 Roskam, Dr. J., Airplane Design: Part V - Component Weight Estimation. Copyrighted by Roskam Aviation and Engineering Corporation, 1985.

5 Lecture Material, AAE 241. John Henderson, 1988.

TABLE 7-2
Summarized Weight Breakdown

	Initial	Final
Operational Empty Weight (OEW)	1604N	3936N
Payload Weight (W_P)	1200N	1200N
Maximum Zero Fuel Weight (MZFW)	2804N	5136N
Fuel Weight (W_F)	690N	864N
Maximum Take-off Weight (W_{TO})	3494N	6000N
Maximum Landing Weight (W_{LA})	---	5900N
Useful Load Fraction (1 - OEW/W_{TO})	0.520	0.344
Maximum Fuel Fraction (W_F/W_{TO})	0.198	0.144

In the above table, N = Newton

TABLE 7-3
Center-of-Gravity

Configuration	Weight (N)	WxMA (N-m)	CG Location (m aft of nose)
A : Two Pilots - Maximum Fuel			
(1) Pre-flight	6000	36,878	6.15
(2) Cruise	5900	36,168	6.13
(3) Post-flight	5786	35,360	6.11
B : One Pilot - Maximum Fuel			
(1) Pre-flight	5400	35,606	6.59
(2) Cruise	5300	34,896	6.58
(3) Post-flight	5186	34,088	6.57
C : Zero Pilots - Maximum Fuel (*)			
(1) Pre-flight	4800	34,934	7.28
(2) Post-flight	4586	33,416	7.29
D : Two Pilots - Zero Fuel (*)	5136	32,682	6.36
E : One Pilot - Zero Fuel (*)	4536	31,410	6.92
F : Zero Pilots - Zero Fuel (*)	3936	30,738	7.81

* Aircraft would not be flying in these configurations.

In the above table,
W = weight
MA = moment arm
CG = center-of-gravity
N = Newton
m = meter

FIGURE 7-1

Center-of-Gravity Travel - Two Pilots

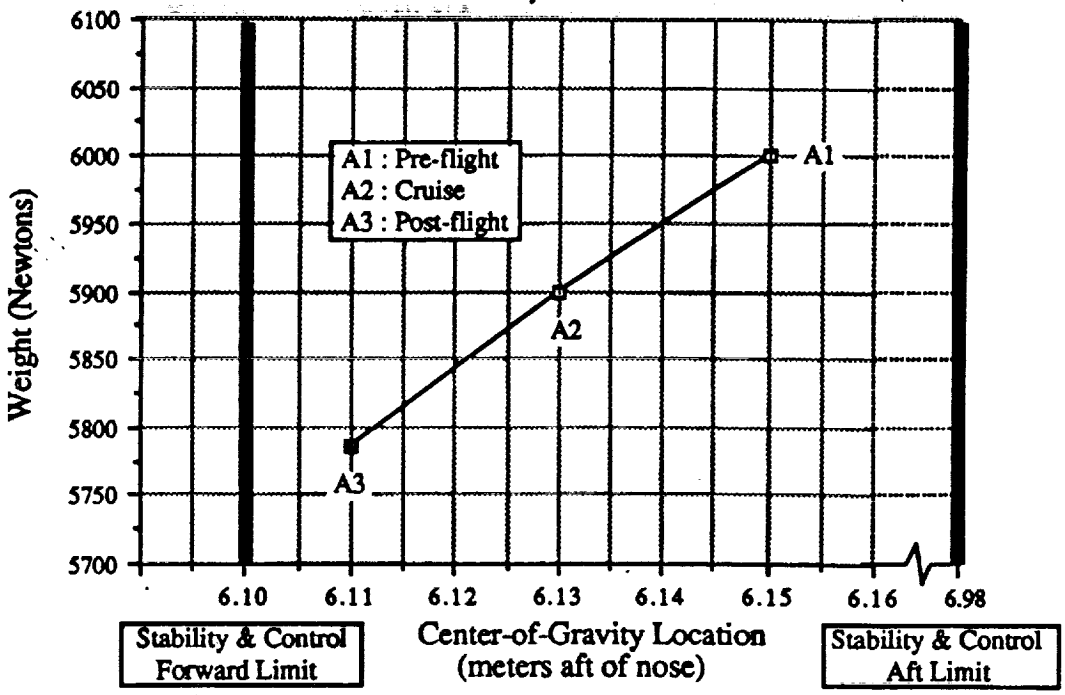

FIGURE 7-2

Center-of-Gravity Travel - One Pilot

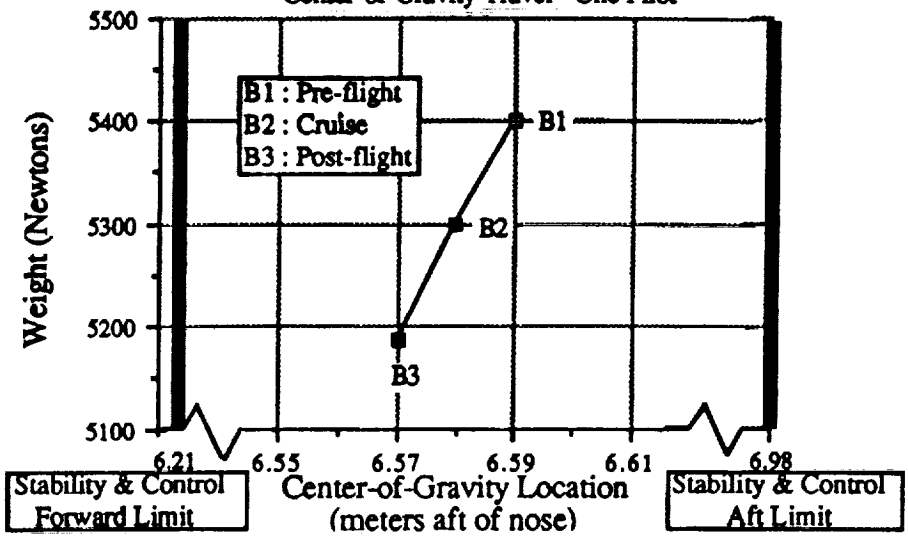

AUXILIARY SECTIONS

Fig. 5-9

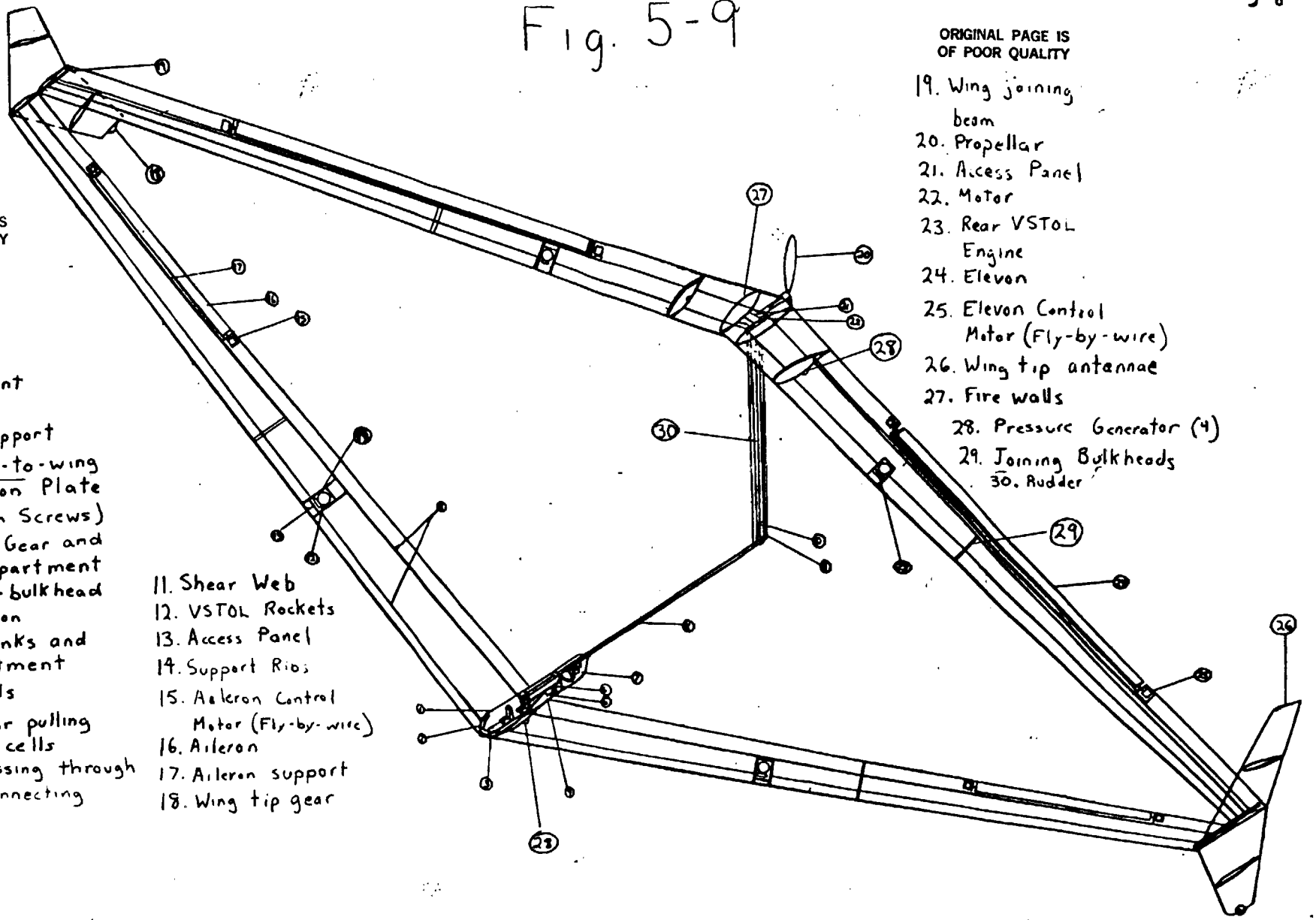

1. Cockpit
2. Instrument Antennae
3. Floor Support
4. Fuselage-to-wing Connection Plate (Titanium Screws)
5. Landing Gear and LG compartment
6. Gear-to-bulkhead Connection
7. Fuel Tanks and compartment
8. Fuel Cells
9. Hatch for pulling out fuel cells
10. Spar passing through boom connecting tail
11. Shear Web
12. VSTOL Rockets
13. Access Panel
14. Support Ribs
15. Aileron Control Motor (Fly-by-wire)
16. Aileron
17. Aileron support
18. Wing tip gear
19. Wing joining beam
20. Propellar
21. Access Panel
22. Motor
23. Rear VSTOL Engine
24. Elevon
25. Elevon Control Motor (Fly-by-wire)
26. Wing tip antennae
27. Fire walls
28. Pressure Generator (4)
29. Joining Bulkheads
30. Rudder

FOLDOUT FRAME

FOLDOUT FRAME

MAINTENANCE AND SERVICING

Scott Hildreth

Fuel Cells.

The fuel cells will be manufactured in a cylindrical fashion so that they can be inserted as a single unit in to the rear of the aircraft. This allows for easy access to perform routine maintenance and makes the most efficient use of space in the aircraft.

The fuel cells will require servicing approximately every 7 missions, although inspections and a thorough system check will be performed before and after every mission.

Fuel/Reclamation System.

The fuel tanks will require little maintenance, except checking for possible leaks in the tanks and couplings. The water reclamation tank will be fitted with heating coils so that when the aircraft returns the water can be thawed and extracted for later decomposition and reuse.

VTOL Rockets.

The rockets can be accessed and removed for servicing from the underside of the wings, or an access panel is provided on the top of each wing for fueling and regular inspections.

PACKAGING FOR TRANSPORT FROM EARTH TO SPACESTATION

Ron Golembiewski

The mars plane has been subjected to a restriction, when disassembled, of a 21 m by 6 m cylinder provided by the space shuttle bay. To meet this requirement, the 70 m wing span will be disassembled into eight sections. Since the wings are tapered, (3.28 m width at fuselage) the ends of the wings will be turned and then slid into the larger portion of the wing. Resulting in a approximate length of 18 m.

The wings will then be placed next to the 15 m fuselage along with the control mechanisms. The tail, which is 10 m, will be disassembled and will also be placed along side the wings and fuselage. This is the standard packaging procedure whether it be from earth to space shuttle or space shuttle to the martian surface.

Graphics needed

Transportation to Mars

Bruce Zimmerman

Due to the size of the Mars Plane, a means of storing the craft in a relatively small and convenient space during transportation to Mars is mandatory.

The large wings will be separated into 8 sections with the end of the wings being turned and slid into the larger portions. These wings will then be placed alongside the fuselage. Elevon mechanisms, tail and wingtip sections are also placed alongside the fuselage. All instrumentation affected by the part separations will be stored in the fuselage. Finally, packing foam on the inside of the fuselage would be desirable to protect the delicate avionics.

A storage area of at least 17.5 meters in length 4 meters wide would be required for the aircraft. Given the spacecraft group dimensions of the storage cylinder (21 meters long, 6 meters in diameter), the aircraft should fit nicely for the journey.

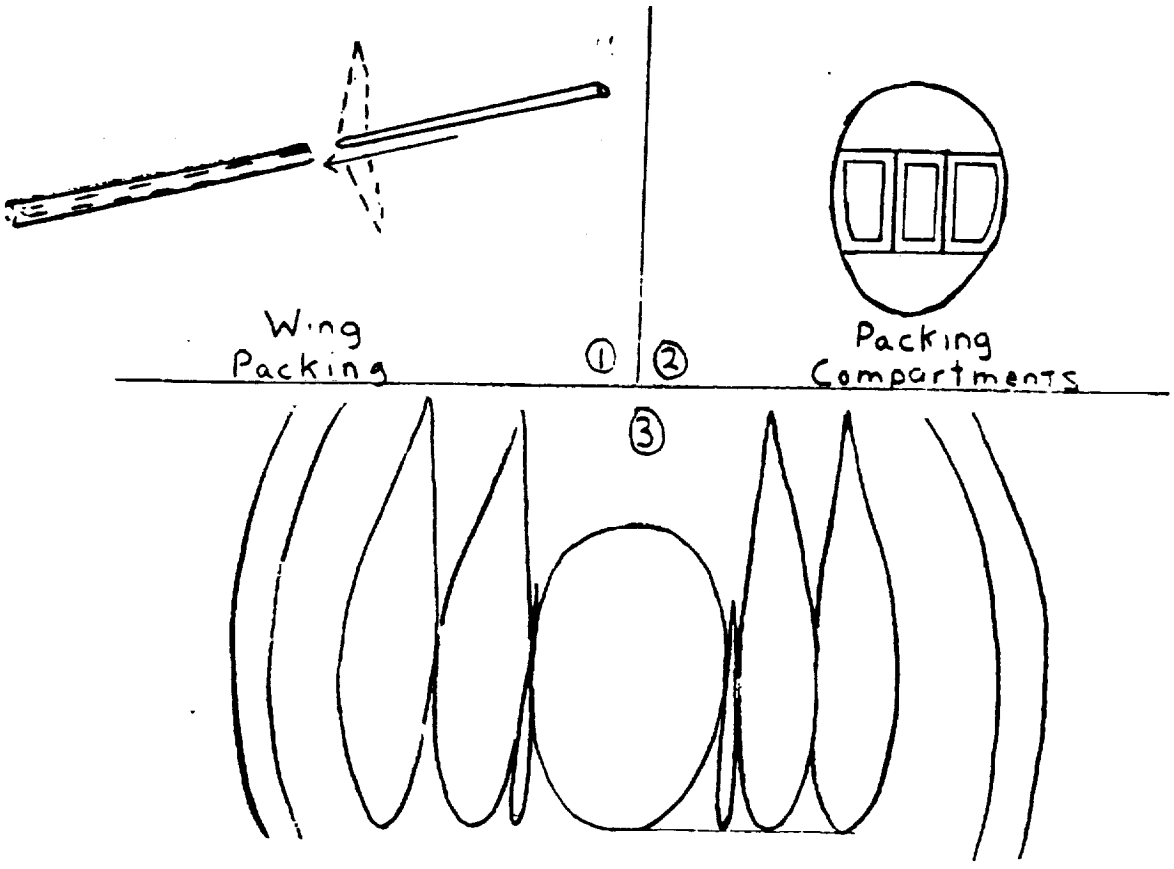

Rescue Scenario

Ron Cihak

At cruise of 70 m/s the craft would have a round trip range of 2050 km using one VTOL fuel cycle and 225 kg of fuel for the main propulsion system. This would allow a pilot an operational radius of 1025 km. If 600 N or 162 kg payload where removed from the rescue craft, an additional 87 kg of fuel and oxidizer could be placed in containers in the cargo area.

Assuming the containers and pumps weigh no more than 25 kg this would leave 50 kg of fuel. The rescue craft would then have an operational radius of about 1250 km and be capable of rescue operations up to the unaugmented range. Upon location of the marooned personnel the pilot could vertically land the plane, put the extra fuel into the main tanks and dump the containers. The rescue could then be placed in the passenger/cargo area and brought back to base.

Until help arrived the downed pilot cold be maintained by the delivery of a ballistic care package (BCP), which would contain oxygen and life support. The BCP could home in on ab emergency locater device.

The possibility of ejection has been ruled out due to the system mass of a large enough parachute to supply a sufficiently low terminal velocity from 15 km. Survivability of this type of escape is questionable at best.

Assembly on Mars

Bruce Zimmerman

Given the difficult conditions that the Mars pilot will face on the planet, it would be beneficial if the aircraft was as easy to assemble as possible. However, due to the height of the aircraft, a pulley or crane system must be considered available.

The fuselage/boom structure will arrive in one piece, requiring only placement of avionics and other instrumentation. For the first assembly, the eight wing sections should be joined at the main wing ribs using adhesives (glue joints have been developed that are as strong as the graphite-epoxy material itself, See figure). Bolts are not as effective with graphite-epoxy materials.[1] During this process, the elevons are to be aligned and locked in position. Second, join the front and rear wing sections by slipping the wingtips over the joining rod. Add winglets by tipping wings in the appropriate direction and slipping winglets into notched section of the joining rod. Next, add tail by sliding spar through boom and use adhesive along top of boom. Using available lifting devices, tilt wing to appropriate position and attach fuselage/boom/tail assembly to wings.

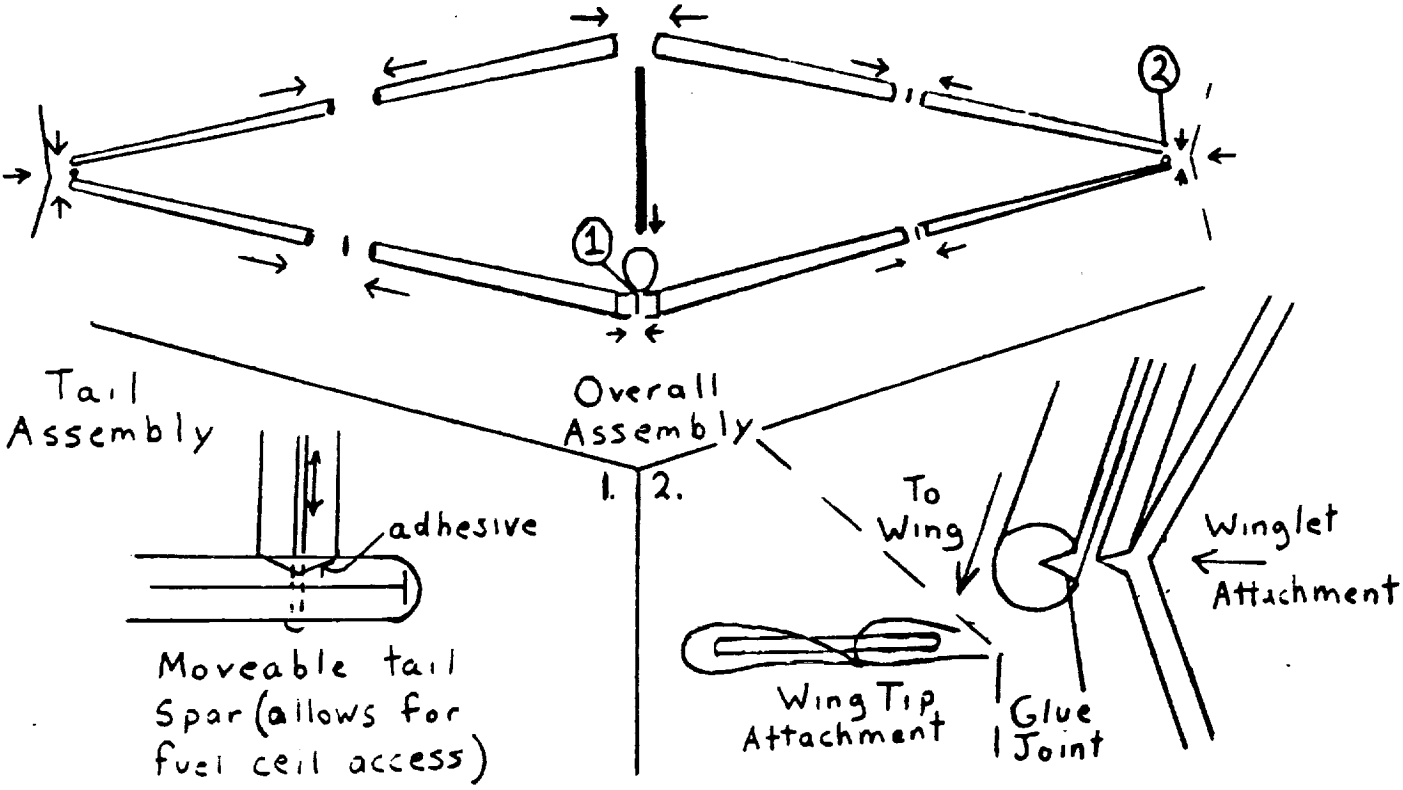

MARTIAN ATMOSPHERE

PAUL BECKWITH

The physical and chemical properties of the martian atmosphere had to be known before the plane could be designed. The temperature in the lower atmosphere varies from 225 degrees Kelvin at ground level to 130 degrees Kelvin at 100 kilometers (km). The temperature in the upper atmosphere varies from 225 degrees Kelvin at 100 km to 400 degrees Kelvin at 900 km. The pressure in the lower atmosphere varies 5.9 mb at ground level to .000174 at 100km. Densities very between 0.0143 kg/m*m close to the ground and 0.0000000706 at 100km. The composition of the lower atmosphere is made up of mostly carbon dioxide (95.3 %). Nitrogen is the next abundant material (2.7%). There is also a good amount of argon (1.6%). Other materials found in small amounts in the martian atmosphere are oxygen, carbon monoxide, water vapor, neon, krypton and xenon.

REFERENCE

Space and Planetary Environment Criteria Guidelines for Use in Space Vehicle Development, Robert E. Smith and George S. West, 1982, Revised (Volume).

COST ANALYSIS

Terri Pulsford

TABLE 9-1
Summary of Costs

Component	DDT&E ($ million)	FHA ($ million)	TOTAL ($ million)
Structures	47.9	14.8	62.7
Attitude Control & Determination	7.0	1.5	8.5
Communications and Data Handling	115.8	27.7	143.4
Propulsion	0.6	0.0	0.6
Subtotal	**171.3**	**44.0**	**215.3**
System Test Hardware	81.9	0.0	81.9
System Test Ops	26.1	0.0	26.1
Software	0.0	0.0	0.0
GSE	23.5	0.0	23.5
SE & I	34.6	7.9	42.5
Program Management	21.2	4.8	26.0
Subtotal	**358.6**	**56.8**	**415.4**
Contingency	71.7	11.4	83.1
Fee	43.0	6.8	49.8
Program Support	9.5	1.5	11.0
TOTAL	**482.8**	**76.4**	**559.2**

Total cost of one unit = $559.2 million

The above costing program was provided by Michael Lembeck. When developing this cost analysis, an unmanned spacecraft was assumed. Also, the total cost above was determined using the weights for aluminum structural components. Noting that pre-fabricated carbon-reinforced composites presently cost approximately 100 times as much as aluminum alloys, [1] it was determined that the structural cost of this aircraft would increase considerably. This would result in a total cost increase of approximately $5 billion, making the total cost $5.6 billion, approximately.

DDT&E above refers to costs incurred during design, testing, and engineering of the aircraft. FHA refers to the costs of production and management. It was noted that the latter costs were considerably less than those for design and testing.

Since the above cost analysis was done assuming a very different aircraft than the actual design, this cost analysis was more of an exercise in introducing the concept of costs to the design groups. Also, since rough estimates were used to determine the added costs due to graphite-epoxy, the total cost of $5.6 billion is a rough approximation at best. It was discovered that the cost analysis of the actual aircraft would be much more detailed when the appropriate complexity factors are considered.

Reference

1 Ashby, M. F. and D. R. H. Jones, Engineering Materials - An Introduction to Their Properties and Applications. International Series on Materials Science and Technology, Vol. 34; Pergamon Press, Oxford, 1980.

Spacecraft Interface

William H. Woodruff

The spacecraft group imposed very few restrictions on the aircraft. They stipulated that no part of the package could be longer than 18.5 meters. In addition, the pieces must be packed as flat as possible. To meet the criteria, the wingtips and the fin must be removed. The two wings must be divided into a total of eight sections. The four smaller parts of the wings can then be fit into the larger sections. According to the structural group, there is no problem in doing this.

Conclusion

William H. Woodruff

It is the opinion of the design group that flight on Mars is a viable method to survey the planet surface. But there are several areas that still require research. There needs to be a way for the aircraft to crash land on the planet surface and still provide the pilot with a reasonable chance of survival. As outlined in the aerodynamics section, the overall size of the aircraft needs to be reduced. At the time of this report, a fuel cell was found that was recently developed by General Dynamics which would have allowed the 35 meter span design briefly discussed in the aerodynamics report to fly. It is clear from this information that several more years of technology will make the mars aircraft a reality.

No. 6 KRS

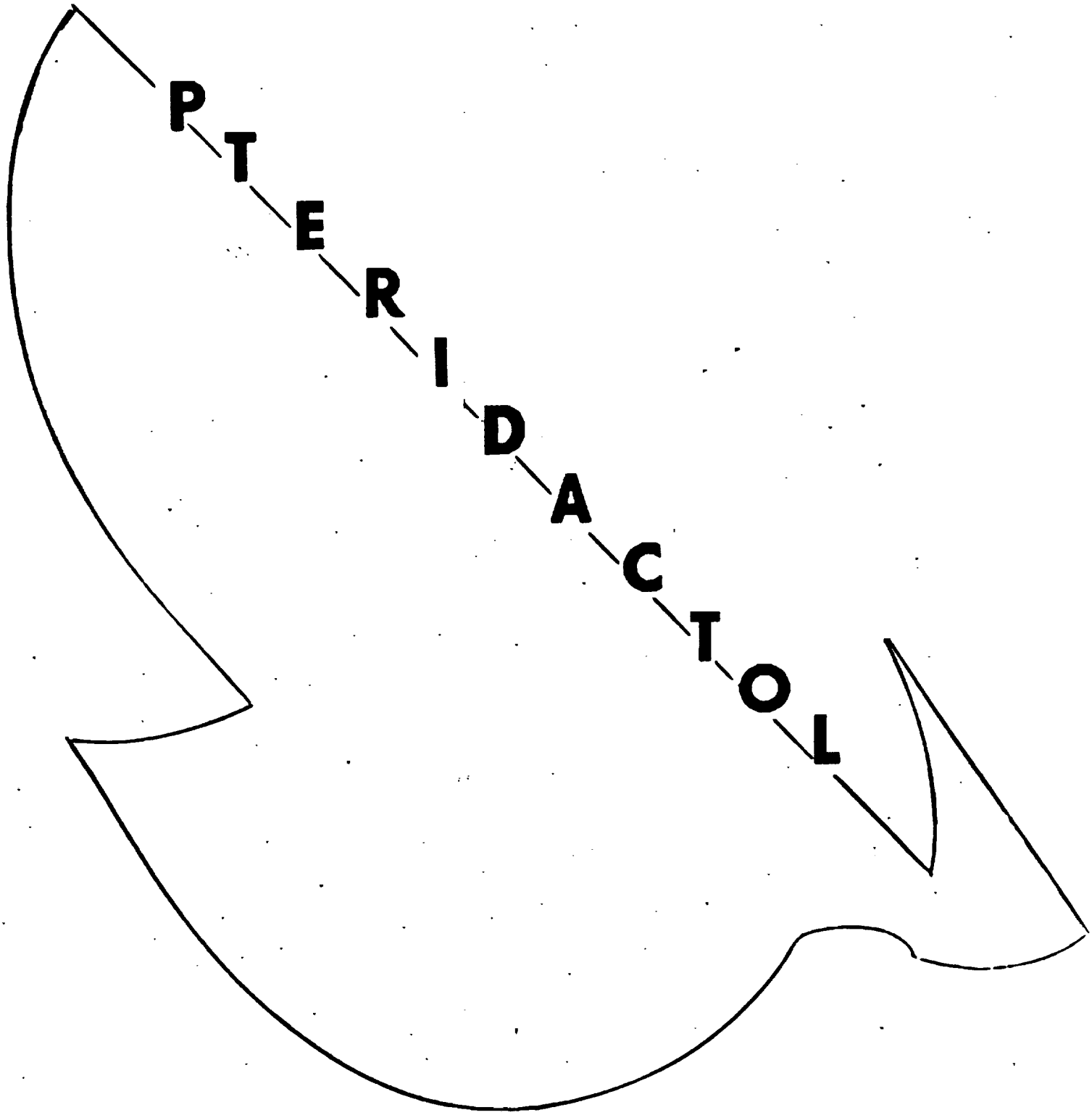

PROJECT PTERIDACTOL

C-7

<100
KRS

PROJECT PTERIDACTOL

DESIGN TEAM

AERODYNAMICS.....DON STROBERG
PERFORMANCE.....SONJA SCHILLMOELLER
POWER AND PROPULSION.....JOHN BLACKWOOD
STABILITY AND CONTROL.....JIM MOCARSKI
STRUCTURES.....GREG CIMMARUSTI
SURFACE OPERATIONS.....DAVID CLOUGHLEY
WEIGHTS.....BRIAN FUDACZ

TABLE X.1

TECHNICAL AREA	RESPONSIBILITY
Aerodynamics	-wing design -cruise configuration -drag analysis -wing lift and pitching moment distribution
performance	-cruise characteristics -climb characteristics -descent characteristics -missed approach
power and propulsion	-propulsion system(s) -propeller analysis -fuel system selection -power system(s)
stability and control	-sizing of horizontal and vertical tails -wing location -neutral point -acceptable c.g. range
structures	-wing loading -materials selection -structural layout
surface operations	-take off and landing scenarios and systems
weights	-weight breakdown -c.g. ranges

PROJECT OVERVIEW

Mars has always been of interest to scientists. Originally interest centered upon the possibility of life existing on Mars and now it focuses on the possibility of colonization. The Viking projects answered many questions about the red planet but it also raised many more. The project PTERIDACTOL is intended to give a means to answer the unanswered questions left by Viking. PTERIDACTOL will make remote areas of Mars accessible for scientific investigation.

The underlying design philosophy of the PTERIDACTOL design team was: "Simple is Better". The design took a common aft tail configuration. Simple designs were not only easier to work with but were also generally found to be lighter. For example, the Sail Wing selected has a relatively simple design and has the characteristics of being lightweight and having good lift to drag characteristics. The basic design objectives were to minimize weight and drag and to maximize lift. While the preliminary design used a square planform for simplicity it became necessary to implement more advanced technologies to achieve the desired characteristics.

The PTERIDACTOL design team was divided into 7 design areas: aerodynamics, power and propulsion, performance, stability and control, surface operations, structures, and weights. Each major technical area set goals and had requirements to meet. Each also had a set of problems to overcome. Aerodynamics set an underlying goal to keep the plane light while maintaining a high lift to drag ratio. However, the technologies selected for the PTERIDACTOL are untested in the dimensions of the marsplane and more importantly they are untested on Mars. Power and Propulsion found it

necessary to have high system efficiency; the system being the propeller, gear box, engine, and fuel cells. Performance needed to minimize excess power during climb and cruise. This enabled the team to reduce the weight of the fuel needed for missions. Stability and Control took the philosophy that since no plane has ever flown on Mars, a margin of safety should be incorporated into the design to account for unpredicted difficulties due to the Mars atmosphere. A standard configuration was chosen for the tails, sticking with the "simple is better" motto, however adjustable camber (similar in principle to that used by the Wright Brothers) was found to give sufficient lateral stability and control without ailerons. Structures needed materials with two properties: strength and light weight. Composite materials were the obvious choice. It was necessary also to incorporate means to enable packaging in the design. Surface Operations had to deal with the problem of a large propeller and a lot of power required to take off. Take off was accomplished through the design of a rocket cart. A glider landing was found to be the best alternative so that long landing gear was not needed. The goal weight for the **Pteridactol** was set and reached at 4800 N. Reductions in weight were found in avionics, flight control systems and in the electrical systems.

A few assumptions were necessary to make the designing of a marsplane feasible. The first was that there would be a runway in operation for use by the **Pteridactol.** Next it was assumed that there would by adequate support facilities for maintenance and assembly. These were felt to be justified because before a manned plane will be flown on Mars, technology will not only make these available but a practical safety measure. Also, for a Marsplane project to be productive these were deemed to be necessary facilities.

DESIGN DATA SUMMARY

Gross Weight: 4800.00 N

Wing Loading: 80.40 N/m^2

Maximum Fuel Weight: 750.0 N

Useful Load Fraction: .25

Maximum Take-Off Power ?

Power Loading: N/A X

Fuel Fraction: .1562

Geometry

Ref. Wing Area: 59.70 m^2
Aspect Ratio: 25.40
LE: 0.0 ?
.667
t/c: .13

Propulsion

Engine Description: Electric Motor
Number of Engines: 1
P_{0max}/Engine: 25 kW
Weight/Engine: 67.9 N
c_p at Cruise: .175
Prop. Diameter: 3.0 m
No. of Blades: 2
Blade Cruise Re: 6.41 E 04

Performance

Cruise Re: 2.93 E 05
Cruise h: 1.50 km
Cruise M: .44
Cruise V: 100.00 m/s
Take-Off Field Length: 1000.00 m
Take-Off Speed: 88.72 m/s
Landing Field Length: 944.1 m/s
Landing Speed: 92.75 m/s
Maximum Landing Weight: 4800.00 N
OEI Climb Gradient (%): N/A
2nd Segment: N/A
Missed Approach: .2033 degrees
Sea Level $(R/C)_{max}$: .3385 m/s

Aerodynamics

Airfoil: LA2566 Sailwing
High Lift System: N/A

Cruise: C_{D0}: .01706
e_0: N/A
C_L: 1.125

Take-Off: C_L: 1.5054
C_{Lmax}: 1.5846

Landing: C_L: .3625
C_{Lmax}: 1.5846

Stability and Control

Static Margin Range: 10.0 %
Acceptable C.G. Range: From Tip (2.27 m - 2.71 m)
Actual C.G. Range: From Tip (2.45 m - 2.47 m)

INITIAL SIZING DATA SUMMARY

Gross Weight: 4000 N

Wing Loading: 44.5 N/m^2

Fuel Weight: 1700 N

Useful Load Fraction: .30

Maximum Take-Off Power ?

Power Loading: 244 kW/m^2

Fuel Fraction: .425

Geometry

Ref. Wing Area: 52.6 m^2

Aspect Ratio: 24.2 Wing #1
14.34 Wing #2

Propulsion

Engine/Motor Type: Hydrazine

No. of Engines/Motors: 1

P_{omax}/engine: 22 kW

c_p at cruise: 0.14

Aerodynamics

Cruise; C_{DO}: 0.01342

e_o: N/A

C_L: 1.125

$(L/D)_{max}$: N/A

Take-Off; C_L: 1.35

C_{Lmax}: 1.5

Landing; C_L: 1.35

C_{Lmax}: 1.5

Cruise Performance

Altitude: 1.50 km

Velocity: 74.5 m/s

INBOARD PROFILE

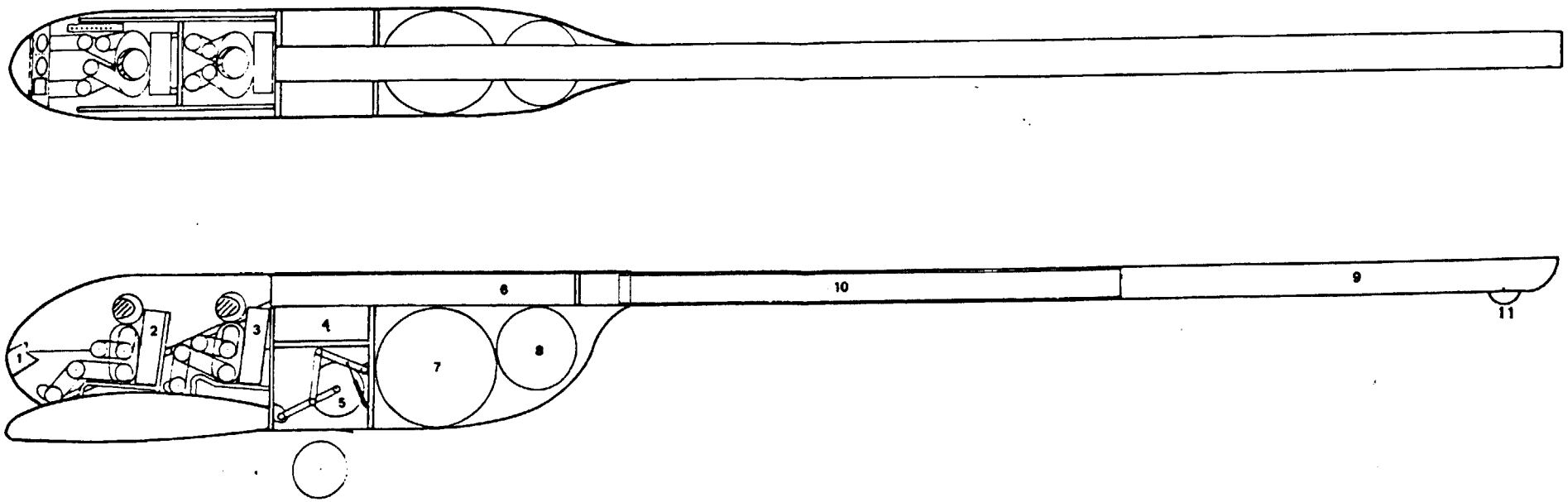

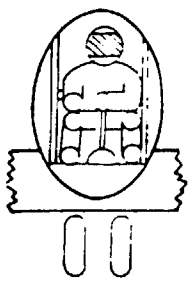

(1) INSTRUMENT PANEL
(2) PILOT
(3) PASSENGER OR PAYLOAD
(4) AVIONICS AND FLIGHT COMPUTERS
(5) LANDING GEAR (STOWED)
(6) WATER RECLAMATION TANK
(7) FUEL TANK (H_2)
(8) OXIDIZER TANK (O_2)
(9) TAIL BOOM
(10) FUEL CELLS
(11) TAIL WHEEL

FOLDOUT FRAME

SCALE 1" = 1 m

FOLDOUT FRAME

AERODYNAMICS SECTION

By

Don Stroberg

Introduction:

The idea of a reuseable flight vehicle for use on Mars is a challenging one requiring some relatively new and untested technologies. The inhospitable enviornment, such as extremely low temperatures and densities, has created some obstacles not ordinarily dealt with on Earth. The aerodynamics of the vehicle were no exception where the low density placed a premium on high lift-to-drag ratios. In keeping with the design team's philosophy of stressing simple and lightweight solutions, the aerodynamics group decided to use a conventional single wing with tail aft configuration. The wing was of a sailwing design and incorporated a mild taper. The fuselage was kept small and simple but proved adequate in the quest for uncomplicated solutions to complicated problems.

Definition of Symbols:

S = Planform area of wing
Wg = Weight of aircraft
(Wg/S) = Wing loading
b = Wingspan
c = Mean aerodynamic chord
AR = Aspect ratio
λ = Taper ratio
t/c = Sectional thickness to chord ratio
Cl = Lift coefficient
Cd = Drag coefficient
Cm = Moment coefficient about quarter chord point
Cl@ = Change in lift coefficient with respect to @
Cdmin = Minimum drag coefficient at nonzero Cl
$(Cd_o)b$ = Body drag coefficient at zero lift (parasite drag)
^Cdb = Body induced drag coefficient at nonzero @b
$(Cd_o)t$ = Tail drag coefficient at zero lift (parasite drag)
^Cdto = Coefficient of drag increment at take-off
@ = Absolute angle of attack of wing
@ol = Zero lift angle of attack of wing
@b = Angle attack of the body
@i = Incidence angle of wing
Re = Reynolds number
e = Efficiency factor
Swetb = Wetted surface area of the fuselage
l/Dmax = Fineness ratio
V = True airspeed
Vstall = Airspeed at stalling condition
h = Geometric altitude above Mars surface

Design analysis:

As mentioned earlier a sailwing design was chosen by the aerodynamics group mainly because of the fine lift to drag characteristics it provides at low Reynolds numbers while employing simple lightweight construction. The particular airfoil chosen (from Ref. 1) was the LA2566 sailwing, shown in Fig. 5.6. The airfoil was tested at Reynolds numbers of 250,000 and 500,000 with the data from the test at 250,000 shown in Fig. 1.1. Basically, the structural configuration (detailed in Ref. 2) of the sailwing consists of a leading - edge spar with ribs, made in the shape of the airfoil, attached at each end of the spar. At the ends of the ribs are strung a wire which is kept taut forming the trailing edge. Around this framework is wrapped a non-porous, non-stretchable cloth membrane, usually made from a material like dacron. Because of its light weight, simple construction, and good aerodynamic performance the LA2566 sailwing made for a good alternative to a conventional hard wing design.

The wings were designed to minimize size, weight, and complexity. The maximum wing span was principally determined by the length of the vehicle transporting it to Mars, and the fact that it was essential, for structural uniformity reasons, that each leading edge spar remain a solid piece, during transfer to Mars, rather than being broken into many pieces to be joined later. The chord length, and in essence the taper ratio selection, was a give and take compromise between using a value small enough to ensure the integrity of the airfoil test data, at the test Reynolds number, and still providing enough wing area to keep the wing loading down. A mild taper ratio was used in an attempt to develop a nearly elliptical wing loading which would decrease the moment at the root due to the aerodynamic loads at the wing tips. An added benefit to a more elliptical wing loading is the increase in the efficiency factor and therefore a decrease in the three dimensional induced drag. It was also felt that not enough data was available about the airfoil section (more was unattainable because of limited distribution) to warrant the use of wing twist or winglets. The cruise mach number was low enough to eliminate the need for wing sweep. The center portions of a sailwing deform in such a way to in effect increase the camber of the airfoil section and provide some of the aerodynamic characteristics of its design. However, ribs were added along the span to maintain some of the airfoil shape as well as to support the dacron membrane. Flaps and ailerons are impractical because of the use of a sailwing but the trailing edge cable tension can be adjusted to provide rolling control. The performance of the airfoil is felt to be adequate enough to overcome the lack of high lift devices. Airfoil and wing data are in Table 1.1 and Fig. 1.1.

With the fuselage the primary design parameter was to keep the size down reducing the parasite drag that comes with the greater size. One important consideration in the fuselage design was that it must provide enough room for everything that will go into it especially since the wing construction severely limits carrying anything within them. Another consideration into the design of the fuselage was the tail since trimming the aircraft is heavily dependent on the location of the tail with respect to the wings, the center of gravity, and the neutral point of the aircraft. The airfoil section chosen for the tail was the symmetric NACA 0012-64 (taken from Ref. 5) which provides adequate lifting and parasite drag characteristics. The tail design is discussed in more detail in the stability and control section of this report. Moderate changes in cross section diameter and shape of the fuselage were also employed to reduce the form drag of the body. The high wing loading was the main influence on the determination of the cruising speed by the fact that it drove the stalling speed so high. The particular speed chosen was a good compromise between strutural limits, power requirements, and the stall speed. Data for the fuselage and aircraft configuration can be found in Tables 1.2, 1.3 and Fig. 1.2.

The determination of the drag polar for the entire vehicle was a difficult process due to the irregular drag polar of the airfoil section. The drag polar for the entire vehicle is given in Table 1.3 under the aircraft data section. The C_d term, in the drag polar equation, is read off of Fig. 1.1 as the difference between the drag coefficient at the particular lift coefficient in question and the minimum drag coefficient not the drag coefficient at zero lift. These values comprise the 2-D induced drag contributions and were tabulated numerically and given to the performance group. This was determined to be more accurate than trying to fit an equation to the curve and is not as cumbersome as it appears due to the use of a computer program by the performance group. Reynolds number calculations were made at -20° C. Despite colder temperatures found on Mars, the data these calculations were made from were deemed acceptable. A complete breakdown of the drag coefficient at cruise is given in Table 1.4.

The Schrenk approximation method (from Ref. 4) was used to determine the lift distribution along the span of the wing. The ensuing results, at the cruise condition, were turned over to the structures group along with the pitching moment data about the quarter chord point along the span of the wing. The lift distribution was put into graphical form and can be seen in Fig. 5.1. The lift curve slope was calculated using equations found in reference 6 as were values for the trimmed lift coefficient. The results of these calculations can be seen in Fig. 1.2.

Summary:

Throughout this project one thing became clear from an aerodynamic standpoint; the smaller the aircraft was the better. Every increased dimension greatly increased the weight and complexity of the aircraft yielding a viscious circle. The main obstical to overcome with this philosophy is the prohibitively high wing loadings and subsequent high stall velocities associated with a small wing design. The sailwing configuration has proved to be quite successful in theory so far but some questions still prevail. One is whether the fabric will be able to hold up to the cold harsh enviornment of Mars. Another question is if a sailwing can perform up to its aerodynamic characteristics at such huge dimensions. At this point only testing will tell.

References:

[1] Liebeck, R.H., "Design of Subsonic Airfoils for High Lift," Journal of Aircraft, Vol. 15, September 1978, pp.547-561.

[2] Maughmer, M.D., "A Comparison of The Aerodynamic Characteristics of Eight Sailwing Airfoil Sections," The Science and Technology of Low Speed and Motorless Flight. Pt. 1, March 1979, pp.155-176.

[3] McCormick, B.W., Aerodynamics, Aeronautics, and Flight Mechanics. New York, 1979.

[4] Sivier, K.R., AAE 316 Applied Aerodynamics. Champaign, Illinois, August 1987.

[5] Abbott, I.H., and Albert E. Von Doenhoff. Theory of Wing Sections. New York: Dover, 1959.

[6] Sivier, K.R., AAE 319 Flight Mechanics. Champaign, Illinois, January 1988.

$S = 59.70\ m^2$	$@o1 = -2.0^\circ$
$b = 38.92\ m$	$@i = 7.97^\circ$
$c = 1.524\ m$	$t/c = 13\%$
$AR = 25.40$	$t_{MAX} = 0.1981\ m$
$\lambda = 0.667$	$e = 0.90$
$Clmax = 1.5$	$Re = 2.93 * 10^6$, $h = 1.5$ km
$Cl@ = 6.139$ (1/rad)	$Re = 3.21 * 10^6$, $h = 0$
$Cd = 0.01125 + 0.01392Cl^2 + \hat{}Cd$	$(Wg/S) = 80.40\ N/m^2$

Table 1.1 Wing design data.

$Swetb = 25.33\ m^2$

$1/Dmax = 6.48$

$(Cd_o)b = 0.00194$

$\hat{}Cdb = 0.245@b^2 + 1.532@b^3$

$@b = 0.00$ (at cruise)

Table 1.2 Fuselage design data.

Wg = 4800 N

V = 100 m/s (at cruise and h = 1.5km)

Vstall = 80.65 m/s (at h = 0)

Clmax = 1.585

Cl = 1.125 (at cruise)

Cl@ = 6.527 (1/rad)

^Cdto = 0.0122

$Cd = 0.01519 + 0.01392Cl^{e} + \hat{}Cd + \hat{}Cdb + \hat{}Cdto$

Table 1.3 Aircraft configuration data.

Cd terms	values
Cdmin	0.011250
^Cd	0.001870
$(Cd_o)b$	0.001940
$(Cd_o)t$	0.0020
^Cdb	0.0
$0.01392Cl^{e}$	0.015880
^Cdto	0.0
Cd	0.032940

Table 1.4 Coefficient of drag breakdown at design cruise.

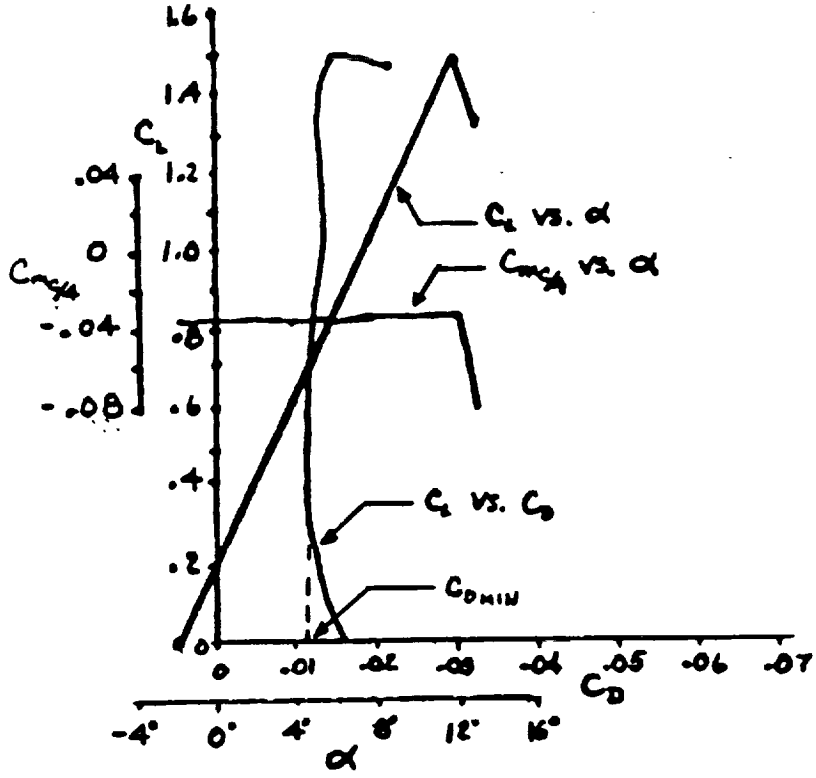

Fig. 1.1 Experimental data for airfoil LA2566

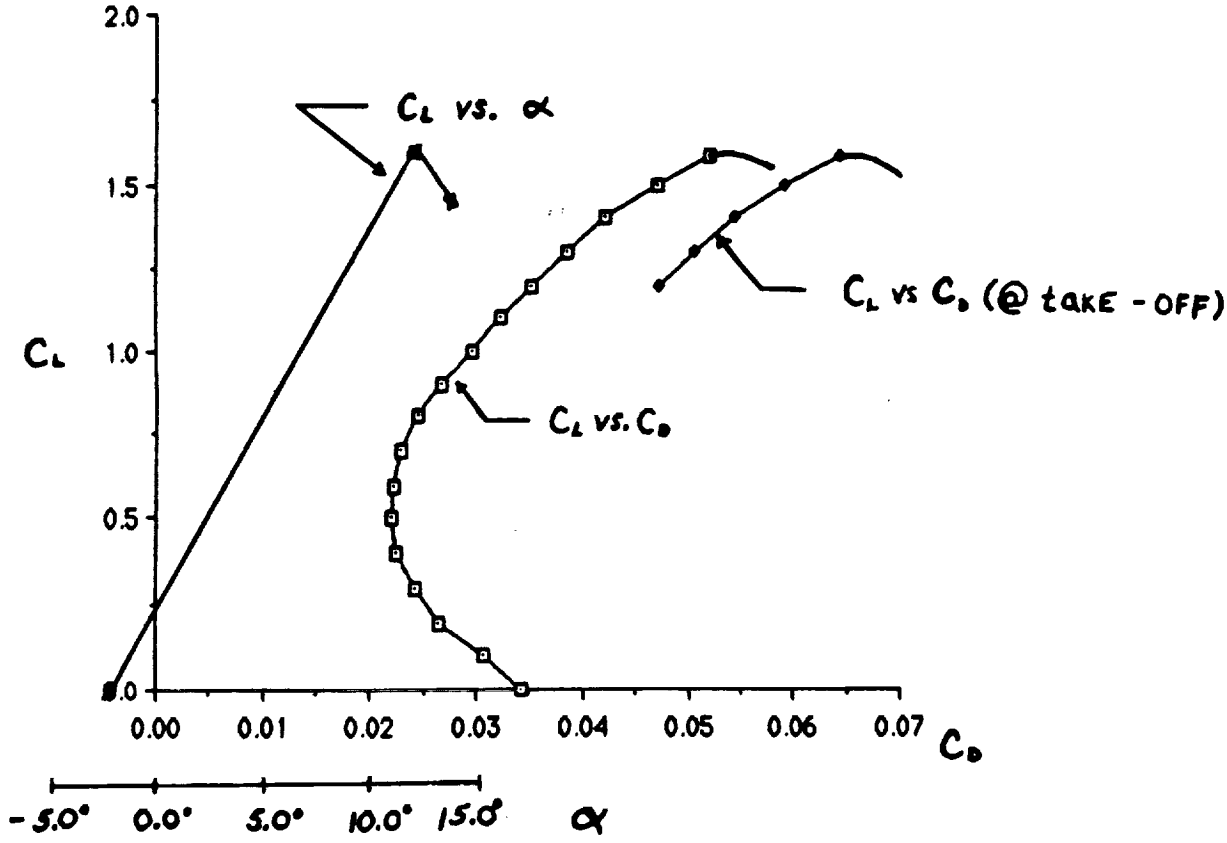

Fig. 1.2 Cl vs. @ and drag polar at trim conditon for entire aircraft.

Performance

by

Sonja Schillmoeller

INTRODUCTION

Three major areas of aircraft performance were analyzed. These areas consisted of cruise, climb, and descent. Also presented are missed approach and the level flight envelope. Aerodynamic and propulsive parameters that will be used frequently in later calculations are presented in Table 2.1 . Application of Equation 2.1 yields, at a cruising altitude of 1.50 kilometers, a stalling velocity of 86.80 meters per second. The Pteridactol was chosen to cruise at a velocity 100.00 meters per second. As was chosen in the preliminary report, the power available for cruise, climb, and descent would be independent of the aircraft's true airspeed. Also determined by the power and propulsion section was the decision to retain all fuel used during the mission. Therefore, the fuel flow rate and change in total weight of the Pteridactol will both obtain a value of zero. Also, since only one engine is being employed, a one engine inoperative performance analysis cannot be performed. Many decisions, which will be mentioned at their appropriate times, were induced due to the fact that at cruise the angle of attack of the aircraft's body will be considered. In the preliminary report, this angle of attack was assumed to be zero. This consideration caused a substantial change in the calculation of the drag coefficient which, in turn, affected the power required value that was obtained.

CLIMB

Just mentioned was the fact that at cruise, the aircraft's angle of attack causes many complications. One of them was the substantial increase in the power needed from the propulsion system during the cruising portion of the mission. This results in an increased weight of the fuel and therefore an increase in the total weight of the Pteridactol. To minimize this effect, the power and propulsion section requested

that the amount of time for the climb and descent be increased therefore resulting in less time for the cruise segment of the mission. To maximize the climbing time, rate-of-climb values must be minimized as can be seen from Equation 2.3 . This, in turn, can be accomplished by minimizing excess power. Initially, calculations were performed with a constant power available of 22.00 kilowatts. With this power, the time to climb amounted to approximately half an hour. After giving this piece of information to the power and propulsion section, it was determined that the fuel weight would increase tremendously so as to exceed the desired aircraft weight of 4800.00 Newtons. Therefore, the decision to climb at a constant power available of 19.00 kilowatts was reached. When maximum time to climb was computed, velocities which were in the range of five to seven meters per second above the stalling velocity at each incremental altitude were used. Referring to Graph 2.1, these velocities gave minimum excess powers which were very close in magnitude to minimum excess powers at the stalling velocities. The time to climb to an altitude of 1.50 kilometers was 104.10 minutes and covered a range of 568.16 kilometers. Results of this climb are summarized in Table 2.2 .

CRUISE

Once at the cruise velocity of 100.00 meters per second, The Pteridactol will travel 2087.46 kilometers and this trip will last 347.91 minutes or 5.80 hours. This calculation was based on a total flight time corresponding to eight hours. Returning to Graph 2.1, the maximum velocity at 1.50 kilometers is observed to be approximately 111.90 meters per second.

DESCENT

As mentioned earlier, it was desired that the Pteridactol spend as much time as possible cruising and descending. Again this corresponded to a minimum excess power ; in this case excess power corresponds to power required minus power available. This conclusion is obvious after observing Equations 2.4 and 2.5 . A constant power available of 13.50 kilowatts was decided on because anything lower, with a corresponding constant power available during climb of 19.00 kilowatts, would cause the aircraft to obtain a weight greater than 4800.00 Newtons. Velocities for

minimum excess power were very close to the cruising velocity of 100.00 meters per second for the altitudes in the range of 600.00 to 1500.00 kilometers. For altitudes from 0.00 to 600.00 meters, the same concept used in the climb analysis was employed; the velocity at which the excess power was computed was in the range of five to seven meters per second above the stalling velocity. With this in mind, the descent will last 27.99 minutes and will cover a range of 160.37 kilometers. The descent will begin at the cruising altitude of 1.50 kilometers and end at the approach altitude of 15.00 meters. Results of the descent are shown in Table 2.3 . doesn't agree with Fig 2.3. I think it does

MISSED APPROACH

From Graph 2.3, one can see that the excess power at the approach speed of 92.75 meters per second will be 1.68 kilowatts. The rate-of-climb at this airspeed will be .3292 meters per second and the corresponding climb angle for this missed approach will be .2033 degrees.

LEVEL FLIGHT ENVELOPE

The level flight envelope is depicted in Graph 2.4 . Observe that a maximum velocity of 112.00 meters per second occurs at an altitude of 900.00 meters. Also note that the altiude where the maximum and minimum velocity are equal, the absolute ceiling, is 2.90 kilometers. The value of the velocity at this point is 90.98 meters per second. The maximum velocity at sea level was 111.75 meters per second. A major point, which should be noted, is that the minimum velocity was indeed the stalling velocity at all altitudes.

CONCLUSION

Because of consideration of the Pteridactol's angle of attack, many complications arose. Coefficients of drag changed therefore altering power required calculations. Had this effect been taken into account in the earlier stages of the design process, perhaps the constant fear of the aircraft weight increasing due to the need for more fuel would never have had to been encountered.

Table 2.1

Aerodynamic and Propulsive Parameters

Varaiable	Definition	Value
WG	Gross Take-Off Weight	4800.00 Newtons
WGS	Wing Loading	71.64 N/m^2
S	Wing Planform Area	67.00 m^2
C_{Lmax}	Maximum Coefficient of Lift	1.50
HCR	Cruising Altitude	1.50 km
VCR	Cruising Velocity	100.00 m/s
PACL	Power Available for Climb	19.00 kW
PAD	Power Available for Descent	13.50 kW
VA	Approach Velocity	88.72 m/s
VTO	Take-Off Velocity	92.75 m/s
PX	Excess Power	(kW)
PXMAX	Maximum Excess Power	(kW)
V_{stall}	Stalling Velocity	(m/s)
V_{max}	Maximum Velocity	(m/s)
Rho	Density	(kg/m^3)
ROC	Rate-of-Climb	(m/s)
ROS	Rate-of-Sink	(m/s)
TCL	Time to Climb	(min)
TD	Time to Descend	(min)
H_1	Altitude	0.0 meters
H_2	Altitude	300.00 meters
H_3	Altitude	600.00 meters
H_4	Altitude	900.00 meters
H_5	Altitude	1200.00 meters
H_6	Altitude	1500.00 meters

Table 2.2

Climb Statistics

Height	Avg. ROC (m/s)	Velocity (m/s)	Time (min)	Range (km)
0-300	.3182	88.947	15.71	83.86
300-600	.2851	89.663	17.53	94.35
600-900	.2510	90.938	19.92	108.69
900-1200	.2159	91.154	23.51	126.63
1200-1500	.1799	92.750	27.79	154.63

Table 2.3

Descent Statistics

Height (m)	Avg. ROS (m/s)	Velocity (m/s)	Time (min)	Range (km)
1500-1200	.9738	100.00	5.13	30.81
1200-900	.9203	100.00	5.43	32.60
900-600	.8963	100.00	5.60	33.57
600-300	.8608	89.66	5.81	31.25
300-0	.8304	88.95	6.02	32.14

Appendix

Equation 2.1 $V_{stall}=[(WGS)(2.0)/(Rho)(C_{Lmax})]^{.5}$

Equation 2.2 ROC-PX/WG-(PACL-PR)/WG

Equation 2.3 $TCL-\ (H_{i+1}-H_i)(2.0)/(60.0)(ROC_{i+1}+ROC_i)$

where $H_{i+1}-H_i$-300 meters

ROC_{i+1}-ROC • H_{i+1}

ROC_i-ROC • H_i

Equation 2.4 ROS-PX/WG-(PR-PD)/WG

Equation 2.5 $TD-\ (H_{i+1}-H_i)(2.0)/(60.0)(ROS_{i+1}+ROS_i)$

where Hi+1-Hi-300 meters

ROS_{i+1}-ROS • H_{i+1}

ROS_i-ROS • H_i

Graph 2.1

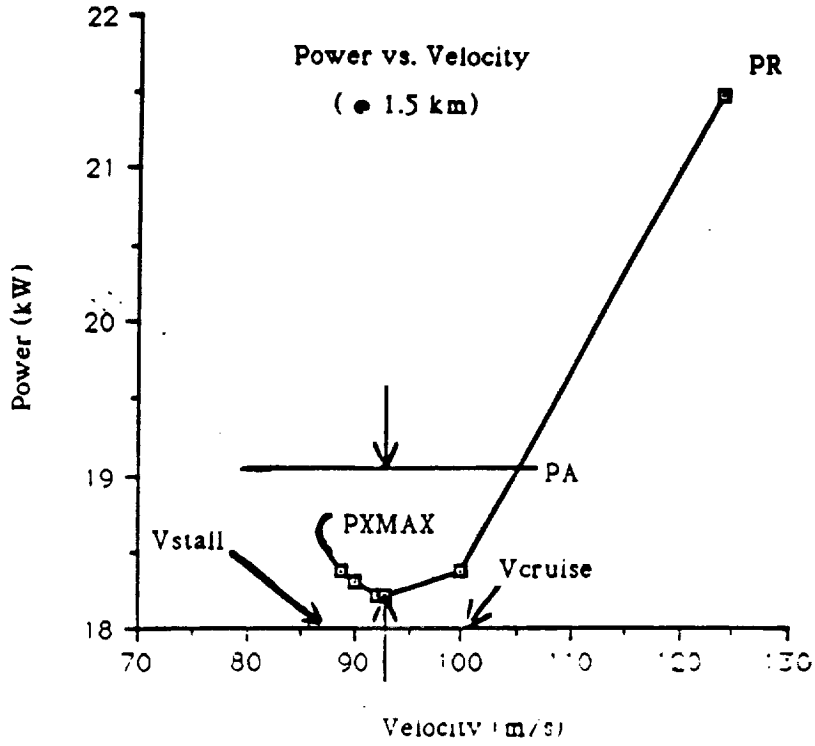

Graph 2.2

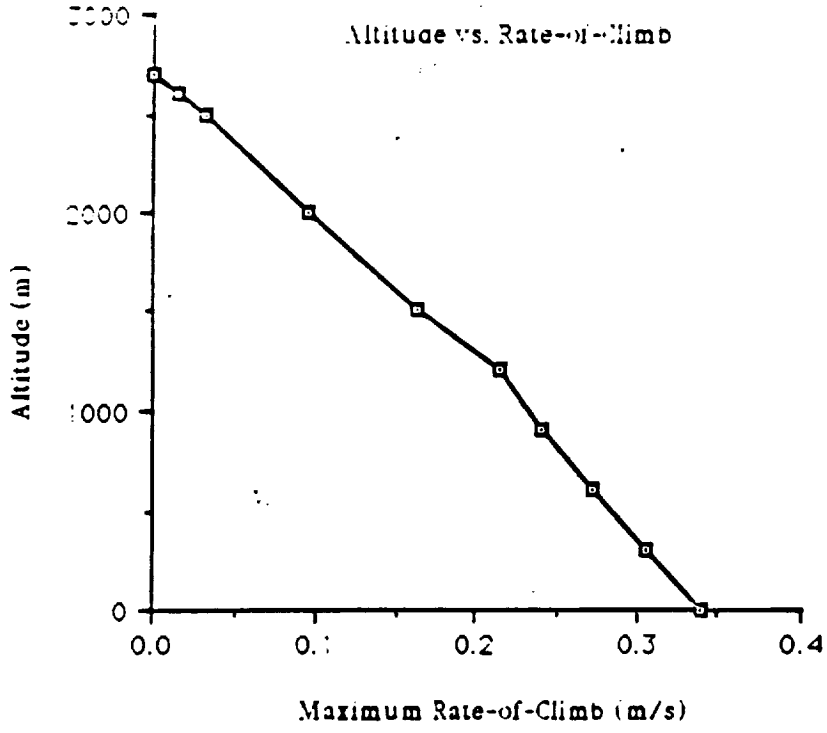

Graph 2.3

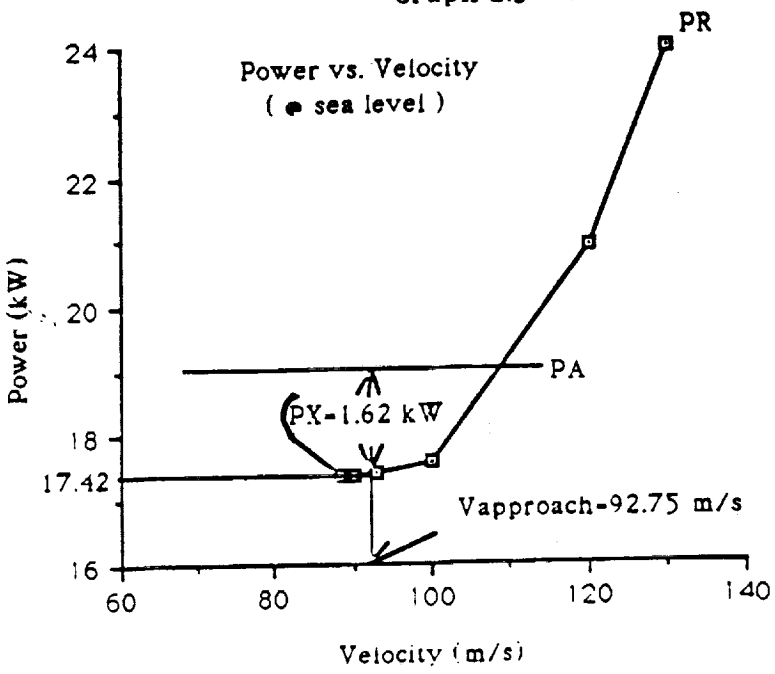

Graph 2.4

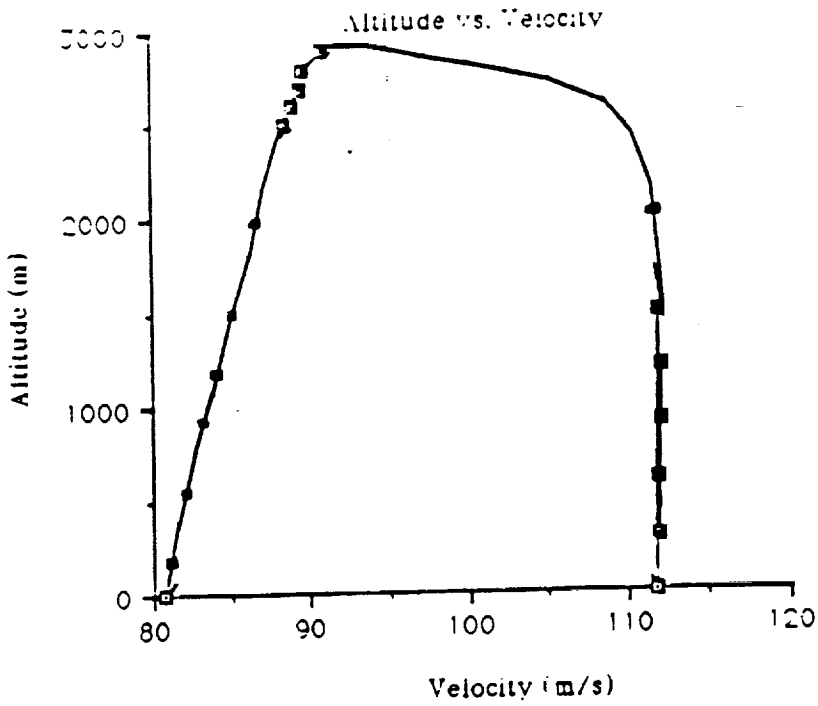

POWER and PROPULSION

by
John Blackwood

Introduction:

The properties of the Mars environment present some problems which are not necessarily dealt with when designing a conventional airplane. The lack of oxygen and low density prevent the use of an airbreathing engine. The purpose of the power and propulsion section is to ensure, if possible, that propulsion requirements for flight are met and provide power for the onboard electrical equipment. For the Pteridactol (Marsplane) design a rocket powered cart will be used for takeoff; therefore, no power from the Pteridactol's propulsion system will be required. Since the Pteridactol is projected for the future some compensation for technological advancements are made and are stated throughout the section, when appropriate. These assumptions are in the form of improved efficiencies while maintaining current weights. A fuel cell system combined with an electric motor prove to be a suitable choice for this project and are discussed at length.

Significant Data

	Climb	Cruise	Descent
Pr (ideal)	19 kw	18.37 kw	13.5 kw
Pr (assumed)	22.66 kw	21.91 kw	16.1 kw
Fuel Flow	5.95 g/s	5.75 g/s	4.23 g/s
Fuel Needed	167.15N	540.12N	31.93N
RPM	1935.96	1914.34	1727.71
Engine Inop. Drag	0.361N	0.427N	0.356N

Design Analysis

The liquid hydrogen (LH_2) and liquid oxygen (LOX) fuel cell system is being used for the Pteridactol project because it has a high energy value and a good efficiency. The fuel cells combine with an electric motor, gearbox and propeller to provide reliable power and propulsion, while weighing less than other systems which have been considered.

The fuel is LH_2 and LOX that is cryogenically stored. Data come from the Space Shuttle design (in 1971) and shows a fuel cell efficiency of 71%. It is assumed that an increase to 84% is possible before the time of actual construction (the only major assumption of this report). A maximum continuous design power (Pomax) of 25 kw is being used, which requires that the fuel cells produce 36 kw of power. Each cell is capable of producing 12 kw at the time of design (1971); therefore, it is also assumed that now the needed 36 kw can easily be obtained using only 3 cells in series. For a more extensive look at the properties of the fuel and fuel cell see table 3.1. The ~~mixing~~ reaction of LH_2 and LOX produces water which is stored in a separate tank in order to reproduce the LH_2 and LOX at the base facilities. Due to the low temperatures on Mars, insulation will be used around the tank to prevent the water from freezing.

Doesn't agree with Per

The velocity for climb steadily increases with altitude until the cruise velocity of 100m/s is reached at 1500 meters. Also, the power required during climb will vary and the 19 kw of power is the average climb power required. The power and velocity for descent decrease until the landing velocity of 92.75 m/s is reached. The 13.5 kw of power needed during descent is the average power required for that segment; see significant data listed above. Using the assumed efficiencies, the fuel needed for the propulsion system is 739.2N and 3.40N for other onboard electrical equipment, which gives 742.60N of fuel being required. A 750N limit for fuel is chosen for weight reasons, any higher and the target weight of 4800N will be exceeded. The fuel flow rate at various velocities in climb and cruise conditions are shown in Fig. 3.1. The fuel and water (3 tanks, total) will be stored in long, cylindrical shaped tanks for both strength and convenience, the locations can be seen in fig.7.1.

The electric motor chosen is the General Electric samarium-cobalt motor, rated at 141hp at 20,000 rpm, measures 17.8 cm in diameter and weighs 53.2N (14.1 kg).[1] The motor is scaled down to give an output power of 30 kw and now weighs 45.9N. Currently, this motor has an efficiency of 90%, but an increase to 92.5% is assumed

obtainable in 20 years or so. This type of motor tends to have maximum efficiency and minimum weight at high shaft speeds, requiring the use of a gearbox.[2]

The Sundstrand Corp. has a preliminary design for a 7.46 kw gearbox from which an appropriate gearbox is scaled. The gearbox weighs 59.7N, has an efficiency of 97% (98% is assumed for calculations) and a reduction ratio of 9.5:1.

This Marsplane is best suited for a single propeller design. The general characteristics of a two-blade design and three-blade design were compared. A three-blade design will have a lower blade chord and Reynolds number than a comparable two-blade propeller, causing a lower lift-to-drag ratio (L/D) and efficiency. Therefore, a two-blade propeller is being used. Another reason, and perhaps more importantly for a two-blade propeller, is that it is necessary for landing the Marsplane as a glider. The propeller is locked in a horizontal position to avoid damage. A fixed 3 meter diameter propeller with a fixed blade angle of 40^0 with an efficiency of 91.8% is chosen.[3] The propeller has a high advance ratio (J) which keeps the tip mach numbers down to 0.788, 0.859 and 0.790, maximum, for climb, cruise and descent conditions respectively. An efficiency increase to 92.5% is assumed possible in the future. The rpm and engine inoperative drag values for climb, cruise and descent conditions are given in table 3.2. Choosing a propeller with such a short diameter, with respect to the wingspan, increases the required rpm, which doesn't present a problem, and allows the motor to be started before takeoff.

The remaining onboard electrical equipment consists of an air-to-ground radio, camera equipment, variable tension cable motor and fly by wire flight controls, all of which are controlled by a central computer, see the weights section for indepth details. A power requirement of 100w is considered to be sufficient for these components. The 100w of power will be taken directly from the fuel cells and will require an additional fuel weight of 3.40N. The locations of all components are in fig.7.1.

The fuel requirements are based on power requirements necessary to fly the Marsplane and power the onboard electrical equipment. Any changes that occur during flight effect the amount of fuel being consumed, such as velocity, drag or weight variations. The Pteridactol has been designed using control surfaces on the tail only. This type of control system allows for decreased overall weight, which in turn helps to keep the power and fuel requirements down to an acceptable level.

Conclusion:

The major problems which have been overcome during the design process are fuel cell selection, fuel weight and propeller tip mach numbers. The fuel cell is being chosen for its high energy value and high efficiency. The fuel weight is at a minimum due to increases in component efficiencies which are assumed obtainable. If the assumed efficiency increases cannot be reached then more fuel will be needed, resulting in exceeding the overall target weight and requiring a shorter flight time. Using a different propeller than originally chosen allows for an acceptable tip mach number at each flight condition. Overall, there are no foreseeable problems with this power and propulsion design.

REFERENCES

1. DeMeis, R., "Control Muscle For Agile Aircraft," Aerospace America, p.32, February 1988.

2. Hall, D. W., Fortenbach, C.D., Dimiceli, E. V., and Parks, R. W., "A Preliminary Study Of Solar Powered Aircraft And Associated Power Trains," NASA CR-3699, December 1983.

3. Hamilton Standard, Generalized Method of Propeller Performance Estimation, 1963.

4. Auer, P. L., Advances In Energy Systems and Technology, Academic Press, Inc., Florida, 1986.

5. Clarke, V. C., Kerem, A., and Lewis, R., "A Mars Airplane?," AIAA, January 1979.

6. French, J. R., "The Mars airplane," Jet Propulsion Laboratory, 1978.

Table 3.1

Fuel Cell Data

Energy (ideal)		3800 kj/kg
Energy (assumed)		3192 kj/kg
Mass Ratio (LOX:LH_2)		6:1
Empty Weight (ea.)		343N
Density	-LOX	1141 kg/m^3
	-LH_2	70.79 kg/m^3
Volume	-LOX	0.149m^3
	-LH_2	0.401m^3
	-H_2O	0.1989m^3

Table 3.2

System Efficiencies

	At Time of Data (year)	Assumed Possible
Propeller	91.8% (1961)	92.5%
Gearbox	97% (1983)	98%
Motor	90% (1983)	92.5%
Fuel Cell	71% (1971)	84%

Fig. 3.1 Velocity vs. Fuel Flow Rate

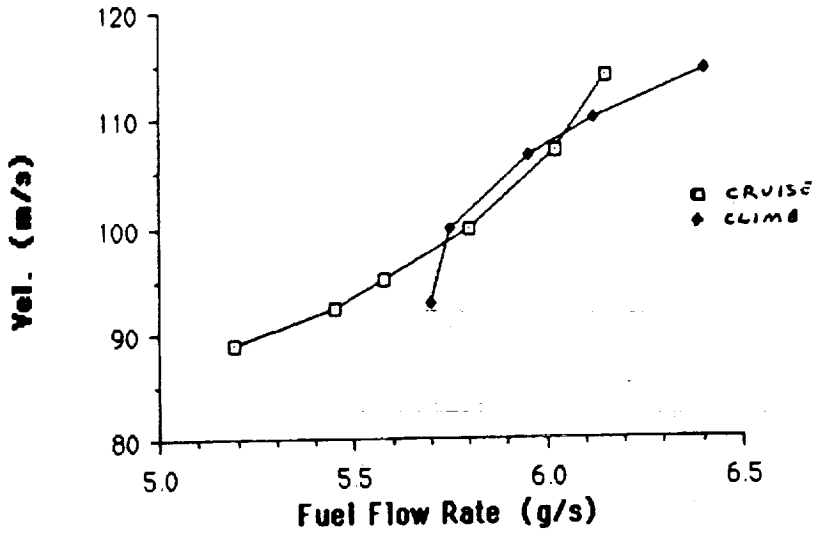

Fig. 3.2 Velocity vs. RPM

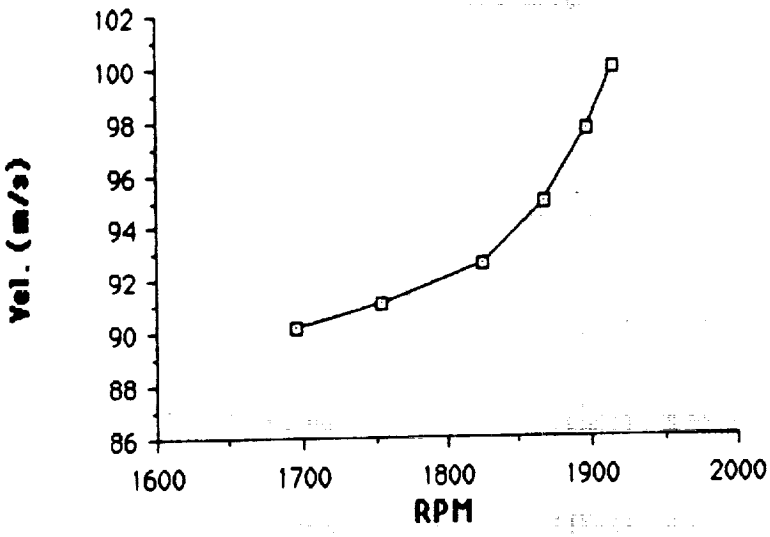

STABILITY AND CONTROL

by

Jim Mocarski

A stability & control tutorial is not appropriate

Introduction:

The stability and control problem is a complex one with many steps and computations. The concentration of this report will therefore center upon a basic explanation of the stability and control problem and the incorporation of the solutions into the design of the **Pteridactol**; not the mathematical calculations. A summary of the results to the problem are tabulated at the end of the report.

Design Analysis:

The stability of an airplane is its ability to return to some particular condition (after being disturbed from the condition) without any efforts on the part of the pilot. An airplane may be stable in some configurations and unstable in others. It should be noted, however that stability is not desirable in all conditions. If a plane is stable in a nose-dive, it would resist the efforts of the pilot to pull out. The stability of an airplane is definitely due to features incorporated in the design and thus stable conditions and un-stable conditions can be planned for, predicted and designed for.

There is a medium between stability and instability. A stable airplane tends to return to an original condition, an un-stable airplane tends to move further from the original condition if disturbed. But what of a plane which does neither and just stays in the new condition? This is called neutral-stability and in some cases is a desirable feature.

Figure 4.1 illustrates some of the ways an aircraft may behave in response to a disturbance. The top is an illustration of the usual type of stability, one in which

stability, one in which there is an oscillation which is eventually damped out. The second is what was called neutral stability and shows a steady oscillation. And the bottom is an unstable aircraft, an oscillation which steadily grows worse.

With stability so defined it is now possible to make further classifications. In order to do this axes must be defined. Figure 4.2 is an illustration of the three axes considered in stability and control. The **longitudinal axis** is a straight line running fore and aft through the center of gravity, and is horizontal when the plane is in the attitude of normal horizontal flight. The **normal axis** is a straight line through the center of gravity and is vertical for normal horizontal flight. The **lateral axis** is a straight line through the center of gravity at right angles to the longitudinal and normal axes. It will be horizontal during normal horizontal flight and parallel to a line joining the two wing tips.

Three types of stability may now be considered. Rolling about the longitudinal axis concerns **Lateral stability and control**. Yawing about the normal axis concerns **directional stability and control**. And pitching about the Lateral axis concerns **longitudinal stability and control**. Figure 4.2 also illustrates these motions.

Longitudinal Stability will be addressed first since it can be considered independently of the other two. An example will best describe this type of stability. Suppose an airplane is flying such that the angle of attack of the main wings is 4^{o} and the angle of attack of the tail is 2^{o}; for one reason or another the nose rises inclining the plane by 1^{o}. What will happen? The momentum of the airplane will cause it to continue moving practically in its original direction and with its previous velocity. So, the angle of attack of the wings is now effectively 5^{o} and the tails's is now 3^{o}. This causes the lift on the

wings and tail to increase. If the restoring moment caused by the increase in lift on the tail multiplied by the distance to the center of gravity is greater than the upsetting movement caused by the increase in the lift of the wings then the plane will be stable. The tail basically causes a restoring moment if the plane is disturbed returning it to the original condition, i.e. if the angle of attack is temporarily increased, forces will act on the plane in such a way as to depress the nose and thus decrease the angle of attack once again.

Lateral stability ensures that if a slight roll takes place forces acting on the plane will restore it to an even keel. Sideslip is the cause of the major restoring forces of lateral stability. The **Pteridactol** will ensure lateral stability with the use of a dihedral. During flight the sailwings will bow upwards effectively creating a dihedral angle. If one wing becomes lower than the other the resultant lift will be slightly inclined in the direction of the lower wing. This causes the lift and weight forces to be out of balance. Therefore there will be a small resultant force sideways and downward acting on the plane, causing it to sideslip. Sideslip causes a flow of air opposite to the slip which will strike the lower wing at a greater angle than the upper wing and as a result the lower wing will receive more lift and roll the aircraft back to an even keel.

Directional stability ensures that if the plane is directed off its course, the forces acting will restore it to its original direction. Directional stability is almost entirely a question of the vertical tail and side surfaces. There is a very close resemblance between the directional stability of a plane and the action of a weather vein which always turns into the wind. However two differences must be kept in mind when considering the analogy. First is that not only may an airplane yaw but it may also move sideways. And second, the wind is caused by the motion of the plane. The **Pteridactol** uses a

standard vertical tail section to produce the correcting forces needed for directional stability.

Lateral and directional stability are closely inter-related. Sideslip, essential to lateral stability will cause pressure on the side surfaces, which provide directional stability, turning the airplane towards the direction of sideslip. Just as a slight roll results in sideslip and then a yawing motion; a yawing motion will cause one wing to travel faster than the other, obtain more lift and produce a rolling motion. Thus a yaw causes roll and roll causes yaw.

Whether stable or unstable it is necessary for the pilot to be able to cause or stop rotation about any of the three axes. Longitudinal control is provided by the elevators. The **Pteridactol** uses a conventional elevator set up which is depicted in Figure 4.3. A fly by wire system will be used to control elevator deflection. This elevator configuration yields sufficient longitudinal control to satisfy the requirements set for the marsplane. Lateral control is provided conventionally by ailerons, but in the case of the **Pteridactol** adjusting the wings camber will be used to provide control. By adjusting the tension of the trailing edge cable the camber of each wing can be changed and thus the lift and drag characteristics of the wing will be changed giving the pilot control. And finally the rudder will provide directional control. The **Pteridactol** uses a conventional rudder arrangement which is also illustrated in figure 4.3. In each case the system of control is the same. If the flap is moved (or wing camber changed) it will change the force upon the surface. Since the pilot has control of the surfaces he also has control of the forces acting on the plane and therefore has control. Figure 4.4 illustrates the physical configuration of the **Pteridactol** and shows the location of the wing and tail as well as the location of the neutral point. Table 4.1 gives sizings of the **Pteridactol**'s control surfaces and other data concerning the vertical and

horizontal tail, and Figure 4.3 is an illustration of the tail surfaces designed to satisfy the **Pteridactol's** stability and control requirements. Table 4.2 demonstrates the satisfaction of the stability and control specifications. It should be noted that since camber change was used in place of ailerons, estimations of the change in the characteristics of the wing with respect to percent camber change were used. The C_l for cruise (1.125) was taken to be 0% change and Cl max as 100% change and a linear distribution was assumed from there. Therefore percent camber change was analogous to aileron deflection for the calculations made. It should be noted though that testing is needed to see if this assumption will hold true. It is not known if or at what point the wing begins to lose its shape or if and when separation takes place when adjusting the camber. Yet with this assumption, at maximum camber change, the **Pteridactol** exceeded the requirements set forth and therefore the need for the proposed floating aileron was eliminated.

In conclusion it is necessary to acknowledge the fact that sail-wings of this size have never been tested so the lateral stability and control predicted may not in practice be the case. But, a margin of safety was designed for in all three classifications of stability and control to protect against unanticipated problems due to the Martian atmosphere.

REFERENCES

Bradley Jones, Elements of Practical Aerodynamics, (John Wiley and Sons, Inc. 1939)

A. C. Kermode, Mechanics of Flight (Sir isaac Pitman and Sons, ltd., 1940)

Jan Roskam, Methods For Estimating Stability and Control Derivatives of Conventional Subsonic Airplanes (University of Kansas, 1977)

TABLE 4.1

HORIZONTAL TAIL

airfoil: NACA 0012-64

$S_h/S_w = 12\%$	AR = 6	$\Lambda = 0$	$i_t = 2.0^o$
$S_h = 7.164m^2$	$S_e/S_h = 45\%$	$\Gamma = 0$	$\delta_{emin}=20^o$?
$l_h = 7m$	$t/c = 0.1$	$\lambda = 0$	$\epsilon_\alpha = 0.1817$

VERTICAL TAIL

$S_v/S_w = 6\%$	$S_r/S_v = 60\%$
$S_v = 3.582m^2$	$S_r = 2.15m$
$S_v/S_t = 50\%$	taper ratio = 0.64

$\delta_{min} = 20^o$

minimum ?

CENTER OF GRAVITY RANGE

FORWARD LIMIT FORM TIP = 2.27m

AFT LIMIT FROM TIP = 2.71m

?

TABLE 4.2

STABILITY AND CONTROL REQUIREMENTS

CONDITION	REQUIREMENT	PERFORMANCE
all flight cond.	10% static margin	min S.M. = 10%
takeoff	lift nosewheel at 90% of takeoff speed w/ c.g. at forward limit	lift nosewheel at 88% takeoff speed
cruise	sustain 30^{o} coordinated banked turn	sufficient control for 35^{o} turn
cruise	develop 30^{o} bank angle in 2.0 seconds	30^{o} bank reached in 1.7 seconds
landing approach	stall w/c.g. at forward limit	need 75% of max elevator deflection
landing approach	crosswind landing	need 65% of max rudder deflection
landing approach	full-rudder sideslip	camber change yields necessary control

FIGURE 4.1

TYPES OF REACTIONS

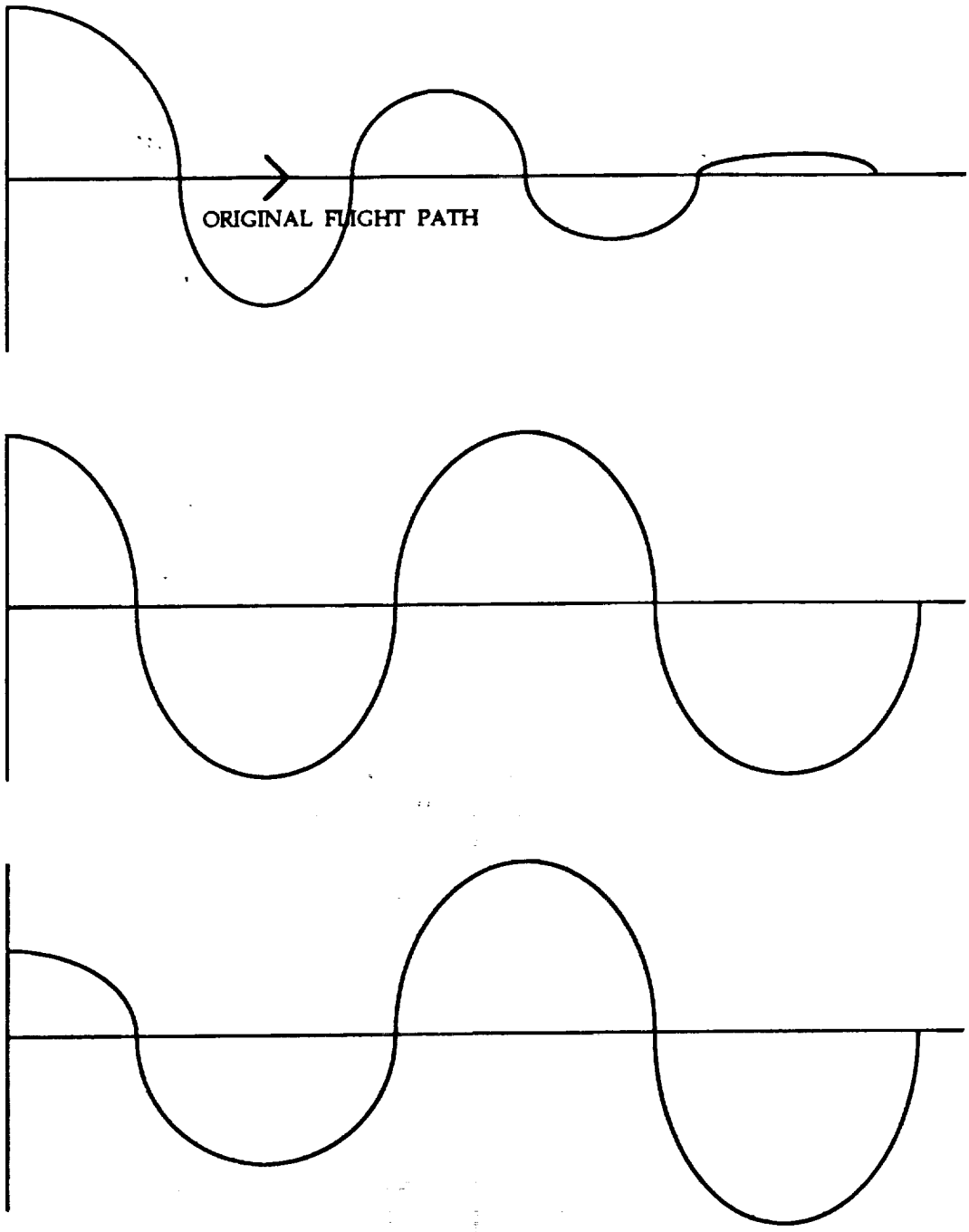

FIGURE 4.2

AXES OF MOTION

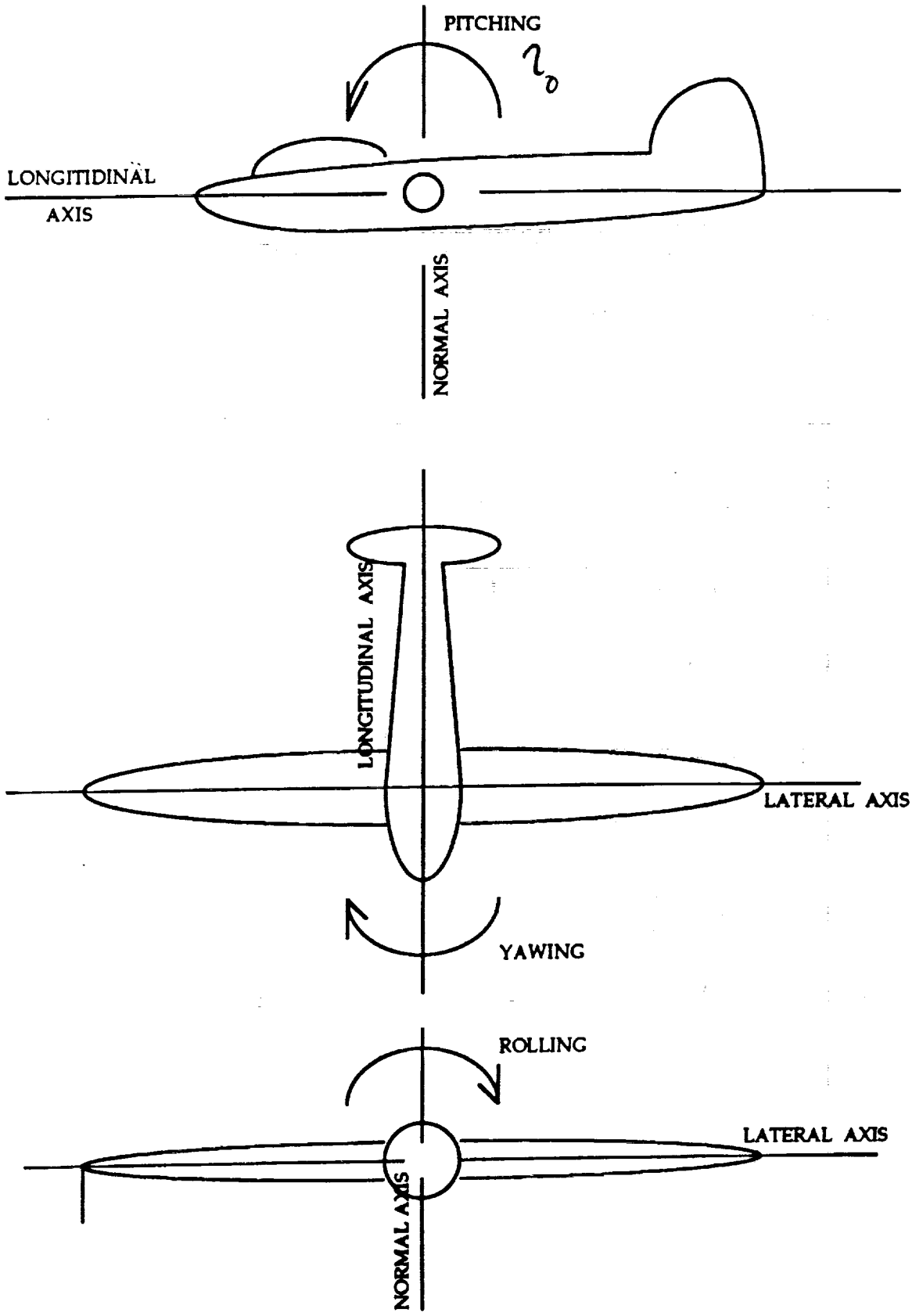

FIGURE 4.3

TAIL SURFACES

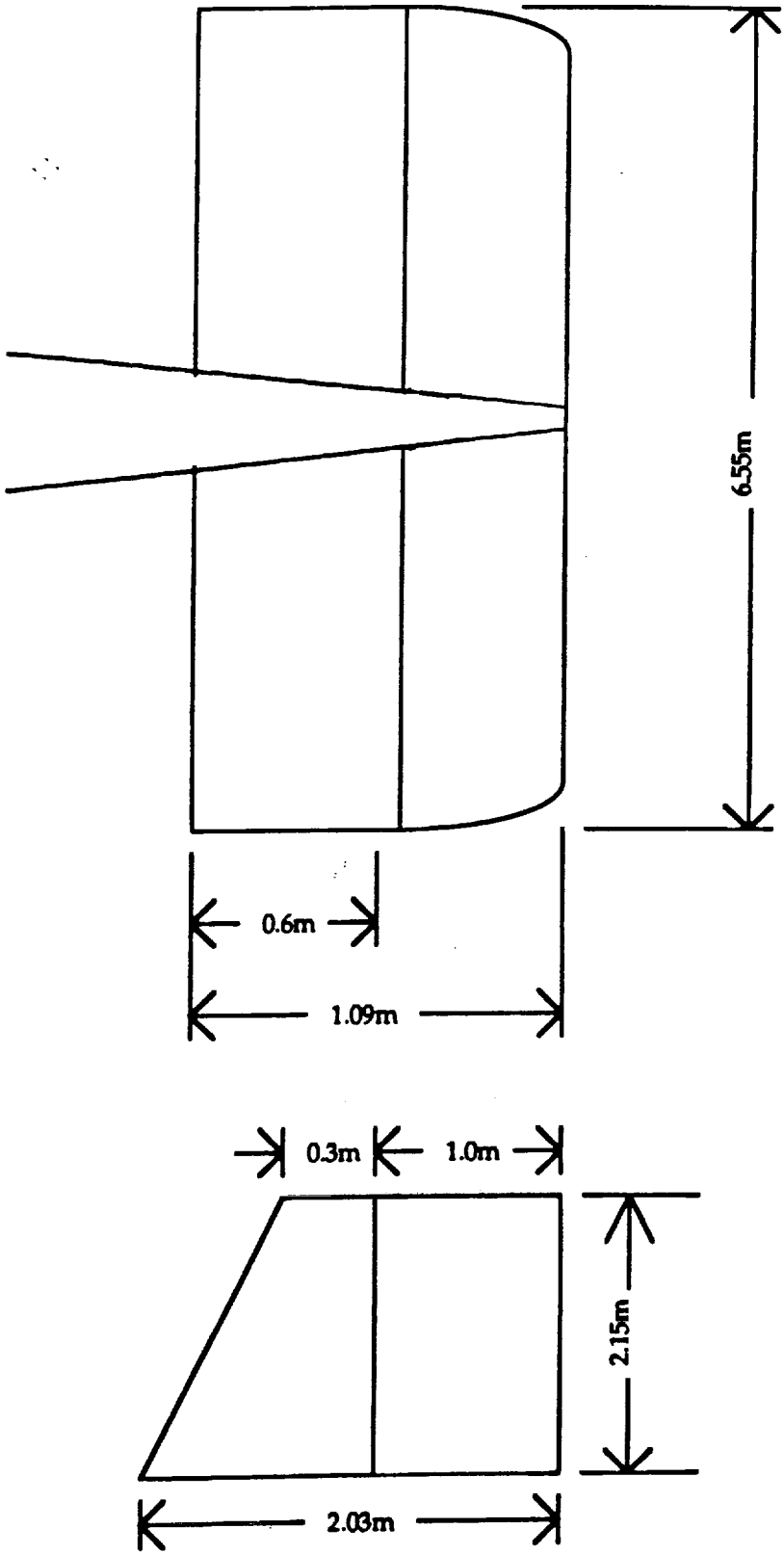

FIGURE 4.4

PHYSICAL CONFIGURATION

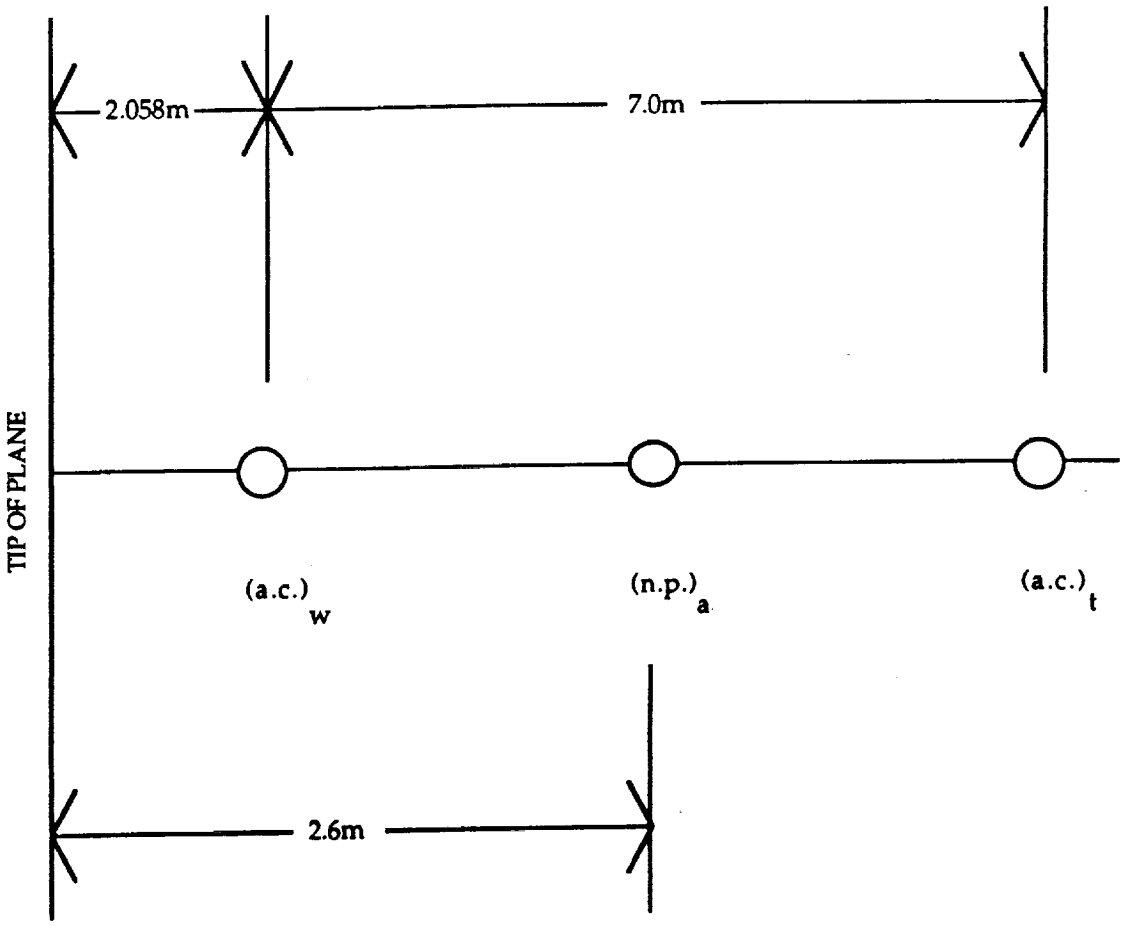

STRUCTURES

by
Greg Cimmarusti

INTRODUCTION:

Throughout the design process of the Pteridactol, atmospheric and mission constrains had to be dealt with. The primary concern of the Structures Group was to get the structural weight as low as feasibly possible. Due to the low density of the Martian atmosphere, a massive wing area was needed to generate the necessary lift. Problems arose in finding a material which had a very low density while having a very high strength. Another major concern was fitting the plane into the aerobrake designed by the Spacecraft Group. It was obvious from the initial sizing that the Pteridactol could not be shipped as a whole. Somehow, the plane had to be designed so that it could be shipped in as few components as possible and be easily assembled after reaching Mars. The Pteridactol's structure also had to be designed for the possibility of 4g flight and have a 1.5 factor of safety for an ultimate load factor of 6g's. These are just a few of the things which challenged the Structures Group during the design of a plane suitable for flight on Mars.

DESIGN ANALYSIS:

After considering the above constraints, among others , it was decided that the best wing configuration to use was a sailwing. It appeared to be the best decision based on weight and simplicity. After the initial sizing and other factors, a gross weight of 4000N was chosen as a goal. That was found to be unattainable and was changed to 4800N. After receiving the wing span from the Aerodynamics Group, a wing loading diagram was done. A wing weight goal was set at 1000N by the Structures Group. The Schrenk approximation for lift and a constant wing weight were used. The placement of powerplants or fuel in the wings was never considered as a possibility due to the use of a sailwing, although they would have helped in the reduction of the bending

moment when in flight. From the loading diagram, shear and moment diagrams were generated. An estimate of the possible leading edge spar thickness could then be found. A decision was then made to use a tapered wing to reduce the drag and the maximum moment at the wing root. Another way to decrease the wing weight was to decrease the thickness of the leading edge spar along the span as the wing tip was approached. A constant linear decrease from 1.5mm to 0.5mm was decided upon. After these changes, it was realized that a lower wing weight of 900N could possibly be achieved. With these new numbers, the final loading diagram was drawn and can be seen in figure 5.1. The assumption was made that with a decreasing chord length and a decreasing spar thickness, a linear wing weight would be obtained. Also, other parts such as ribs would be included in the wing weight but not shown as point loads due to their small weights compared to the rest of the wing. The last assumption made was that the leading edge spar would carry the load of the entire plane and that the horizontal tail and the other wing parts such as the trailing edge cable would not carry any. This would add an extra factor of safety to the leading edge spar. The next step was to generate the shear and bending moment diagrams which can be seen in figures 5.2 and 5.3. The value of the maximum moment was found to be 16,201.5Nm and occurred at the wing root. Several points along the span were tested to see if their thicknesses were greater than the minimum allowed and all were sufficient. A maximum torsional moment diagram was also done and can be seen in figure 5.4. It can be seen that the highest moment occurs at the wing root and since it was so small it was never considered a problem during the wing design. Cross-sections of the wing at the tip and root can be seen in figures 5.5a and 5.6a respectively.

Depends on tail trim load

The sailwing design consists of several parts. First was the leading edge spar which was approximated by the shape of a semi-ellipse for the simplicity of calculations. The cross-sections of these approximations can be seen for the wing tip and root in figures 5.5b and 5.6b respectively. The material chosen for the leading edge spar was a carbon fiber-reinforced composite. Sheets of this composite will be layered at $\pm 45^0$ to increase it's strength. The needed tensile strength of 9×10^8 N/m^2 could be found in this type of composite, especially when orienting the fibers properly.[1] Another great advantage found in this material was a low density of approximately 1.49×10^4 N/m^3. It was also chosen for it's fatigue and corrosion resistance, and the fact that the low temperatures on Mars do not greatly diminish it's properties.[2,3] A dacron membrane was used for the flexible part of the sailwing. It's good strength and light weight was very beneficial in the wing design; however, it is not known how the low temperatures on Mars will affect this material. A trailing edge cable with varying

tension is used to help produce the proper airfoil section needed. The cable is made of stainless steel and runs from the trailing edge of the wing tip to a small motor in the fuselage which controls the tension. The sailwing also consists of five carbon fiber composite ribs and the end plate which help it keep it's shape. In order to diminish the possibility of buckling and increase it's strength, the leading edge spar is filled with honeycomb. Honeycomb is strong, but did not add much weight to the wing. A small stainless steel strip is also placed at the bottom of the wing tip to protect it when landing. Although the wing tip was found to deflect only 19.1cm when not in flight, the wing tips will still touch the ground due to the glider type landing. There is also an extra section added to the spar for use in the problem of assembly and will be further discussed in that section. The overall wing construction can be seen in figure 5.7 and a weight breakdown can be seen in table 5.1.

where?

Although a thorough structural analysis of the fuselage and tail was not done, steps were taken to ensure a structurally safe plane while trying not to have an overabundance of excess weight. The approximate sizes and spacings of the fuselage structural components can be seen in table 5.2. For extra safety, the spacings listed are smaller than the distances usually used in small planes.[4] Extra frames and longerons were placed in areas where more strength seemed necessary.

The horizontal tail was designed using wing structures found in current small planes.[4] A cylindrical spar and rectangular stiffeners were used along with ribs placed about .75m apart. Another small stainless steel strip is used to prevent damage to the horizontal tail when on the ground and landing. The vertical tail was also designed using the basic structures found in small aircraft. The vertical and horizontal tails were attached together in the fuselage for weight savings. The landing gear was also placed under the forward wing and the tail and could use the same bracings. The material used in the majority of the plane was the same composite used in the wing construction.

Two bay doors are also included in the structure. The first is on top of the fuselage and was designed for the purpose of having access to the inside of the fuselage to do maintenance and replace parts. The second is a cargo door and is on the bottom and to the side of the fuselage. It's operation will be further discussed in the rescue scenario. The overall structure of the fuselage and tail can be seen in figure 5.8a. Important cross-sections of the fuselage were also drawn and can be seen in figure 5.8b.

CONCLUSION:

Because there are still many questions about the planet Mars and it's atmosphere, whether or not a plane can be designed and built to fly and be useful is still unknown. Theoretical calculations seem to show that it can be done. Many steps were taken by the Structures Group to ensure the safety of the pilot. The plane had to be designed to handle any unexpected problems which may occur. Extra factors of safety were incorporated into the structure whenever possible. Also, many of the components of the Pteridactol have never been used or tested before. Testing is the best way to determine if this endeavor could be successful. Many may think the idea of a plane which would be able to fly on Mars is somewhat of an unreal goal. The final conclusion is that it is certainly possible in the near future.

REFERENCES

1. Delmonte, John, Technology of Carbon and Graphite Composites, New York, Van Nostrand Reinhold Company, 1981.

2. Fritz, W., and Huttner, W., "Carbon Fiber-Reinforced Composites: Processing, Room Temperature Properties, and Expansion Behavior at Low Temperatures," Nonmetallic Materials and Composites at Low Temperatures, Plenum Press, New York (1979), pp. 245-267.

3. Kasen, M.B., "Mechanical Performance of Graphite- and Aramid -Reinforced Composites at Cryogenic Temperatures," Advances in Cryogenic Engineering Materials, Vol. 28, Plenum Press, New York (1982), pp. 165-175.

4. Roskam, Jan, Airplane Design part III: layout design of cockpit, fuselage, wing, and enpennage : cutaways and inboard profile, Published by Roskam Aviation and Engineering Corp., 1986.

5. Kensche, C., "Service Life of Sailplanes Made of CFRP," Fiber Science and Technology, Vol. 18, pp. 95-108, 1983.

6. Nicolai, Leland M., Aircraft Design, Published by Mets, Inc., 1975.

7. Schramm, R.E., "Cryogenic Mechanical Properties of Boron-, Graphite-, and Glass-Reinforced Composites," Materials Science and Engineering, Vol. 30, pp. 197-204, 1979.

TABLE 5.1
Wing Weight Breakdown

leading edge spar	330.6N
dacron membrane	76.3N
trailing edge cable	27.9N
wing ribs(six total)	10.7N
honeycomb filler	3.5N
landing plate	1.0N
	450.0N/wing
TOTAL WING WEIGHT	900.0N

TABLE 5.2
Fuselage Construction

frame depths	0.3cm
frame spacing at cockpit	0.25m
frame spacing of main body	0.45m
frame spacing at tail section	0.34m
longeron spacing of main body	0.3m

FIGURE 5.1
LOADING DIAGRAMS

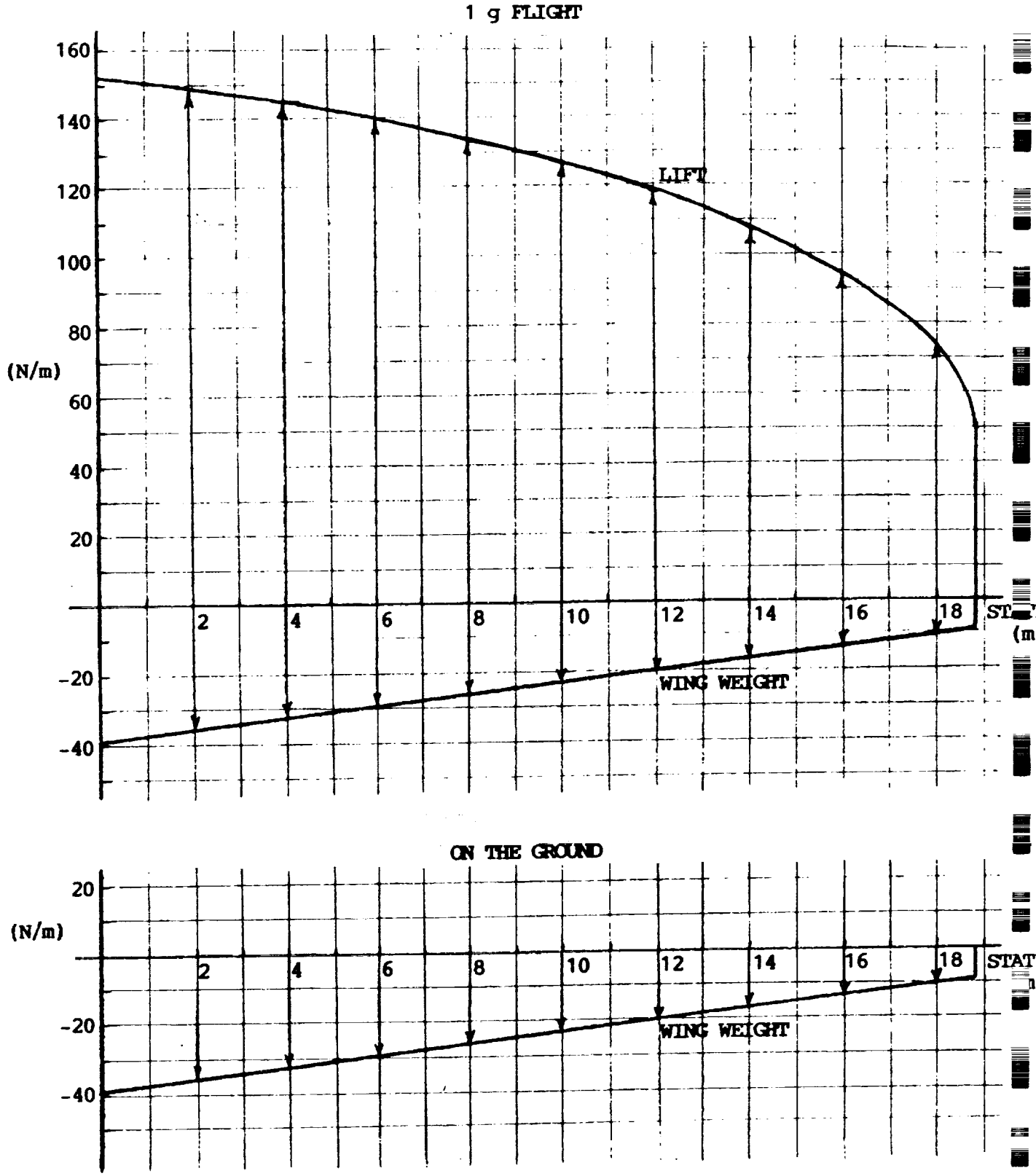

FIGURE 5.2
SHEAR DIAGRAMS

1 g FLIGHT

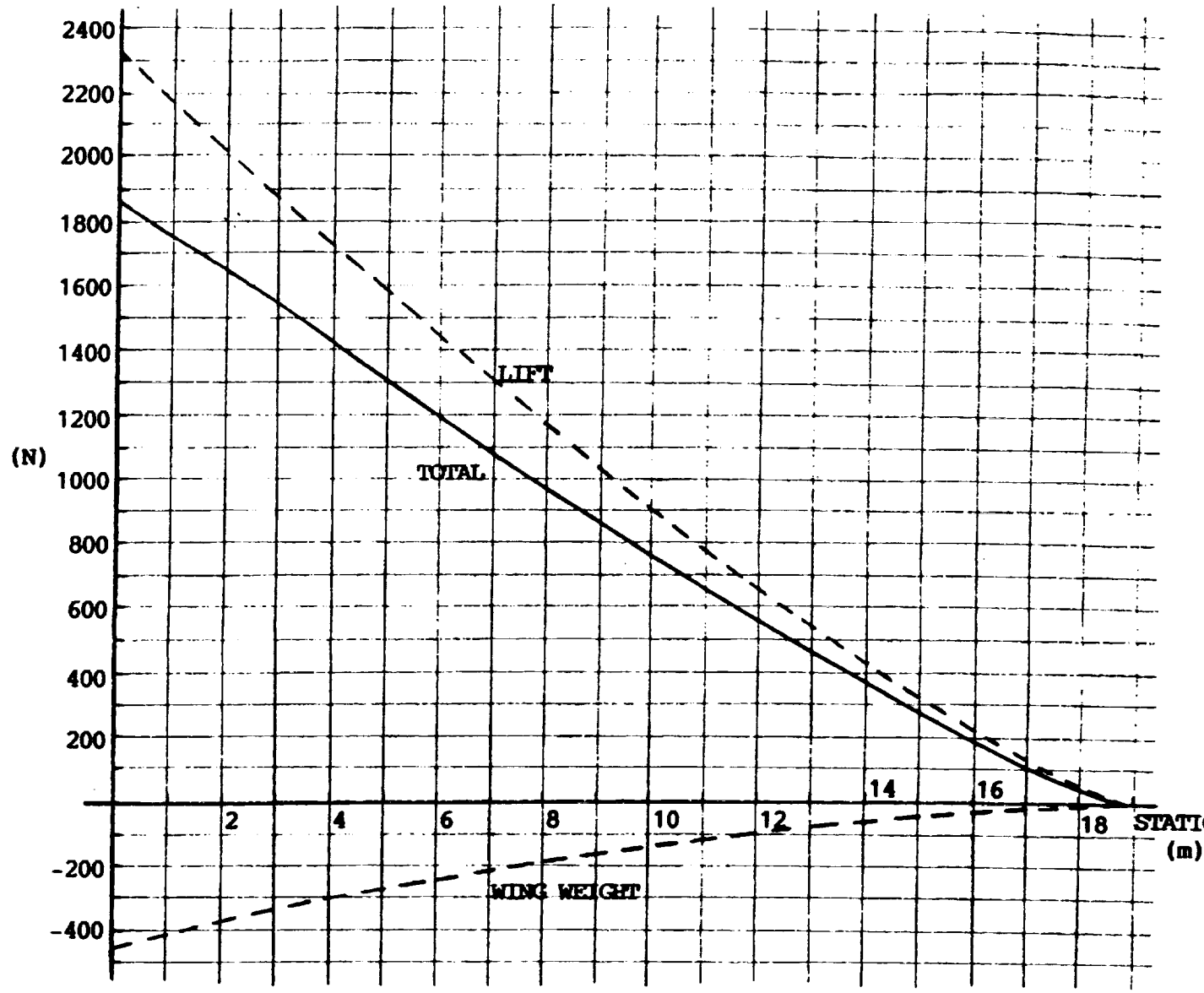

ON THE GROUND

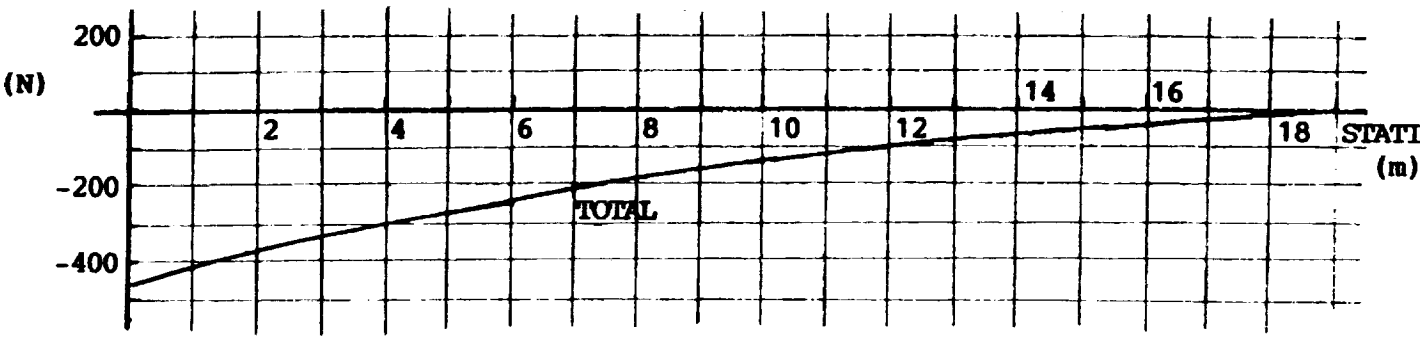

FIGURE 5.3
MOMENT DIAGRAMS

1 g FLIGHT

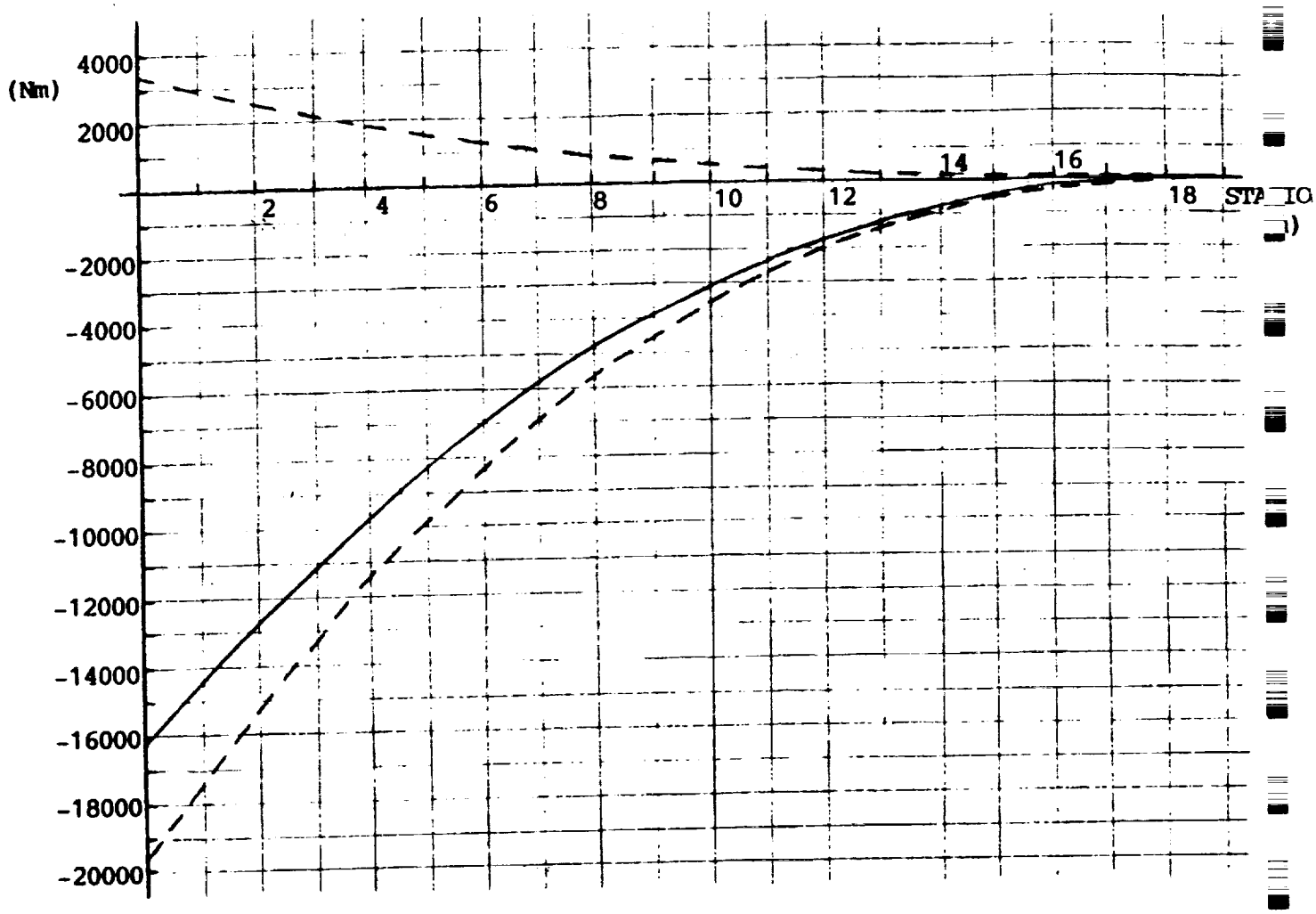

ON THE GROUND

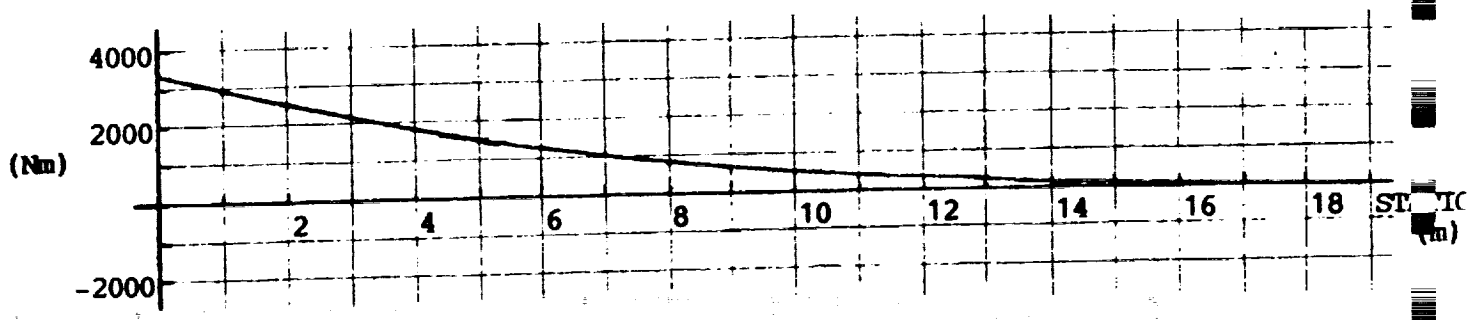

ORIGINAL PAGE IS
OF POOR QUALITY

FIGURE 5.4
TORSIONAL MOMENT

1 g FLIGHT

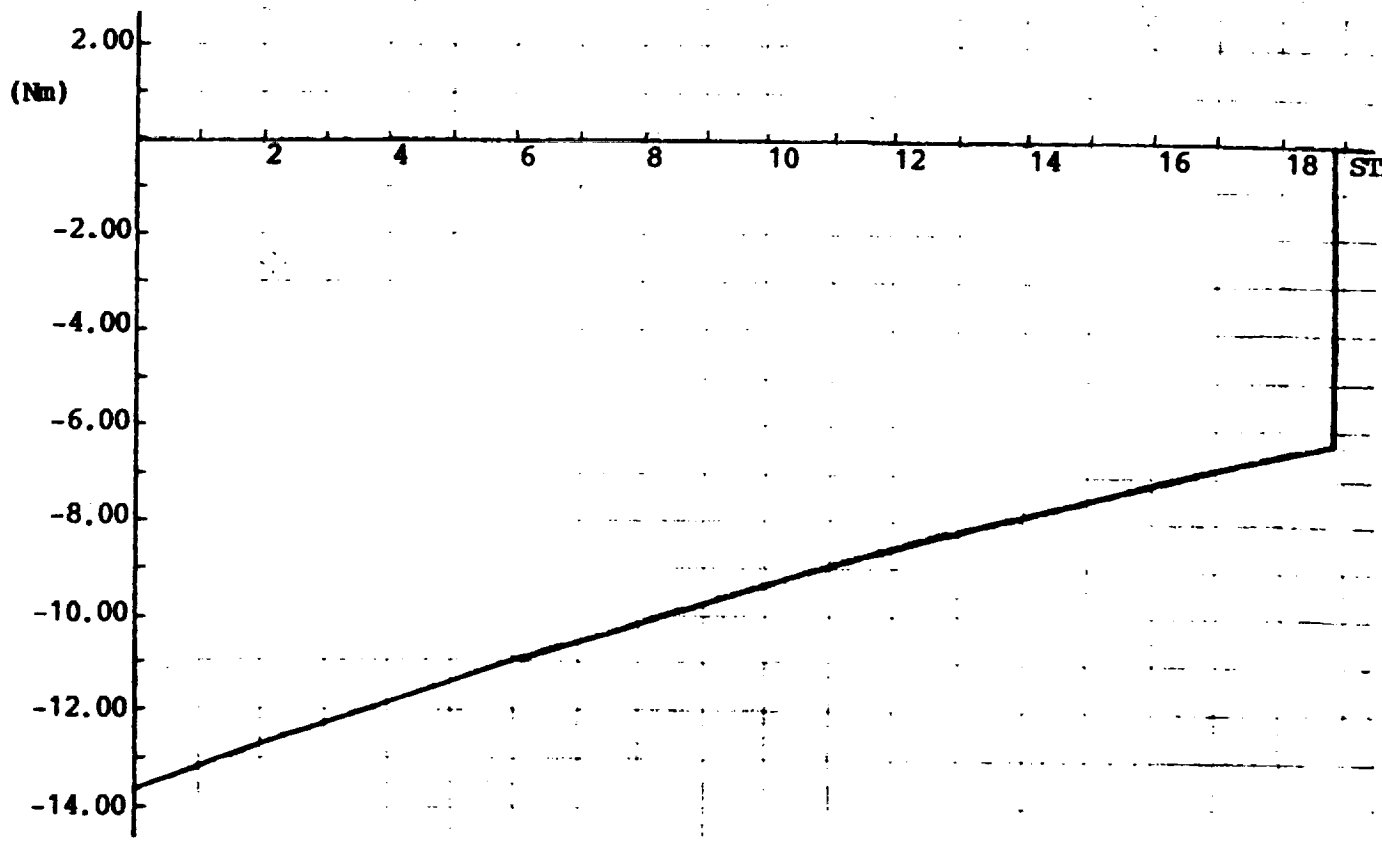

5.5 b

FIGURE 5.5 a
Airfoil Section at Wing Tip

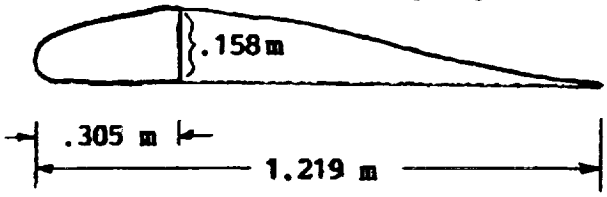

FIGURE ~~5.7~~
Leading Spar Approximation at Tip

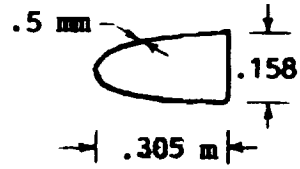

5.6 b

FIGURE 5.6 a
Airfoil Section at Wing Root

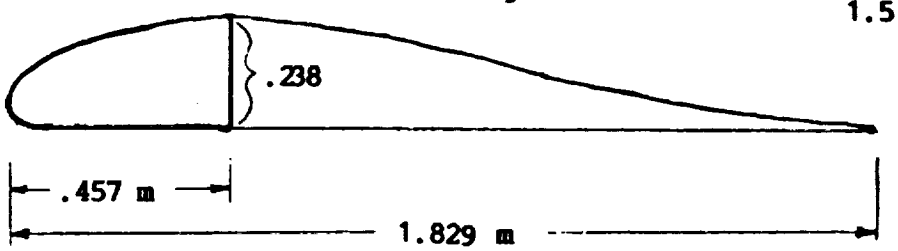

FIGURE ~~5.8~~
Leading Spar Approximation at Root

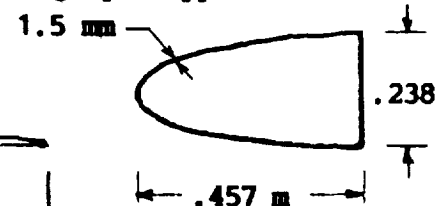

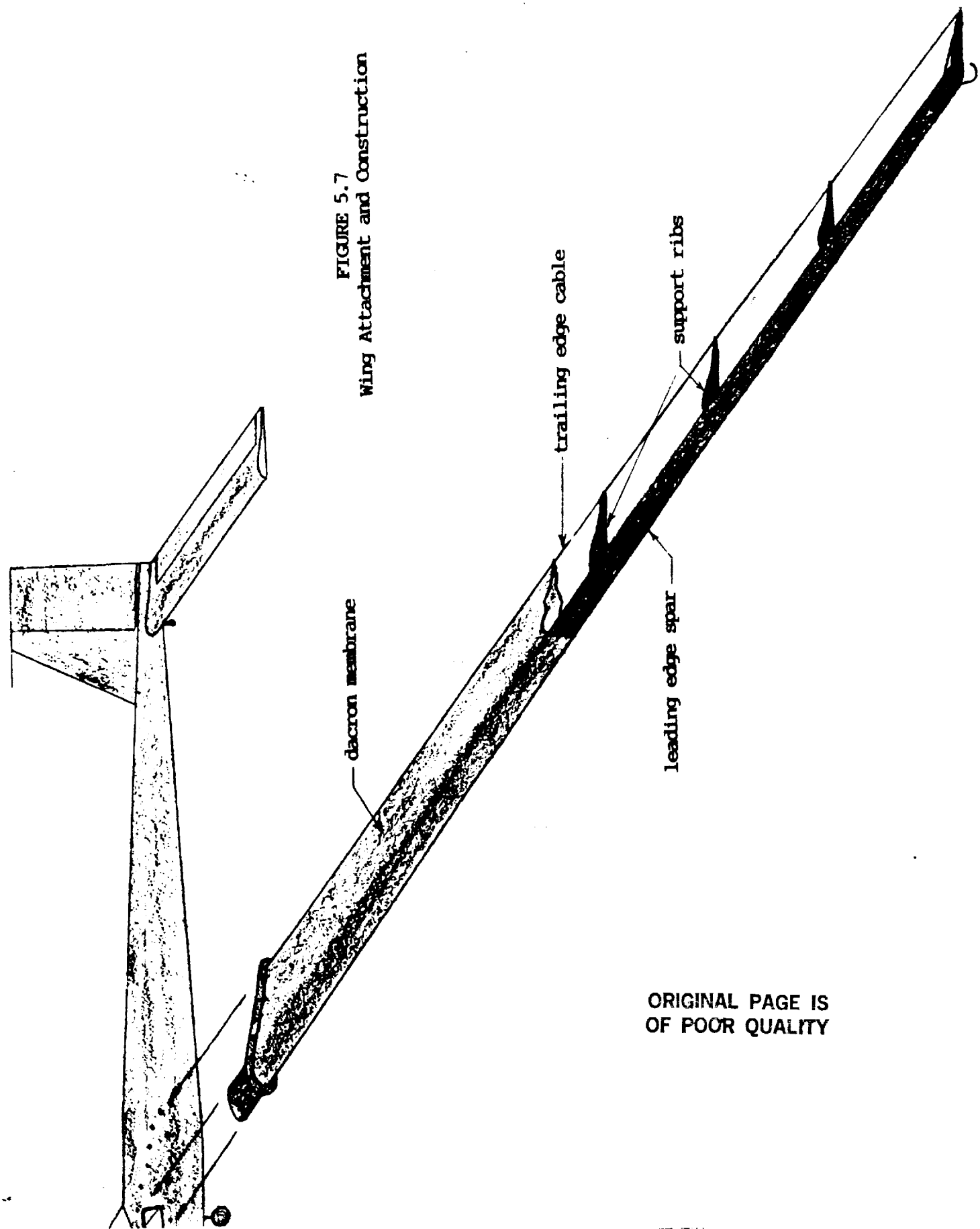

FIGURE 5.7
Wing Attachment and Construction

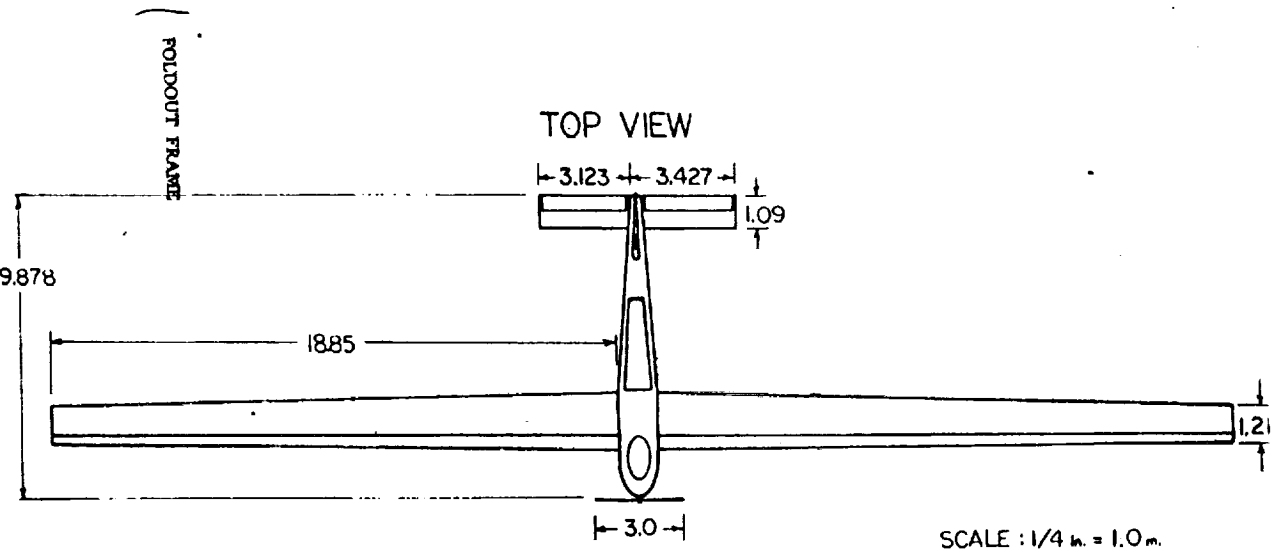

SCALE : 1/4 in. = 1.0 m.

* ALL DIMENSIONS ARE IN METERS

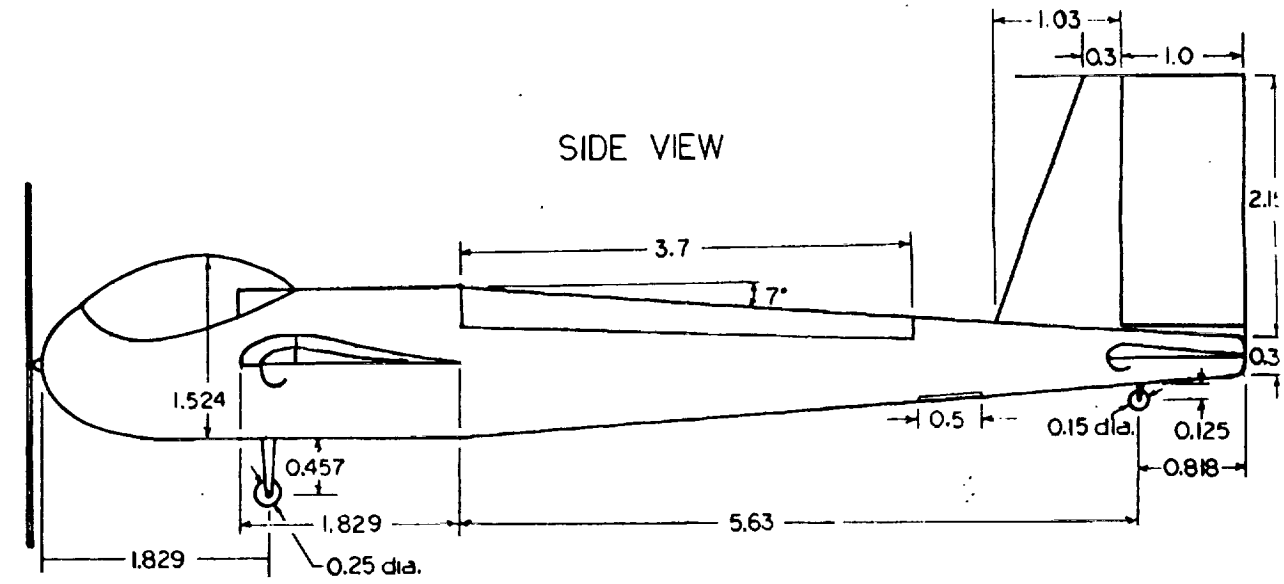

SCALE : 1 in. = 1.0 m

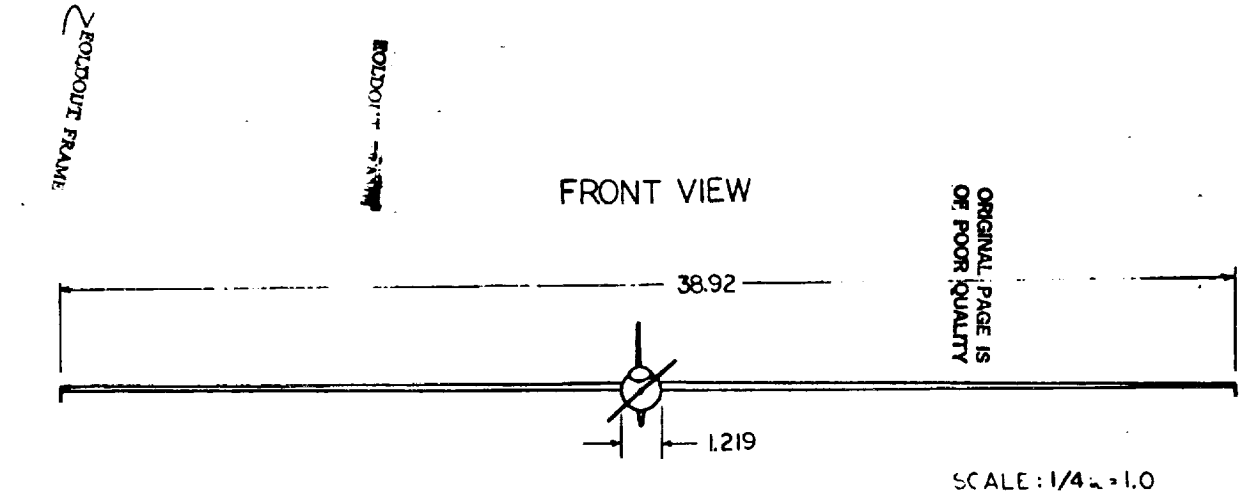

SCALE : 1/4 in. = 1.0

ORIGINAL PAGE IS
OF POOR QUALITY

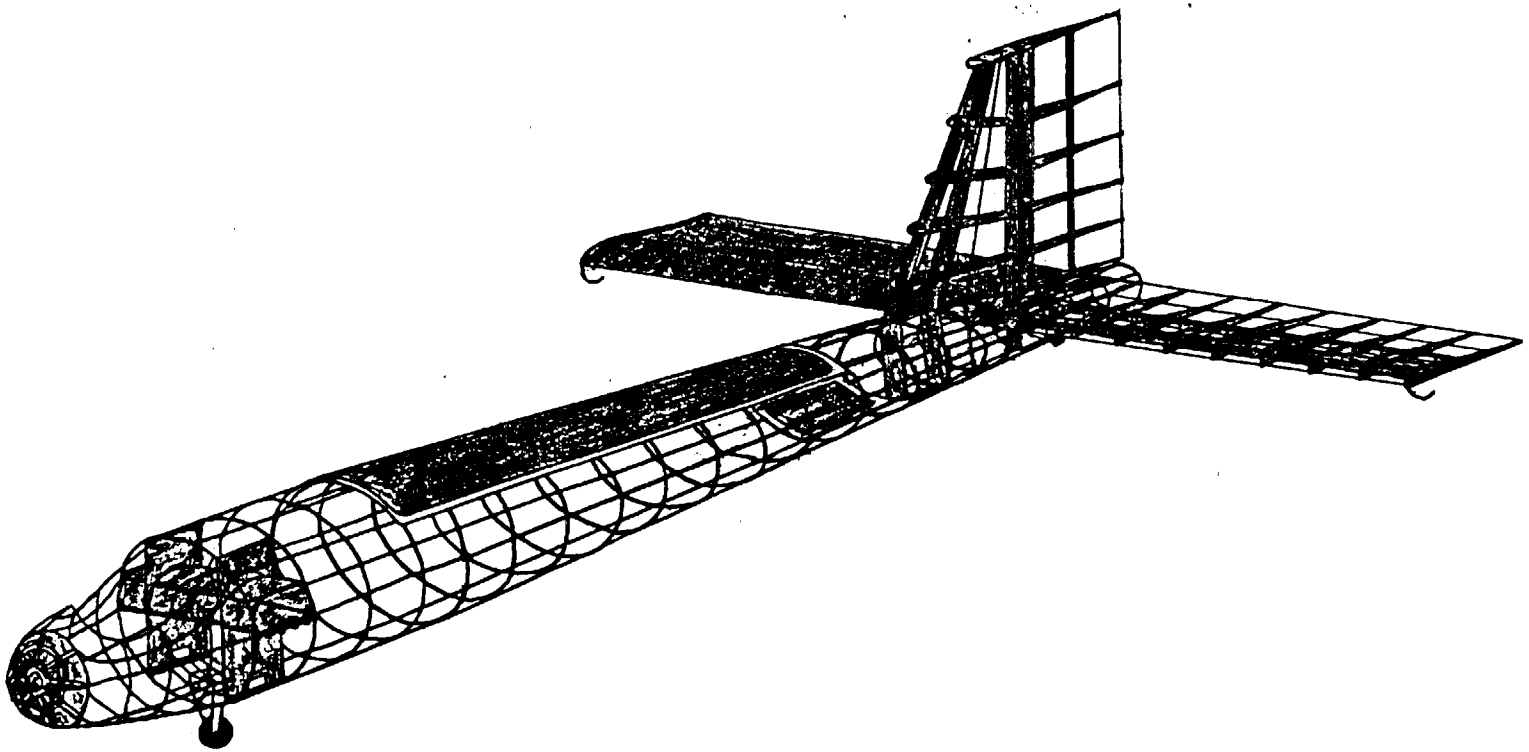

EOLDOUT FRAME

EOLDOUT FRAME

FIG. 5.8a
FUSELAGE AND TAIL SKELETON

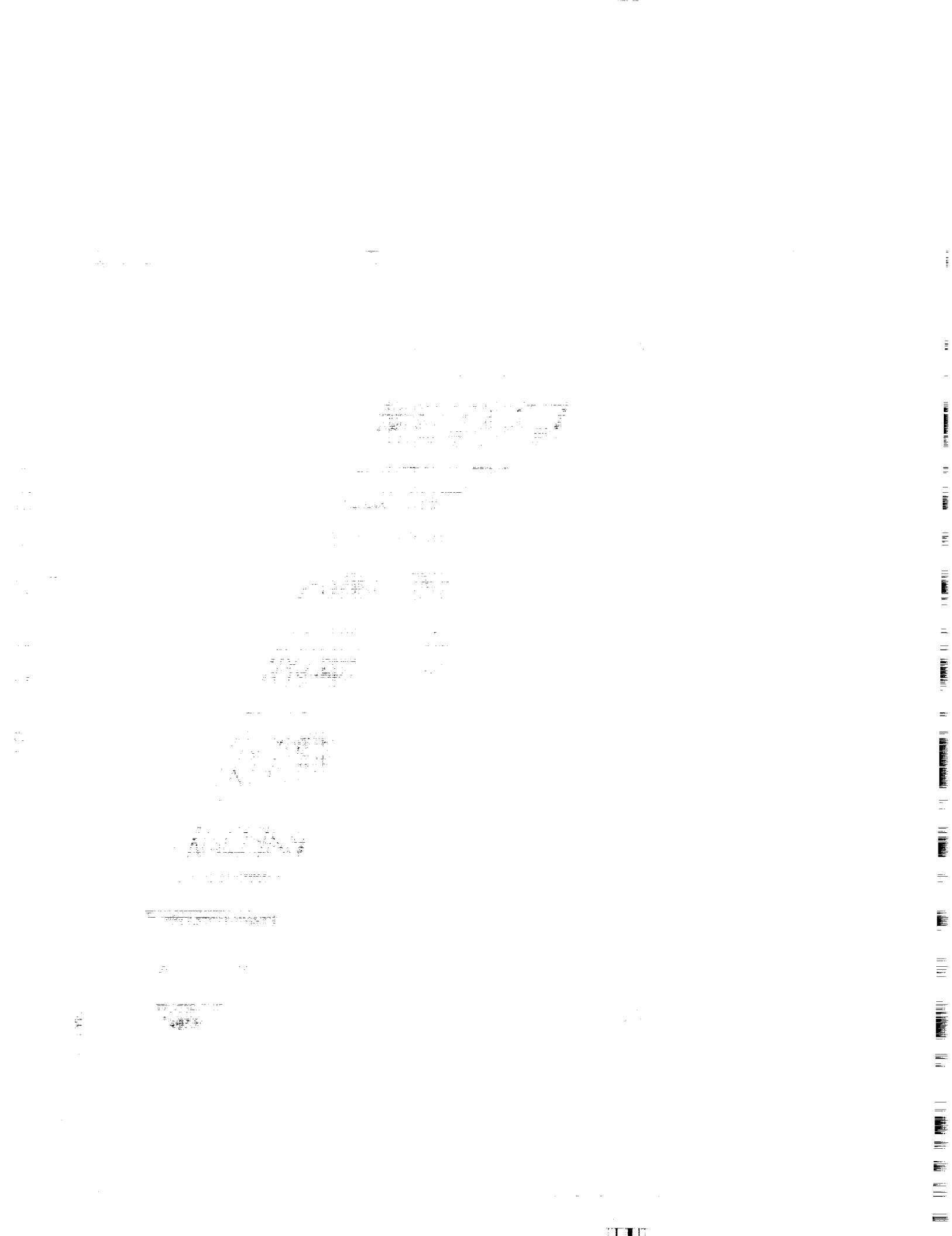

FIG. 5.8b

L-L
K-K
J-J
I-I
H-H
G-G
F-F
E-E
D-D
C-C
B-B
A-A
FOLDOUT FRAME
ORIGINAL PAGE IS OF POOR QUALITY
ORIGINAL PAGE IS OF POOR QUALITY
FOLDOUT FRAME

SURFACE OPERATIONS

by

David C. Cloughley

INTRODUCTION:

Large obstacles, high winds, and low temperatures are a few characteristics of the Mars environment which must be considered when analyzing landing and take-off maneuvers. After reviewing the different types of take-off and landing configurations, the following type seems to be the most favorable. The take-off of the Marsplane is achieved by the utilization of a rocket cart. The Marsplane is anchored on top of the cart, while the cart is guided down the existing runway by the use of steel cables. When taking off, a rocket thruster on the back of the cart is fired; subsequently, the cart and Marsplane both begin to accelerate down the runway. When the lift-off speed is obtained, the Marsplane lifts off the cart and begins to climb to it's design flight altitude. Landing the Marsplane will be similar to the procedure of landing a glider. The Marsplane will descend, after clearing the required obstacle, and land on a single wheel. The Marsplane will come to a stop by using a single wheel conventional braking system.

Definition of terms:

a_L = Deceleration During Landing

a_{TO} = Acceleration for Take-Off

C_D = Lift-Off Drag Coefficient of Marsplane

C_{Dc} = Lift-Off Drag Coefficient of the Cart

C_{LA} = Approach Lift Coefficient

C_{LF} = Flare Lift Coefficient

C_{LCL}	= Climb Lift Coefficient
C_{LLO}	= Lift-Off Lift Coefficient
C_{Lmax}	= Maximum Climb Angle
cm	= Centimeters
D_A	= Drag on the Marsplane at Take-Off
D_C	= Drag on the Cart at Take-Off
g	= Gravity on Mars
h_{ob}	= Obstacle Height
m	= Meters
N	= Newtons
ρ_M	= Density of Mars
ρ_{mmh}	= Density of Mono Methyl Hydrazine
ρ_{N2O4}	= Density of Nitrogen Tetraoxide
R	= Radius of Flight Path
rpm	= Revolutions Per Minute
S	= Planform Area of Wing
S_A	= Distance Covered on Approach
S_F	= Distance Covered on Flare
S_G	= Ground Roll Distance
S_R	= Distance Covered during Rotation
S_{TO}	= Total Distance
S_{TR}	= Distance Covered During Transition
W_{fuel}	= Weight of Fuel
W_g	= Weight of Marsplane
V_A	= Approach Velocity
V_{LO}	= Lift-Off Velocity
V_{stall}	= Stall Velocity
μ	= Ground Friction Coefficient
μ_b	= Frictional Braking Coefficient
γ_A	= Decent Angle of Approach
γ_C	= Climb Angle after Lift-Off
ϕ	= Diameter

DESIGN ANALYSIS :

Analyzing the various types of takeoff and landing configurations, the following environmental constraints and design limitations must be kept in mind. The Marsplane must take-off and clear a 15m obstacle after traveling 1000m. When landing, the Marsplane must clear a similar 15m obstacle before touchdown and still come to rest within 1000m of the obstacle. It is assumed that, a flat runway does exist on the planet and may be utilized.

The first proposal was having the Marsplane perform conventional take-offs and landings. The Marsplane would use only a propeller for the entire flight, including take-off. However, the problem was getting the Marsplane up to its take-off speed, using only the propeller and the limited take-off distance. When the propulsion system was unable to produce the necessary thrust to obtain the take-off speed an alternative system was sought. Analysis for the Marsplane to perform a vertical take-off and landing appeared the most logical.

With the employment of thruster rockets, the Marsplane could land and take-off vertically almost anywhere.[1] The thrusters analyzed were the same type as used on the Viking Landers. Though the hydrazine thrusters studied were small and light weight relative to other thrusters, the problem was that the Marsplane would have to use (2) 2500N thrusters in order to obtain the necessary lift-off speed. Also, the weight of the required fuel needed for one take-off and landing was over 1400N. This obviously did not seem feasible; therefore, this configuration was not chosen.

Since vertical take-off and landing maneuvers proved impractical, the following take-off and landing configuration is proposed. The take-off of the Marsplane is obtained by using a rocket cart, as shown in fig. 6.1. The rocket cart is 1.0m high by 1.0m long. The height of the cart is necessary in order to house the rocket thruster and it's needed equipment and to provide ground clearance for the Marsplane's propeller during ground roll. The cart is constructed out of steel bars and assembled in a cross-hatched way to insure the stability of the cart during its ground roll. The open box type configuration proves to produce less drag on take-off than a closed box type cart. Inside the cart sits a Sentry type high performance throttling rocket engine shown in fig. 6.2. Developed by TRW, this rocket is a high pressure, deep throttling, ultra fast response, bipropellant rocket engine.[2] The performance characteristics of the thruster are shown in Table 6.1. Also on the cart, in addition to

the thruster, are two propellant tanks, a water tank, and a battery, whose dimensions and specifications are shown in Table 6.2.

The overall take-off configuration is shown in Fig. 6.3. When taking off both the propeller is started prior to the thruster. The propeller is started initially in order to obtain the designed rpm for climb. The thruster is started by the pilot with an electrical switch, which sends 3.5 volts of direct current from the battery, which exists on the cart, to the thruster.

The cart is directed down the runway steel cables shown in Fig. 6.1. The cables are fed through the cart and extend down the length of the runway, before being secured in the Mars surface, as shown in Fig. 6.4. Fastened to the front of the cart is a steel plate shown in Fig. 6.1. This plate is employed as an "air dam" to prevent the cart from lifting off the ground during its high speed ground roll. The carts tires are made of Polyurethane. This type of solid tire is chosen instead of standard rubber air tires, because at low temperatures, like that on Mars, rubber air tires become extremely brittle.[3] Since there exist such a drastic change in the properties of rubber, at low temperatures, a solid type tire is best.

To obtain the necessary lift-off speed of 88.72 m/s, the rocket thruster will be fired for a 7.96 second duration during ground roll. This corresponds to a rocket cart ground roll distance of 353m at which time the rocket engine will be electrically shut off. The needed thrust to take-off is 14.391N; therefore, the rocket thruster will be working at 65% of maximum thrust. Calculations show that the combined total weight of both propellants is 204.1N, during take-off. The calculated acceleration of the Marsplane during the ground roll period is 11.15 m/s^2 or 2.96 g's. Considerations are taken so that the that the load on the wings, parallel to the velocity and acceleration vectors during take-off, do not exceed the structural stability of the wing.[4]

The Marsplane is to be seated on the cart at its climb angle of 3.33° above horizontal, which corresponds to 0.95(C_{Lmax}). This angle is necessary in order for the Marsplane to get lift when departing from the cart. This angling of the Marsplane on th cart also allows it to climb at its design climb angle without having to rotate upon lift-off. When the cart reaches the lift-off speed of 88.72 m/s the Marsplane is released from its sitting position by a simple clamp and the rocket engine on the cart is shut off. The Marsplane will continue to climb at 3.33° until it successfully clears the 15m obstacle at the end of 1000m runway. Is not compatible with missed approach climb given in Perf.

The landing procedure of the Marsplane will be similar to that of a glider, shown in fig. 6-3. After clearing the 15m obstacle the Marsplane will descend at an angle of 7.96° relative to the horizontal and at approach speed of 92.75 m/s. The

Marsplane will begin to flare, after passing the obstacle by 107.6m. This flare procedure will decrease its approach angle to one half its original value or 3.98°. Prior to touchdown the pilot will lock the propeller in a horizontal position and glide the remaining distance. Therefore, the final touchdown of The Marsplane will occur 160.1m after clearing the obstacle. After touchdown, the Marsplane will have a ground roll stopping distance of 839.9m. The Marsplane will be decelerating at at a rate of 5.486 m/s^2 and will actually come to a stop in 784 m.

The landing gear is a single wheel configuration, shown in fig. 6.5.[5] The landing gear consisting of a 0.25m diameter solid polyurethane tire, which weights 20N, and disc brakes to stop the Marsplane within the specified ground roll distance. A dampening shock consisting of a linear spring, is connected to the bottom of the fuselage and to the single wheel. This spring type landing gear is used to dampen out the vertical force component of 333.3N, when touchdown occurs. There also exist a smaller wheel, which weights 2N, near the tail, whose function is to stabilize the tail section during ground roll and to protect it from possible damage on poor landings. Considerations were taken when developing this useful landing dampening system. Due to the increase in fluid viscosity, by the low temperatures found on Mars, landing the Marsplane with any type of fluid shocks or air filled tires might prove to be disastrous.[3] Disastrous because typical oils become gels and rubbers become brittle at low temperatures, therefore a spring is used to absorb the energy when landing.

The boarding of the pilot occurs through the plastic window hatch, which is located on the top of the fuselage, as shown in fig. A. A small ladder is needed for the pilot to get in the Marsplane due to the height of the hatch location. The ladder will brace against the cart for stability when the pilot is climbing in. For the landing the pilot simply opens the hatch and steps out onto the ladder provided by the groundcrew.

Given the conditions of the Mars atmosphere, maintenance and servicing of the Marsplane will prove to be of vital importance to insure its' longevity. The Marsplane is equipped with a large bay door located on top of the fuselage to allow easy access to its internal components. This access is necessary for refueling fuel tanks, draining the water produced by the propulsion system and for periodic lubrication of mechanical parts. The maintenance of the wings and fuselage will occur as necessary. The open cage concept of the cart also allows for easy maintenance. Maintenance on the cart consists of refilling the propellant tanks, emptying the water tank and recharging the starter battery. Overall, testing needs to be performed to fully determine regular periods of maintenance and servicing for the vehicle and subsequent equipment.

CONCLUSION

This rocket cart type configuration was needed due to the high stalling speed and the corresponding high lift-off speed. Also, the thrust needed to achieve take-off was much too high to get from the propulsion system used for cruise condition. After reviewing other take-off configurations, the rocket cart system proves to be most feasible. When analyzing the landing of the Marsplane with the single wheel approach, the configuration seems to be the simplest and the most reliable way to stop the Marsplane. This simplistic light weight type design also helped keep the overall weight of the Marsplane low. After thorough investigation of this take-off and landing configuration, there are no foreseeable problems in ingress and egress procedures, operation of the systems, and the sizing of the equipment that can not be corrected at the base site, should the need arise.

Values Used During Calculations:

a_L	$= 5.486\ m/s^2$	R_L	$= 760.6\ m$
a_{TO}	$= 11.15\ m/s^2$	R_T	$= 13965.6\ m$
C_D	$= 0.0476$	S	$= 59.7\ m^2$
C_{Dc}	$= 0.0122$	S_A	$= 107.3\ m$
C_{LA}	$= 0.3625$	S_F	$= 52.79\ m$
C_{LF}	$= 1.45$	S_G	$= 784.0\ m$
C_{LCL}	$= 0.42$	S_R	$= 0.0\ m$
C_{LLO}	$= 1.5054$	S_{TOL}	$= 944.1\ m$
C_{Lmax}	$= 1.5846$	S_{TOT}	$= 1000\ m$
D_A	$= 148.23\ N$	S_{TR}	$= 647.1\ m$
D_C	$= 22.36\ N$	W_{fuel}	$= 750\ N$
g	$= 3.77\ m/s^2$	W_g	$= 4800\ N$
h_{ob}	$= 1.5\ m$	V_A	$= 92.75\ m/s$
ρ	$= 1.56 \times 10^{-2}\ kg/m^3$	V_{LO}	$= 88.72\ m/s$
ρ_{mmh}	$= 807.1\ kg/m^3$	V_{stall}	$= 80.65\ m/s$
ρ_{n204}	$= 1447\ kg/m^3$	μ	$= 0.04$
γ_A	$= 7.96^\circ$	μ	$= 0.5$
γ_C	$= 3.33^\circ$		

REFERENCES

1. AIAA Student Branch, "Aries," 1980 AIAA/Bendix Design Competition, June 1980.

2. Hardgrove, J., and Krieg, H., "High Performance Throttling and Pulsing Rocket Engine," AIAA/SAE/ASME, 20th Joint Propulsion Conference, Cincinnati, Ohio, June 1984.

3. Astle, M. J. and Beyer, W. H., CRC Handbook of Chemistry and Physics, CRC Press, Inc., Florida, 1983.

4. Allen, D. H., and Haisler, W. H., Introduction To Aerospace Structural Analysis, John Wiley and Sons, New York, 1985.

5. Currey, N. S., Landing Gear Design Handbook, Lockheed-Georgia Company, 1st Addition, January 1982.

Table 6.1 Sentry Type Thruster Data:

Design Thrust	22250N
Throttling Range	9:1
Design Life	12 yrs.
Weight of Thruster	127.5N
Propellants: Fuel	MMH
	(Mono Methyl Hydrazine)
Oxidizer	N_2O_4
	(Nitrogen Tetraoxide)
Mixture Ratio (O/F)	1.65
Firing Time	7.96 sec.
Command Voltage	3.5 volts dc.

Table 6.2 Additional Cart Equipment

Propellants :			
	Total Propellant Flow :		$15\ ^{m}/_{S}$
	Weight of propellants :		MMH = 77.02N
			N_2O_4 = 127.07N
	Volume OF Tank :		MMH = $42000cm^3$
			N_2O_4 = $23000cm^3$
	Dimension Of Tanks :		MMH = (12.20 x 90L) cm^3
			N_2O_4 = (9.020 x 90L) cm^3
Water Tank :	Volume	=	$65000\ cm^3$
	Dimension	=	(30w x 90L x 25H) cm
Battery :	Max. Volts	=	12 Volts dc.
	Dimension	=	(20.32w x 30.48L x 25.64H) cm

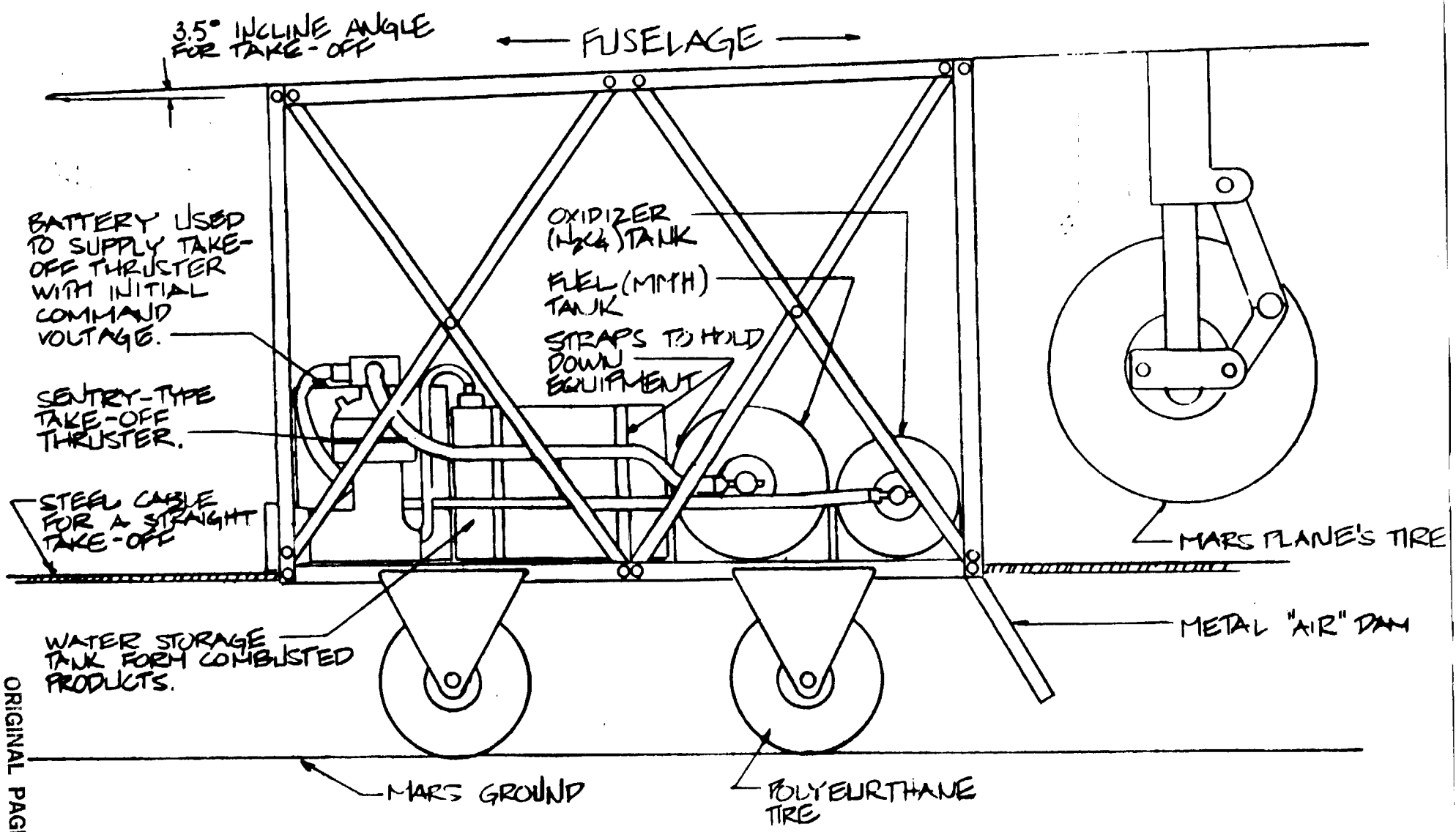

FIG. 6.1

TAKE-OFF CART CONFIGURATION

SCALE: 1" = 20 CM

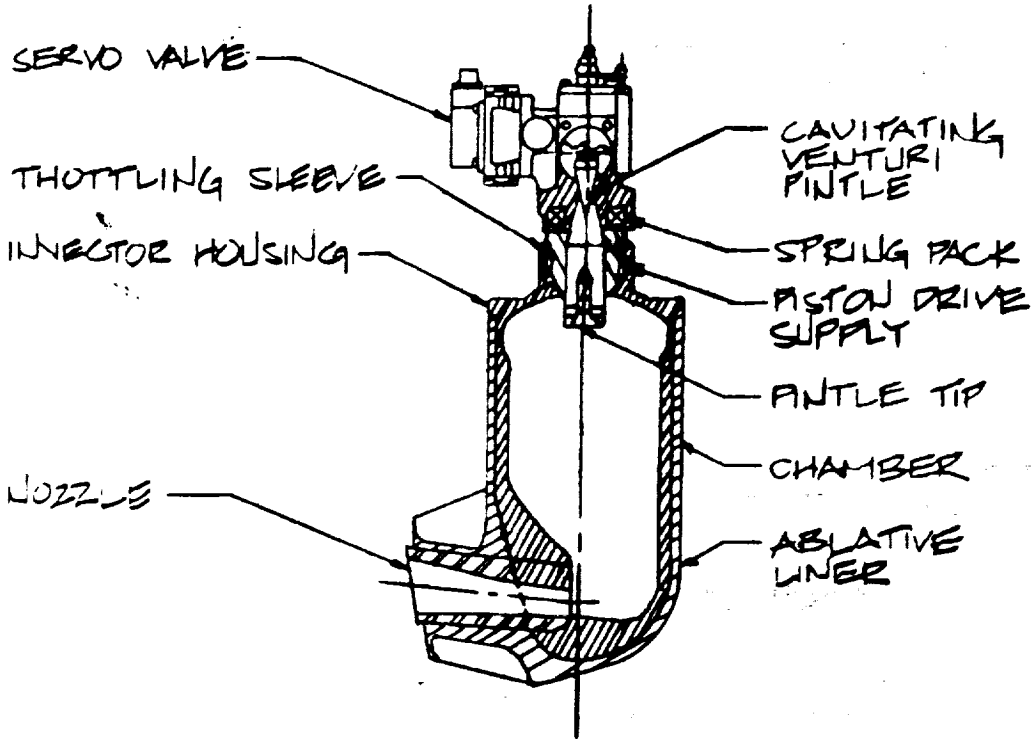

FIG 6-2 SENTRY TYPE TAKE-OFF THUSTER
SCALE: NONE

NOTE: TAKE-OFF WILL TAKE PLACE AS SHOWN. THE AIRCRAFT WILL BE STRAPED TO A ROCKET CART WHICH IS ON RAILS. THE AIRCRAFT WILL LIFTOFF AND CLEAR THE 15M. OBSTICLE WITHIN THE 1000M. RUNWAY.

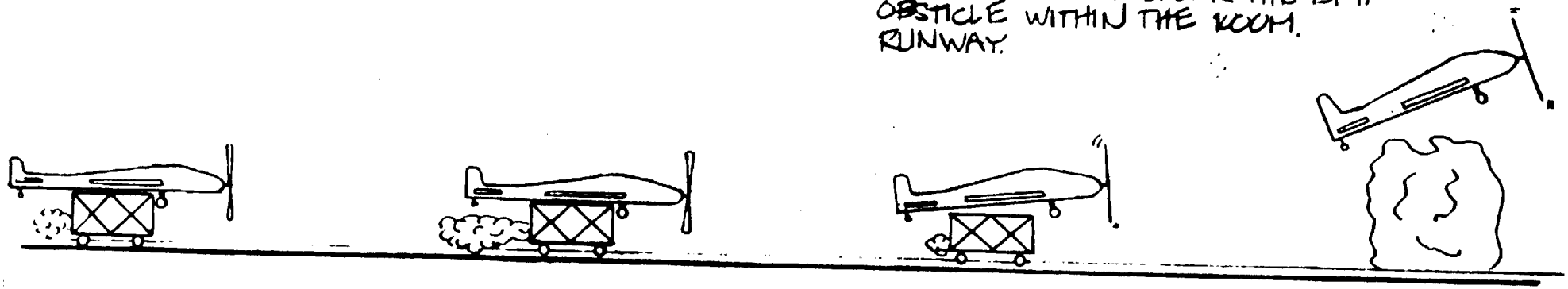

FIG. 6.3 TYPICAL TAKE-OFF PROCEDURE
SCALE: NONE

NOTE: LANDING WILL TAKE PLACE AS SHOWN. THE AIRCRAFT WILL CLEAR THE 15 M. OBSTICLE UPON ENTRY AND WILL COME TO REST WITHIN THE 1000M. RUNWAY. AFTER STOPPING THE CRAFT WILL REST ON ITS WING.

FIG 6.3 TYPICAL LANDING PROCEDURE
SCALE: NONE

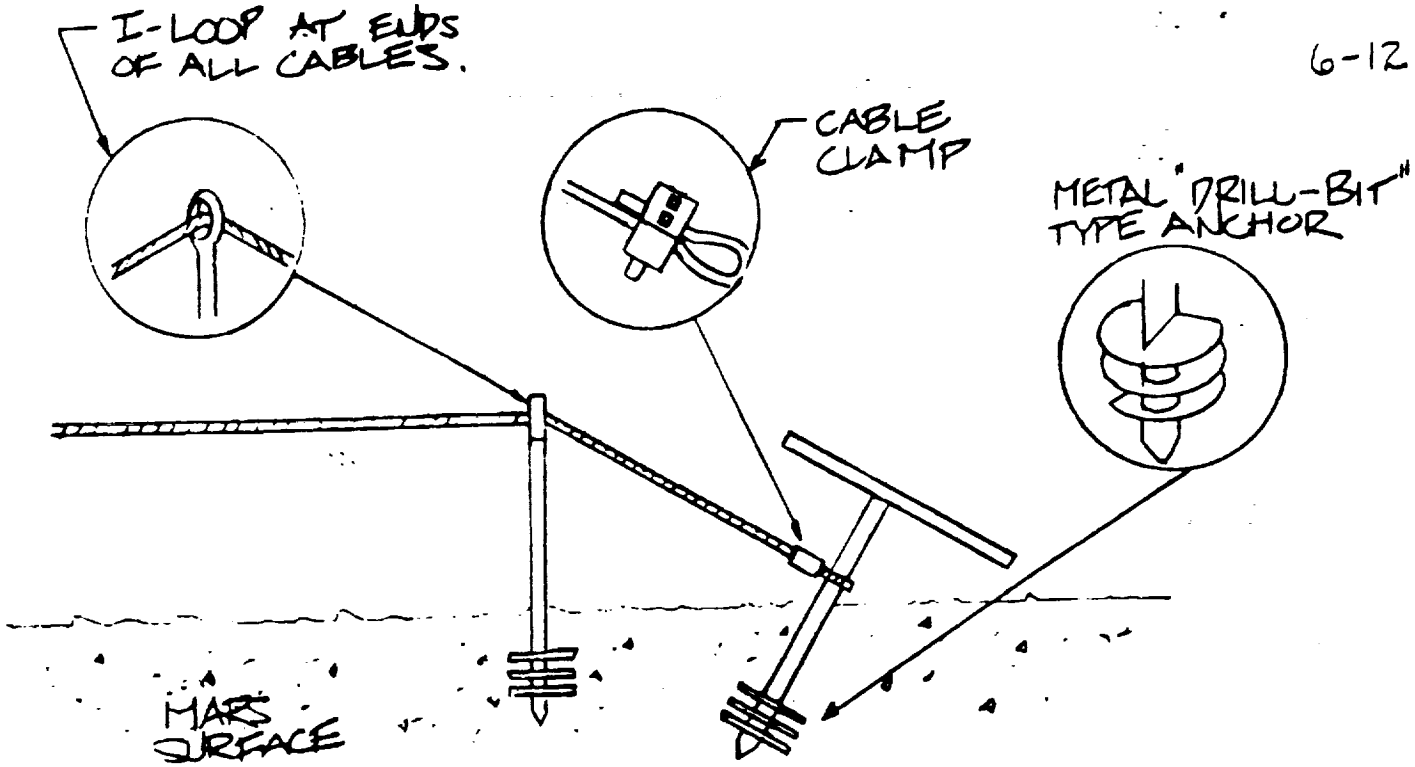

FIG. 6.4 MARS ANCHORING DETAIL
SCALE: NONE

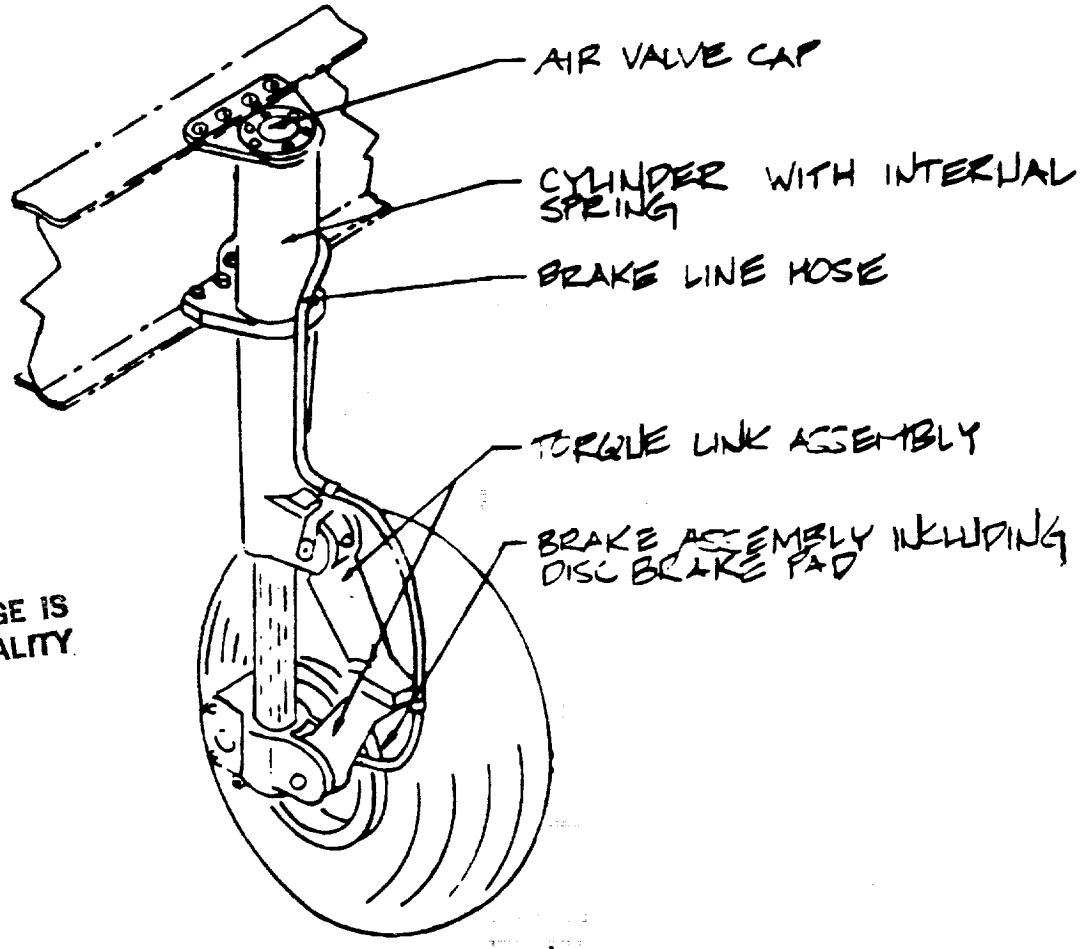

FIG. 6-5 EXTERNAL LANDING GEAR
SCALE: NONE

WEIGHTS AND BALANCE

by

Brian J. Fudacz

NOTE: ALL WEIGHTS ARE GIVEN ON MARS

INTRODUCTION:

The Marscraft has presented many problems to the weights group. The most obvious is the weight of the craft. The final weight of the craft is 800 N higher then the group originally estimated. Through out the design process of the craft, the weight steadily rose. The design group together decided on a goal weight of 4800 N. This weight was obtained and maintained. Keeping the center of gravity location within the acceptable range was done by simply rearranging the crafts major components.

DESIGN ANALYSIS:

The current weight breakdown for the Marsplane is given in table 7.1. W_g (gross weight) is calculated at 4800.0 N. This is only a twenty percent increase from our original goal. The initial sizing W_g was calculated to be 4000 N.

As the breakdown shows, the airframe structure group makes up 29.78% of the crafts W_g. The wing weight of 900 N was calculated by the structures group, while the the gear weight was calculated by the surface operations group. Both of these weights are exact calculations. The tail group, body group, and the nacelle group were calculated using Cessna and Torenbeek equations for weight estimation (Ref 1). The estimations for the tail and body group vary with W_g, while the nacelle group estimation varies with the total required take-off power. They were then reduced by 25% to account for composite use (Ref. 2). These estimations have been written into a

computer program designed to give W_g. The program performs a loop starting with a guessed value for W_g and continues until it converges to the true value of W_g. The weight group used 3000 N for its first guess. A counter in the program shows that 4 loops were needed for convergence at 4800.0 N (Ref. 3).

The propulsion system makes up 27.62% of the craft. All of these weights are exact figures as determined by the propulsion group. The only exception being the weight of the tanks. This is was estimated by the propulsion group. This wieght is based on the future development of high strenght, light weight plastics. The fuel cell weight is the sum of the three individual cells that provide power for the craft. Some of this power is used to operate the crafts fixed equipment.

The fixed equipment consists of the crafts furnishings, a camera system, and a highly sophisticated electronic control system. The furnishing weight is an estimation of a simple light weight seat and belts. The camera system will consist of a simple camera used to take photographs of the Martain surface. It will be controled by the crafts electronic control system. This system will also control the crafts electronic flight control system and its avionics, which is a small sophisticated air to ground radio. The radio will be incorporated into the pilots flight suit.

A central computer will operate the electronic control system (Ref. 4). A simple joy stick will allow the pilot to control the total craft and a computer screen will allow him or her to monitor all functions. The computer will process the pilots inputs, and control the crafts flight. Electro-hydrostatic actuators will be used to operate the crafts control surfaces, (Ref. 5) while the sail-wing's trailing edge cable will be controled by a simple motorized device. The weight of the actuators are included in the tail group, and the weight of the tension device is part of the airframe group. By taking into account flight conditions, desired performance, and drag minimization, the computer will be able to simpfly operations.

The operational items include the pilots weight, the fuel weight , and the rescue cargo weight. The design team decided the craft would carry one pilot who will drop rescue supplies to needing individuals. Therefore the weight of this cargo must be half the required payload. The fuel weight was determined by the propulsion group. These weights are all exact figures.

Table 7.2 lists the maximum take-off weight, the maximum landing weight, the operational empty weight, the useful load fraction, and the maximum fuel fraction. The maximum take-off weight and the maximum landing weight were

determined by the surface operations group, while the others were simple calculations performed by the weights group.

The center of gravity for the major components of the plane are presented in fig 7.1(Ref 6). The figure lists each component and gives the components distance from a reference line. This reference line is located one meter in front of the propellers center of gravity, an arbitrary distance. Once again these are only estimations.

Again the weight group has written a computer program to calculate the crafts overall center of gravity at the three different situations. These are all given in fig. 7.2. As shown by the figure, the crafts center of gravity fits into stability and control's acceptable range.

RERERENCES

1. Roskam, Jan Airplane Design Part V: Component Weight Estimation, Roskam Aviation, 1985.
2. Nicolai, L. Fundamentals of Aircraft Design, METS, Inc., 1975.
3. Program written in IBM Basic
4. Stengel, R. "Time To Reinvent The General Aviation Aircraft" Aerospace America, Vol. 25, No. 8, August 1987, pp.24-27.
5. "New Products And Literature", Aerospace America, Vol. 25, No. 9, Sept. 1987, pp. 64.
6. Roskam, Jan Airplane Design Part V: Component Center of Gravty Estimation, Roskam Aviation, 1985.

GROUP WEIGHT BREAKDOWN

table 7.1

GROUP INDICATION	WEIGHT (N)	MOMENT ARM x (m)	%
AIRFRAME STRUCTURE			
WING GROUP	900.0	3.0	18.75
VERT. TAIL	24.0	9.4	0.50
HOR. TAIL	61.5	10.06	1.28
BODY GROUP	400.0	2.9	8.33
FRONT GEAR	20.0	2.8	0.42
REAR GEAR	2.0	10.06	0.04
NACELLE GROUP	21.9	1.3	0.46
TOTAL	**1429.4**		**29.78**
PROPULSION GROUP			
MOTOR	45.9	1.3	0.96
GEAR BOX	59.7	1.15	1.24
FUEL CELLS	1029.0	3.86	21.44
FUEL &WATER TANKS	50.0	6.18	1.04
PROPELLER	141.0	1.0	2.94
TOTAL	**1325.6**		**27.62**
FIXED EQUIPMENT			
ELECTRONIC CONTROL SYS.	80.0	1.61	1.67
FURNISHINGS	11.0	2.3	0.23
CAMERA EQUIPMENT	4.0	2.3	0.08
TOTAL	**95.0**		**1.98**
OPERATIONAL ITEMS			
PILOT	600.0	2.3	12.50
RESCUE CARGO	600.0	8.5	12.50
FUEL	750.0	6.18	15.62
TOTAL	**1950.0**		**40.62**
			100.00
GROSS WEIGHT	**4800.0**		

RELATED DATA

table 7.2

MAXIMUM TAKE-OFF WEIGHT	4800.0 N
OPERATING EMPTY WEIGHT	2850.0 N
MAXIMUM LANDING WEIGHT	4800.0 N
USEFUL LOAD FRACTION	0.25
MAXIMUM FUEL FRACTION	0.156

COMPONENT & CENTERS OF GRAVITY BREAKDOWN fig 7.1

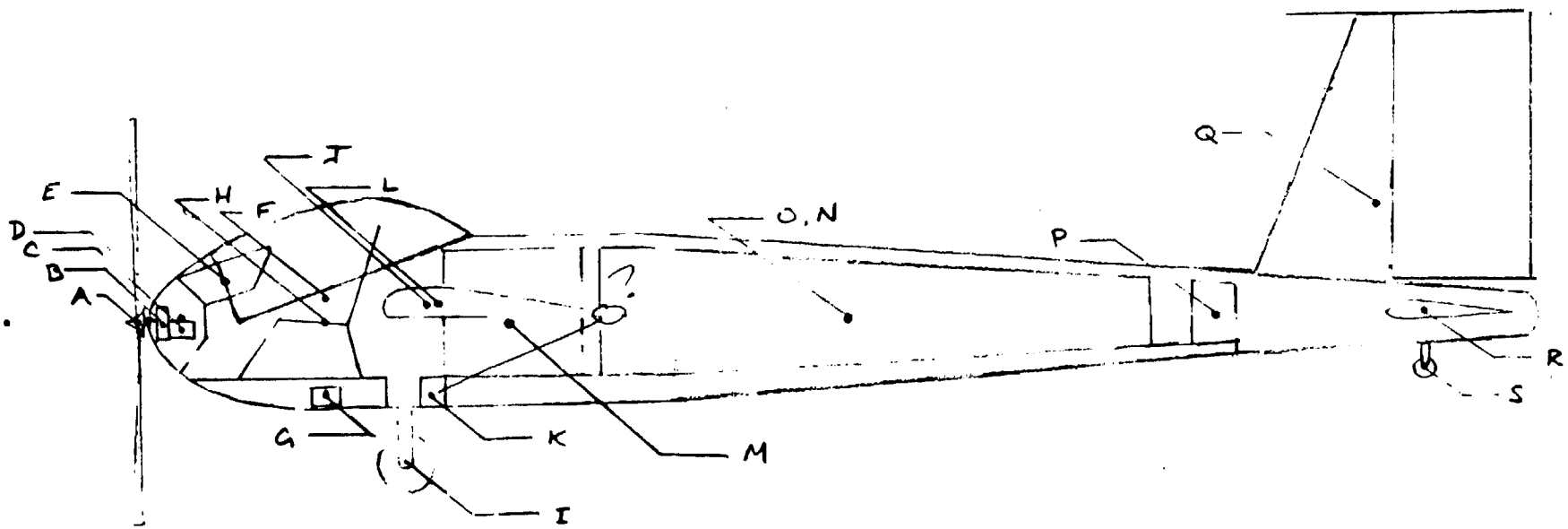

COMPONENT	C.G. LOCATION (m)	COMPONENT	C.G. LOCATION (m)	COMPONENT	C.G. LOCATION (m)	COMPONENT	C.G. LOCATION (m)
A=PROPELLER	1.0	F=PILOT	2.3	K=TENSION DEVICE	2.9	P=CARGO	8.5
B=GEAR BOX	1.15	G=CAMERA	2.3	L=WING	3.0	Q=VERT. TAIL	9.4
C=MOTOR	1.3	H=FURNISHING	2.3	M=FUEL CELLS	3.86	R=HOR. TAIL	10.06
D=NACELLE	1.3	I=FRONT GEAR	2.8	N=TANKS	6.18	S=REAR GEAR	10.06
E=CONTROL SYS.	1.61	J=AIR FRAME	2.9	O=FUEL	6.18		

CENTER OF GRAVITY TRAVEL

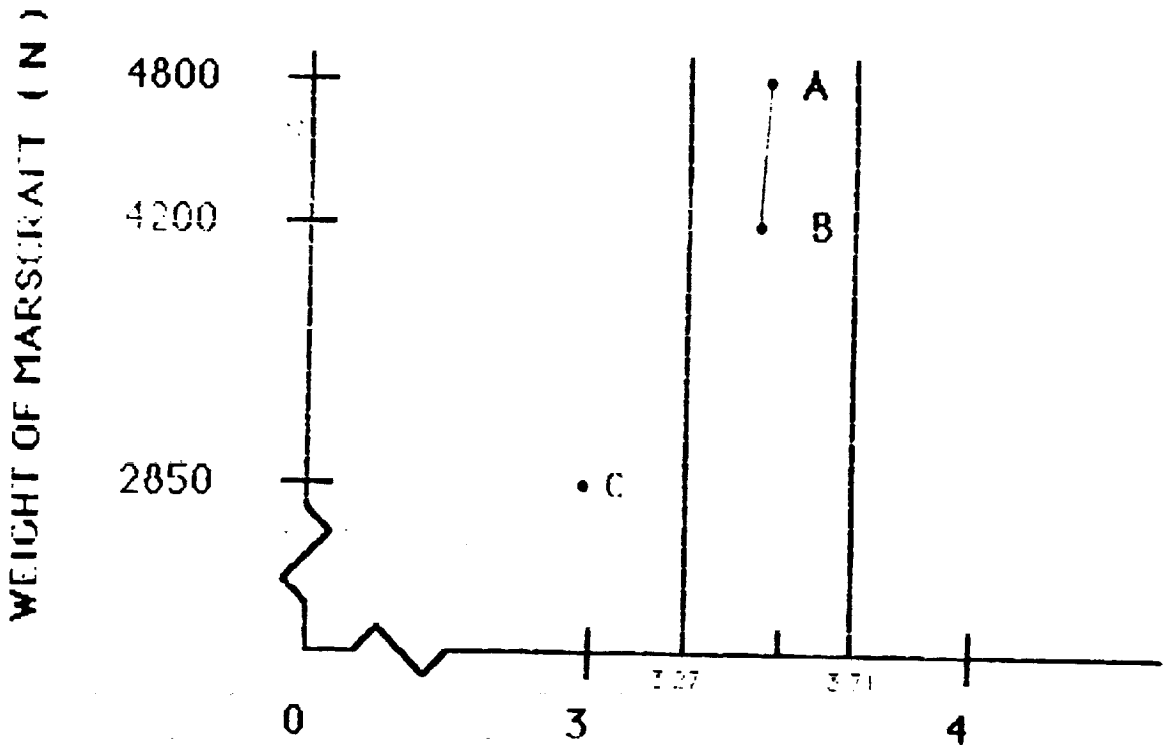

3.27 m -> forward limit

3.71 m -> aft limit

A -> pilot and payload at 3.47 m

B -> pilot with no payload at 3.45 m

C -> empty weight at 2.98 m

Assembly of Pteridactol on Mars

by

Greg Cimmarusti

A severe problem which had to be overcome in the design of the Pteridactol was shipping it to Mars. The Marsplane has to first fit in the Space Shuttle cargo bay, and second in the aerobrake designed by the Spacecraft's section. It is obvious from th beginning that the wings, with their incredible span, have to separated from the plane. What wasn't obvious until just recently was the fact that the horizontal tail span would also be too large to fit. A somewhat simple, but seemingly efficient way to solve the wing problem was approached. Each wing would be an entire separate piece containing the leading edge spar, sail fabric, trailing edge cord and ribs. An extra 0.6m of spar was added to the length at the root of the wing for attachment purposes. This section of the spar was designed to slide tightly into the fuselage. The fuselage was structurally designed to accommodate the spar. After sliding into the fuselage, the spars will meet in the center and be bolted properly into place. For access to the spar connection, the backrest of the pilot's seat can be tilted forward. Where the sail section of the wing ends it is attached to a thin metal plate. This plate will press flat against the fuselage and be bolted to it to keep the sail section in place. The trailing edge cable will pass through a small hole in the fuselage and run to the varying tension motor. For detailed drawings of the assembly, see figs. 5.7, 5.8a and 5.8b. The problem of the tail was approached differently. To each side of the fuselage the horizontal tails will be hinged. When packaged, the tails will be rotated up to a vertical position and lie against the vertical tail. When pulled down into place they are safely and tightly locked and extra supports are added. These methods will enable the Marsplane to be packaged small enough to accommodate the given sizing.

Cost

by

Sonja Schillmoeller

Cost was evaluated using a LOTUS program supplied by Michael Lembeck. The analysis was broken down into seven categories: structures, thermal, attitude control and determination, reaction controls, communication and data handling, electrical power, and propulsion. The breakdown, in terms of weight in kilograms, of each of these categories was as follows:

Structures	386 kilograms
Thermal	0 kilograms
Attitude Control	21 kilograms
Reaction Controls	0 kilograms
Communication	1 kilograms
Electrical Power	0 kilograms
Propulsion	345 kilograms

After application of the program, the total cost of the Pteridactol assumed a value of 195.8 million dollars. The numbers, in terms of millions of dollars, are summarized on the following page.

	DDT&E	FHA	TOTAL
Structures	35.2	8.9	44.1
Thermal	0	0	0
Attitude Control	21.9	4.9	26.8
Reaction Controls	0	0	0
Comm. & Data Handling	.7	.1	.8
Electrical Power	0	0	0
Propulsion	.5	0	.5
SUBTOTAL	58.2	13.9	72.2
System Test Hardware	21.3	0	21.3
System Test Ops	14.8	0	14.8
Software	0	0	0
GSE	12.4	0	12.4
SE&I	12.6	3.1	15.7
Program Mngmt.	7.8	1.2	9.0
SUBTOTAL	127.2	18.2	145.4
Contigency	25.4	3.6	29.1
FEE	15.3	2.2	17.4
Program Support	3.4	.5	3.8
TOTAL	171.3	24.5	195.8

MARS ENVIRONMENT

by

Jim Mocarski

The Marstian atmosphere is among the most important parameters to be considered when attempting to design a plane to fly there. Due to the low density of the atmosphere (about 1% of that at sea level on earth) large wing areas with low wing loadings will be required. Subsonic speeds and and low power required are also limitations placed on a marsplane by the atmosphere. The speed of sound on Mars is also significantly lower than on Earth, (about 70%). This will place limitations on propeller rpm's if not to exceed the limiting tip mach number.

The density is not the only characteristic of the Mars atmosphere needed to be considered. The atmosphere is mainly CO_2. This requires the power system to be non-airbreathing. This places limitation on the endurance of the Marsplane. Low tempuratures on Mars force materials selection to be done carefully as well as fuel cells and avionic equipment. High wind velocities will pose a problem in controls and stability.

So it is quite evident that the environment in which the **Pteridactol** will be flying is a harsh one and a parameter which needs to be considered in the design.

give data needed for analyses

Packaging of the Pteridactol for Mars Deployment

by
John Blackwood
Greg Cimmarusti
David Cloughley

Considerations had to be taken into account when designing the Pteridactol to insure that it would fit inside the cargo capsule provided by the spacecraft section. The ability to deliver the entire plane in one drop would be advantageous to all involved. The dimensions of the cylindrically shaped capsule are 60 ft. long with a 15 ft. diameter. The wings are not yet attached to the fuselage and will be packaged from corner to corner. The wings will cross at the center of the capsule and will lie over the fuselage. The horizontal tails fold up next to, and are strapped to, the vertical tail. The fuselage sits on the bottom and is held in place by straps placed over the fuselage at various points. A clamping device is used to hold each wheel stationary. The empty weight of the plane is 2850N. There is also 1000N of fuel stored in heat resistant pressurized tanks. It is assumed the braces and supports for the packaging weighs 100N. A4800N weight was allocated for the capsule which allows for 850N of supplies to be delivered to the base. For a better understanding of the packaging see fig.B.

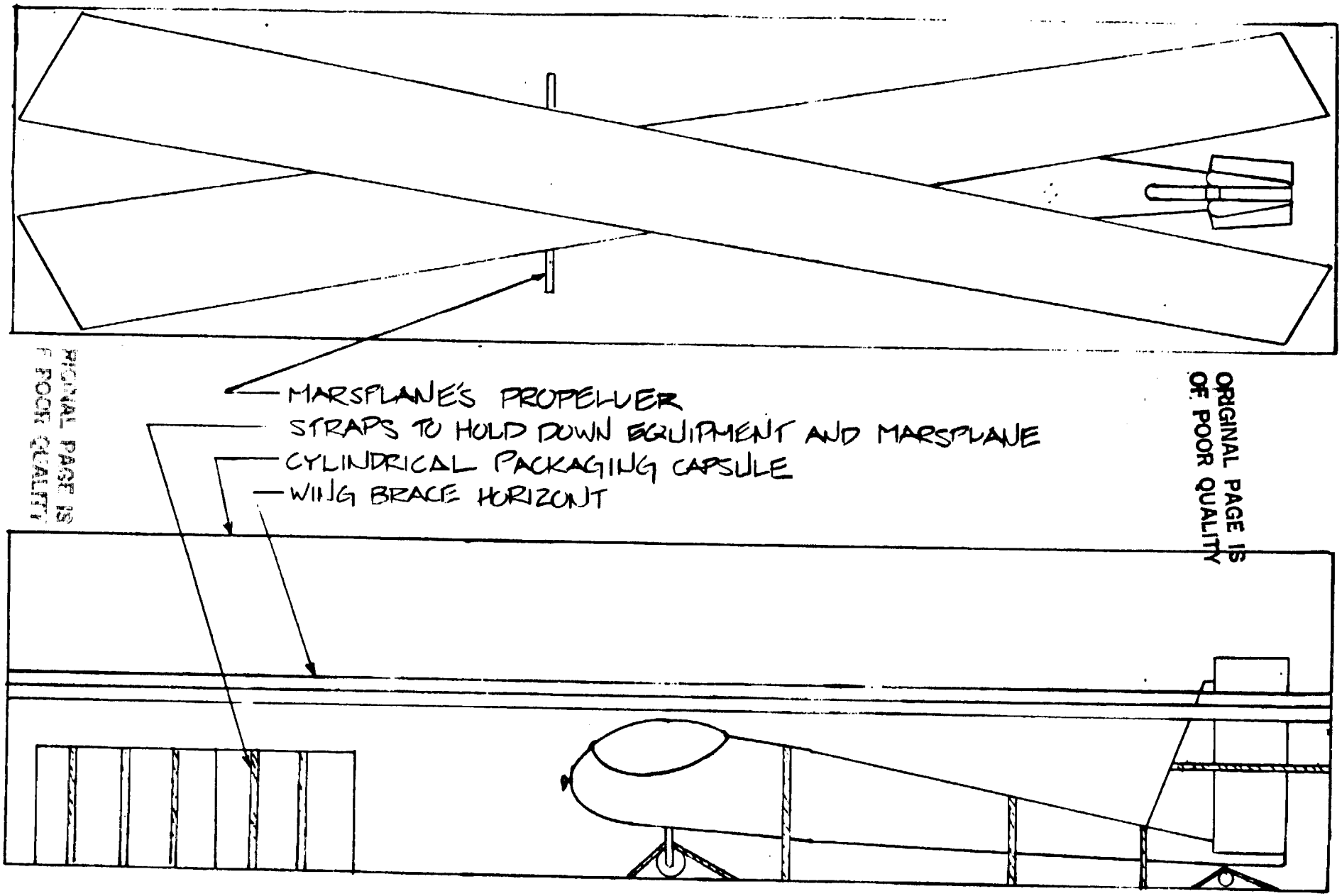

FIG. B PACKAGING OF THE PTERIDACTOL
SCALE: 1.0 CM = 72.0 CM

Rescue Scenario

by
John Blackwood

The rescuing of a stranded crewmember has been a significant problem in the design of the Pteridactol. Since it is not able to land and take-off again without a runway and support equipment, the crewmember cannot be picked up. Instead of retrieving the person the Pteridactol is designed to carry a life support package which can be dropped by the pilot from the plane. This package will contain food, water, oxygen and protection from the harsh elements in order to keep the person safe long enough for groundcrews to arrive. The survival kit weighs 600N and is located near the rear of the plane. Under the fuselage is a mechanically operated cargo door from which the kit is dropped and subsequently parachuted to the ground. The cargo door size and location can be seen in figs. A, 5.8a and 5.8b. The door consists of a cable and latch assembly. This scenario should allow ground crews ample time to locate and reach the stranded crewmember.

The parachute should have been urged.

89 PAGES

MANNED MARS RECONNAISSANCE AIRCRAFT:

FINAL DESIGN REPORT

GROUP 7

Craig Barton, Project Coordinator
Nathan Fawer, Aerodynamics
Rick Kreiger, Performance
Paul Martin, Power and Propulsion
Jim Sullivan, Stability and Control
Kevin Klein, Structures
Wally Lee, Surface Operations
Craig Barton, Weights and Balance

AAE 241
22 April 1988

Group 7 MMRA.2 Overview

Craig A. Barton

Group 7 has designed the Manned Mars Reconnaissance Aircraft; Design 2 (MMRA.2) to operate efficiently and effectively in the vastly different atmosphere of Mars. The groups design philosophy was that the aircraft must be simple enough and rugged enough to perform on a day-to-day basis. Advanced design techniques were employed, but overall the design is rather conservative stressing a simple design rather than futuristic configurations.

Design Requirements

The group was given several design requirements that needed to be met for the design to be considered successful. These included a 1200 N payload, the ability to operate from a 1km, preparted airstrip, and an eight hour endurance. Additional requirements include the ability to rescue a stranded astronaut. The entire aircraft must be able to be packaged in the 18.3m long and 4.57m diam. shuttle bay.[1] All of these requirements have been met by this design.

The group imposed additional restrictions upon the design. A gross weight of less than 5000 N was needed to keep power requirements at a managable level. The aircraft also had to have excellent visibility from the cockpit. Finally, the aircraft had to be servicable by personnel on Mars.

Configuration

The MMRA.2 is basically a reconaissance vehicle. It has a 1213 N payload (pilot+payload) ability, and can perform veritcal take-offs and landings (VTOL).THe design incorporates an advanced fly-by-wire flight control system and a very "user-friendly" cockpit. The cockpit instrumentation is only four CRTs which display aircraft data. These CRTs as well as many of the aircraft functions are controlled by pilot voice commands.

The propulsion system uses two 35kW electric motors. These are powered by a powerful battery capable of powering the aircraft for eight hours or more. The use of two engines offers safety for the pilot as the

aircraft is flyable with only one engine operating. The Viking system allows the aircraft to make VTOLs to take samples or perform a rescue. The high wing gives clearance from the rough terrain and leaves the pilot with an excellent view down.

Future

Much more work would have to be done to develop this aircraft into a production model. What Group 7 has designed is a very feasible configuration based on simplicity and effectiveness. Several problems are still lingering, however, such as the control problems associated with the vertical maneuvers. Overall, the aircraft has met or exceeded all of the design requirements placed upon it by the course and the group.

References/Notes

[1] Unfortunately, this requirement was cut in half four days before the project was due. The aircraft was designed to fit into the original cannister but can not be made to fit into the new, smaller cannister. Obviously, this is a problem that would have to be resolved if the design process is to continue.

Mission Scenario

Craig A. Barton

The MMRA.2 was designed to complete three basic missions with the flexibility to perform many duties. These missions fall under two basic categories, data/sample gathering and a rescue mission. They are differentiated by distinct aircraft configurations.

Mission 1 is a data gathering mission. In this configuration the aircraft has a pilot and a full of instruments, atmospheric samplers, experiments, etc.... Only enough fuel for one vertical take-off is put onboard. The aircraft performs a vertical lift-off at the start of the mission. This is followed by up to eight hours of cruise during which data is being gathered. The aircraft then returns to base for a conventional landing. Mission weights are shown in Table MS.1.

Mission 2 is a sample collection mission. The purpose of this type of mission is to collect soil and rock samples from distant sites for analysis by scientists. For this mission part of the payload is left empty for the samples. The mission profile is a vertical take-off followed by a cruise to the "sample site". A vertical landing in the field is performed and samples are collected. This is followed by a vertical lift-off and a cruise home for a conventional landing. Table MS.1 has a detailed mission weight breakdown.

The third mission, Mission 3, is a rescue mission. For this mission it is assumed that no payload will be onboard, other than possibly medical or life-support equiptment. The hydrazine tanks will be filled for three vertical maneuvers. A vertical lift-off is followed by a cruise to the stranded astronaut. The aaircraft lands vertically and the "passenger" is put onboard. The cruise home to a conventional landing folows the vertical lift-off. Table MS.1 details weights for this mission.

TABLE MS.1

Mission Scenarios

Mission 1 Data Gathering
profile: VTO, cruise, conventional landing
mission weights: GTOW= 4725 N
cruise wt= 4641.8 N

Mission 2 Sample Collection
profile: VTO,cruise to site, VTOL, cruise to base
mission weights: GTOW= 4891.8 N
1st cruise= 4808.5 N
2nd cruise= 4641.8 N

Mission 3 Rescue Scenario
profile: VTO, cruise to site, VTOL, cruise to base
mission weights: GTOW= 4344.9 N
1st cruise= 4261.6 N
2nd cruise= 4681.8 N

AAE 241
Spring 1988
DESIGN DATA SUMMARY

Gross Weight: 4932 N
Wing Loading: 32.2 N/m^2
Maximum Fuel Weight: 108.8 N (battery wt)
Useful Load Fraction: .296

Maximum Take-off Power 62.3kW
Power Loading: .080 N/w
Fuel Fraction: .022 (battery)

Geometry

Ref. Wing Area = 153.1m^2
AR = 15.43
Λ_{LE} = 7.10 deg.
λ = 0.4
t/c = 0.1

Propulsion

Engine Description: 40kW electric
Number of Engines = 2
$P_{O_{max}}$ /Engine = 31.15
Weight/Engine = 148.2 N
c_p at Cruise =
Prop. Diam. = 8.2m
No. of Blades = two
Blade Cruise R_e = 148,600

Performance

Cruise R_e = 400,000
Cruise h = 1.5km
Cruise M = 0.36
Cruise V = 90 m/s
Take-off Field Length = N/A
Take-off Speed = N/A
Landing Field Length = 680m
Landing Speed = 68.5 m/s
Maximum Landing Weight = 4808.5 N
OEI Climb Gradient (%): = 1.83 deg.
2nd Segment = 1.55 deg.
Missed Approach = 1.83 deg.
Sea Level $(R/C)_{max}$ = 7.91 m/s

Aerodynamics

Airfoil: Wortmann FX-60-100
High Lift System: plain flaps

Cruise; C_{D_o} = .0197
e_o = .7996
C_L = 0.545
(L/D_{max}) = 19.9
Take-off; C_L = 0.889
$C_{L_{max}}$ = 1.308
Landing; C_L = .8295
$C_{L_{max}}$ = 1.402

Stability and Control

Static Margin Range = .10 to .378
Acceptable C.G. Range = 2.912m fore 3.630m aft
Actual C.G. Range = 3.294m to 3.356m

AAE 241
Spring 1988
INITIAL SIZING DATA SUMMARY
GROUP 7

Gross Weight: 3380 N

Wing Loading: 21.5 N/m^2

Fuel Weight: assumed battery power

Useful Load Fraction: .298

Maximum Take-off Power 31.9 kW

Power Loading: .106 N/kW

Fuel Fraction: N/A (battery power)

Geometry

Ref. Wing Area = 157.2m^2

AR = 15.03

Propulsion

Engine/Motor Type: 40kW electric

No. of Engines/Motors = one

$P_{o_{max}}$ /engine = 31.9kW

c_p at cruise = N/A due to use of battery power

Aerodynamics

Cruise; C_{D_o} = 0.020

e_o = 0.80

C_L = 0.426

$(\frac{L}{D})_{max}$ = unknown

Cruise Performance

h = 1.0km

V = 90m/s

Take-off; C_L = 1.240

$C_{L_{max}}$ = 1.50

Landing; C_L = 1.364

$C_{l_{max}}$ = 1.50

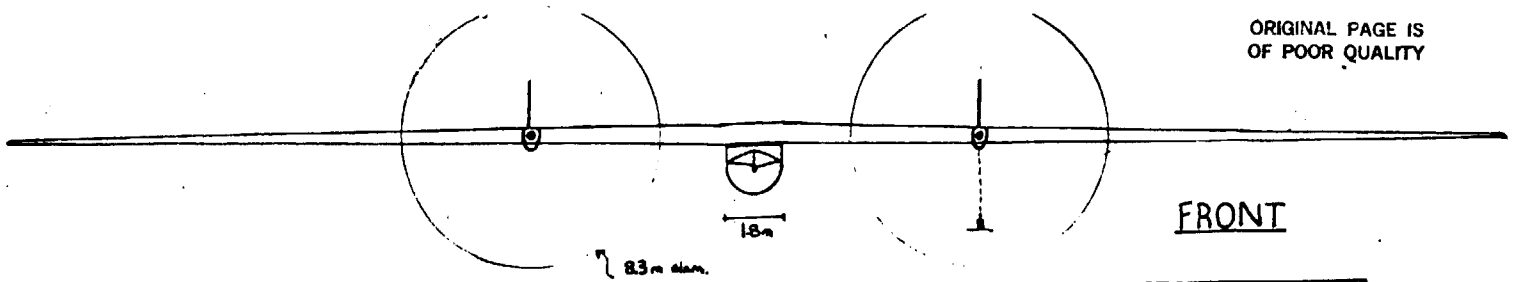

FRONT

ORIGINAL PAGE IS
OF POOR QUALITY

Aircraft Data	
W_g	1932 N
W_g/S	32.2 N/m^2
S	153.1 m^2
b	48.6 m
AR	15.43
P_{max}	623 W
W_g/P_{max}	.080 N/W

Scale

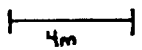

ALL DRAWINGS USE THIS SCALE

0.4m

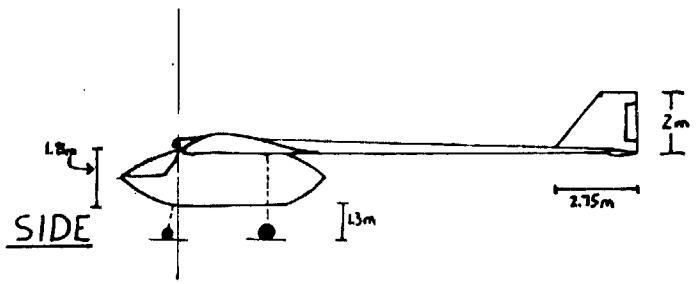

SIDE

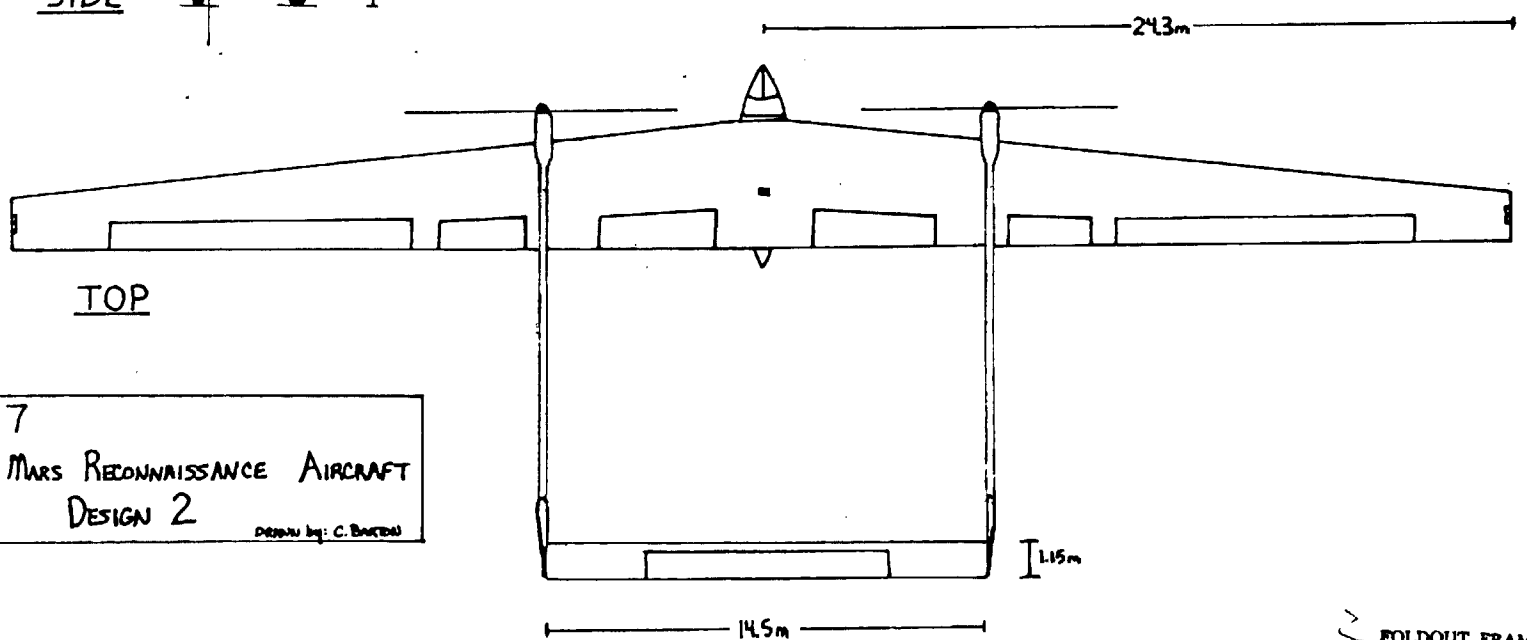

TOP

GROUP 7
MANNED MARS RECONNAISSANCE AIRCRAFT
DESIGN 2
Drawn by: C. Barkdoll

FOLDOUT FRAME

FOLDOUT FRAME

Aerodynamics

Nathan Fawer

Configuration

The Mars Aircraft is composed of a large wing with a box tail and a body at the center of the wing. The box tail was originally chosen to accommodate a single engine with a pusher propeller in the rear of the body. After a single engine was found to lack sufficient power, the box tail was kept because it provided good support for the large horizontal tail. The two engines were then placed in the wing in front of the tail booms.

The cruise condition is at 1.5 kilometers and 90 meters per second. The altitude was a given design condition. A high airspeed is desired because this keeps the lift coefficient necessary for flight low. However, the higher the airspeed, the higher the power required. After considering the wing lift curve and the power available, an airspeed of 90 meters per second was chosen.

The Wing

Flight in the Martian atmosphere is characterized by Reynolds Numbers much lower than those found on earth. The Reynolds Number for this design is approximately 400,000 at the wing root and tapers off to approximately 170,000.[3] Although few airfoils have been designed for these Reynolds Numbers, many of the airfoils designed for sailplanes and model airplanes have been tested at these low Reynolds Numbers. Initially, the Wortmann FX-63-137 airfoil was chosen because of the high maximum lift coefficient of 1.5.[2] However, this airfoil produced too much drag to be part of a practical design. The Wortmann FX-60-100 airfoil was chosen as a replacement; the maximum lift coefficient is 1.1 and the parasite drag coefficient is 0.015.[6] The wing has a span of 48.6 meters and an aspect ratio of 15.43. A taper ratio of 0.4 was chosen because the nearly elliptical loading will keep the induced drag low. The wing loading (fig. 5-1) was found using the Schrenk approximation, which was also used to find the sectional lift coefficient distribution (fig. 1-1).[1] The sectional lift coefficient reaches a maximum at about 15 meters out on the wing. It was believed that this would occur safely inboard of the ailerons, so wing twist was not used. However, final design of the ailerons proved this to be false. Therefore, the wing will need twist, but when this was realized, it was to late to incorporate it into the design. Wing dihedral will not be used because this design has a high mounted wing which produces the same affects as dihedral does. An equation in Reference 1 was used to compute the wing lift curve from the two

dimensional data (fig. 1-2). The maximum lift coefficient is 1.04 and to fly at cruise condition the wing needs an incidence angle of 2.6 degrees.

Drag

The drag polar for the aircraft is shown in fig. 1-3. The equation is $C_D = 0.0197 + 0.0258\ C_L$, where C_D is drag coefficient and C_L is lift coefficient. The parasite drag coefficient can be broken down as follows:

component	parasite drag coefficient
wing	0.015
tail booms	0.0007
horizontal tail	0.001
vertical tails	0.0002
engine nacelles	0.0002
body	0.0018
wing body interaction	0.0008

All parasite drag coefficients were found from equations in Reference 4 except for those of the wing and tail booms. The wing's value was taken from data in Reference 6, while the tail boom drag coefficient was found by assuming the booms to be a flat plate of equal surface area. The induced drag of the wing was calculated by using span efficiency factor data from Reference 5. The body and booms will also produce induced drag, however, the values are so small that they have been neglected. As the aircraft nears stall, flow separation causes the drag to rise. For the wing, data showed the parasite drag coefficient should rise approximately 0.01.[6] The rise due to the body and tail has been assumed to be equal to the rise from the wing, making the total drag coefficient rise 0.02.

Take Off and Landing

The aircraft will take off vertically; as it transfers to horizontal flight the lift will be increased by flaps deflected 25 degrees. The aircraft will land conventionally, with lift increased by flaps deflected 45 degrees and drag increased by flaps and landing gear. Using data supplied by Surface Operations, the lift curves have been found have been found for both configurations (fig. 1-2). The drag polars for the two configurations are almost identical; the take off configuration having slightly smaller drag coefficients. For this reason, only the polar for the landing configuration is shown. Drag data for the flaps was also supplied by Surface Operations. Drag data for the landing gear was obtained from Reference 4.

References

1 AAE 316 Class Notes, Prof. K. Sivier.

2 "The Effect of Trip Wire Roughness on the Performance of the Wortmann FX-63-137 Airfoil at Low Reynolds Numbers", Proceedings of the Conference on Low Reynolds Number Airfoil Aerodynamics, Notre Dame, IN, June, 1985, edited by T. Mueller.

3 Mars Atmosphere Profile, NASA, 1967.

4 Methods for Estimating Drag Polars of Subsonic Airplanes, Jan Roskam, 1974.

5 Airplane Aerodynamics, D. Domasch, S. Sherby, T. Connolly, 1957.

6 "The Design of Airfoils at Low Reynolds Numbers", AIAA Paper 85-0074, M. Selig, Jan., 1985.

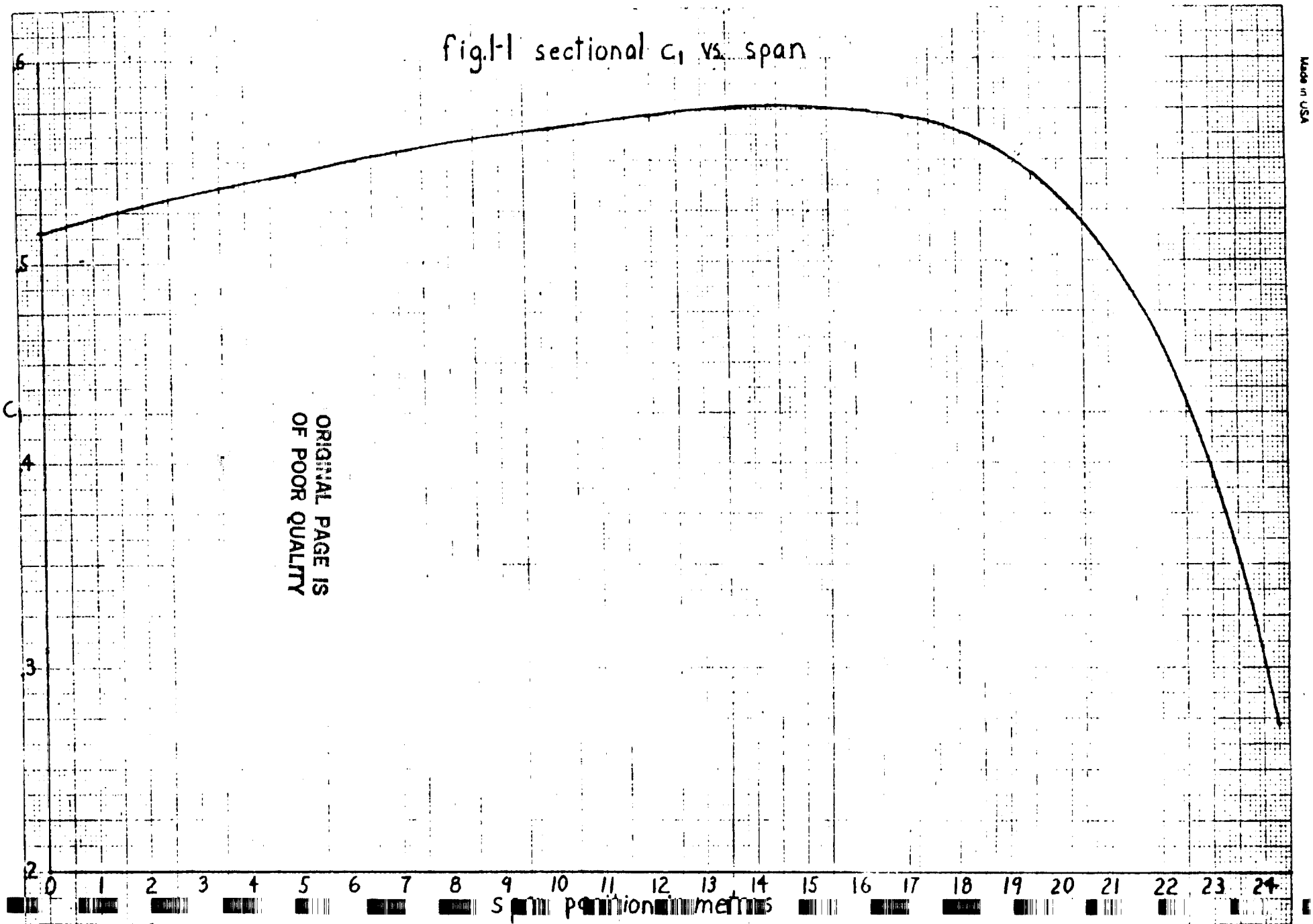

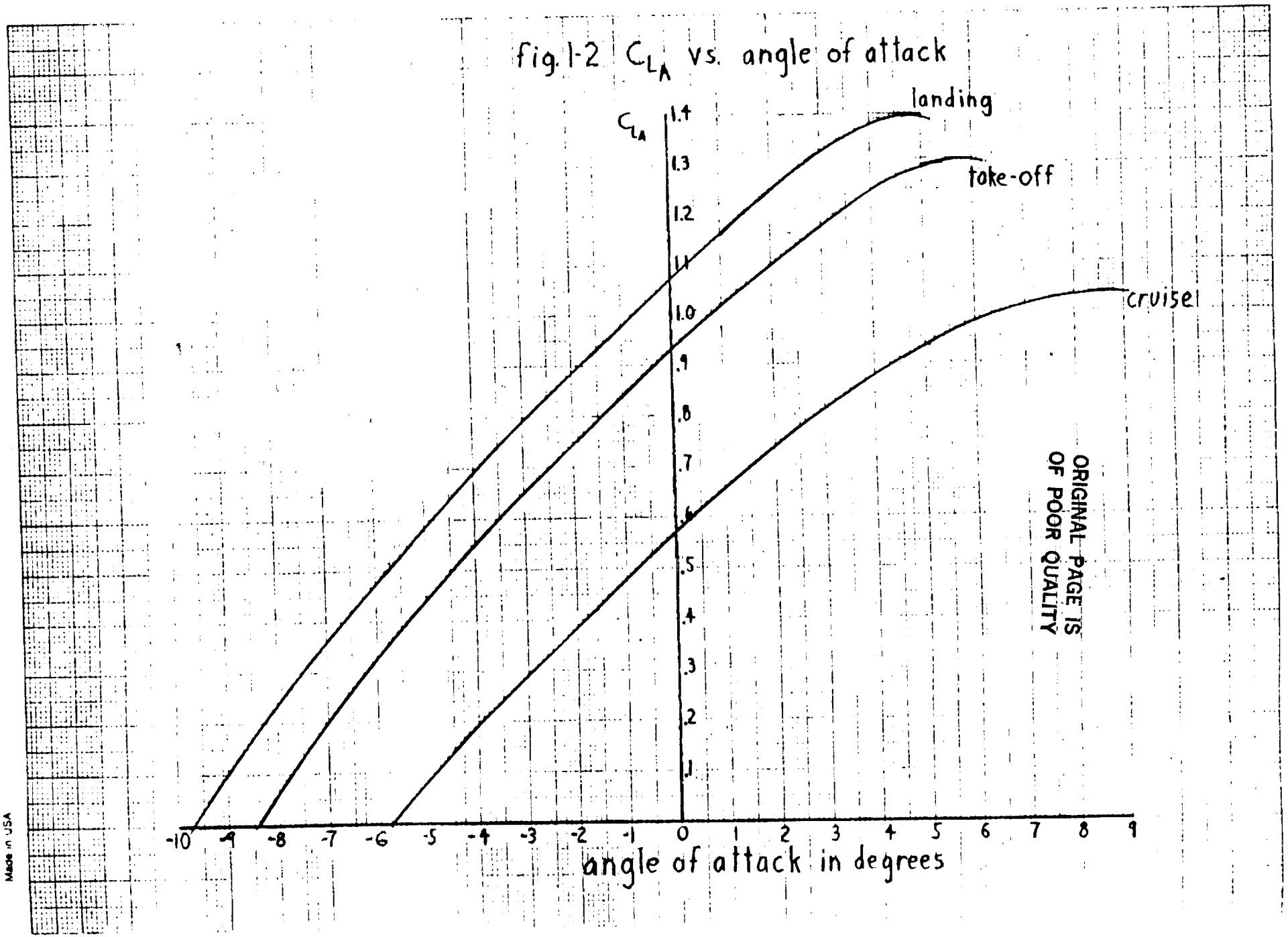

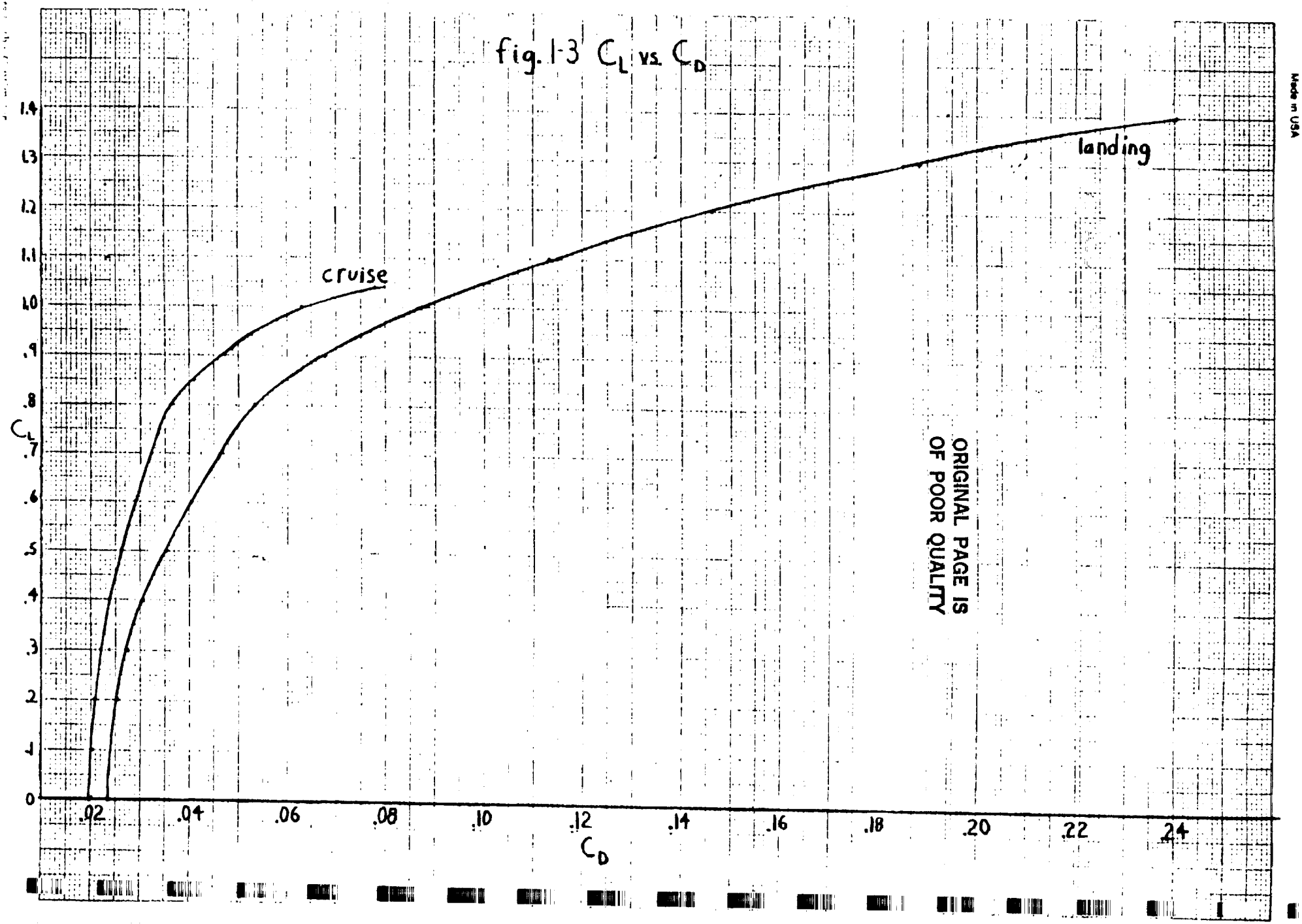

PERFORMANCE

Rick Kreiger

This current configuration of the aircraft is flying. Power available and power required versus velocity for sea-level and at the cruise altitude of 1500. meters are graphed in Figures 2-1 and 2-2. As shown by these graphs, even with only one engine, level flight can still be achieved. These power requireds are for the clean condition only. Since the aircraft will either land vertically or do a power-off conventional landing, no flap deflection or gear down drag is included in these figures. For explanation of the terms used on the figures, and also for terms used throughout this report, see Table 2-10.

PERFORMANCE CHARACTERISTICS

A numerical breakdown of the performance characteristics at sea-level and at 1500. meters is given in Table 2-8. This table, as are all tables except Tables 2-1 to 2-6, is done at

W=4808.5 N

the maximum weight after a vertical take-off. For the sea-level to 1500. meter range, it is apparent that the values do not change much. The largest change is in the maximum excess power, $(P_X)_{max}$, and the terms associated with it, $(R/C)_{max}$ and $(Gamma)_{max}$. It has a large change, from 38.0 to 31.7 kilowatts, a 17.% decrease. The velocities do not vary by more than 6.%. Also listed in the table is the absolute ceiling, which is 9190. meters. The service ceiling, which is when $(R/C)_{max}$ is 100 feet/minute, is calculated to be 8470. meters.

A complete breakdown of performance characteristics is given in the Flight Performance Envelope, Figure 2-3. This shows several items. The minimum velocity

at which flight can be achieved is the stall velocity all the way up to an altitude of 7600. meters. Also note the almost constant maximum velocity. Under 3600. meters, it only varies from 123. meters/second to 125. meters/second. Plotted on the graph is the velocity for maximum rate of climb. Since the $(C_L)_{max}$ of 1.0 is rather low (as compared to values on Earth), the lift induced drag is rather low for this aircraft. The low $(C_L)_{max}$ has raised the stall speed. This is why the velocity for $(R/C)_{max}$ is rather close to the V_{min} (or V_{stall}) line and follows it up in altitude.

MISSION PROFILE

The values for three mission scenarios are calculated, instead of just one. The missions are listed in detail in Table MS-1 in the mission section, with weight changes due to rocket burns and payload changes. Briefly, Mission 1 is a normal flight, with just a take-off, cruise, then landing. Missions 2 and 3 are a flight out, a landing in the field, then a flight back to base. Mission 2 is the delivery of a payload in the field, while Mission 3 is the rescue mission. For each mission two variations are presented. The first one is to completely exhaust the fuel supply, which in this case is battery power. The second variation is to end the mission with 10.% of the battery power in reserve, which is 6.34×10^7 Joules. The profiles for the three missions and two variations of each are given in Tables 2-1 to 2-6. The notes after Table 2-6, and Table 2-8 explain the flight conditions in detail.

The cruise is at 90. meters/second at an altitude of 1500. meters. It is a constant altitude and constant velocity. This can be achieved since the aircraft has two electric engines which run off of batteries. The only change in weights are due to payload changes and when the rockets burn, and they only burn in vertical take-offs and vertical landings. This is why there is no "fuel used" column in Tables 2-1 to 2-6. It is replaced by an Energy Used column. The total energy available for flight is 6.34×10^8 Joules. The cruise speed came out to be 72.% of the maximum velocity at 1500.

meters. This value can be found in Table 2-8.

The climbs and descents are all done at either $(R/C)_{max}$ (climb) or $(R/S)_{min}$ (descent). It was calculated in 5 segments, of 300. meter increments, except for the first climb, from 15. meters to 300. meters, and the last descent, from 300. meters to 25. meters, as listed in the notes to Tables 2-1 to 2-6. This increment was picked because it allowed a variation, while being flyable. A pilot will not be able to make a correction every 1. meters or even every 10. meters. The 300. meters should allow the pilot time to make changes, and still allow a climb that conforms to the optimum, infinitely many variation climb.

The descent at 5.% of power available was chosen for two reasons. A powered descent was desired, so the engines would not have to be restarted in an emergency. It was also decided to keep the sink angle around 2.0 degrees. As shown in Table 2-9, this is achieved at the power setting of 5.% of power available.

A quick comparison of the last two columns of Tables 2-1 to 2-6 shows the flight time and radius of operation, which is insightful. It shows that the values for the missions are approximately the same for the same reserve power condition. For 0.% reserve power, the endurance is approximately 8 hours and 25 minutes with a radius of operation of approximately 1350. kilometers. For 10.% reserve power, the values are 7 hours and 34 minutes, and 1214. kilometers. This group's design goal was an 8 hour endurance with 10.% reserve power. This was not met, but a quick interpolation of the presented findings shows that an 8 hour endurance would be achieved with approximately 5.% reserve power.

MISSED APPROACH PERFORMANCE

The performance for one engine in landing is given in Table 2-7. This is done with gear down and flaps in the landing condition. It is done at an altitude of 25. meters. This is when the gear and flaps are deployed, and when the engine is shut-off. The engine is shut-off because in touchdown the propeller will hit the ground before the

landing gear. At this point, the plane can climb at a $(R/C)_{max}$ of 2.3 meters/second. This is comparable to the $(R/S)_{min}$ of 2.71 meters/second from Table 2-9.

SUMMARY

The aircraft as it stands know is in good shape as far as performance is considered. It meets the endurance requirement with some energy to spare. It has the ability to climb and fly with one engine out. One problem is the vertical take-offs and landings. The values supplied from Surface Operations do not seem too realistic. To make them more realistic would be to increase the burn times, which would increase the fuel. By comparing the climbs and descents from different mission, however, which have different weights, it can be seen that a weight change of 300 Newtons or less would not have a great effect on performance. Another area to look into is the engines. Two engines offer a safety factor, but if a more powerful engine or a highly reliable engine is installed, the aircraft might need only one. This is based on its ability to fly now (although poorly) on one engine. Two engines are preferred, however, basically for the safety factor.

Figure 2-1: P_A and P_r versus V at sea-level

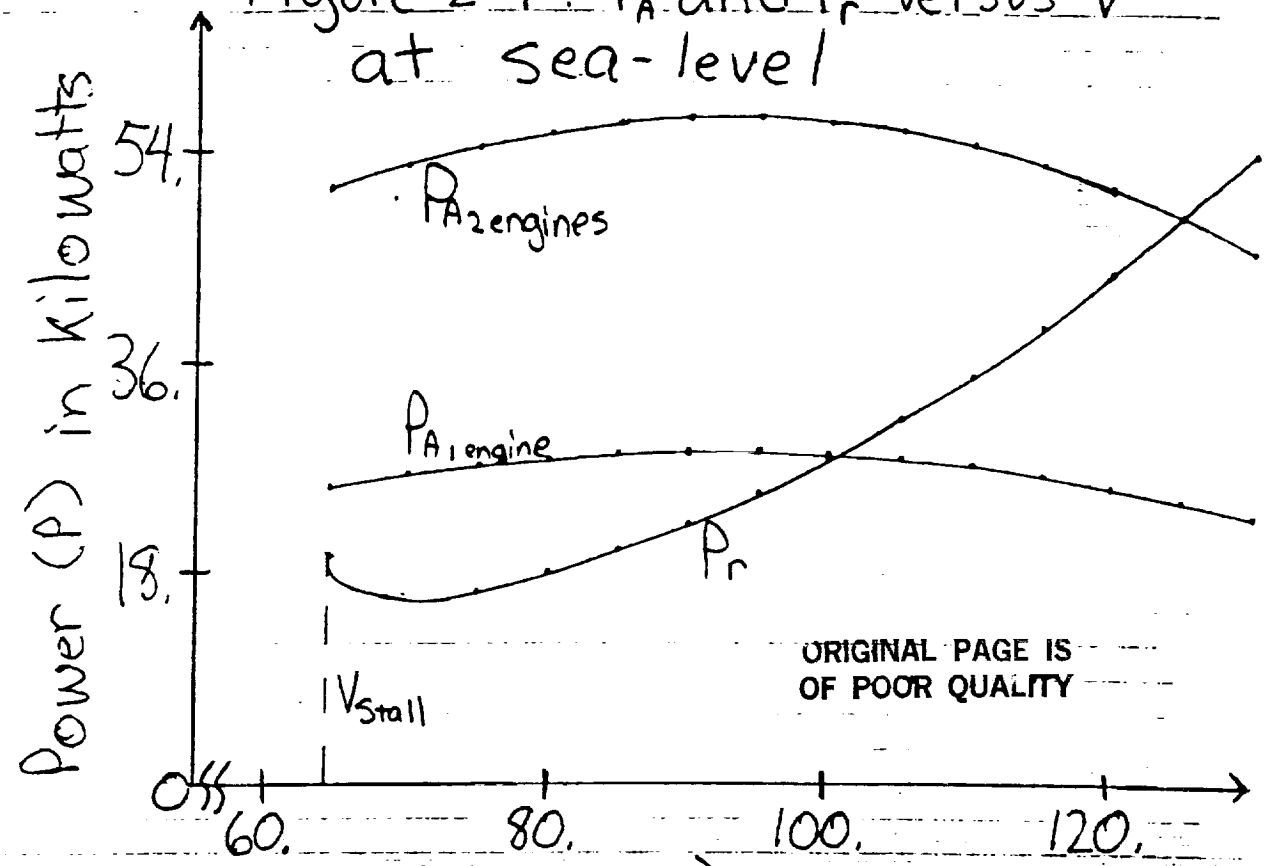

Figure 2-2: P_A and P_r versus V at 1500. m

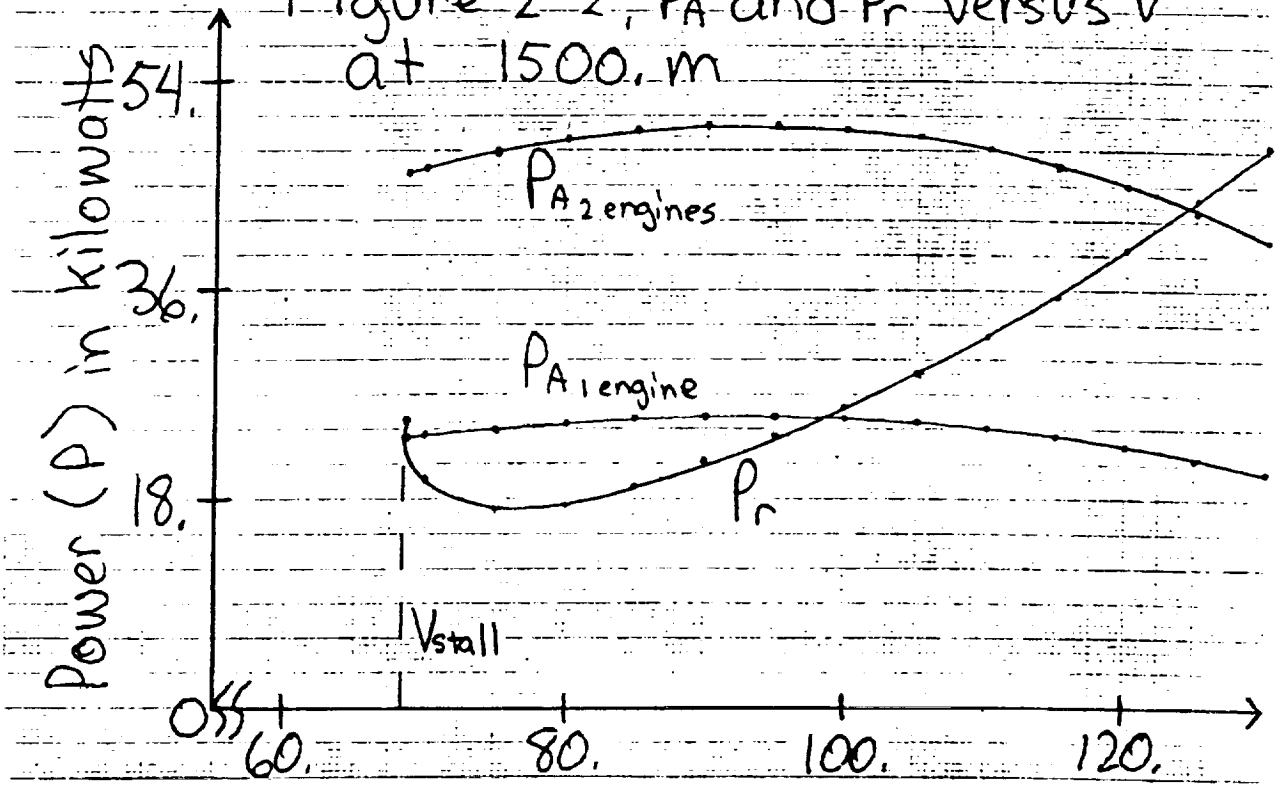

Figure 2-3: Level Flight Performance Envelope

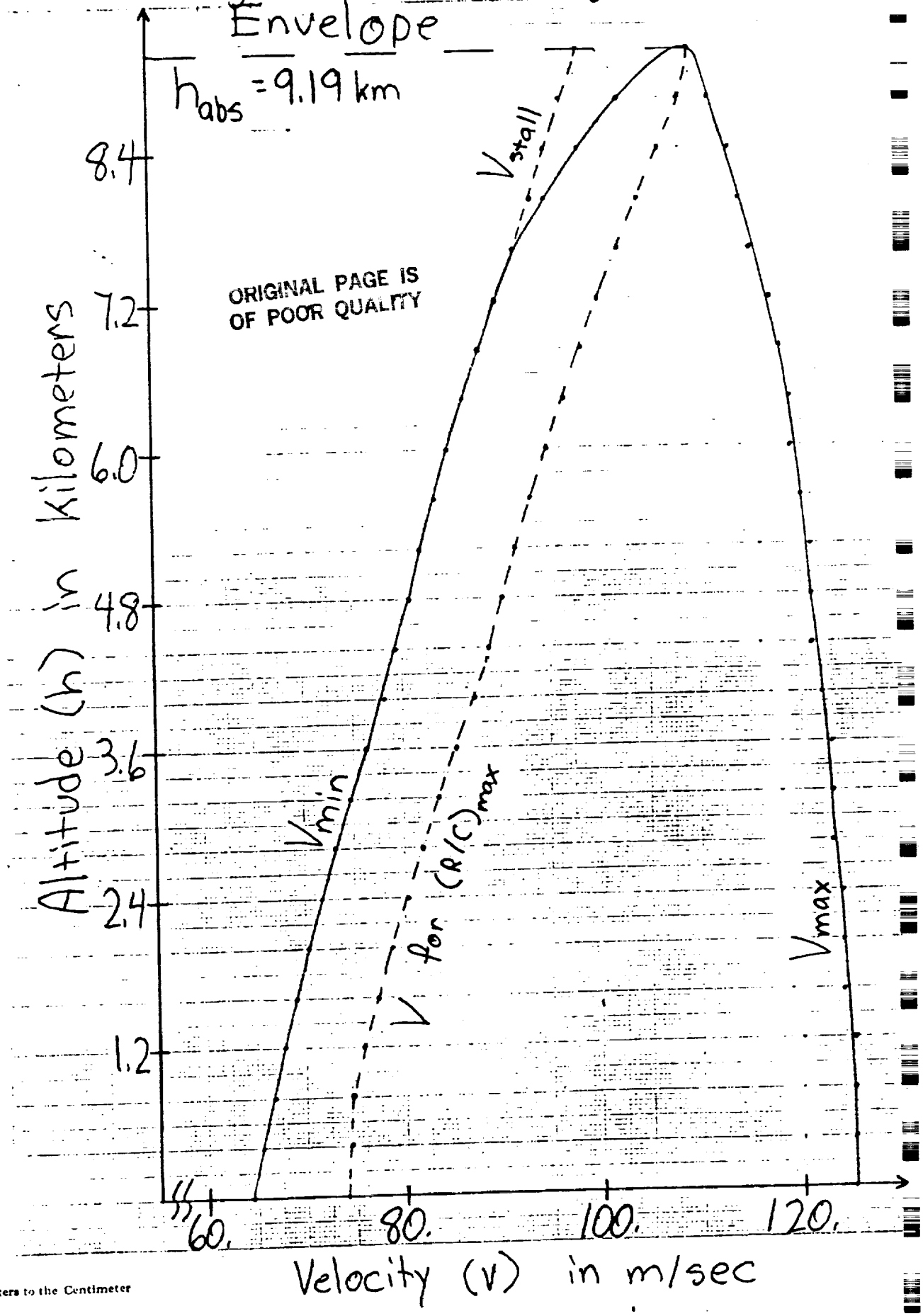

TABLE 2-1

Mission 1, 0% Battery Power Reserve

Maneuver	Time sec	Range m	Energy Used J
Vertical Take-Off	42.0	1885.	2.10×10^6
Climb	197.0	13440.	1.01×10^7
Cruise	29401.5	2646136.	6.20×10^8
Descent	552.9	39920.	1.41×10^6
Conventional Landing	10.0	680.	0.0
TOTALS	30203.4	2702061.	6.34×10^8

Flight Time: 8 hours, 23 minutes, 23 seconds
Radius of Operation: 1351.03 kilometers

TABLE 2-2

Mission 1, 10% Battery Power Reserve

Maneuver	Time sec	Range m	Energy Used J
Vertical Take-Off	42.0	1885.	2.10×10^6
Climb	197.0	13440.	1.01×10^7
Cruise	26397.1	2375738.	5.57×10^8
Descent	552.9	39920.	1.41×10^6
Conventional Landing	10.0	680.	0.0
TOTALS	27199.0	2431663.	5.71×10^8

Flight Time: 7 hours, 33 minutes, 19 seconds
Radius of Operation: 1215.83 kilometers

TABLE 2-3

Mission 2, 0% Battery Power Reserve

Maneuver	Time sec	Range m	Energy Used J
Vertical Take-Off	42.0	1885.	2.10×10^6
Climb	207.1	14380.	1.06×10^7
Cruise	14367.2	1290347.	3.03×10^8
Descent	538.4	39560.	1.38×10^6
Vertical Landing	4.0	100.	0.0
Vertical Take-Off	42.0	1885.	2.10×10^6
Climb	197.0	13440.	1.01×10^7
Cruise	14367.2	1290347.	3.03×10^8
Descent	552.9	39920.	1.41×10^6
Conventional Landing	10.0	680.	0.0
TOTALS	30327.8	2697945.	6.34×10^8

Flight Time: 8 hours, 25 minutes, 28 seconds
Radius of Operation: 1348.97 kilometers

TABLE 2-4

Mission 2, 10% Battery Power Reserve

Maneuver	Time sec	Range m	Energy Used J
Vertical Take-Off	42.0	1885.	2.10×10^6
Climb	207.1	14380.	1.06×10^7
Cruise	12865.0	1157848.	2.72×10^8
Descent	538.4	39560.	1.38×10^6
Vertical Landing	4.0	100.	0.0
Vertical Take-Off	42.0	1885.	2.10×10^6
Climb	197.0	13440.	1.01×10^7
Cruise	12865.0	1157848.	2.71×10^8
Descent	552.9	39920.	1.41×10^6
Conventional Landing	10.0	680.	0.0
TOTALS	27323.4	2427546.	5.71×10^8

Flight Time: 7 hours, 35 minutes, 23 seconds
Radius of Operation: 1213.77 kilometers

TABLE 2-5

Mission 3, 0% Battery Power Reserve

Maneuver	Time sec	Range m	Energy Used J
Vertical Take-Off	42.0	1885.	2.10×10^6
Climb	175.4	11560.	8.93×10^6
Cruise	14410.9	1296977.	3.04×10^8
Descent	590.7	40890.	1.47×10^6
Vertical Landing	4.0	100.	0.0
Vertical Take-Off	42.0	1885.	2.10×10^6
Climb	199.4	13660.	1.02×10^7
Cruise	14392.9	1295357.	3.04×10^8
Descent	549.3	39830.	1.40×10^6
Conventional Landing	10.0	680.	0.0
TOTALS	30416.5	2702824.	6.34×10^8

Flight Time: 8 hours, 26 minutes, 57 seconds
Radius of Operation: 1351.41 kilometers

TABLE 2-6

Mission 3, 10% Battery Power Reserve

Maneuver	Time sec	Range m	Energy Used J
Vertical Take-Off	42.0	1885.	2.10×10^6
Climb	175.4	11560.	8.93×10^6
Cruise	12908.6	1161778.	2.72×10^8
Descent	590.7	40890.	1.47×10^6
Vertical Landing	4.0	100.	0.0
Vertical Take-Off	42.0	1885.	2.10×10^6
Climb	199.4	13660.	1.02×10^7
Cruise	12890.6	1160158.	2.72×10^8
Descent	549.3	39830.	1.40×10^6
Conventional Landing	10.0	680.	0.0
TOTALS	27412.1	2432425.	5.71×10^8

Flight Time: 7 hours, 36 minutes, 52 seconds
Radius of Operation: 1216.21 kilometers

Notes for TABLES 2-1 to 2-6:

1) All vertical maneuvers (take-off and landing) burn 83.3 N of rocket propellant.
2) All climbs are from 15. m to 1500. m at V for $(R/C)_{max}$, calculated every 300. m.
3) All cruises are at 1500. m at 90. m/sec.
4) All descents are at 5.% of full power, and go from 1500. m to 25. m at V for $(R/S)_{min}$, calculated every 300. m.
5) All conventional landings start at 25. m. The engines are shut-off at 25. m.

TABLE 2-7

Summary of Selected Values

Term	Unit	Sea-level	25 m, 1 engine, gear and flaps down	1500m
V_{stall}	m/sec	64.5	61.3	68.7
V_{min}	m/sec	64.5	61.3	68.7
V_{max}	m/sec	125.0	101.0	125.0
V for $(R/C)_{max}$	m/sec	74.1	72.2	76.8
$(R/C)_{max}$	m/sec	7.91	2.31	6.60
$(Gamma)_{max}$	degrees	6.12	1.83	4.93
$(P_x)_{max}$	kWatts	38.0	11.1	31.7

$h_{service}$= 8470. meters
h_{abs}= 9190. meters

TABLE 2-8

Cruise Information

Cruise at constant altitude of 1500. m.
Cruise at constant velocity of 90. m/sec.
At 1500. m, cruise is 72.% of maximum velocity.

TABLE 2-9

Term	Unit	Descent Values Sea-level	1500. m
V_{stall}	m/sec	64.5	68.7
V for $(R/S)_{min}$	m/sec	72.2	76.8
$(R/S)_{min}$	m/sec	2.71	2.97
$(Gamma)_{max}$	degrees	-2.15	-2.22

TABLE 2-10

Variable Descriptions

V: Velocity
V_{stall}: Velocity at stall
V_{min}: Minimum Velocity
V_{max}: Maximum Velocity
$(R/C)_{max}$: Maximum Rate of Climb
$(R/S)_{min}$: Minimum Rate of Sink
Gamma: Flight Path Angle
$(Gamma)_{max}$: Maximum Flight Path Angle
h: Altitude
h_{abs}: Absolute Ceiling
$h_{service}$: Service Ceiling
P: Power
P_a: Power Available
P_r: Power Required
P_x: Excess Power
$(P_x)_{max}$: Maximum Excess Power

Power and Propulsion

Paul W. Martin

System Selection

Due to the original constraints of the Martian atmosphere, an air-breathing propulsion system was deemed unfeasible. Initially a solar powered system was investigated because of the solar power density with respect to gravity on Mars. However, after investigating available material it was found that the power density available from solar arrays could not meet the requirements of this project. The fact that the power density was not optimal was overshadowed by the lack of information on solar arrays concerning size, density and flexibility related to the needs of this project. Even if sufficient information was available, the structural complications associated with implementing solar arrays on the upper surface of the wing and tail surfaces would be a major problem in the design of the aircraft. The use of solar power as a primary source of power was ruled out.

After investigating several different types of electrical power alternatives to solar power, the Lithium family of batteries were found to have suitable characteristics for the needs of this project. Specifically, the Lithium Flouride battery was found to have an excellent power density.[1] In addition to having a higher power density than that of solar arrays, batteries are much more convenient to use. The batteries can be stored on board and recharged inbetween flights.

The batteries will power two motors located in booms in a conventional propeller driven configuration. Two motors are being used for safety as well as structural reasons. The aircraft can maintain altitude with one engine out, however, performance is drastically reduced. In the event of a motor failure, the aircraft would be able to make it back to its base. Moving the motors away from the fuselage also reduces the shear force at the wing root. This reduces the need for additional support at the wing root and hence additional weight.

The motor that was chosen is a GE, special design, copper rotor cage, integral geared motor. The power output and weight have been scaled down to conform to the design requirements. The peak power available from each motor is 35 kw and the weight of each motor is at 40.5 kg. The motors will be used to power two 2-bladed propellers. The propellers are designed to operate at maximum power at a velocity that is slightly higher than the design cruise velocity. Motor and propeller data have been listed on page 3-4.

Power Available

The power available at a cruise altitude of 1.5 km is maximum at a velocity of 94 m/s. This information is presented in graphical form in Figure 3.1. The aircraft will be lifted to a height of 20 m in a vertical take-off. The maximum power available at sea level is 85 percent of peak power or 59.5 kw.

The power supplied by the Lithium Flouride cells has been calculated for an endurance of eight hours. In addition to powering the motors for an endurance of eight hours, the cells will also need to power the electical system/avionics. The power breakdown along with the weight of the power system is shown on page 3-5.

Propeller Design

The propeller that was chosen to power the aircraft is the 5868-9, Clark-Y section, two-bladed propeller. This propeller provides sufficient power after propeller efficiency losses. Maximizing the blade angle at 45 degrees during cruise resulted in a maximum propeller efficiency of 76.4 percent. The specific parameters for the propeller are listed on page 3-4.

Engine Inoperative Drag

The engine inoperative drag was calculated as a function of the drag coefficient of the propeller, the dynamic pressure at cruise velocity and altitude, and the blade planform area. The following equations were used in the calculation of the inoperative drag.

1) $C_D = .1 + \cos^2(\text{Beta})_2 = D/q(\text{Blade Planform Area})$

2) $\text{Blade Planform Area}/\pi D^2 = .05$

Analysis of these equations resulted in a blade planform area of 10.5 m^2 and a drag of 35.7 N at cruise altitude and velocity.

References

1) Gabano, Jean-Paul (1983). *Lithium Batteries,* (p.3)

Motor Data

GE Special Design

- Copper Rotor Cage
- Integral Gearing

Peak Power.....35 kw

Weight.....40.5 kg

Maximum efficiency.....89%

Propeller Data

Propeller Section.....5868-9, Clark-Y, two bladed

Number of props.....2

N.....486.6 rpm at cruise

D.....8.2 m

B.....40 - 45 degrees

Power Breakdown

Motors.....6.34×10^8 J

Avionics.....2.88×10^7 J

Total P_{req}(8 hr).....**6.628×10^8 J**

Battery Power Density.....6254 W-hr/kg

Weights

Battery Weight.....108.8 N

Electrical System..... 8.4 N

Propellers (x2)..... 50.0 N

Motors (x2)..... 91.0 N

Total..... 258.2 N

Figure 1
P_A vs V
@ Cruise

5 Squares
to the Inch

STABILITY AND CONTROL

JIM SULLIVAN

Horizontal Tail

$l_h = 13.000m$ $\quad S_t/S_W = 11.5\%$

$AR = 12$ $\quad S_t = 17.644m^2$

$C_{L\alpha t} = 4.835/rad$ $\quad b_t = 14.500m$

$e_\alpha = 0.240$ $\quad c_t = 1.217m$

The initial phase in the design process for the stability and control of this aircraft was to size a horizontal tail. An initial choice for the distance between wing and tail aerodynamic centers, l_h, was 15.000m. This was later found as too high for structural stability, so it was reduced. An aspect ratio, AR, was chosen, and a downwash gradient, e_α, was extrapolated from a graph in the notes. With this information and a relation in the notes, the tail size was found.

Since the aircraft's tail is mounted on booms, careful consideration was taken as to where they would attach to the tail. Since the engines are mounted on the booms, they had to be far enough apart so the propellers cleared the fuselage. When this information was calculated, the booms were found to be effective attached to the tips of the tail.

Vertical Tail

$S_V/S_t = 45\%$ $\quad \Lambda = 37.5^\circ$

$S_V = 3.970 m^2$ each $\quad \lambda = 0.440$

$b_V = 2.000 m$

Since the horizontal tail is so long, two vertical tails are used for added directional stability and control. Sweep and taper ratio were found from geometry.[2] The entire area fo the vertical tails was chosen as an appropriate percentage of the horizontal tail area.

Using relations in the notes, a neutral point location was found; see Fig 4-1. To continue in the design process, an allowable center of gravity range had to be found. This range changed after alterations were made from the initial design, and a suitable range was found; see Fig 4-2. As the figures show, the aircraft is stable at all weights; i.e. the neutral point is aft of any allowable c.g., and the c.g. range demanded by the weight of the aircraft is within the stability limit. A minimum static margin of 10% had to be maintained at all flight conditions, and this aircraft's minimum possible static margin is 19%. Since this aircraft design is well within the range of stability, a wide variety of changes could be made in the future if needed; i.e. a different mission, increased carge, etc.

Next in the design process was to size and place control surfaces on the aircraft. Using longitudinal and directional control derivative relations, along with sideslip and roll derivative relations given in the notes, appropriate control surface designs and capabilities were acheived that would give the aircraft positive directional stability and control power at all flight conditions.

Elevator

$S_e/S_t = 43\%$

$S_e = 7.519m^2$

$b_e = 8.200m$

$c_e = 0.914m$

$\delta_{e\,max} = \pm 40$

Ailerons

$S_a/S_w = 12\%$

$S_a = 9.360m^2$ each

$b_a = 9.720m$

$c_a = 0.963m$

Rudders

$S_r/S_V = 7.56\%$

$S_r = 0.300 m^2$

$\delta r\ max = \pm 30$

For detailed dimensions, see Figs. 4-3, 4-4.

All control surfaces are deflected using a compressed atmosphere system described by Surface Operations.

Take-Off

This aircraft will use a vertical take-off manuever for its mission, thus take-off analysis is not applicable.

Cruise

$V_{cruise} = 90 m/s$

Capability: 35° sustained banked coordinated turn

30° bank in 1.832s

Landing

This aircraft will make one conventional runway landing in its mission scenario.

Stall is capable when center of gravity is 2.800m aft of nose, which is much less than at minimun center of gravity location of 2.912m aft of nose.

$$V_{approach} = 80^{m}/_{s}$$

Capability: 32° sustained banked coordinated turn

30° bank in 1.946s

A rudder deflection of 24° will give a steady sideslip angle 0f 10°.

With a full-rudder sideslip, 70% of lateral control power is needed to maintain wings-level flight.

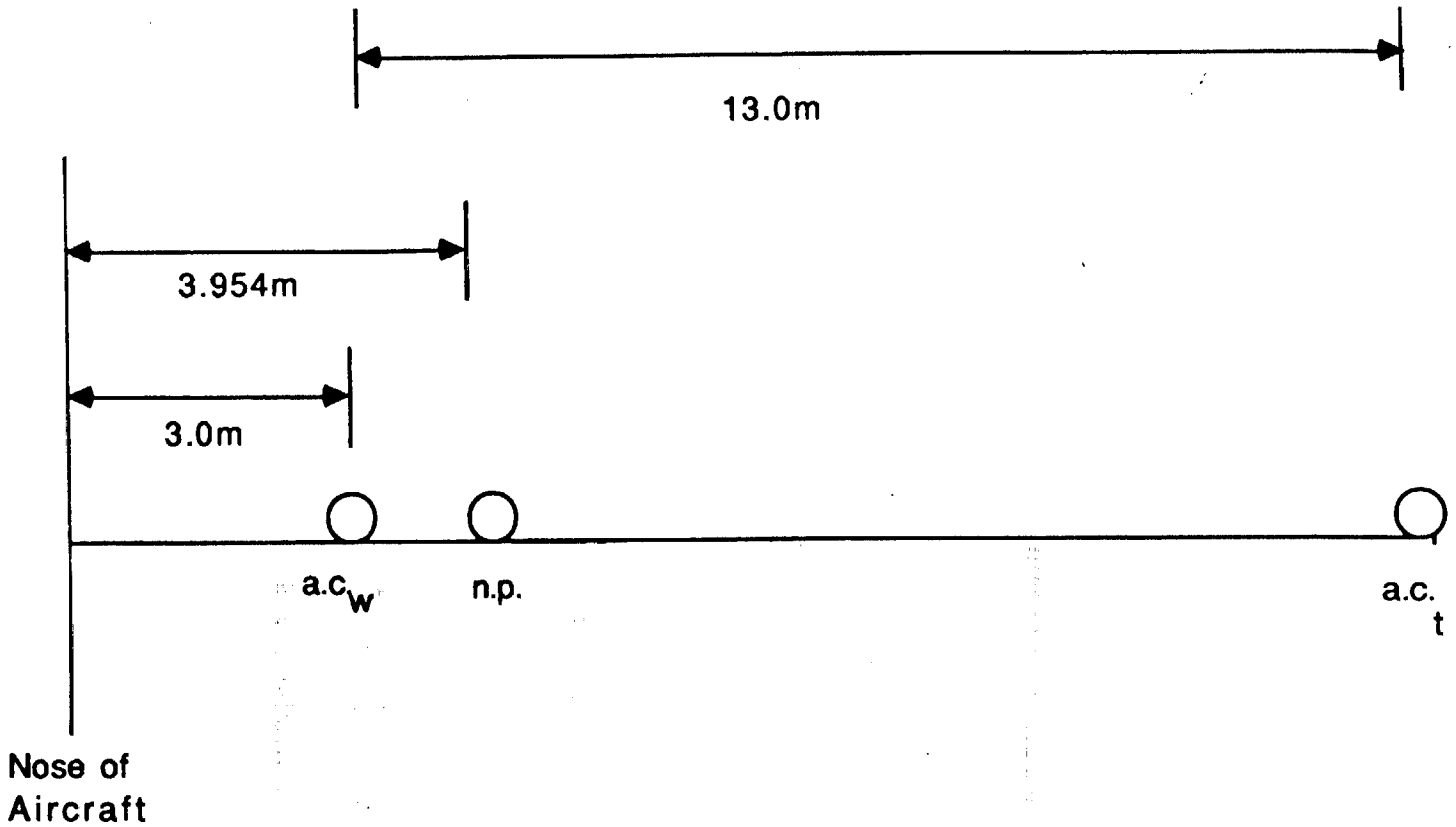

FIG. 4-1

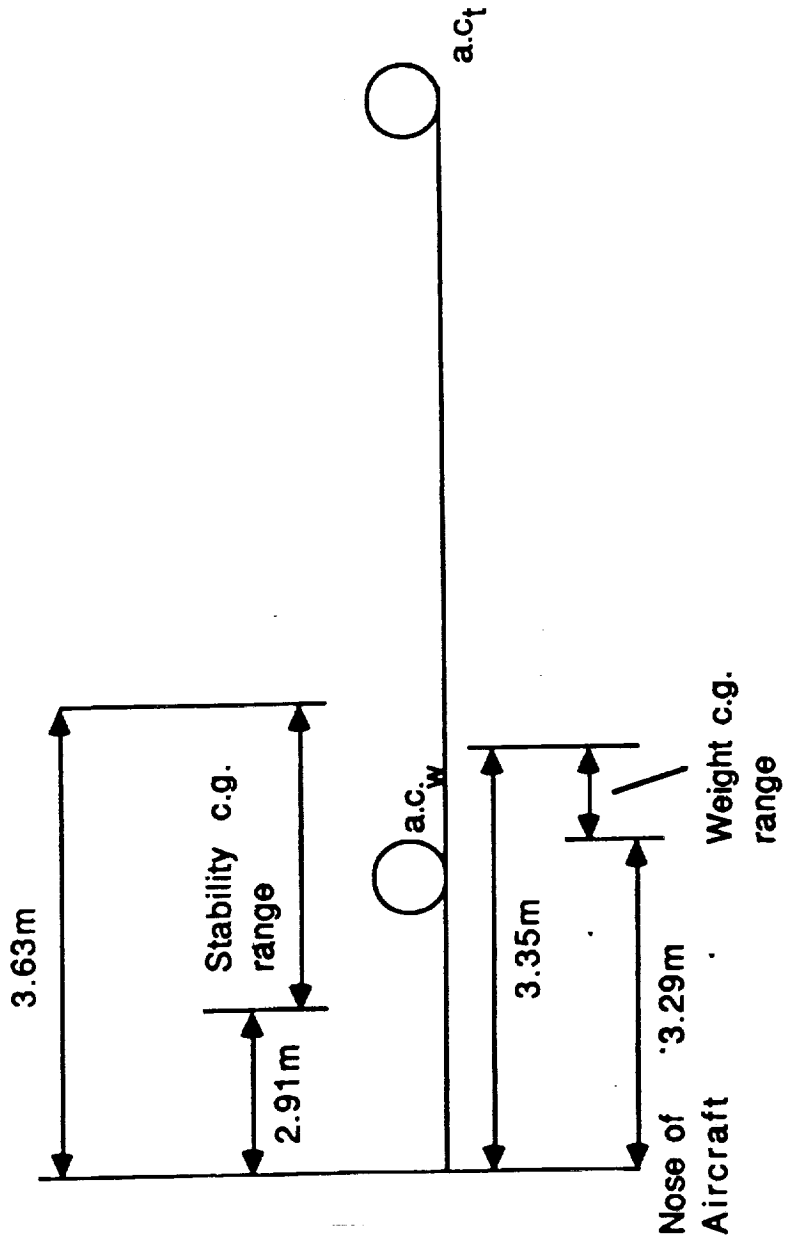
a.c$_t$
a.c$_w$
3.63m
Stability c.g. range
2.91m
3.35m
3.29m
Weight c.g. range
Nose of Aircraft

FIG. 4-2

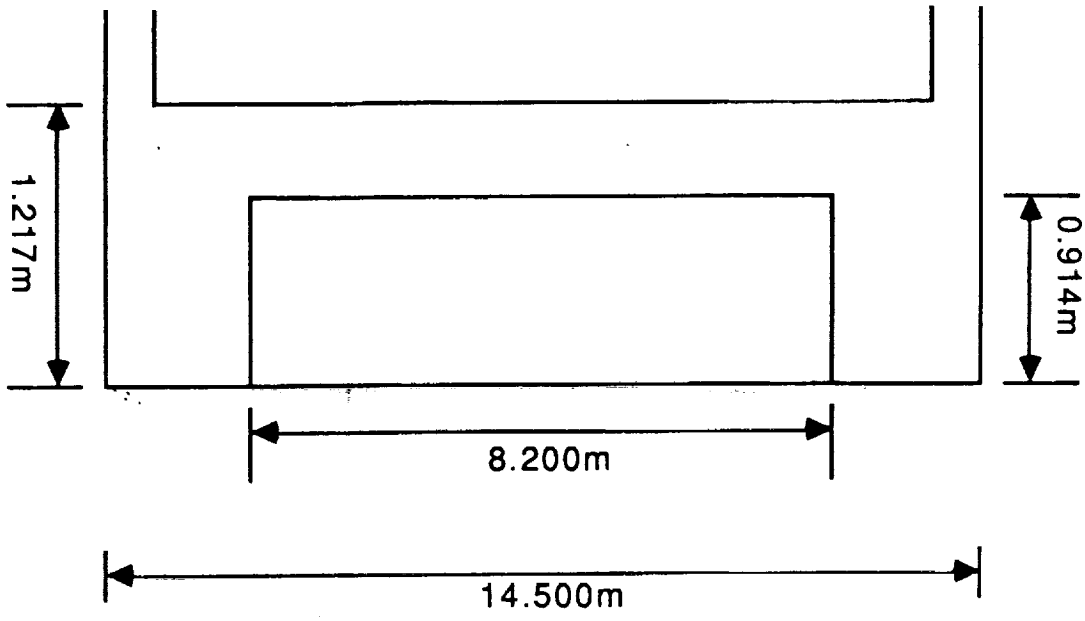

Top view, horizontal tail

FIG. 4-3

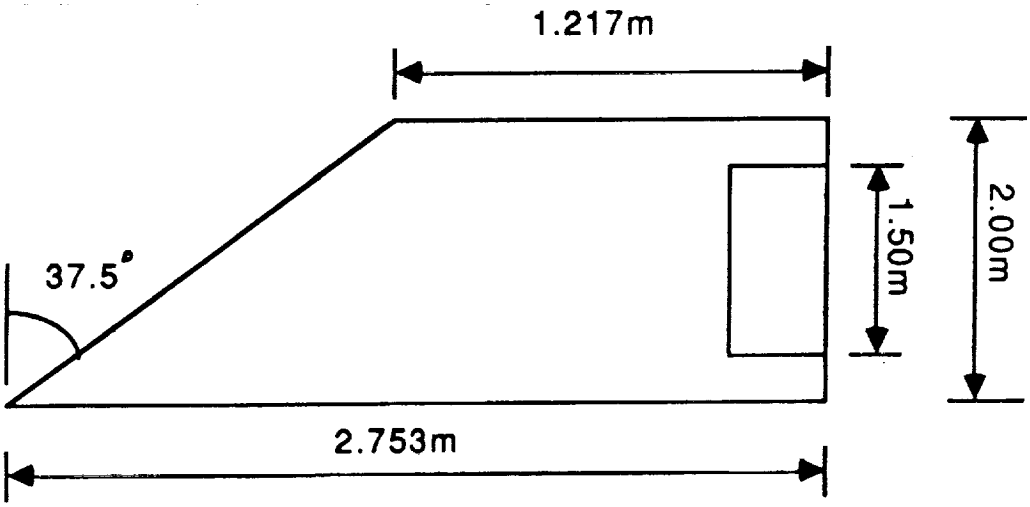

Side view, vertical tail with rudder

FIG. 4-4

STRUCTURES

Kevin J. Klein

Using the weights and dimensions calculated for the MMRA.2, an in depth structural analysis was performed. This analysis consisted of the determination of load distributions, shear force and bending moment diagrams, as well as a torsional moment diagram. The reasoning behind this analysis was to determine the forces that the aircraft could expect to encounter. Once the results of this structural testing were determined, it was possible to begin the structural design of the aircraft. The details of this process will be shown in the following paragraphs.

It was necessary to first calculate the load diagrams. Figures 5.1 and 5.2 show the load conditions for level steady flight and while on the ramp. The level flight condition consists of a lift distribution, a point load, and a weight distribution. The lift distribution was found using the Shrenk approximation, and consists of the lift necessary to keep the aircraft in level flight. The point load consists of three components, all acting at X=7.25m. These three loads are the weight of the engine and its accessories, the landing gear weight, and one-half of the tail weight. The wing weight distribution was also calculated, and is also shown. The ramp condition is shown in Figure 5.2. The lift contribution disappears, and a new force is formed due to the reaction of the landing gear. This force is shown as a point load acting at 7.25m. It was assumed that each of the main landing gear would support 45% of the gross weight, and the nose gear would support 10%. The reaction force was adjusted accordingly.

Once the load distributions were found, the shear force due to each individual component was calculated, and using the sign convention that an upward acting force causes positive shear and negative moment, the total shear force was found. Figures 5.3 and 5.4 show how the shear force varies as a function of span for level flight and

while on the ground. The maximum shear force was found to be 1215 N acting at X=7.25m while on the ramp. This was due to the large reaction force due to the landing gear.

After the shear equations were computed, the moment equations were found by taking the integral of the shear. Figures 5.5 and 5.6 give the total moment distributions for the two load conditions. The maximum net moment was found to be 14349.5 Nm at the root of the wing during level flight. The torsional moment was also computed, and is shown in Figure 5.7. The torsional moment is the pitching moment about the aerodynamic center of the airfoil, and is independent of angle of attack.

Once the loads acting on the wing were determined, it was possible to begin sizing an internal wing structure. This wing design consists of two spars of constant radius and varying thickness, and ribs placed an average of one meter apart throughout the span, with extra ribs added to areas which needed extra support. The spar design was determined to provide the majority of the structural support, but to also allow for the use of flaps and ailerons in the rear of the wing. Figure 5.8 shows the spar placement. Blt consists of one spar located at the aerodynamic center of the airfoil, or 25% of the chord, and the other spar at 55% of the chord length. This spar design leaves ample room for flaps and ailerons in the rear of the airfoil. Figure 5.8 also shows a sample calculation of the spar thicknesses. Due to the smaller radius of the rear spar, the needed thickness for the rear spar was slightly greater than that needed for the front spar. Since buckling must also be analyzed to determine a final structural sizing, an estimate had to be made on the needed thicknesses for each spar. This estimate was that the buckling analysis would cause the spars to be no more than five times their calculated minimum thicknesses. In order to help insure that buckling will be less severe, it was decided to use a reinforcement method like that in the report on the Gossamer Condor by J. D. Burke. These reinforcements will be circular graphite-epoxy plugs that will be inserted into the spars at intervals of 4m. These plugs will reduce the buckling be reducing the effective spar length. By using a decreasing thickness spar,

the weight of the spar can be further reduced. A rough calculation of spar weights using the constraints outlined above yielded a front spar weight of 354 N and a rear spar weight of 273 N.

The ribs will also be made out of graphite-epoxy, and will be placed to insure a constant airfoil geometry, and to give added structural support. Figure 5.9 shows the wing structural layout with rib positions clearly defined. It was necessary to add ribs in places where the wing needed to be more structurally sound. Such places are the wing-fuselage attachment points, the landing gear and engine locations, and the wing breakdown points. In order to obtain an estimate of rib weight, rib sizing had to be determined. It would be very difficult to determine the forces on the ribs without the use of a finite element program so the rib width was estimated at one-half inch. An analysis was performed on a rib in the middle of the semi-span to determine the average volume of a rib. It was found that a rib in this position would weigh about 21 N, allowing for a honeycomb structure. It is very probable that most of the ribs will weigh less than this average value, since most do not cover the entire airfoils area.

The wing skin will be made out of Kevlar sheeting wrapped over the airfoil. Kevlar has a density of .0188lb/ft2, which is very light, and has a very high strength to weight ratio which makes the material ideal for this purpose. Forming a two sheet layer of Kevlar over the 153.09m2 wing area resulted in a weight of only 19.4 lbs. This is a tremendous weight savings over the normal aircraft skin.

Consideration was also given to the tail structure. Figure 5.9 shows the tail structural layout. It was decided that since the tail encountered loads much less than those of the wing, that two small rectangular spars would be used instead of the two circular spars used in the wing. The ribs were placed 1.5m apart in the horizontal tail, and every 0.5m in the vertical tail. The tail-boom will be ovular in shape, and decrease in radius as the tail is neared. Since the loads on the tail-boom will be mostly in the vertical direction, a smaller horizontal radius was not only desired, but was structurally feasible.

The next step was to determine the fuselage structure. Using the design algorithm given in Airplane Design Part III: Layout Design of Cockpit, Fuselage, Wing and Empennage: Cutaways and Inboard Profiles by Jan Roskam, the internal structure was determined. Figure 5.10 shows the fuselage structural layout. The structural members are not drawn to scale, but they are scaled in relation to themselves. Special consideration was given to the internal configuration of the fuselage so that structural synergisms would exist. This resulted in the placing of the payload bays to coincide with the spar attachment bulkheads. The batteries will also be placed in between the floor supports of the rear half of the aircraft in order to save space. Since an accurate load analysis on the airframe is beyond the scope of this course, only size and weight estimates can be made for the fuselage structure.

REFERENCES

Roskam, Jan, Airplane Design Part III: Layout Design of Cockpit, Fuselage, Wing and Empennage: Cutaways and Inboard Profiles . Pub. by Roskam Aviation and Engineering Corp, 1986.

Nicolai, Leland M. , Aircraft Design. , Pub. by Mets, Inc. 1975.

Allen, David H.,and Haisler, Walter E., Introduction to Aerospace Structural Analysis. Pub by John Wiley and Sons, 1985.

Burke, J. D., The Gossamer Condor and Albatross: A Case Study in Aircraft Design. Report No. AV-R-80/540, June16, 1980.

Materials Selector Handbook. 1987

FIGURE 5.1 : LOAD DISTRIBUTION FOR LEVEL FLIGHT

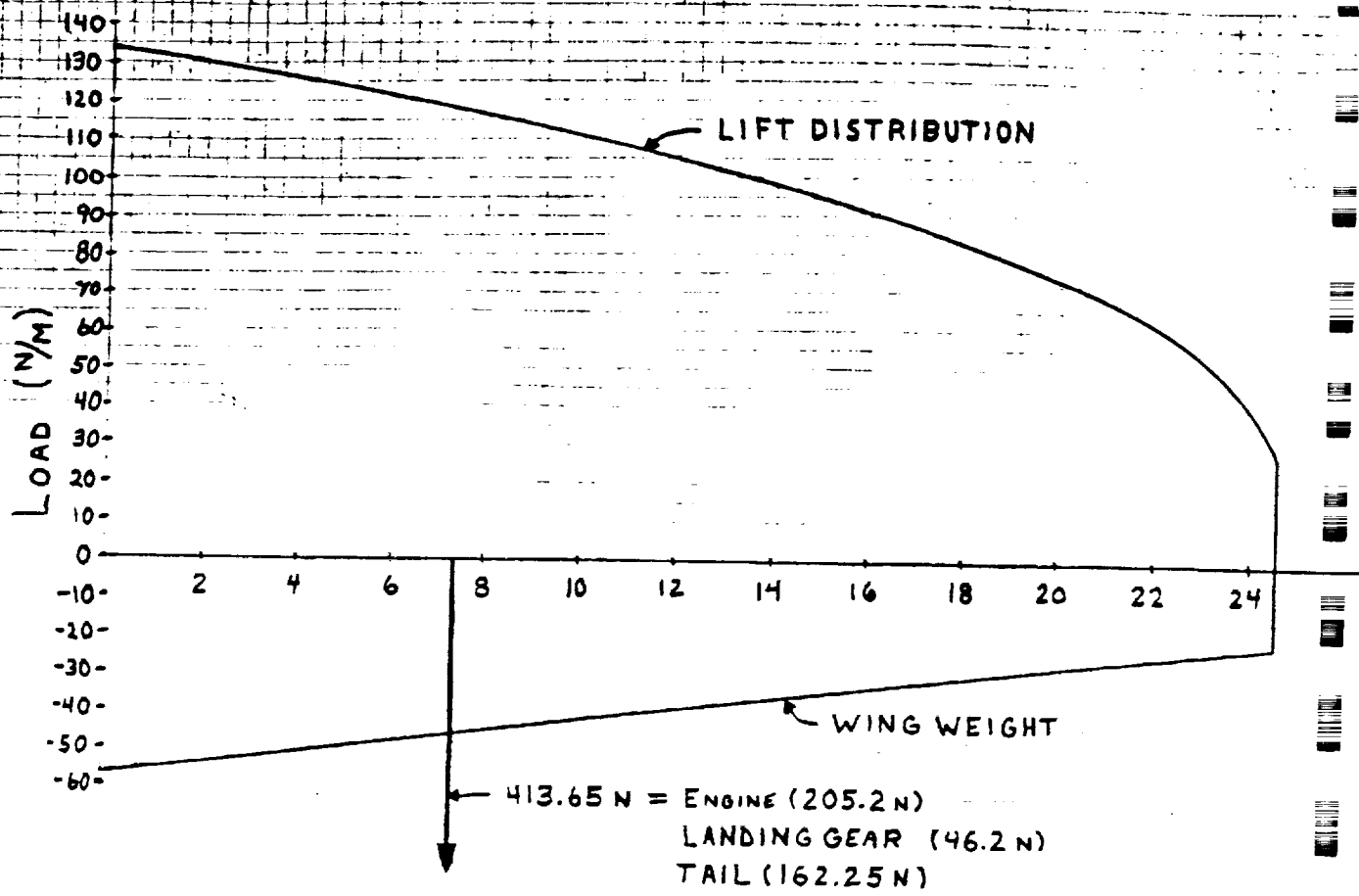

FIGURE 5.2 : LOAD DISTRIBUTION ON THE RAMP

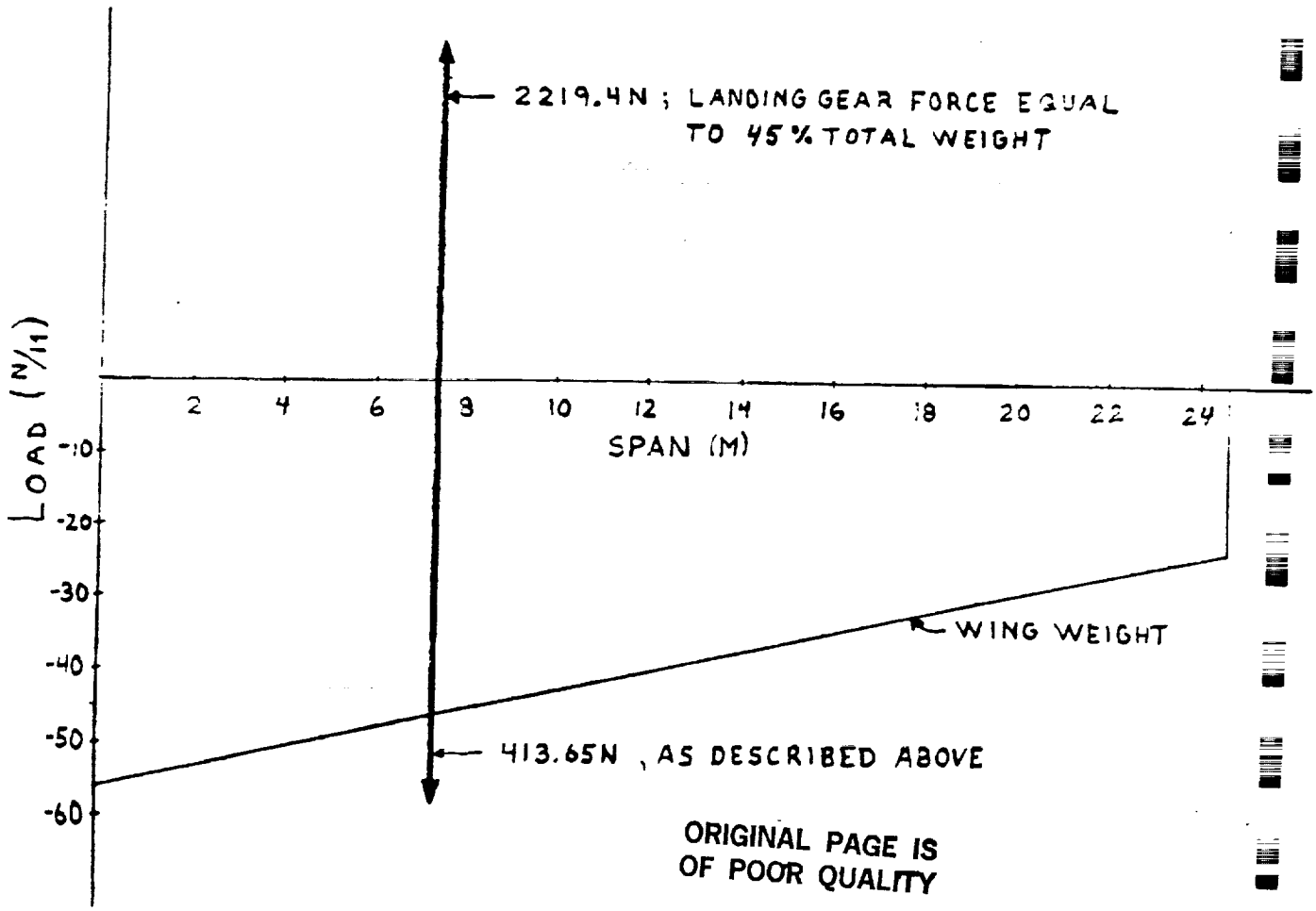

FIGURE 5.3: SHEAR DIAGRAM FOR LEVEL FLIGHT

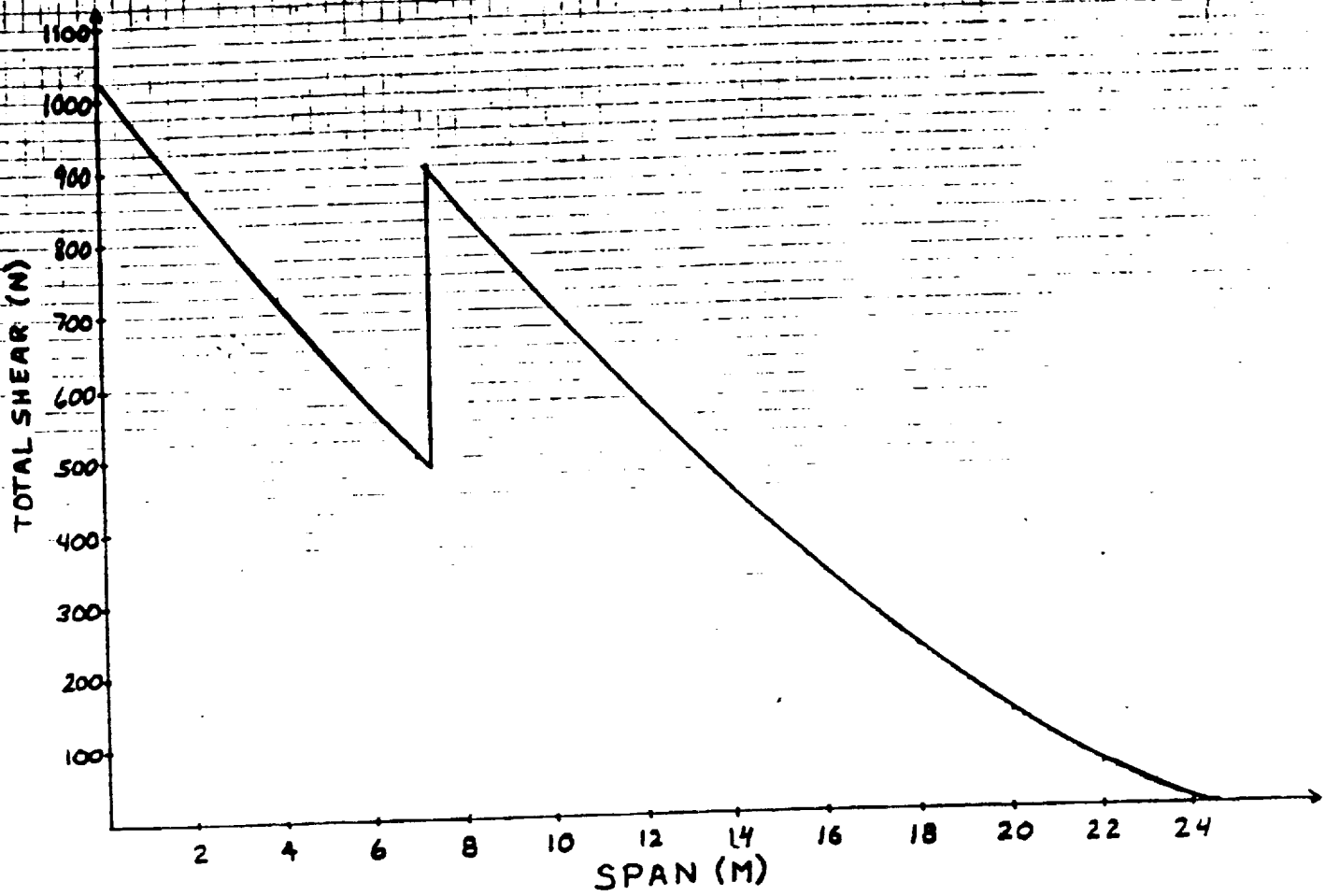

FIGURE 5.4: SHEAR ON THE RAMP

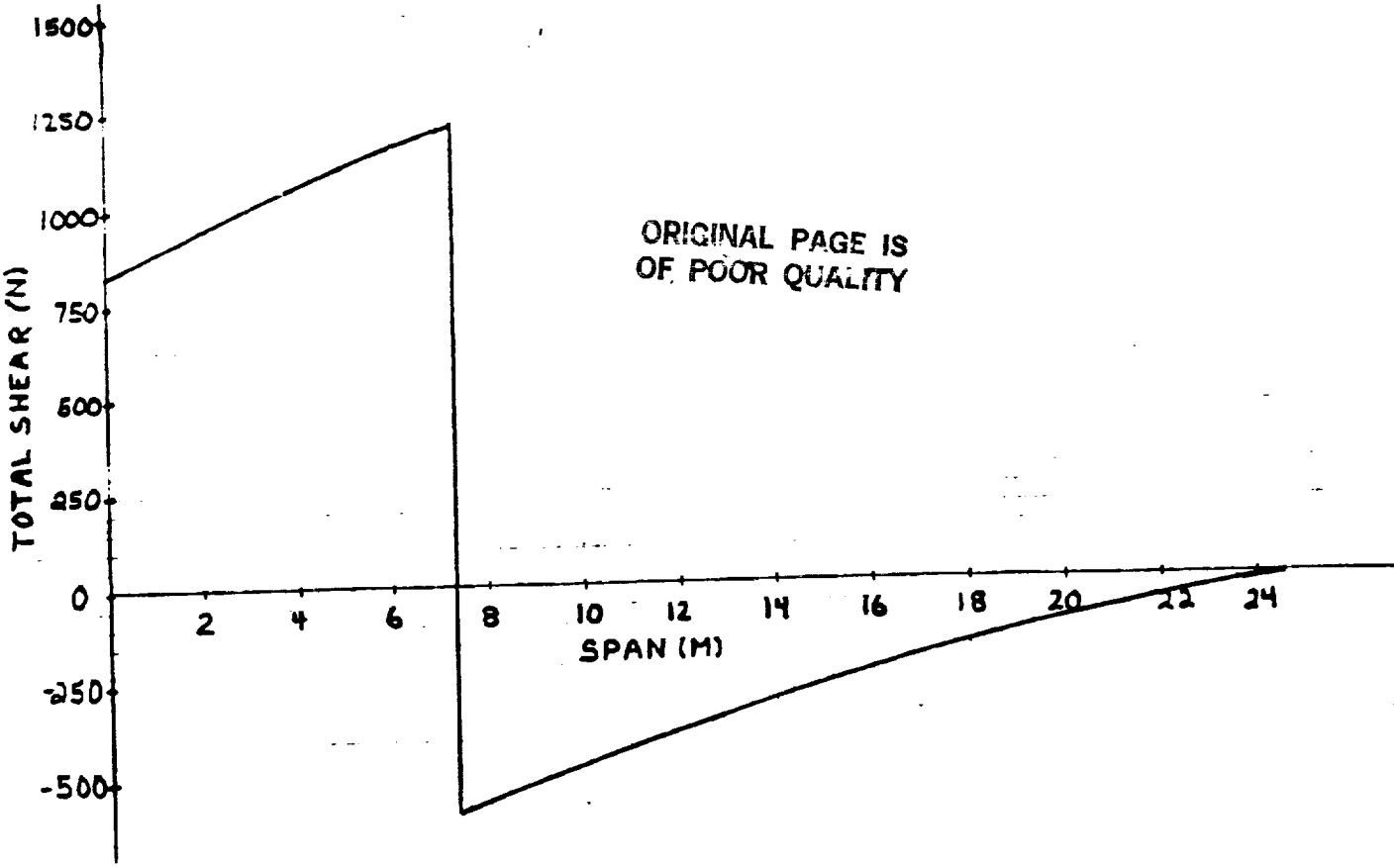

FIGURE 5.5 : MOMENT DIAGRAM FOR LEVEL FLIGHT

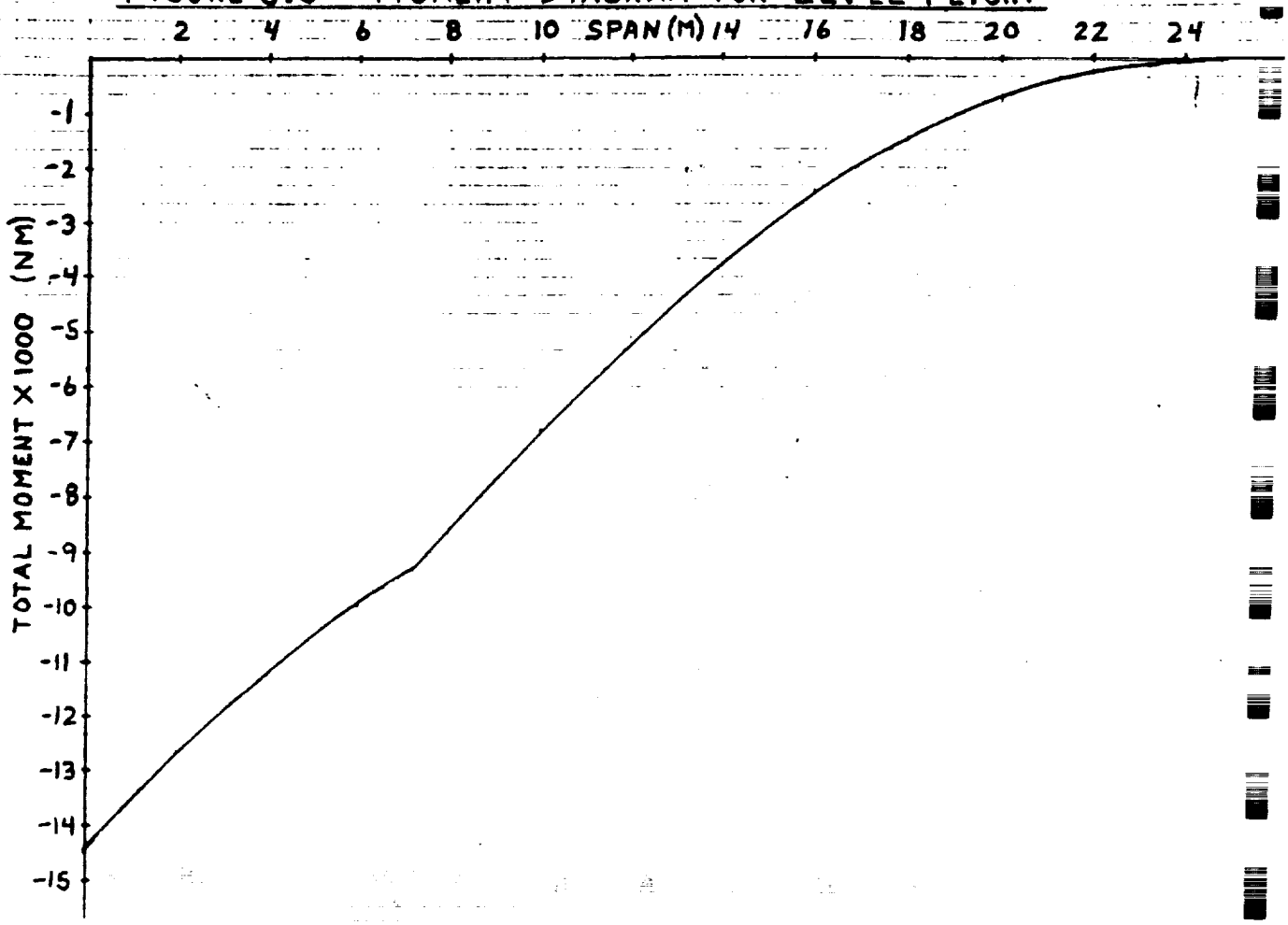

FIGURE 5.6 : MOMENT DIAGRAM ON THE RAMP

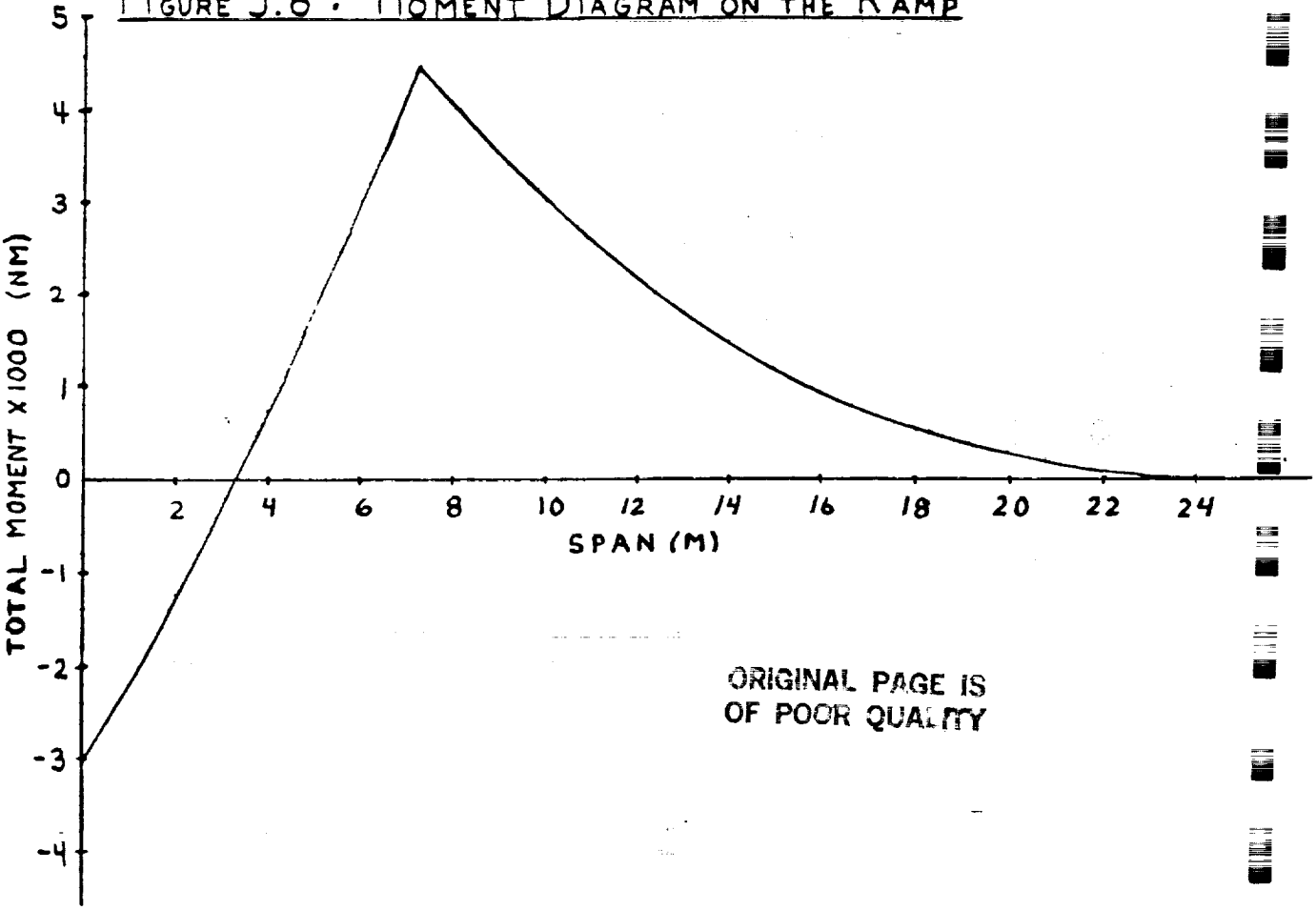

FIGURE 5.7: TORSIONAL MOMENT VS. SPAN

$M_{AC} = (q)(c)^2 C_{mac}$

"$q_{max.}$" = 131.55 $\frac{N}{M^2}$

$C_{mac_{sect.}} = -.12$

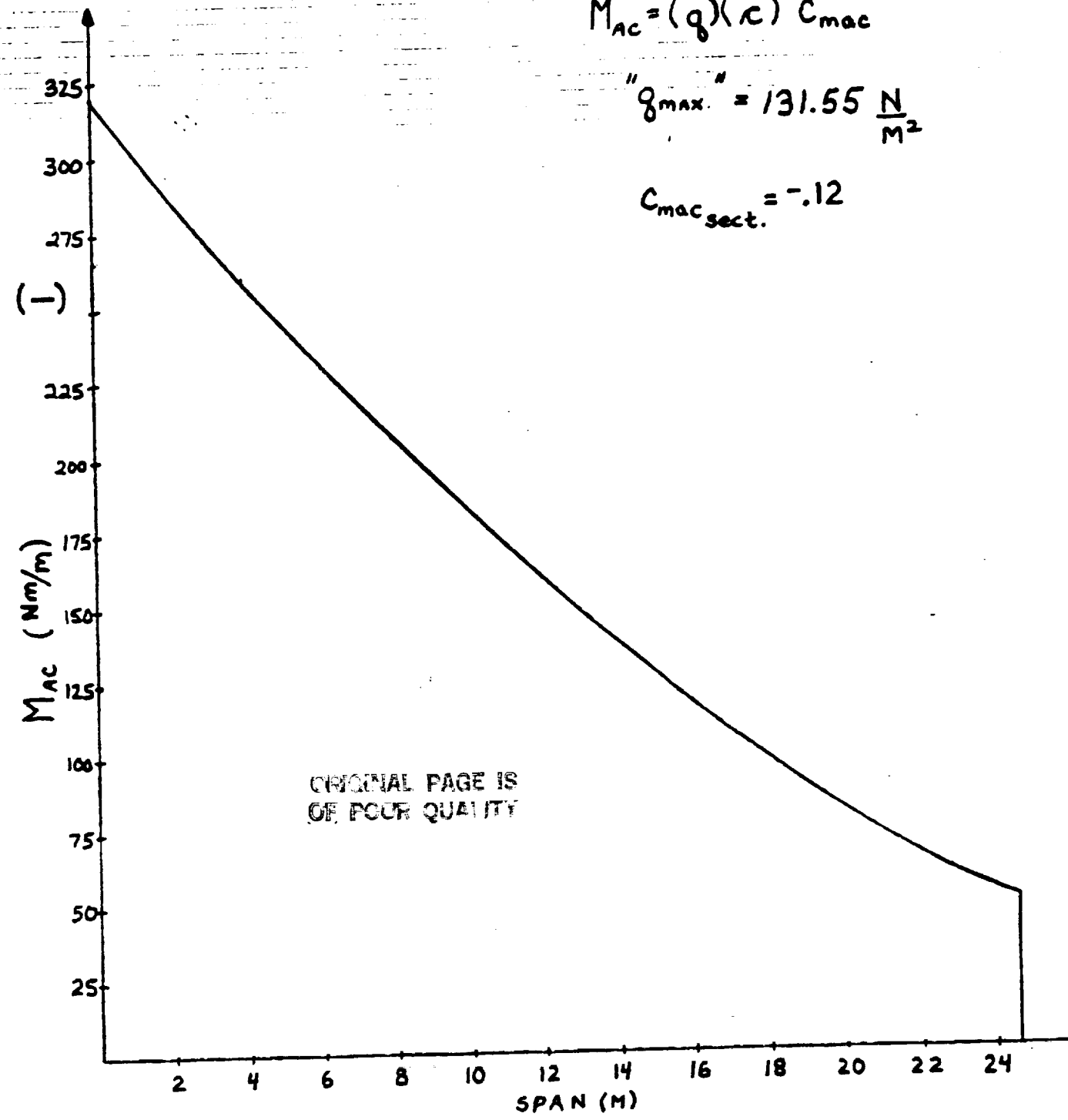

FIGURE 5.8 : SPAR LOCATION AND THICKNESS CALCULATION

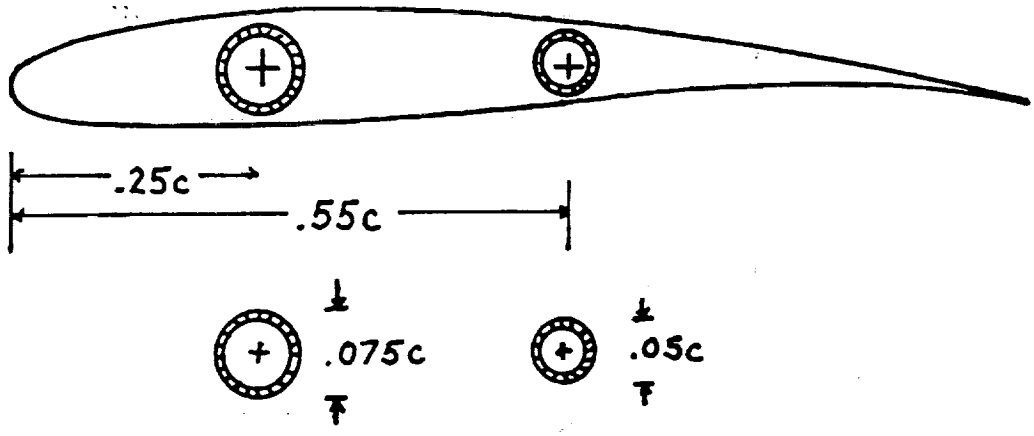

MATERIAL : GRAPHITE-EPOXY

$\sigma_y = 200$ ksi

$\rho = .057$ lb/in^3

$M_{NCT_{MAX}} = 14349.5$ Nm (c = 0

LOAD FACTOR = 6

SAFETY FACTOR = 1.5

$$\sigma_y = \frac{Mv}{I_{yy}} \quad \text{WHERE } I_{yy} = \pi r^3 t$$

EXAMPLE CALCULATION : ASSUMING THE FRONT SPAR CARRIES 2/3 OF THE LOAD.

Front: $I_{yy} = \pi r^3 t = \frac{Mv}{\sigma_y}$ $\quad t = \frac{Mv}{\sigma_y \pi r^3} = \frac{(14349.5\ \text{Nm} \times 2/3 \times 6 \times .18\text{m})}{(\frac{200000}{1.5}\ \text{lb/in}^2 \times \frac{6894.4\ \text{N/m}^2}{1\ \text{lb/in}^2} \times \pi \times .18\text{m})^3}$

$t = .613$ mm

rear: $t = \frac{(14349.5 \times 1/3 \times 6 \times .1125)}{(\frac{200000}{1.5} \times 6894.4 \times \pi \times .1125)^3}$

$t = .785$ mm

FOLDOUT FRAME

FIGURE 5.9: WING AND TAIL INTERNAL CONFIGURATION

NOTES: · VERTICAL AND HORIZONTAL SCALES ARE DIFFERENT IN ORDER TO SHOW BETTER DETAIL VERT. = 6sq./m, HOR. = 4sq./m

· RIBS ARE NOT DRAWN TO SCALE: THEY ARE ENLARGED TO SHOW DETAIL

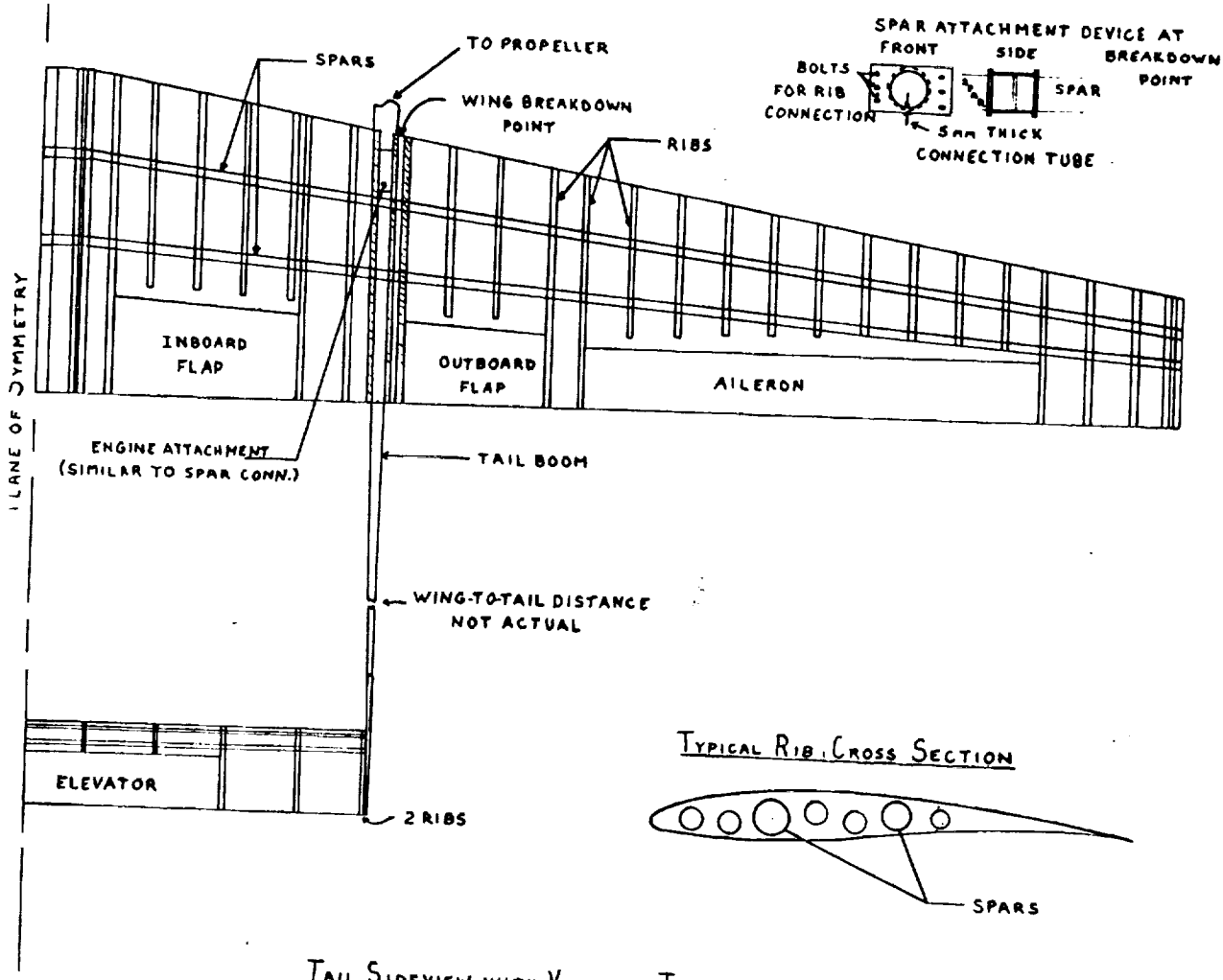

TYPICAL RIB CROSS SECTION

TAIL SIDEVIEW WITH VERTICAL TAIL

1 sq. = .1m

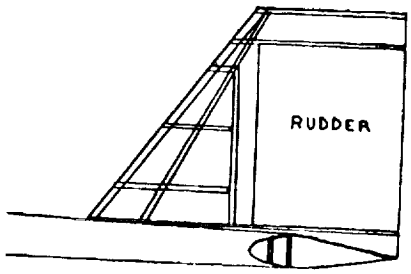

2 FOLDOUT FRAME

FOLDOUT FRAME

FIGURE 5.10: FUSELAGE STRUCTURAL LAYOUT

NOTE: FUSELAGE STRUCTURAL MEMBERS ARE NOT DRAWN TO SCALE. THEY ARE SCALED IN RELATION TO EACH OTHER.

SIDE VIEW 1 sq. = .1m

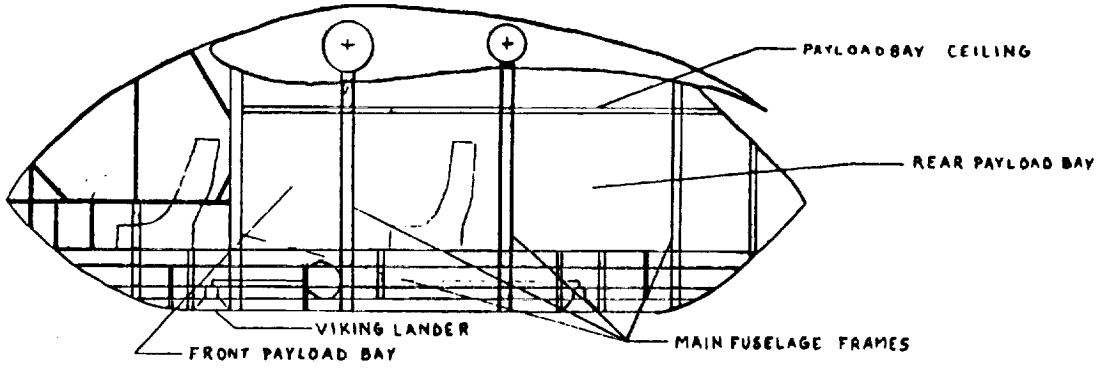

TOP VIEW

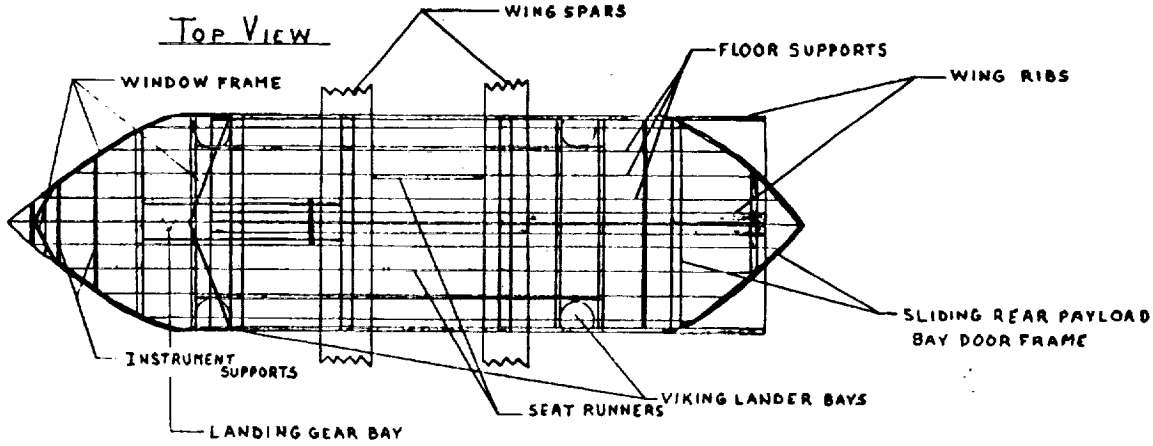

FOLDOUT FRAME

FRONT VIEW

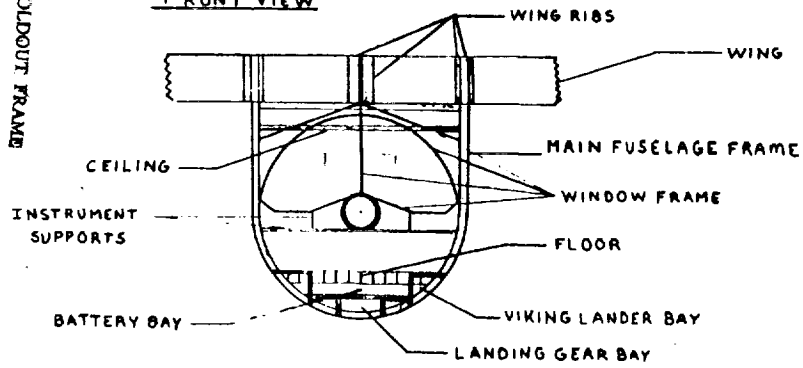

Surface Operations

by

Hwasup Lee

The goal of the Surface Operations division is to design and analyze the take-off and landing system for the Marsian aircraft. Because of the difference in planetary qualities between Earth and Mars, the problem of taking-off and landing on Mars proves to be challenging. Many modes of take-off and landing were considered for this design problem. The selection of the best configuration of take-off is first considered.

With the given power information from the Power division (table 6-1), the analysis for conventional take-off indicated that the the power available is insufficient for the aircraft take-off within the given bounds (table 6-1). Consideration for other types of take-off modes were given such as: catapaults, tow-line and parachute,and dolly-skids. These types of take-off modes need support from a ground crew and the ground crew would be required to work outside in the Marsian atmosphere. A NASA study on maintenance of the space station indicated that it would be less efficient and counterproductive to require ground people to work outside with life support systems. Due to these facts, the above methods of take-off was not chosen. VTOL by tilt rotor was considered next, the analysis on the rotor VTOL indicated that a power of twice the power available would be required. Thus, the decision against it. Finally, a rocket VTOL was considered. The initial study of rocket VTOL showed its feasibility. Thus, the decision was made for the Rocket VTOL system. Also, the initial analysis indicated that less fuel (less weight) would be

required if the aircraft landed conventionally. The ability to land conventionally increases the safety of the airplane in case of rocket VTOL system failure in flight. With the knowledge of how to take-off and land, three mission scenario were planned. There are as follows:

Case1

Aerial Scientific Mission

The aircraft will take off vertically and do an aerial survey. When the mission is complete, aircraft will return to base and land conventionally.

Case2

Aerial/landing Scientific Mission

The aircraft will take off vertically and do an aerial survey. It will then go to a point of interest and do a VTOL for some scientific samples. When the mission is complete, aircraft will return to base and land conventionally.

Case3

Rescue Mission

The aircraft will take off vertically. After reaching the rescue site, the aircraft will do a VTOL to pick up the rescuee. When the mission is complete, aircraft will return to base and land conventionally.

The weight breakdown for each of the above mission is on table 6-2. The

weight breakdown is necessary because the aircrafts performance is a function of weight.

The analysis and design of the MMRA. 2 marsian aircraft will be presented in individual sections. There are as follows:

Vertical Takeoff

The vehicle is equipped with four Viking rockets mounted on the fuselage. The analysis for the vertical takeoff was done with the derivations from Newton's second law (Sample 6-1). In the initial study, the aircraft was to reach a vertical altitude of 600 meters then perform a constant energy altitude dive to get up to stall velocity. This expended too much energy and not practical.

It was decided to take the aircraft up vertically to 15 meters with the viking rockets(at max. thrust) while inducing a forward velocity with the main propulsion system. The main propulsion system would provide the max. horizontal thrust so that the aircraft would reach required horizontal velocity for climb-cruise flight. Calculations for the vertical takeoff to 15meters were done(table6-3). At the height of 15m, the aircraft would reduce the viking engines to provide for a hover. The initial calculations before the design freeze showed that 83.33N would be enough for the each vertical takeoff and landing maneuver. But, latter analysis indicated that 83.33N would not be enough. This comes about in the further investigation of the vertical takeoff.

The analysis of the vertical takeoff upto 15 meters vertical height

was correct. But, the calculation to the hover flight was out of the ball park.

From the analysis done on hover flight, the stall velocity of 62.68(m/s) was reached 38.8 seconds after the the start of the hover flight. For this analysis, the fundamental equations in sample 6-1 were applied in the horizontal direction. This analysis was especially complex because considerations had to be given to the change in mass, lift, and thrust to maintain the aircraft at hover until horizontal stall speed. Only the assumptions and results are presented:

The hover takeoff was modeled like a conventional takeoff but without the ground friction and flare. Thus , the only forces acting on the aircraft is the lift,the vertical thrust,the horizontal thrust and the drag. The horizontal thrust and drag are a function of velocity. Since the aircraft is accelerating, the mean velocity (62.68/Sqrt(2)) was used in the calculation for the horizontal thrust and drag. Also, for this take-off mode, flaps of 25 degrees deflection were used(look at later) to enhance the lift. As the aircraft is accelerating the lifts force begins to increase. This mean that the vertical thrust must be reduced inorder to maintain hover. Thus, there is the reduction of the mass flow of the fuel. The total mass is getting lighter at a different rate throughout this maneuver. At the beginning of the hover the mass flow of the fuel is 2.25Kg/s. When velocity of the stall is reached, the mass flow of the fuel is .3225Kg/s. This not a linear relationship as the curve in graph 6-1 indicates. So, the average mass flow of 1.37Kg/s was assumed.

The final results is that it takes total time of 42.6 seconds to reach stall speed via vertical takeoff. The aircraft's viking engines also burn 216N of fuel for one vertical takeoff.

Vertical control and stability

During flight at speeds below stall, the control surfaces such as ailerons,rudder, and elevator are not effective. So, for this marsian aircraft with VTOL capabilities, a control system much like the Harrier S/VTOL is needed (Figure 6-2). Compressed atmosphere from a compressor motor in the fuselage will be supplied to four control valves. The control valve at the tip of the nose will provide pitch control. The two control valves on each of the wing tips will provide the roll control,and the control valve located at the trailing edge of the left boom will provide the pitch and yaw control. The control valve at the wing tips(figure 6-2b) are coordinated with the ailerons; so, that when the ailerons are up; the compressed atmosphere is directed in the same direction and vis-versa. The control valve at the trailing edge shoots down and sideways(figure 6-2). The compressor provides 20 pounds (89.6N) of thrust toeach of the valves . These valves give the following moments:

weight ?.

rolling moment = 2204.16 N-m either direction

pitching moment = 336.9 N-m

Yawing moment = 1105.6 N-m

These control moments are controlled directly by the pilot ,just as he would control any regular control surface. This would stabilize the aircraft during gust loadings,etc.

Highlift System

For the conventional landing, a high lift system is required. Initial analytical iterations indicated that simple plain flaps would be sufficient for the conventional landing configuration. Because larger the flaps are the more effective and due to the structural considerations of the wing, a constant C_f/C=.30 is the optimal. It leaves 5% of the chord for the mechanical devices to control the flaps. Using the Datcomm manual of flaps, values were calculate for the changes in coefficient of lift, max. coefficient of lift, coefficient of pitching moment,and coefficient of drag (table 6-4). The flaps cover 19.66m^2 of the wing and is 34.98 % of the wingspan (figure 6-1). The reason behind picking the flap angle of 25 degrees for takeoff is due to fact that the ratio of lift over drag is the greatest at 25 degrees. The reason behind picking the flap angle of 45 degrees for landing is because that is where drag is the greatest.

Vertical landing

Vertical landing analysis as complex as the vertical takeoff analysis with almost similar modeling of the maneuver (figure 6-3). In this

analysis, the aircraft starts at height of 15m and at the stall speed (52.65m/s) with 45 degrees of flap deflection. The aircraft would pitch up with the use of the pitch control valve. It would pitch to a pitch angle of 8 degrees which is beyond stall angle. The thrust needed from the viking rockets would be 4808.5N. It would take 4 second to land the aircraft from a horizontal distance of 100 meters. It would used 84.6 N of fuel.

Conventional landing

Conventional landing analysis was done with the flaps deflected at 45 degrees and non-power glide. Using Prof. Sivier AAE 319 methods with the following assumptions:

μ = .5 $\qquad C_{Lopt} = .5(PI)(e_0)(AR)(\mu)$

for 4641.8N

Velocity of stall	52.67 m/s	with C_{Lmax}=1.40
Radius of flare	6230.58m	
Angle of approach	3.97 deg.	
Velocity at touchdown	60.55 m/s	
Ground deceleration	7.51m/s^2	
Total Landing distance	676.37m	

for 4681.8N

Velocity of stall	53.65 m/s with C_{Lmax}=1.40
Radius of flare	6469.49m
Angle of approach	3.90 deg.
Velocity at touchdown	61.69 m/s
Ground deceleration	7.90m/s^2
Total Landing distance	680.00m

The total landing distance for both cases at under the required boundary of 1000m.

Landing gear

The placement of the landing gear is very important for conventional landings. Since this MMRA 2 marsian aircraft is to perform conventional landing, a landing gear analysis was done. Following the landing gear design manual by Currey. Figure 6-4 was the method to determine the landing gear length and placement. The following resulted: (nose as ref. x=0 and the bottom of fuselage y=0)

Mean aerodynamic chord = 3.34m (MAC)
Vertical center of gravity = 1.3m (y-direct.)
Forward center of gravity = 3.35m (x-direct.)
Aft center of gravity = 3.76m (x-direct.)

Taking a vertical line from the 50% of MAC and a 15 degree line from the aft c.g. The intersection of these two lines determine the most forward placement of the main landing gear. For this aircraft, the main landing gear is place 4.65m from the nose(x=0). Laterally, the main landing gear are placed in the booms at 7.25m from the airplane's centerline. The nose gear is 1.3m behind the nose. The length of the nose gear is .7m and the length of the main gear is 2.0m. The main gear tucks into a pod in the boom (figure 6-5). The static loading of the gears are as follows;

Max. static load main gear per strut = 1840.29N

Max. static load nose gear = 1987.52N

Min. static load nose gear = 1251.40N

Max. braking nose gear load = 3130.61N

The parasite drag of the landing gear was not incorporated because it is negligible compared to wing reference area.

The tipping angle was also calculated. It came out to be 47.76 degrees.

Conclusion

The main goal of the takeoff and landing performance was met. The only problem is the miscalculation of the amount of fuel need. As of the

present design, the aircraft can takeoff and land only once. It just requires more hydrazine fuel for the viking engines.

The material to the landing gear is determined to be graphite epoxy, but, further investigation is needed. As for the ground maintenance, the aircraft would be stored and serviced inside an indoor hanger.

The pilot will Ingress and egress by lifting the glass canape and ingressing or egressing in the nose direction. The prop. will not be a safety factor on the ground, because they will never rotate on the ground.

whew!

CANAPÉ: A PIECE OF BREAD OR TOAST OR A CRACKER TOPPED WITH A SAVORY FOOD

Table 6-1

Given data

Take-off and landing required

Runway field length = 1 Km obstacle height = 15m

Power Data

Shaft Power = 70 Kw Efficiency = 0.85

Aerodynamic data

$C_{Lmax} = 1.04$ $C_L = 4.80$ $C_{Lcruise} = 0.531$

$e_o = 0.8$ $AR = 15.43$ $t/c_{at\ 27\%\ of\ chord} = 0.1$

$$C_D = .0193 + .0258\,C_L^2 + .0004\,C_L^3 - .0007\,C_L^2 + .0004\,C_L - .0001 + .0176 \sin^3(C_L/1.662 - .1105)$$

Wing Span	48.6m
Planform Area	$153.09m^2$
Taper Ratio	.400
Base Chord	4.5m
Tip Chord	1.8m

Change in Drag due to Flaps $C_D = C_L^2/AR - 2.3x10^{-6}(6)^2$

Viking Rocket Data From Jim Thompson-NASA/MSFC

Four Model MR 80 Variable Thrust Engine

Fuel + System : Blowdown Hydrazine Pressure
Chamber; 250psi-27psi

ISP	220 sec
Max. Thrust per engine	2668.8 N
Mass of each engine	7.7 Kg
Mass flow of fuel per engine	1.24 Kg/s (at Max. Thrust)

Marsian gravity **3.76 m/sec^2**

Amount of fuel allowed **250.0 N**

Table 6-2

Weight breakdown for missions

All weights are in Newtons on Mars

Case1

Aerial Scientific Mission

Take off weight	4725.13 N
Landing weight	4641.80 N

Case2

Aerial /Landing Scientific Mission

First Take off weight	4891.80 N
First Landing weight	4808.50 N
Second Take off weight	4724.50 N
Second Landing weight	4641.80 N

Case3

Rescue Mission

First Take off weight	4344.90 N
First Landing weight	4261.60 N
Second Take off weight	4764.50 N
Second Landing weight	4681.70 N

Table 6-3

Results for vertical altitude calculations

Values were calculated for the differ takeoff weight given in table 6-2. All values given values used are on table 6-1. The equations used are on sample 6-1. For vertical takeoff up to 15m, the viking engine are at max. thrust.

For aircraft weight of 4725.13N

vertical velocity(m/s)	time of burn(sec)	distance(m)
16.0	3.65	14.64
16.5	3.79	15.65
17.0	3.93	16.71

Amount of fuel used (N)

time x mass flow of fuel x gravity = 70.68 N

For aircraft weight of 4891.8N

vertical velocity(m/s)	time of burn(sec)	distance(m)
15.0	3.67	14.24
16.0	3.90	15.64
17.0	4.18	17.92

Amount of fuel used (N)

time x mass flow of fuel x gravity = 72.73 N

For aircraft weight of 4724.5N

vertical velocity(m/s)	time of burn(sec)	distance(m)
16.0	3.65	14.56
16.5	3.79	15.66
17.0	3.93	16.71

Amount of fuel used (N)

time x mass flow of fuel x gravity = 70.68 N

For aircraft weight of 4724.5N

vertical velocity(m/s)	time of burn(sec)	distance(m)
16.0	3.15	12.60
17.0	3.37	14.37
17.5	3.49	15.31

Amount of fuel used (N)

time x mass flow of fuel x gravity = 65.09 N

The change of $C_{L_{max}}$, C_m, C_D and C_L due to flaps

Used the Datcomm manual and the following givens (Table 6-1):

$C_f/C = .30$ $S_{wf}/S_w = .4676$

C_f=chord of flap C=chord of wing

S_{wf}=wetted area of flaps S_w=wetted area of wing

Angle of (deg.) flap deflection	*Change of $C_{L_{max}}$*	*Change of C_L*
10	.1259	.2132
15	.1810	.3165
20	.2282	.3410
25	.2675	.3571
30	.2990	.3901
35	.3226	.4253
40	.3422	.4849
45	.3619	.4986

Angle of (deg.) flap deflection	*Change of C_m*	*Change of C_D*
10	-.0487	.0114
15	-.0724	.0148
20	-.0780	.0158
25	-.0816	.0163
30	-.0892	.0175
35	-.0972	.0189
40	-.1108	.0213
45	-.1140	.0219

National 12-188
Made in USA

Upside down

Fig 6-1
FLAPS DIMENSIONS

TOTAL AREA of flaps = 19.65 m^2

ORIGINAL PAGE IS
OF POOR QUALITY

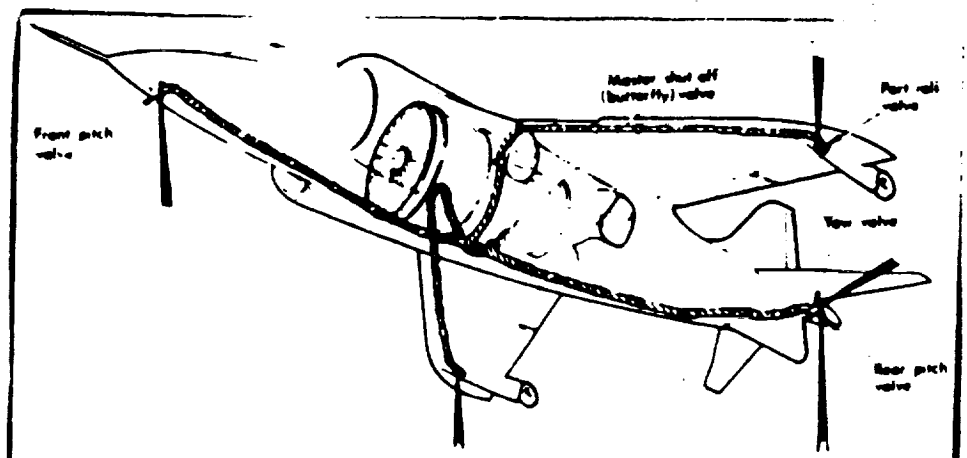

Fig.3.6.6 Reaction control system layout

FIG. 6-2

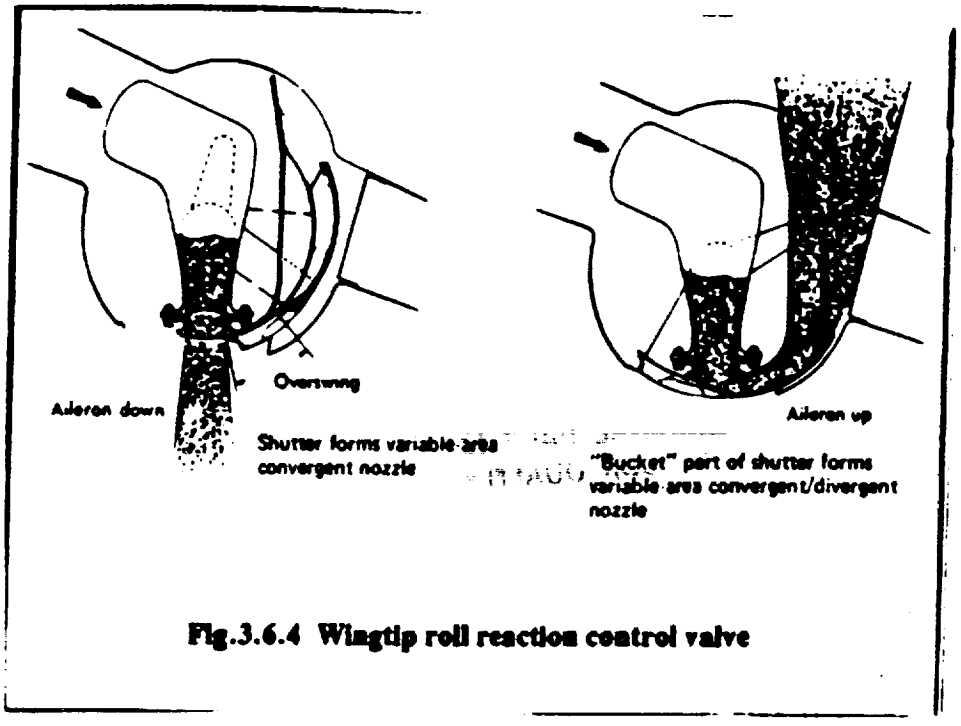

Fig.3.6.4 Wingtip roll reaction control valve

FIG 6-2b

FIG. 6-3

VERTICAL LANDING

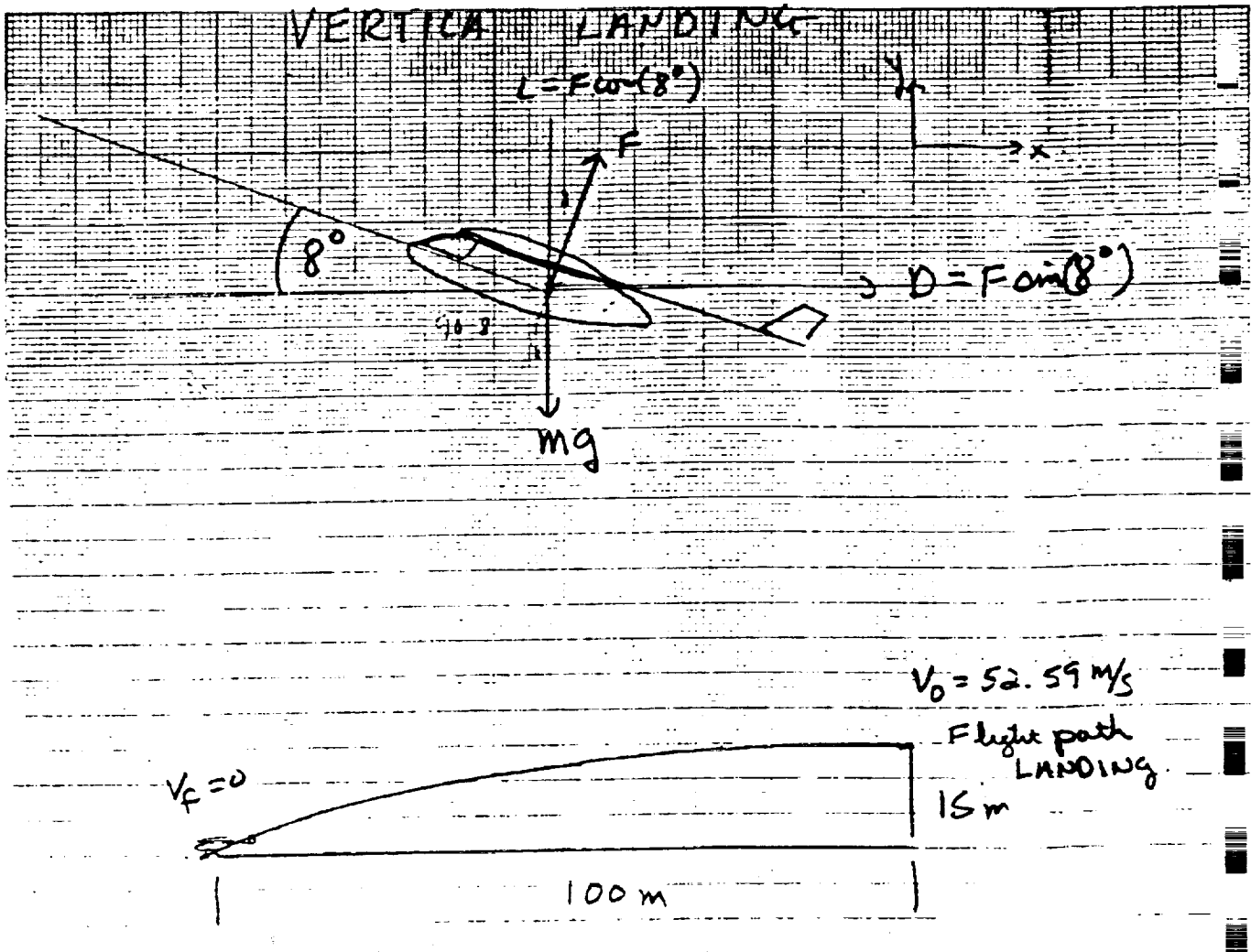

$$m - \dot{m}(t)\frac{dV_x}{dt} = F\sin(8^\circ)$$

$$m - \dot{m}(t)\frac{dV_y}{dt} = F\cos(8^\circ) - [m - \dot{m}t]g$$

FIG. 6-4

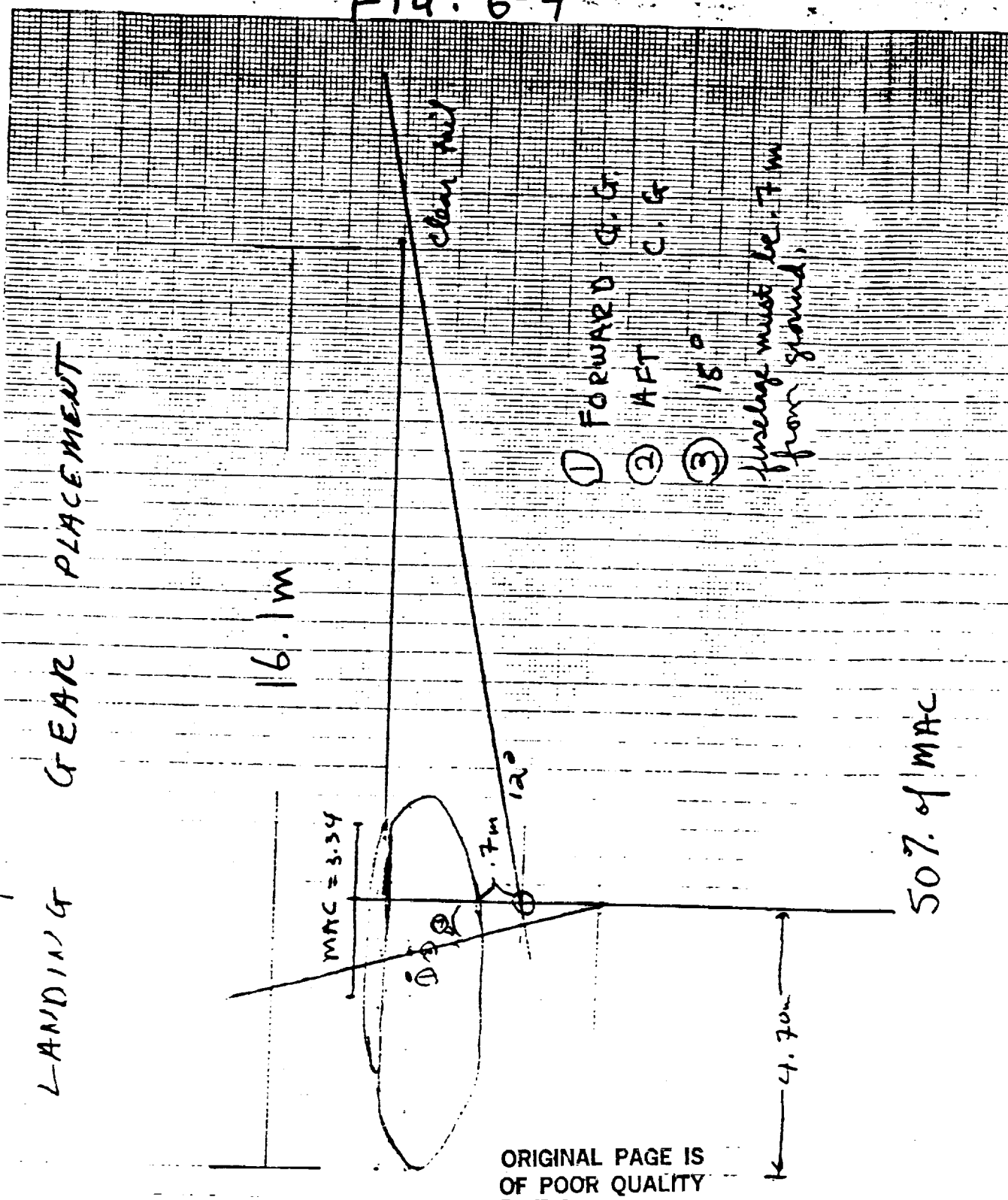

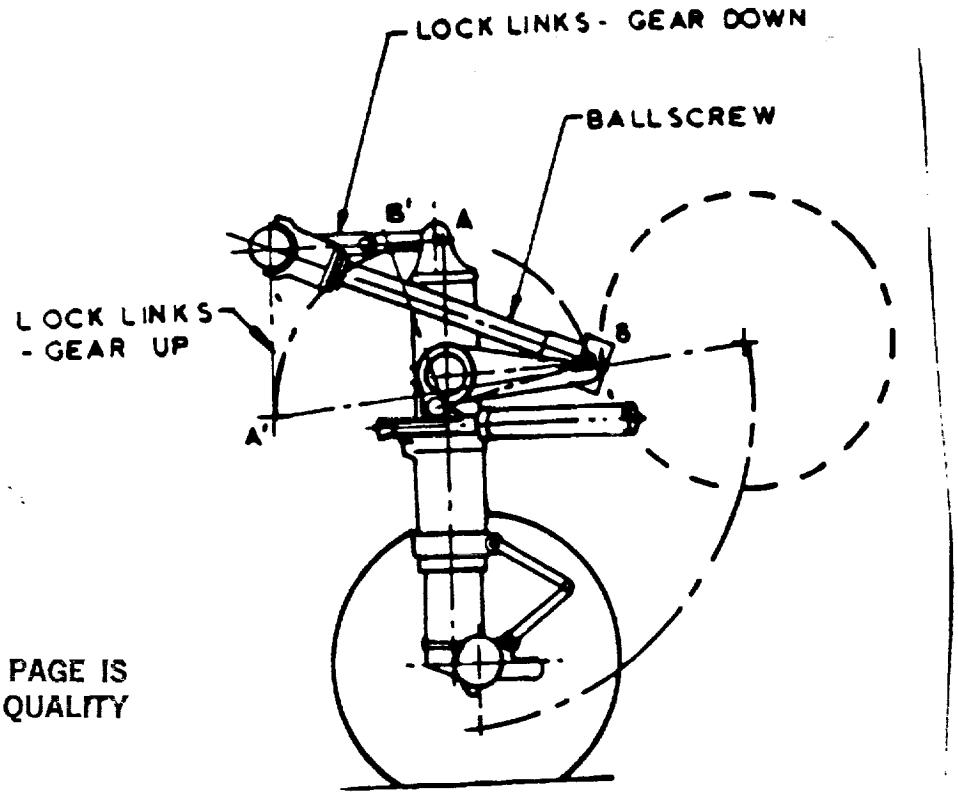

NOSE GEAR

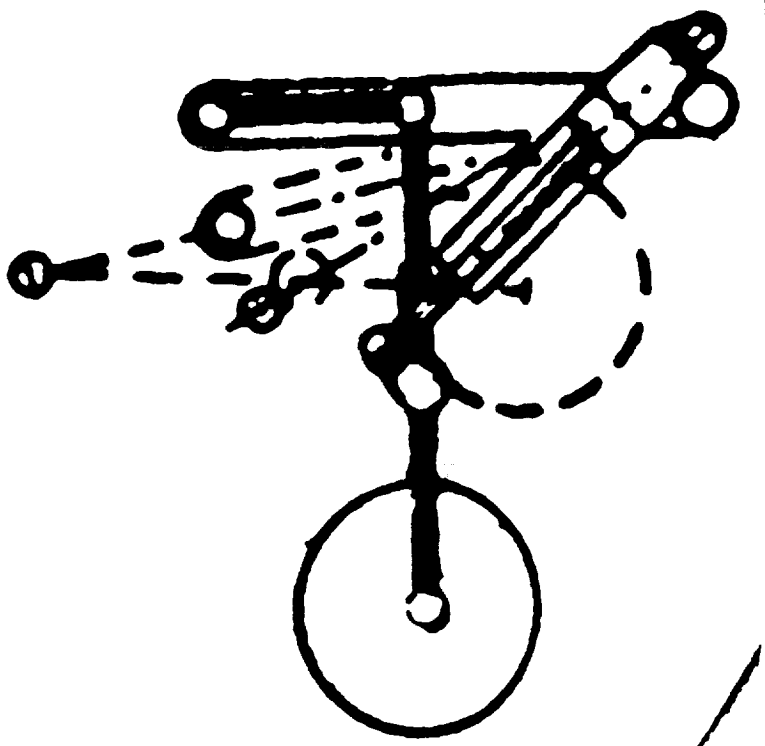

MAIN GEAR

FIG. 6-5

To find mean mass flux of fuel during take off.

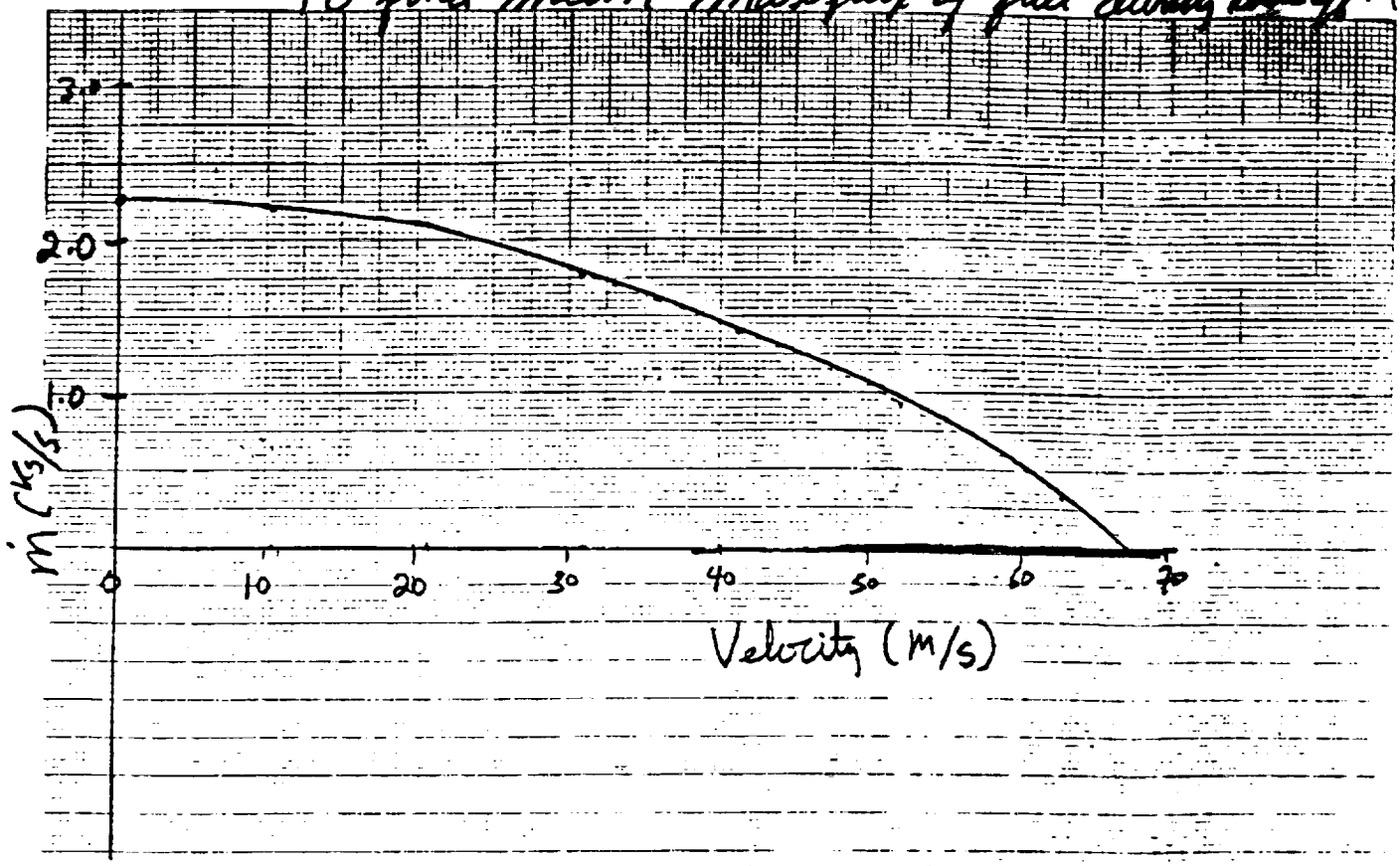

ORIGINAL PAGE IS
OF POOR QUALITY

Velocity (m/s)	Lift (N)	Thrust (Vertical) (N)	ṁ (kg/s)
0	0	4858.14	2.25
10.44	115.53	4742.60	2.20
20.34	437.45	4420.68	2.10
31.34	1044.13	3817.01	1.77
41.79	1850.31	3007.82	.40
52.32	2941.66	1966.47	0.92
62.52	4250.52	643.62	0.30
67.64	4258.14	0	0

AVE or mean $\dot{m} = 1.3713$ kg/s

Sample 6-1

Fundamental equations used for VTOL analysis

From Newton's 2nd Law

$$F=ma$$

For our analysis, we must consider the change in mass and aerodynamic forces. Thus;

$$M\, dv/dt = Thrust - weight - F_D \quad (1)$$

Where M=Mass of the aircraft, m^*=mass flow rate of fuel, t=time in sec., and F_D=aerodynamic drag. The mass change is $M=M-m^*(t)$. For the vertical assent, we will consider the wing and tail as flate plates. From Horner's Drag book, the following drag coefficient was used.

$C_{D_{wing}}=C_{D_0}(1-K(H/B)$ Where K=4.09, H=chord length and B=wingspan

Substituting in all values into (1) and integrate, we get

$$V=-[thrust-weight-\{.5\ V^2[S_{wing}(C_{D_{wing}})+S_{tail}(C_{D_{tail}})]\}] \times 1/m^* \times \{\ln[M-m^*(t)] - \ln[M]\}$$

We integrate again to get vertical distance;

$$Z= -[thrust-weight-\{.5\ V^2[S_{wing}(C_{D_{wing}})+S_{tail}(C_{D_{tail}})]\}] \times 1/4m^* \times \{\ln[M-m^*(t)]\,[m^*(t)/M] - \ln[M]\}$$

Bibliography

Fozard, John W. *The british aerospace harrier case study in aircraft design,* AIAA,July, 1978.

Currey, Norman S. *Landing gear design hand book,* Lockheed-Georgia Co., Jan., 1982

Horner, *Aerodynamic drag,* private, ??

Datcom/ Material on High lift wing systems

Sivier, Kenneth *AAE 316/ Applied Aerodynamics notes*

WEIGHTS AND CENTERS OF GRAVITY

Craig A. Barton

Table 7.1 shows the weight breakdown for the MMRA.2 aircraft. The weights for the components marked with an asterisk were calculated using the algorithms introduced in class.[1] These algorithms were originally intended to be used for weight calculations of light, general aviation aircraft. They were modified for use on the futuristic Martian aircraft using techniques presented in L. Nicolai's book Fundementals of Aircraft Design.[2] Nicolai, assuming advanced composite structures, suggests a 25% weight savings for a composite wing, fuselage, and tail over a metal part. A 12% weight reduction is suggested for the landing gear. These two factors were used when calculating the corresponding component weight.

Several of the weights are, at best, educated guesses. Avionics weight was estimated assuming a highly advanced cockpit and flight control system. Traditional cockpit designs had hundreds of dials, knobs, and instruments. Modern transport and military aircraft use high technology to ease the work load of the pilot. The MMRA.2 incorporates many of the same "instruments" that modern aircraft have. Not only do the modern systems work better, but thet offer substantial weight and volume savings.

The avionics weight includes communications, navigation, and flight control equiptment. The cockpit instrumentation consisits of four CRTs to display all of the aircrafts operating conditions. These displays will be activated by voice command and controls on the stick. The communications gear consists of UHF/VHF/HF radios for short and long range communications. A millimeter-wave radar is incorporated for collision avoidance and nightime operations. A data link and INS system are used for navigation. The weight for these vital components was set at 41.9 newtons.

A weight for the battery system was a little easier to calculate. Extensive researh was undertaken by the Propulsions Group to find a lightweight energy source. At first, this search proved unsuccessful as battery weight hovered near 900 newtons. Finally, a battery with a high energy density was found. The batteries have an energy density of 6250 watt-hours per kilogram (Wh/kg). This density was converted to Joules per kilogram to find a weight. The energy requirements for the aircraft were obtained by calculating the joules required to power the aircraft for an eight hour flight. Using the cruise power required for flight and avionics and adding a 10% "buffer" a total of 6.63×10^8 joules are required.

This energy requirement is equal to 108.8 N of batteries. This weight does not take into account the power needed by the payload. All payloads will include an auxilliary power source.

One area of concern for the weights group was the weight of the landing system. The decision to go with a VTOL system as well as a conventional system put two "landing systems" on the aircraft. This was an unavoidable weight addition due to the broken terrain on Mars. If the aircraft was to perform a landing in the field a vertical landing was the only possible type. Also, propeller size precluded a normal take-off.

The alighting system is composed of a tricycle landing gear and a set of four Viking VTOL thrusters. The landing gear weight was found using the weight equations. This weight was consistently higher than expected, but further study revealed it to be consistent with gear weights of similar aircraft. The weight of the Viking system was calculated using real data supplied by Surface Operations. Weights group had hoped for a more modern VTOL system but the Viking system offers no great weight penalties. Overall the alighting system weighs 278.5 N which is 5.6% of the GTOW. When 250 N of hydrazine fuel is added the landing system weighs 528.5 N or 10.7% of gross weight. This is a rather substantial portion of the total weight, but the two systems are needed for the MMRA.2 to operate effectively on Mars.

Payload for the aircraft consists of one pilot (586.9 N), and either 586.9 N of passenger or instrumentations. The location of this passenger/payload bay was optimized so that the center of gravity would be in the same spot for either configuration. Furthermore, when flying with a passenger, such as during a rescue mission, an extra seat is added in the payload bay. This seat has a weight of 40 newtons. This brings the total payload to 1213.8 N which is 13.8 N above desighn specifications. This extra weight is no problem since the aircraft will rarely, if ever, fly at maximum ramp weight.

WEIGHT HISTORY

The maximum take-off weight (GTOW) for the MMRA.2 is 4932 newtons. The basic empty weight (BEW) is 3468.4 newtons. Most of the flight scenarios picture the aircraft flying between 4200 N and 4900 newtons.[3]

The weight for this aircraft has changed drastically since the project began three months ago. The sizing example returned a GTOW of 3280

newtons. It soon became clear that this weight was only a ballpark figure and would change once the design process began in earnest.

It is easiest to see how the weight has changed by following the path of GTOW and wing weight. These two paramaters best describe the up and down cycles that the Weight Group encountered. The cycles began with a general design with a low weight. The weight would increase as this design was thought through. But, as the design evolved the weight would be reduced below the previous weight only to increase again as the design process continued. The weight went through several of these cycles before the final weight was finally determined.

The initial sizing example GTOW of 3380 N returned a wing weight of 1036.9 newtons. This weight was 30.7 percent of the GTOW. As more data became available it became possible to perform a weight iteration for the first time. This iteration yielded a gross weight of 5609 N and a wing weight of 2915.8 newtons. The component weight percentage is 52 percent. This percentage is so high because real data at this time was limited to the wing. Therefore, many of the other weights were much to low. The GTOW at this time was deemed much to high and work was begun to cut weight.

A maximum weight of 5557.2 N was reported for the midterm. This weight was only slightly lower than the previous weight. This caused concern that the GTOW would hover around this high mark and severly hamper the aircraft's performance. Wing weight for this stage of the design was calculated to be 2153, or .39GTOW.

After a radical design change (new airfoil, smaller engines, etc..) the weight began to come down. As stated before, this happened in cycles. The weight would decrease , the increase, then decrease again. The fact that weight was decreasing more than increasing was very reassuring. Using new data a GTOW was calculated to be 4650 newtons and a wing weight of 1535 newtons was found. This wing weight was 33% of the maximum weight. This would not be the final weight as several more systems were added to increase weight. This would be the last "cycle" and would lead to a final design weight.

The final GTOW was found to be 4932 newtons and the corresponding wing weight is 1933.1 newtons, or 39.2 percent. This weight reflects several systems (VTOL compressor, seat, more fuel) that were added late in the design process. This weight of 4932 N is also within the design limits set by the group. The maximum weight limit was placed at 3000

lbs. (5031 N) and the design goal weight was set at 2750 lbs. (4600 N). The extra 300 N do not have a great effect on on performance since most missions will be flown several hundred newtons below GTOW.[4] Table 7.2 shows the operating limits , useful load fraction, and maximum fuel fractions for the MMRA.2.

CENTERS OF GRAVITY

An interior configuration was developed so the centers of gravity could be calculated fo various aircraft components.[5] Aircraft centers of gravity could then be calculated. The c.g. location is very important in an aircraft of this type. Due to the adverse weather conditions on Mars the MMRA.2 needed to be very stable and controllable. Stability and control presented fore and aft c.g. limits of 2.912 and 3.630 meters, respectively. These limits are referenced to the nose tip (0m). The aft limits represent the minimum static margin of 0.1 allowed by the design requirements. The centers of gravity for the aircraft all fall within the limits and the minimum static margin is 0.19. The center of gravity travel diagram, Fig. 7.3, shows c.g. locations for all three main missions as well as other operational configurations. The lines connecting the points in Fig. 7.3 do not represent fuel burn. The only fuel "burnt" is hydrazine during vertical maneuvers. Therefore the c.g. travel diagrams for the MMRA.2 are quite different than a conventional c.g. diagram. The lines connecting the points are only used to show the direction of travel during different parts of the missions.

The centers of gravity do not move significantly, they are all near 3.3m, because the aircraft does not burn fuel. Figue 7.4 is a detailed view of the region near 3.3m from Fig. 7.3. Hydrazine fuel is carried for vertical maneuvers but , since it is only 5% of the GTOW, it's use does not effect the c.g. location. Also, the c.g. for the payload is in the same place as the c.g. for an extra passenger. This creates a wide variety of operating configurations with the payload or an extra passenger.

Overall, the centers of gravity are within the limits set by Stability and Control. One exception is at Basic Empty Weight (BEW) where the c.g. is located aft of the aft limit. This is alright since at BEW the aircraft can not fly. However, the aircraft is balanced on the ground at BEW. In flight, though, the MMRA.2 is statically stable.

REFERENCES, NOTES

1 Roskam, Jan, Airplane Design, Part V: Component Weight Estimation, Roskam Aviation and Engineering Corp., 1985.

2 Nicolai, Leland N., Fundementals of Aircraft Design, METS Inc., 1975.

3 For a detailed description of scenarios see Mission Scenarios section

4 For a detailed mission weight breakdown see Mission Scenarios section

5 Roskam, Jan, Airplane Design, Part V: Component Weight Estimation, Roskam Aviation and Engineering Corp., 1985.

TABLE 7.1
Component Weights and Center of Gravity

COMPONENT	WEIGHT(N)	%GTOW	CG(m)
Wing*	1933.1	39.2	3.30
Fuselage*	306.0	6.2	2.47
Horizontal Tail*	79.1	1.6	15.80
Vertical Tails*	26.6	0.5	15.80
Tailbooms	218.8	4.4	8.00
AIRFRAME	**2563.6**	**51.9**	–
Engines	296.4	6.0	1.88
Nacelles	30.4	0.6	2.00
Propellers	50.0	1.0	1.70
Gear Reduction	33.6	0.7	1.75
Batteries	108.8	2.2	4.00
Electrical	8.4	0.2	2.40
PROPULSIONS	**527.6**	**10.7**	–
Landing Gear*	124.6	2.5	2.97
Viking Thrusters	113.9	2.3	3.15
Viking Fuel System	15.0	0.3	2.60
VTOL Compressor	25.0	0.5	3.70
ALIGHTING GROUP	**278.5**	**5.6**	–
Com/Nav/Avionics	41.9	0.9	0.40
Flight Controls	16.8	0.3	4.15
Crew Provisions	40.0	0.8	1.32
AICRAFT SERVICE	**98.7**	**2.0**	–
BASIC EMPTY WT	**3468.4**	-	–
Payload	1213.8	24.6	2.34
MAX ZERO FUEL	**4688.2**	-	–
Hydrazine	250.0	5.1	2.60
MAX TAKE OFF	**4932.0**	-	–

TABLE 7.2

AIRCRAFT WEIGHT PARAMETERS

Maximum Take Off Weight	4932 N
Operational Empty Weight	3468 N
Maximum Landing Weight	4849 N
Maximum Battery Fraction	2.2%
Maximum Hydrazine Fraction	5.1%
Useful Load Fraction	29.6%

FIGURE 7.3

CENTER OF GRAVITY TRAVEL DIAGRAM

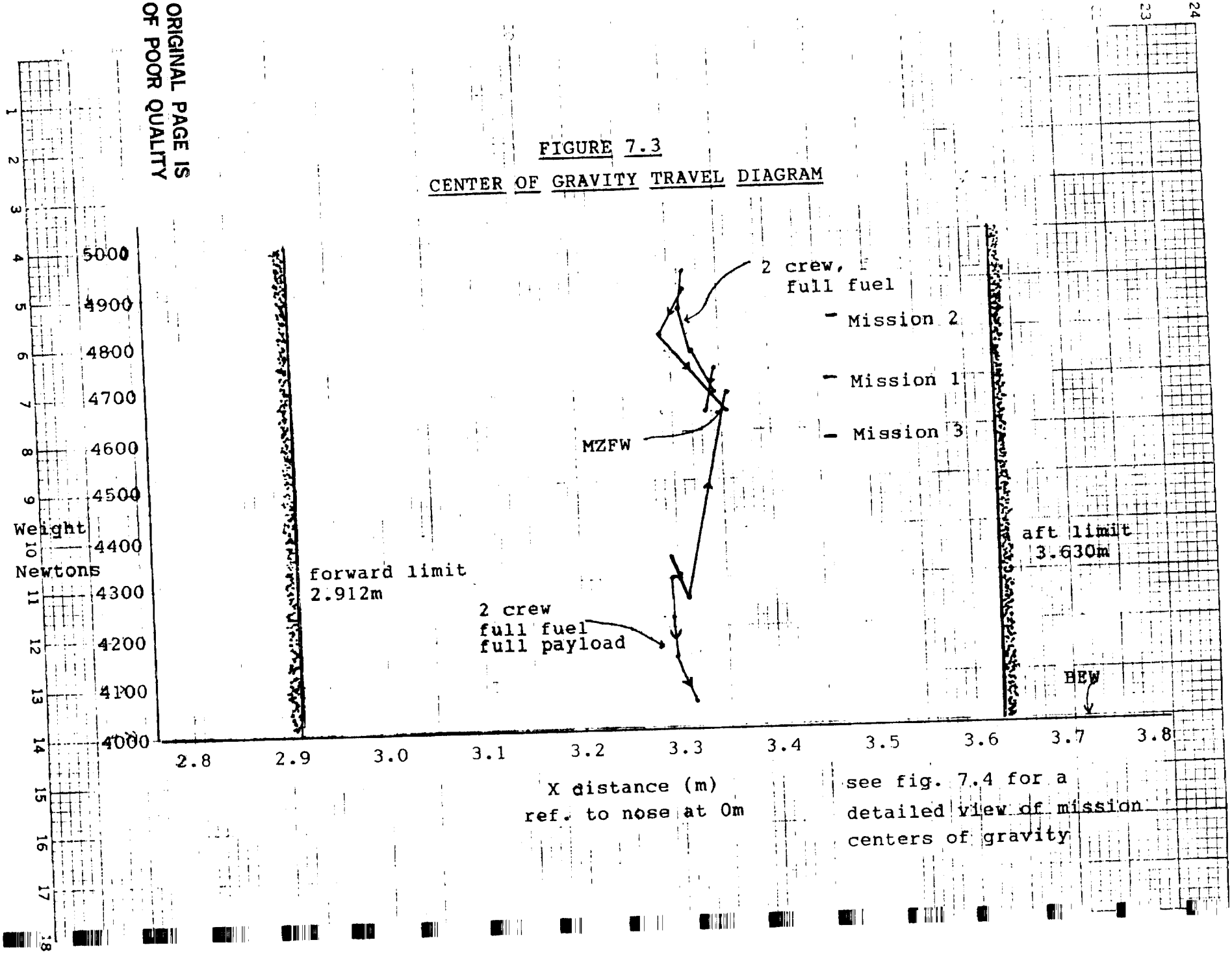

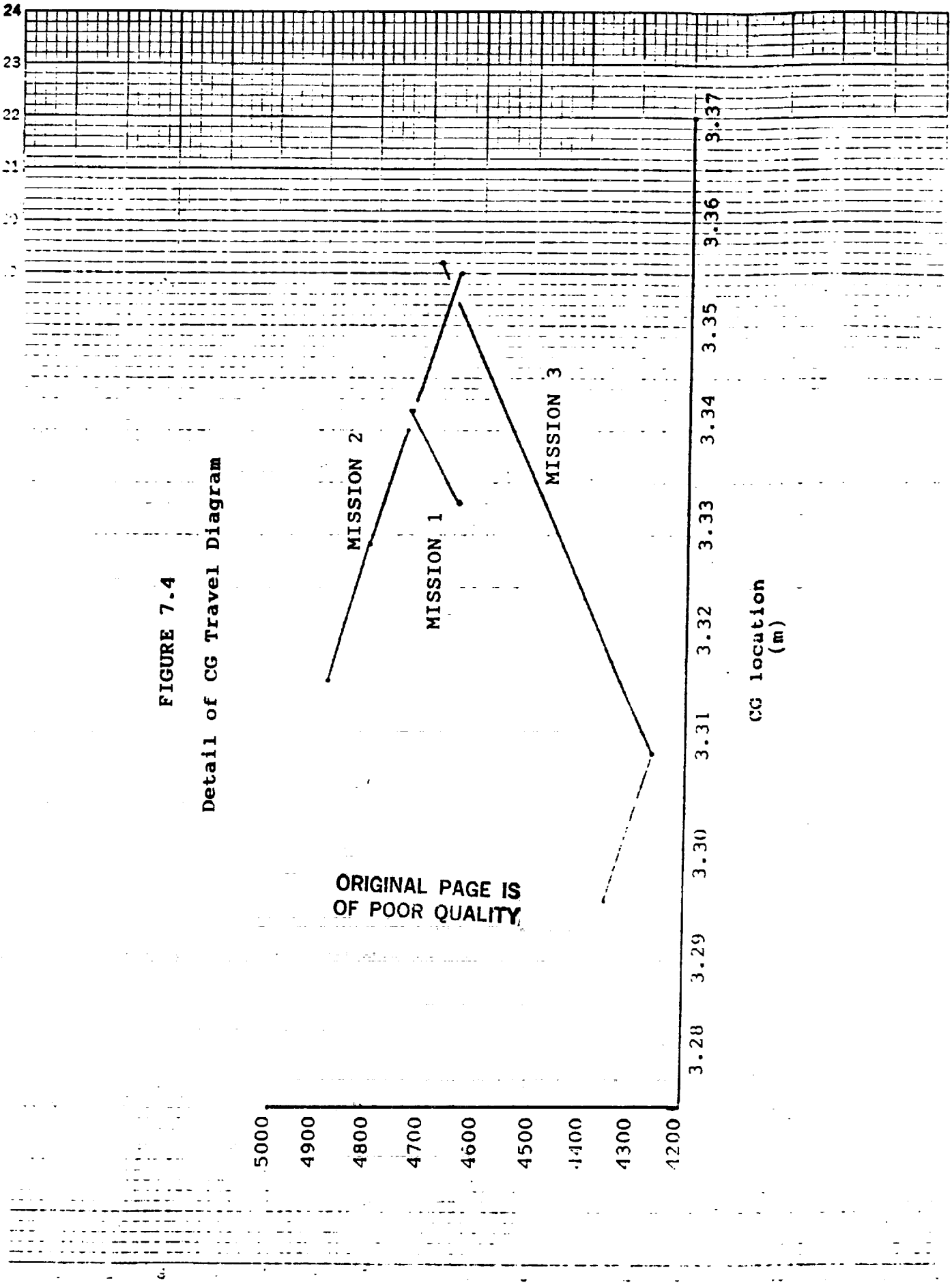

FIGURE 7.4

Detail of CG Travel Diagram

ORIGINAL PAGE IS
OF POOR QUALITY

COSTS

Rick Kreiger

The total cost for the construction only of the current design is estimated at $238.5 million. This was evaluated using the supplied computer program plus the corrections to it. A breakdown by the seven sub-areas is in Table C-1. It is also broken down by the categories design, develop, test, and engineering, or DDT&E, and fixed hardware costs, or FHA. The masses in kilograms are also supplied.

Table C-2 shows a run of the program with some of the variables changed. In this run, all of the factors involved in the computation of the Structures cost were changed from 1.00 to 2.00. This was done for several reasons. First, the program is for spacecraft, not aircraft. The structures of each one are different. The spacecraft from which the initial values were set for was not man-rated, while this aircraft is. Also the current design is to make extensive use of composites in all areas of structure. This will cost more, has never been done to this extent, will get no "off-the-shelf" parts, and people have no experience in doing this. This is what the changed factors take into account. The result is an increase in the Structure's cost by the same factor of 2.00, as shown in Table C-2. The new total cost for this set-up is $299.1 million.

There are several reasons this cost might be off. As stated before, this is a spacecraft cost model. Also, the placing of components into the sub-areas is not too scientific. Some areas, such as Reaction Control, were left blank. The majority of the mass was categorized into Structures. This gave out a small cost in relation to its mass. Propulsion also produced a low cost for its mass. Table C-3 shows the percentage of total mass, and the percentage of total cost for both computations. The costs for items that are not functions of mass were not calculated. An example of this is Software costs. This was done since there was no data to put into the program. The total costs supplied are the costs to build the "hardware" of the aircraft only.

At best, the costs supplied here are a very rough estimate. A better estimate would have a more accurate breakdown of the weights. It would require more knowledge of the variable factors so that they can be determined accurately. It would also include the costs that were not estimated due to lack of information.

TABLE C-1

Sub-area	Mass kg	DDT&E millions of dollars	FHA millions of dollars	Total millions of dollars
Structures	747	46.5	14.1	60.5
Thermal	0	0.0	0.0	0.0
Attitude Control	16	17.4	3.9	21.3
Reaction Control	0	0.0	0.0	0.0
Communications	168	120.0	28.9	148.9
Electrical Power	32	7.3	0.1	7.5
Propulsion	107	0.3	0.0	0.3
TOTALS	1070	191.5	47.0	238.5

TABLE C-2

Sub-area	Mass kg	DDT&E millions of dollars	FHA millions of dollars	Total millions of dollars
Structures	747	92.9	28.1	121.1
Thermal	0	0.0	0.0	0.0
Attitude Control	16	17.4	3.9	21.3
Reaction Control	0	0.0	0.0	0.0
Communications	168	120.0	28.9	148.9
Electrical Power	32	7.3	0.1	7.5
Propulsion	107	0.3	0.0	0.3
TOTALS	1070	238.0	61.1	299.1

TABLE C-3

Sub-area	Percentage of mass	Percentage of cost		
		Original	Changed	
Structures	69.8	25.4	40.5	
Thermal	0.0	0.0	0.0	
Attitude Control	1.5	8.9	7.1	
Reaction Control	0.0	0.0	0.0	
Communications	15.7	62.4	49.8	
Electrical Power	3.3	3.1	2.5	
Propulsion	10.0	0.1	0.1	
TOTALS	100.3	99.1	100.0	

INTERNAL CONFIGURATION

CRAIG A. BARTON
KEVIN J. KLEIN

The internal configuration of the MMRA.2 is shown in Figure IC.1. This configuration was devised by the Weights and Structures Groups to optimize the c.g. locations and to make the fuselage structure as simple as possible. Volumes for individual components were calculated when possible. The component volume was estimated when no exact size was known.

The placement and size of the payload bay was the most difficult task while determining the internal configuration. Because the payloads size was unknown, as much volume as possible was allotted. Therefore, the payload bay is split. This allows for extra volume as well as placing the c.g. in the proper location. This split design also allowed Structures to place ribs and bulkheads directly beneath the wing spars for increased strength.

The hydrazine fuel system consists of two spherical tanks. Each is located on either side where pictured. Each tank can hold up to 125 N of fuel and is used to fuel the two thrusters on the same side. These tanks are loaded from beneath where a pump pressurizes the tanks for proper operation.

The internal configuration is very simple. It stresses simplicity and a variety of configurations. The design creates a very neat fuselage structure and gives the aircraft a large volume for payload.

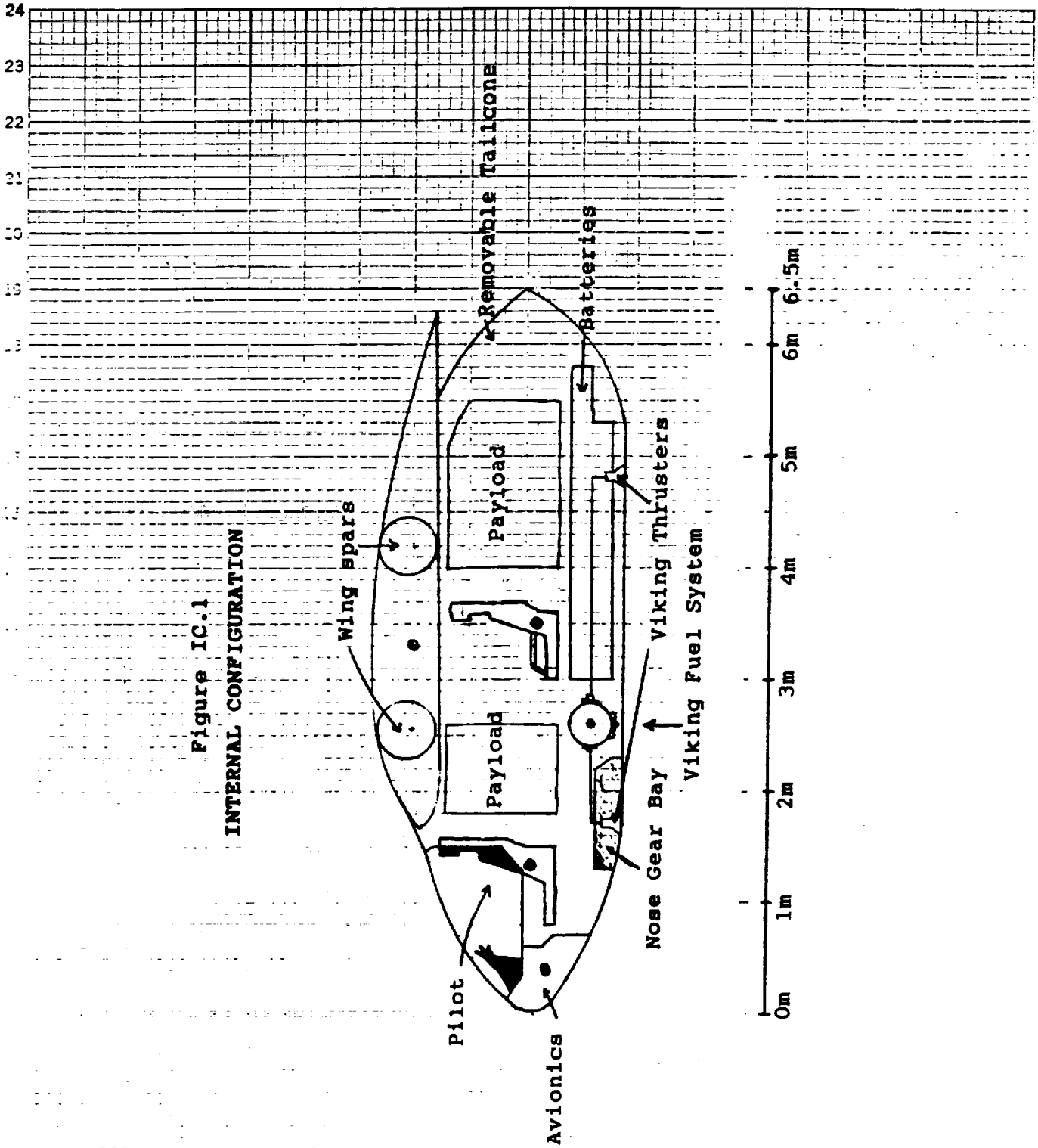

Figure IC.1
INTERNAL CONFIGURATION

PACKAGING AND ASSEMBLY

Kevin J. Klein

The dimensions given for the Shuttle bay were 18.3m by 4.57m. Due to the large size of the MMRA.2 aircraft, it was necessary to incorporate a way to break the aircraft down into several components which could then be shipped to Mars. This design also had to be simple, since it would have to be assembled again on the Mars surface.

The packaging procedure consists of first disassembling the aircraft into small enough components, packaging them, and shipping them to Mars. Figure PA.1, along with Figures 5.9 and 5.10 show the basic breakdown points. The fuselage will be broken down into three pieces, a front and rear cone, and the main cylindrical frame. The front and rear cones will then be inserted backwards into the rear payload bay to save space. The bulkheads at these breakdown points will have interlocking edges with a surface to be used for bolting the seperated pieces back together. The wing will also be broken down into three pieces, and the tail/tail-boom structure along with the engine assembly will both be easily removed. The wing segments will be reassembled using the device shown in Figure 5.9. This piece will also provide an easy way to connect the spars while securing the ribs along either side. The tail-booms and vertical tails will fold over onto the horizontal tail to form a very compact structure. Figure PA.1 shows the way that these components will be stored in the transport cylinder. Effort was taken to insure that the center of gravity would remain as close to the center of the cylinder as possible.

Figure PA-1 Aircraft Packaging Diagram

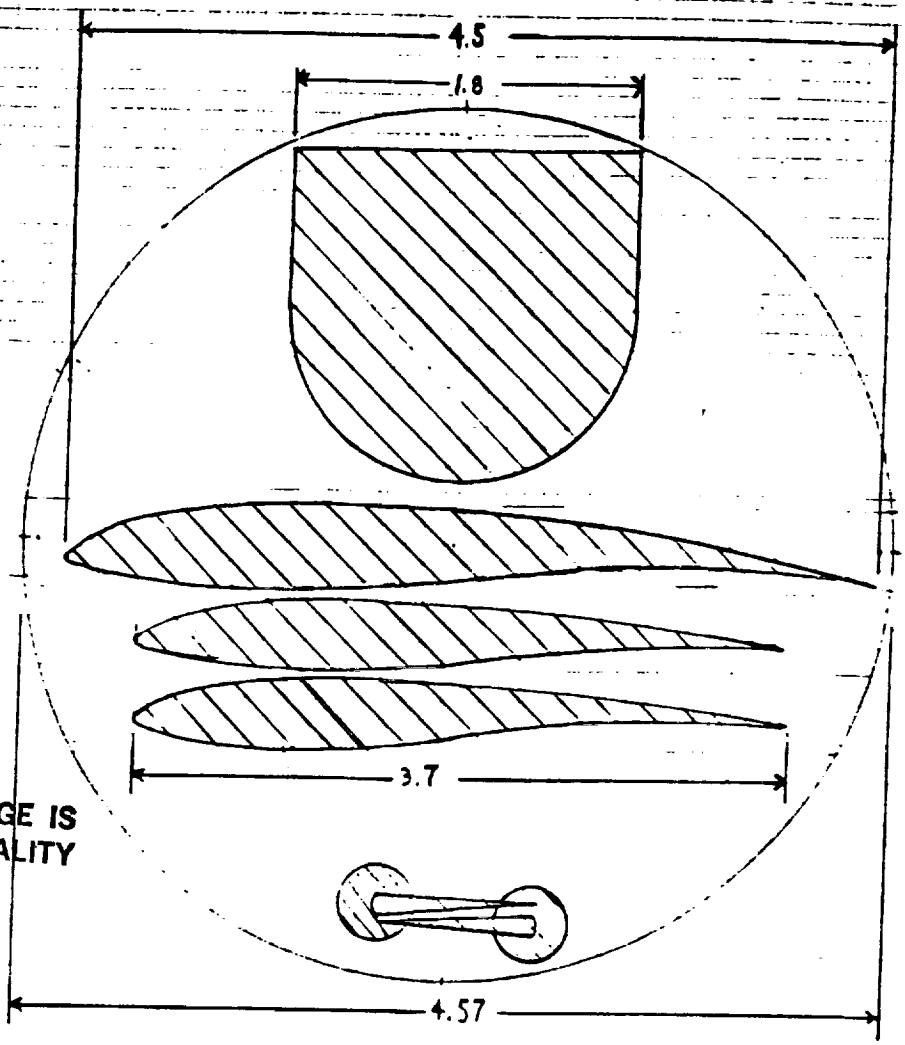

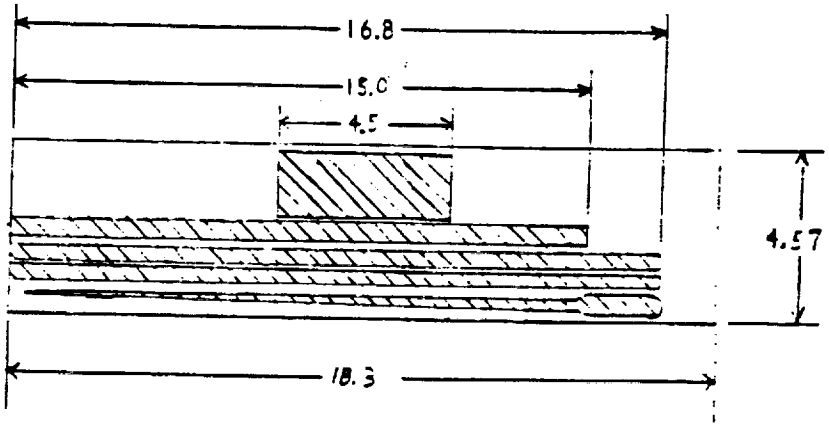

all dimensions in meters

Rescue

by

Hwasup Lee

The rescue of another rescuee will happen only if the rescue site is within the radius 1351 km from the starting point of the rescue airplane. The rescue craft will have all its scientific payload emtied except for some lifesupport equipment. The aircraft will take off vertically. After reaching the rescue site, the aircraft will land vertically to pick up the rescuee. The rescuee will be placed in the payload bay . The aircraft will takeoff vertically and return to base. When the mission is complete, aircraft will return to base and land conventionally. One the ground, airplance will be towed into a indoor compound and the rescuee will be treated.

No. 8 92 PAGES
JFH

SKY C.A.B.

A Manned Mars Aircraft

Mike Croegaert	- Aerodynamics
Steve Schirle	- Performance
Jamie Goggin	- Power and Propulsion
Jamie Edgar	- Stability and Control
Jami Munson	- Structures
Matt Miller	- Surface Operations
Angie Kostopoulos	- Weights

AAE 241

Professor Sivier

4/28/88

DESIGN SUMMARY

The objective of the design group was to design a manned Mars aircraft for reconnaissance that met certain specifications. These specifications include an eight hour endurance, a landing and take-off field length of 1km, and the capability to transport a 1200 N payload. The aircraft must also provide for a rescue scenario and must be suitable for transport from the space station to Mars. These specifications provide the boundaries for the design of Sky C.A.B.

The Mars atmosphere played a major role in the design philosophy of Sky C.A.B. Because of the low density on Mars, an airfoil and wing configuration that would produce a high lift in a low density region was required. The engine selection for the aircraft was primarily based upon the atmosphere conditions also. Sky C.A.B. needed an engine that would not only produce enough power to fly the aircraft, but that would also take advantage of the resources on Mars. Once these two areas of the design process were decided upon, the other areas could determine if specifications could be met.

The joined wing configuration combined with NASA NLF(1) - 1015 airfoil proved to be adequate for the Mars atmosphere. Together, they produce the needed lift for the low density region. The methane engine chosen by the propulsion section meets the power requirement needs and also takes advantage of the resources on Mars. Since methane is a combination of carbon and hydrogen, the production of the fuel should cause few problems since both gases are of great abundance on Mars. The carbon can be found in the atmosphere in the form of carbon dioxide while the hydrogen can be found in ice on the surface of Mars. Using these selections, the remaining design areas found that flight at the goal weight would be possible.

There were several problems which had to be overcome before the final design could be put on paper. The first and most serious problem was the weight of Sky C.A.B. At the time of the preliminary report, a weight of almost 8900 N was needed for the aircraft, almost 3000 N over the goal weight. Also, a wing span of 80 m and a fuselage of length 40 m proved tolarge for transport purposes. The obvious solution to both these problems was to reduce the wing span, the fuselage length, and, in doing so, decrease the gross weight of the aircraft. Reducing the wing span to 50 m and the fuselage length to 20 m helped bring the gross weight down around the desired goal weight. These new dimensions also met the requirements set by the spacecraft section. Also, this reduction in size alleviated the poblem with landing gear. At the time of the preliminary report, it was discovered that a 5 m long landing gear would be needed due to the long wing span and the dihedral angle of the wing. After the reductions were made, an exceptable landing gear length of 2.5 m was achieved.

Many changes have occured in the design of Sky C.A.B. since the initial sizing. Every area of the design process has been met with problems which had to be solved before flight could occur. Through changes in wing span, cruise velocity, engine design, and a number of other areas, these problems were overcome. The result, a manned aircraft capable of flight in the martian antmosphere.

AAE 241
Spring 1988
DESIGN DATA SUMMARY

Gross Weight: 5957 N
Wing Loading: 19.06 N/m^2
Maximum Fuel Weight: 722 N
Useful Load Fraction: .322

Maximum Take-off Power: 28 kw
Power Loading: .0897 kw/m^2
Fuel Fraction: .121

Geometry

Ref. Wing Area = 312.50 m^2
AR = 8
Λ_{LE} = 16 forward 16 aft
λ = .6 front .67 back
t/c = .159

Propulsion

Engine Description: Free Piston Stirling Engine
Number of Engines = 1
$P_{O_{max}}$ /Engine = 32.25 kw
Weight/Engine = 613 N
c_p at Cruise = 1.2 kg/kwh
Prop. Diam. = 8.265 m
No. of Blades = 2
Blade Cruise R_e = NOT AVAILABLE

Performance

Cruise R_e = 5×10^5
Cruise h = 1.5 km
Cruise M = .25
Cruise V = 60 m/s
Take-off Field Length = 836.3 m
Take-off Speed = 60 m/s
Landing Field Length = 891.6 m
Landing Speed = 41.8 m/s
Maximum Landing Weight = 5957 N
OEI Climb Gradient (%): = DOES NOT APPLY
2nd Segment =
Missed Approach =
Sea Level $(R/C)_{max}$ = 0.862 m/s

Stability and Control

Static Margin Range = .10 to .25
Acceptable C.G. Range = 8.0 to 8.6
Actual C.G. Range = 8.0 to 9.55

Aerodynamics

Airfoil: NASA NLF(1)-1015
High Lift System:

Cruise; C_{D_o} = .0182
e_o = .85
C_L = .6078
(L/D_{max}) = 93.29
Take-off; C_L = 1.02
$C_{L_{max}}$ = 1.60
Landing; C_L = 1.48
$C_{L_{max}}$ = 1.701

AAE 241
Spring 1988
INITIAL SIZING DATA SUMMARY

Gross Weight: 5,940 N

Wing Loading: 8 N/m^2

Fuel Weight: 496 N

Useful Load Fraction: .501

Maximum Take-off Power : 23.54 kw

Power Loading: .102 kw/m^2

Fuel Fraction: .299

Geometry

Ref. Wing Area = 742.5 m^2

AR = 10

Propulsion

Engine/Motor Type: Free Piston Stirling Engine

No. of Engines/Motors = 1

$P_{o_{max}}$ /engine = 25 kw

c_p at cruise = 1 kg/kwh

Aerodynamics

Cruise; C_{D_o} = .0515

e_o = .8

C_L = .91

$(\frac{L}{D})_{max}$ = 17.67

Take-off; C_L = 1.505

$C_{L_{max}}$ = 1.83

Landing; C_L = 1.671

$C_{l_{max}}$ = 1.84

Cruise Performance

h = 1.5 km

V = 58.3 m/sec

SKY C.A.B.

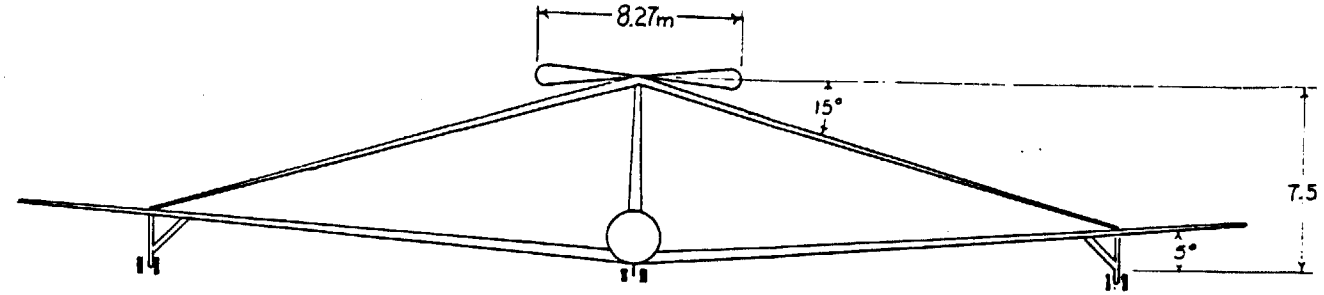

ORIGINAL PAGE IS
OF POOR QUALITY

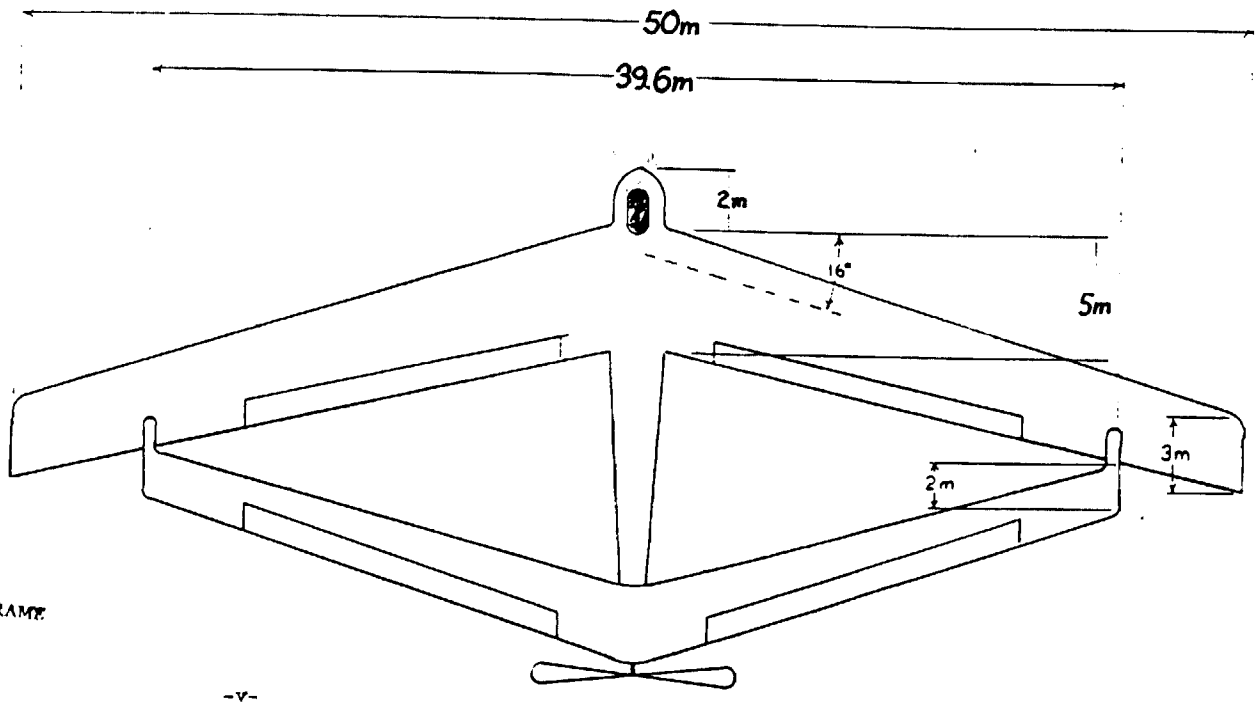

FOLDOUT FRAME

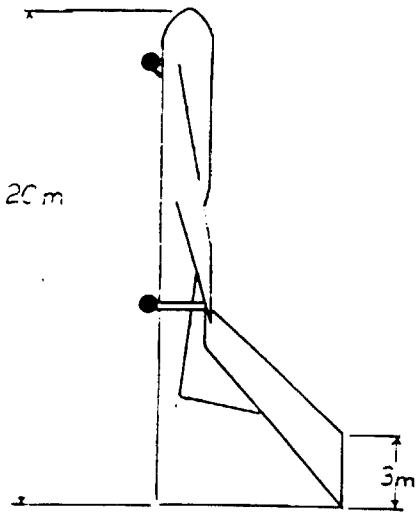

FOLDOUT FRAME

SKY C.A.B. : A MARS AIRPLANE

AERODYNAMICS

MIKE CROEGAERT

NOMENCLATURE

AR	Aspect ratio
b	Wing span
c	Chord length
C_d	Sectional drag coefficient
C_D	Total drag coefficient
C_l	Sectional lift coefficient
C_L	Total lift coefficient
D	Drag
F	Front wing
l	Location
L	Lift
R	Rear wing
S	Planform area
t	Airfoil thickness
V	Airspeed
α	Angle of attack
δ	Elevator deflection angle
Γ	Dihedral angle
λ	Taper ratio
Λ	Sweep angle
Θ	Wing twist

INTRODUCTION

Mars, and its exploration are becoming of major interest to more and more people in the space industry. This seems to be the next logical step since it is Earth's closest neighbor and thereby being the most easily reached. The question is: Once there, how is the exploration going to be completed? The use of a land rover is impractical due to the vast size of Mars, its nearly four times the larger than the Earth's moon[1]. The logical choice seems to be some type of flight vehicle equipped with reconnaissance instruments.

The designing of such a "Mars Airplane" requires the consideration of many factors that are quite different than what would be considered when designing an aircraft to fly on Earth. One such factor is the low atmospheric density which is less than one percent of that on Earth.[2] Other subjects that also have to be considered are the availability of fuel, low atmospheric temperature, and the maintainability of the aircraft. Several of these must be considered when developing the aerodynamic configuration of the aircraft.

AIRCRAFT CONFIGURATION

There were several different configurations that were considered for this aircraft. Monowing with an aft tail, monowing with a canard, and a biplane were just a few of the choices. The approach that was taken was that of a joined wing design. This was chosen due to several advantages over conventional designs. From the structural standpoint, it had high stiffness with a relatively low weight and a reduced fuselage length. It had the aerodynamic properties of low induced drag, a high trimmed C_{Lmax} and reduced parasite drag due to a lower wetted area. The joined wing also provided good stability and control with direct lift and sideforce control capabilities.[3]

The joined wing configuration itself, had several design options which had to be considered to find the optimum design. Probably the most important of these was that chosing the configuration of the wings. This included the location and the type of joint, airfoil design, planform area distribution between the front and rear wing, taper ratio, dihedral and sweepback angles, and wing twist. The decision on the location of the wing joint was made to keep the aircraft as lightweight as possible. It was found that the optimum location of the joint, for this weight consideration, would be inboard of the front wing tip at 70 percent of the half-span.[4] The wings will only overlap slightly. This reduces some of the effect of induced velocity at the joint.

Choosing an airfoil posed some interesting problems. The low density and the initial design criteria of an eight hour flight were the two major concerns in the selection process. Several airfoils that had been designed for low Reynolds numbers were examined and one that also satisfied the endurance requirement was chosen. The airfoil selected was the NASA NLF(1)-1015. A cross-section and design characteristics are shown in Figures 1 and 2 and Table 1. This airfoil had a relatively high C_{lmax} and its behavior near C_{lmax} was independent of surface contamination which helped to reduce drag.[5]

The low density condition was important because of the low Reynolds numbers is allowed for aircraft. For this design they were approximately $5x10^5$ for cruise conditions. This was a problem because even though it reduces parasite drag, it also reduces the lift obtainable for a given wing. Therefore, to produce enough lift for the the aircraft to fly, a large wing area was required. It was found that for the lift required a wing planform area of 312.5 m^2 was necessary. This area was apportioned between the front and rear wing with 64 percent of the total area going to the front wing. The wings were also designed with a taper to help accomadatte the area distribution. For this chosen area arrangement, the ratio of the lift due to the front wing to the lift due to the rear wing was found to be approximately 1.77.

When the wing was designed as a whole, there were several parameters that had to be considered. In order for the front and rear wing to join large sweepback and sweepforward angles are required. The selection process for these angles involved finding the optimum case to match the wing span, fuselage length and weight considerations. It was found from research that as the sweep angles were increased the weight increased disproportionately.[6] Another parameter that had to be determined was the dihedral angles. Increasing the dihedral angle was advantageous to the relative weight so, there was no constraint from that standpoint.[6] The problem with the dihedral arose when the landing gear location was examined. It was discovered that in order to keep the landing gear length reasonable the dihedral for the front wing had to be small. An angle of 5 degrees was decided on. This along with the given height determined the dihedral of the rear wing to be -15 degrees.

Probably the most difficult design conditions to determine were wing camber and twist. These considerations were necessary due to the interference in the airflow across the rear wing produced by the front wing and vice-versa. The front wing produces an induced camber on the rear wing and a negative angle of incidence increasing from the the root to the tip.[6] To reduce the induced drag produced by these effects a positive camber of about 2 percent of the chord and a

twist of 6 degrees were designed into the rear wing. For the front wing the effect was similar and a 4 percent of the chord wing camber and a twist of 3 degrees inboard of the joint and 5 degrees outboard of the joint. This increasea in twist outboard of the joint was added to prevent the tips from stalling before the rest of the wing.

AIRSPEED SELECTION

The velocity at which this aircraft flys was of major concern when it was being developed. The design airspeed has significant effects on the configuration of the plane. If a large velocity was chosen, then compressibility problems could have arrose which may have made it necessary to change or modify the airfoil and wing design. If too small of an airspeed had been used, producing enough lift to cruise at the required altitude would have been impossible. Another determinant for the cruise airspeed was the specified mission. The main purpose of this project was to develop a way to survey the Martian surface, and ths could not be done if the flight speed was too high to get accurate data. Taking into account these facts and optimizing the fuel and weight requirements for a complete flight the cruise airspeed was determined to be 60 meters per second.

DRAG DISCUSSION

After the complete aircraft configuration was determined, it then became possible to determine the values for both parasite and induced drag terms. There were several parasite terms that had to be calculated. They included terms due to the wetted area of both wings, the vertical tail and the fuselage. The induced terms were comprised of those due to the wing body interference, wing twist and angle of attack of the aircraft. A complete list of the drag terms is given in Table 2. Another consideration of the drag analysis was the drag rise as flight conditions approached C_{Lmax}. For the chosen airfoil, this was not important until the flight conditions were within 7 percent of C_{Lmax}. These ΔC_D values that have to be added to the drag polar are listed in Table 3. Table 4 shows additional ΔC_D terms that are present during landing

← and during trim when flap deflections are necessary. This term would not come into play for take-off since the aircraft used a cart assisted lift-off, no flap deflections were necessary. From all these terms drag polars were set up for both level flight and climb or descent. These are shown in Table 5 and are ploted in Figures 3, 4 and 5. From the cruise drag polar and coefficient of lift, which will be discussed later, the cruise drag coefficient, C_D was calculated and a value of 0.0415 was obtained.

LIFT DISCUSSION

As was stated in the aircraft configuration section, the lift was distributed between the front and rear wings with approximately 65 percent produced by the front wing. The exact amount of lift each wing produced was dependent on two conditions. The first of these was the angle of attack at which the plane is flying. This was due to the fact that the wings produce more lift at higher angles of attack upto a limit. The second condition was that the lift changed with the elevator deflection with an increase when it was deflected downward. The effects of elevator deflection on the C_L for several different angles are given in Table 4. Plots of CL vs a show the effects of angle of attack and elevator deflection and are given in Figures 6 and 7 for cruise and landing configurations. With this information and the determined cruise airspeed of 60 m/s, the cruise lift coefficient, C_L was calculated to be 0.6078.

CONCLUSION

With all the considerations that have been taken into account for this project, it seemed that it would be a reasonable assumption that a design of this sort was very feasible for the Mars Airplane. It would probably be very beneficial if a "mock-up" of this design were built and tested in wind tunnel conditions that were similar to those on Mars. If this were done, exact experimental data could be obtained to show how reasonable this design actually was.

REFERENCES

1. CRC Handbook of Chemistry and Physics. 66th Edition, 1985-86, p F-159.
2. French, J.R., "The Mars Airplane," NASA Manned Mars Missions. NASA Conference Proceedings, June 1986.
3. Wolkovitch, Julian, "Principles of the Joined Wing," NASA Commission Report, December 3, 1980.
4. Wolkovitch, Julian, "The Joined Wing: An Overview," ACA Industries Inc., January 14, 1985.
5. Maughmer, M. D. and Somers, D. M., "An Airfoil Designed for a High Altitude, Long-Endurance Remotely Piloted Vehicle," NASA Symposium on Natural Laminar Flow Control Research. Nasa Conference Proceedings, August 1987.
6. Wolkivitch, Julian and Lund, David, "Application of the Joined Wing to Turboprop Transport Aircraft," Ames Research Center, 1984.

TABLE 1.

AIRCRAFT CHARACTERISTICS

$(t/c)_{max}$	=	0.159
$l_{(t/c)max}$	=	0.42c
AR	=	8
c_F	=	5m at root, 3m at tip
c_R	=	3m at tail, 2m at joint
b	=	50m
Γ_F	=	5°
Γ_R	=	-15°
Λ_F	=	16°
Λ_R	=	-16°
λ_F	=	0.600
λ_R	=	0.667

TABLE 2.

PARASITE DRAG TERMS

C_{DoF}	=	0.0059
C_{DoR}	=	0.0046
C_{DoV}	=	0.0043
C_{DoB}	=	0.0034

INDUCED DRAG TERMS

C_{DiB}	=	$0.0498C_L^2$
$C_{Di\alpha}$	=	$0.0628\alpha^2 + 0.816a^3$
	=	$0.0199C_L^2 + 0.2582C_L^3$
$C_{Di\Theta}$	=	$0.0080C_L$

TABLE 3.

ΔC_D NEAR C_{Lmax}

% away from CLmax	ΔCD
0%	0.013
1.25%	0.008
2.50%	0.005
3.75%	0.003
5.00%	0.002
7.25%	0.000

TABLE 4.

INCREASE IN LIFT AND DRAG DUE TO ELEVATOR DEFLECTION

δ	ΔCD	ΔCL
10°	0.00473	0.128
20°	0.01790	0.223
30°	0.03730	0.260
40°	0.06230	0.303

TABLE 5.

DRAG POLARS FOR LEVEL CRUISE AND CLIMB OR DECENT

Level Cruise

$$C_D = 0.0182 + 0.0080C_L + 0.0498C_L^2 + \Delta C_D + \Delta C_{D\delta}$$

Climb or Decent

$$C_D = 0.0182 + 0.0080C_L + 0.0697C_L^2 + 0.0258C_L^3 + \Delta C_D + \Delta C_{D\delta}$$

FIGURE 1.

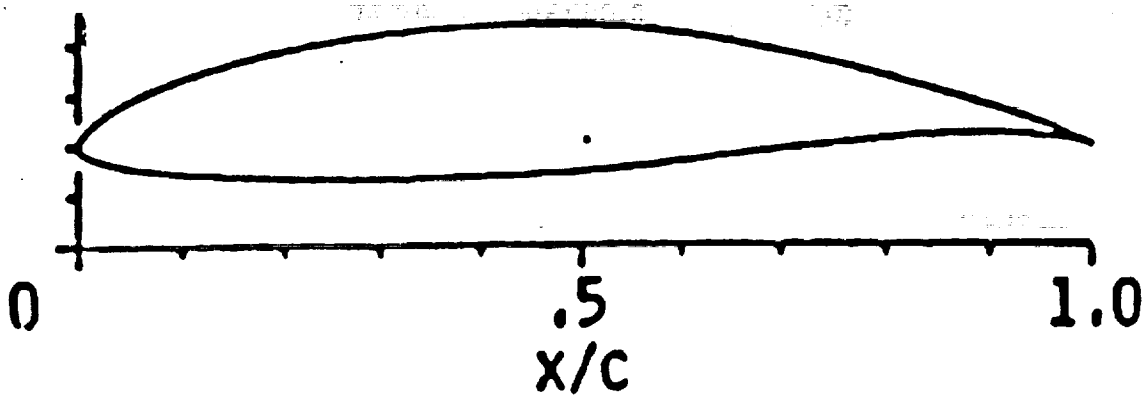

The NASA NLF(1)-1015 airfoil

FIGURE 2

COMPARISON OF THEORY AND EXPERIMENT
NLF(1)-1015

Theory
○ Experiment
□ Hysteresis

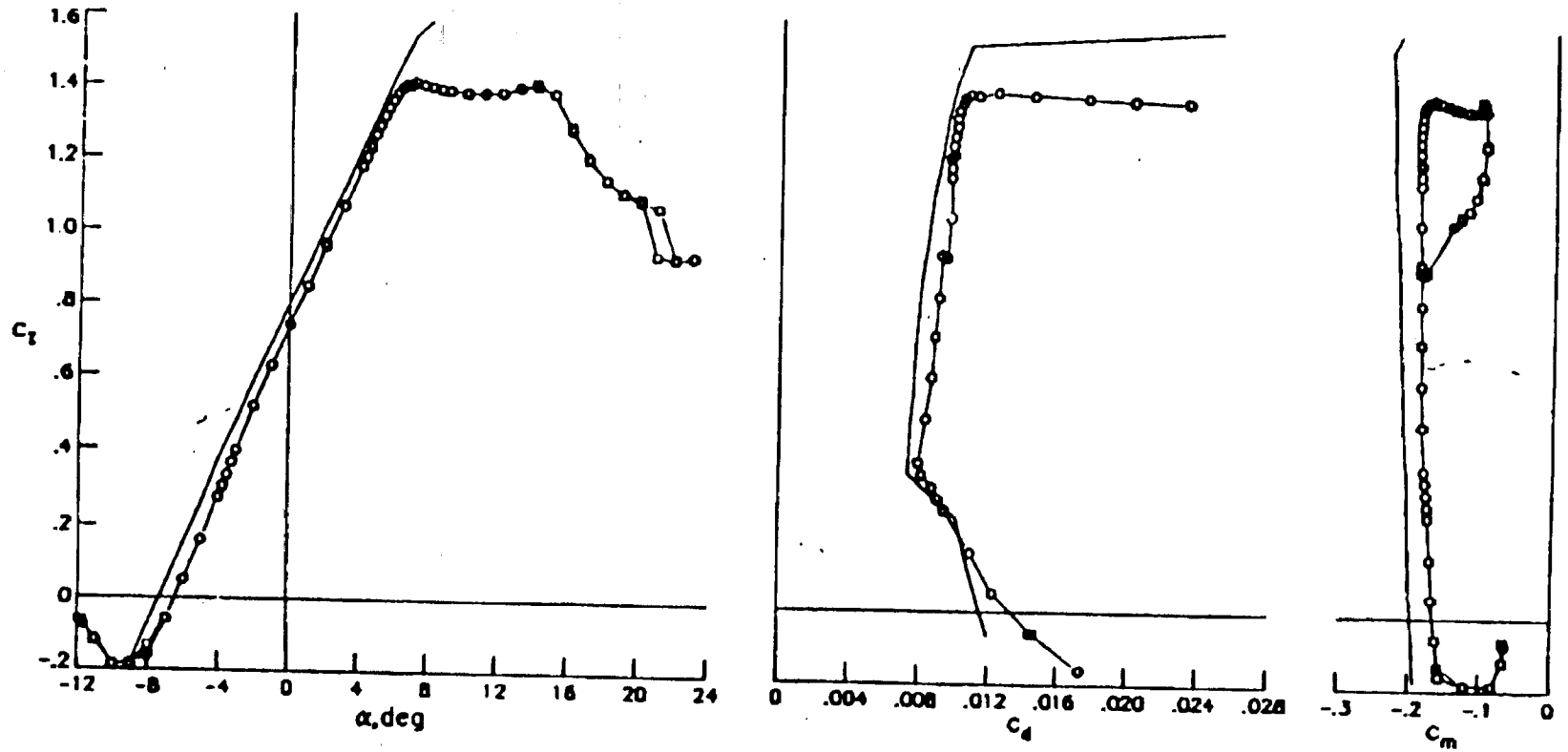

FIGURE 3.

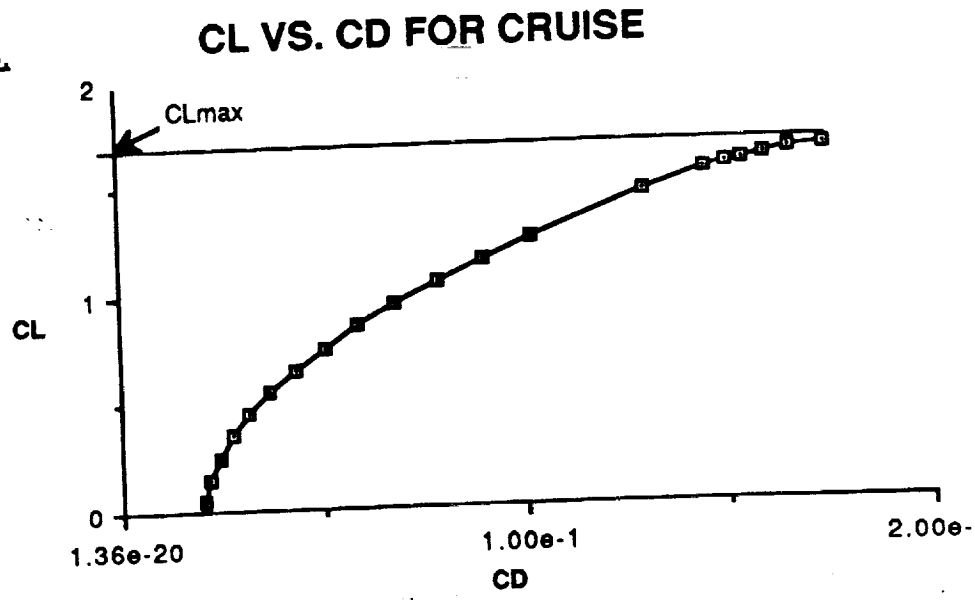

FIGURE 4.

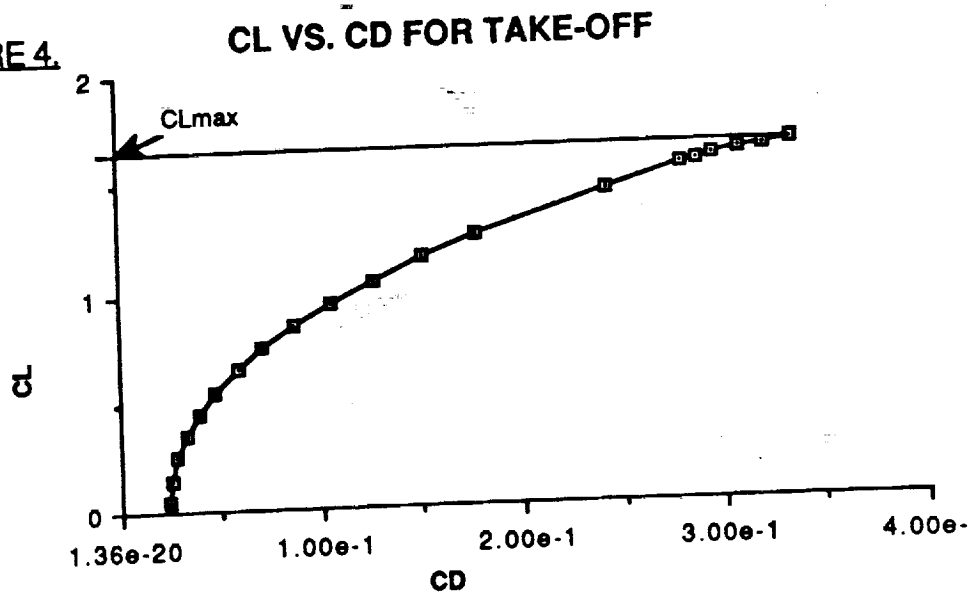

FIGURE 5.

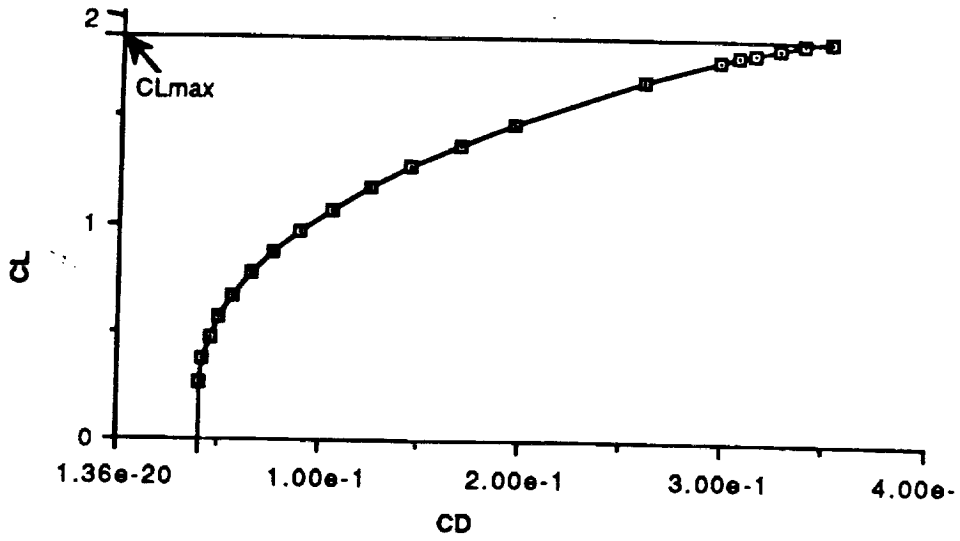

FIGURE 6.

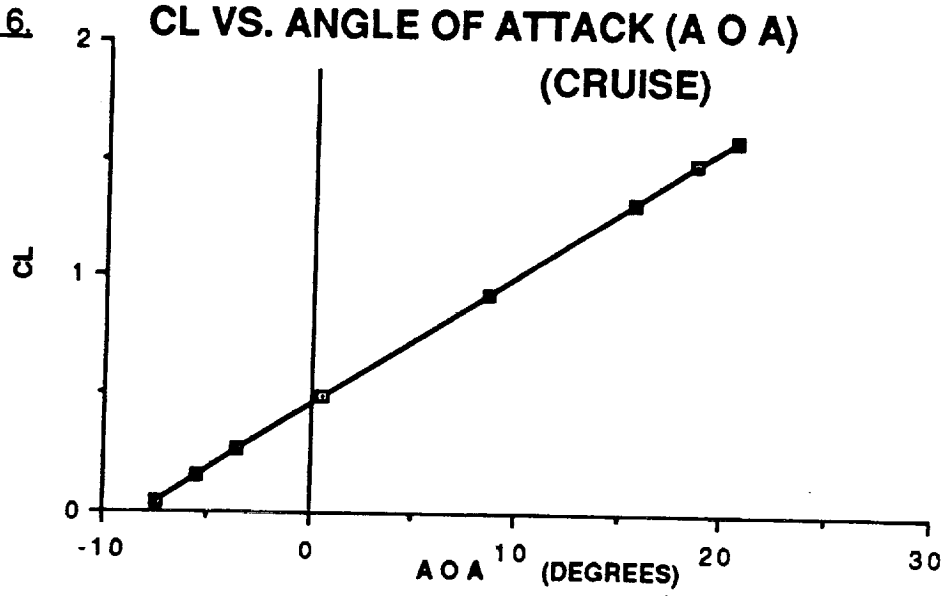

FIGURE 7.

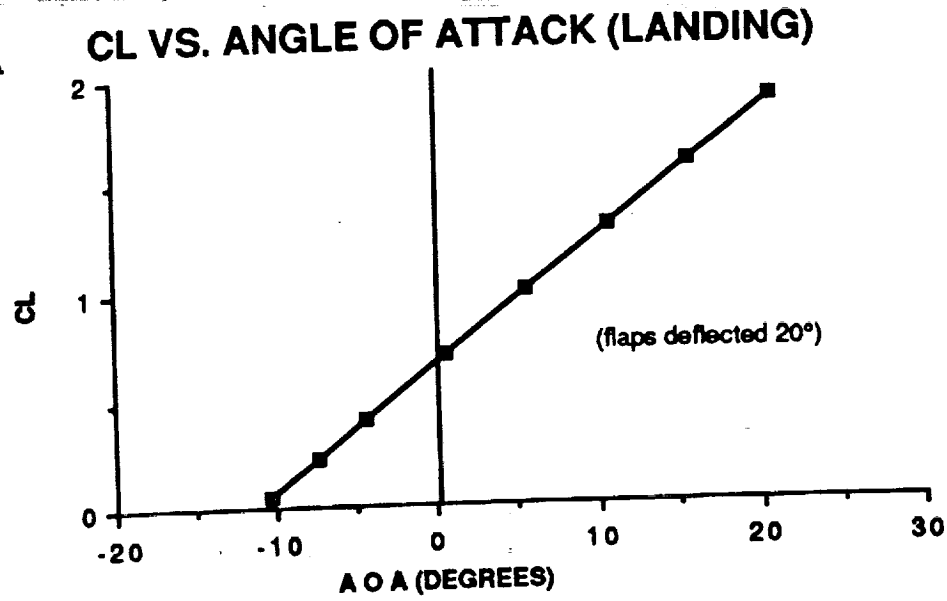
CL VS. ANGLE OF ATTACK (LANDING)
2
1
0
CL
(flaps deflected 20°)
-20
-10
0
10
20
30
AOA (DEGREES)

C-4

PERFORMANCE

Steve Schirle

DATA SHEET:

Climb:

Maximum Rate-Of-Climb	= 0.862 m/s
Velocity at this Rate-Of-Climb	= 55 m/s
Time To Climb	= 0.52 hrs
Fuel To Climb	= 56.18 N
Range Of Climb	= 102.1 km

Cruise:

Constant altitude cruise at 1500 m	
Velocity at beginning of cruise	= 60 m/s
Velocity at end of cruise	= 56.7 m/s
Endurance of cruise	= 7.29 hrs
Fuel used in cruise	= 620 N
Range of cruise	= 1671.9 k
Maximum velocity possible	= 70 m/s
Stalling velocity	= 43 m/s

Descent:

Rate-Of-Sink	= 2.24 m/s
(at 30% of available power)	
Velocity for this rate of sink	= 55 m/s
Time to descend	= 0.194 hrs
Fuel used to descend	= 46.55 n
Range of descent	= 38.4 km

Total Mission (Climb, Cruise, and Descent)

Total endurance	= 8 hrs
Total weight of fuel	= 722 N
Total Range	= 1812.4 km

PERFORMANCE DISCUSSION:

DESIGN PHILOSOPHY:

To begin the discussion on the performance of Sky C.A.B., it is important to first look at the design philosophy used. The performance of Sky C.A.B. centers around two design demands. The first demand on the aircraft is that it must be able to fly at an altitude of 1500m. The second demand is that an endurance of eight hours must be achieved. With these demands in mind, the velocities for cruise, climb, and descent can be chosen so as to yield the most efficient mission profile, that is, the mission profile which yields the minimum amount of fuel needed, without exceeding the flight boundary conditions. Since the aircraft must meet a specified goal weight, any reduction in the weight of the fuel is helpful. With this design philosophy in mind, the performance data for Sky C.A.B. will now be discussed.

FLIGHT ENVELOPE

The level flight envelope shown in Fig 2.1 provides the altitude and velocity boundaries for level flight cruise. The flight envelope was calculated by means of the Performance Data Program (PDP). The PDP calculates the maximum velocity (Vmax) and the minimum velocity (Vmin) at a given altitude by finding the intersection points of the power required (Preq) and the power available (Pa) curves (these intersection points for 1500 m and sea level altitudes are shown in Fig 2.2 and Fig 2.3 respectively). In conjunction with the Vmin values, the stalling velocity (Vstall) must also be considered. If Vstall is greater than Vmin, the stall velocity is the minimum velocity at which the aircraft can fly. As pointed out in Fig 2.1, this is the case for Sky C.A.B. up to an altitude of 4,000m. As the altitude is increased, Vmin and Vmax approach each other until an altitude is reached at which Vmin = Vmax. This altitude is known as the absolute ceiling (Habs), above which flight cannot occur. The absolute ceiling for Sky C.A.B. is 5,500m and is shown in Fig 2.1. Also included in Fig 2.1 is a line labeled RCmax. This line represents the velocities at which the maximum rate of climb occurs for a given altitude. Thus, from the previous discussion, it is apparent that the flight envelope provides the velocity and altitude boundaries for level flight.

CLIMB:

The rate-of-climb (RC) chosen for Sky C.A.B. to climb at is the maximum rate-of-climb (RCmax) of the aircraft. The value for RCmax is 0.862 m/s and occurs at a velocity of 55 m/s.

These values (RCmax and it's corresponding velocity) are actually the average maximum rate of climb and the average corresponding velocity over the region from sea level to 1500m. An average RCmax is needed because the actual RCmax decreases as altitude increases and is therefore not a single value. For the remainder of the discussion, the average RCmax will be referred to as simply RCmax but it should be understood that this value, along with it's corresponding velocity, is an average value. The reason for the selection of RCmax as the rate-of-climb can be seen by examining the following equation:

$$\Delta W_f = \int (Cp \times Pa)dh/(n \times RC)$$

Cp = the specific fuel consumption

n= the propeller efficiency

dh= small increment in altitude

It is desirable for the RC to be the most efficient (i.e. require the least amount of fuel). By studying the above equation for fuel used during climb, it is apparent that the values of Cp/n and Pa/RC must be minimized for the most efficient climb period. As shown in Fig 2.2, Pa/RC is minimized when the Preq is a minimum. This occurs at a velocity of 50 m/s. From Fig 2.4 , it can be seen that Cp/n is a minimum at a velocity of 60 m/s. Thus, a trade-off is needed. If a velocity of 55 m/s is chosen (i.e. RC= 0.862 m/s) only a slight increase of 1% from the minimum value of Cp/n occurs and an increase of only 1% from the minimum value of Preq occurs. On the other hand, if the aircraft climbs with a rate-of-climb corresponding to a velocity of 50 m/s (Preq= mimimum) there is an increase of 4.5% from the mimimum value of Cp/n. If the aircraft climbs at a rate-of-climb corresponding to a velocity of 60 m/s (Cp/n= minimum), there is an increase of 4% from the minimum value of Preq. Therefore, noting these increases in Preq and Cp/n at the different velocities, it is apparent that the most efficient rate of climb will occur at a velocity of 55 m/s, which corresponds to RCmax= 0.862 m/s.

The time to climb, fuel to climb, and range of climb were calculated with the assistance of the PDP (computer program mentioned previously). The time to climb to 1500m for Sky C.A.B. was calculated to be 30.9 minutes. The fuel needed for the aircraft to climb to 1500m is 56.18 N and the range of climb is 102.1 km.

DESCENT:

An average rate-of-sink (RS) of 2.24 m/s was chosen for the descent of Sky C.A.B. This RS occurs at an average velocity of 55 m/s and was calculated by the PDP in the same manner as the RC, except at a power setting of 30% of the total power available. This produces a Preq

greater than Pa and a power deficit is obtained. The reason for this selection for the rate-of-sink follows the same reasoning as that for the rate-of-climb. The most efficient rate of sink occurs at a velocity of 55 m/s. This velocity is the most efficient because it provides the best trade-off between Preq and Cp/n and thus requires the least amount of fuel. ? what about power off ?

The time to descend, the fuel to descend, and the range of descent were calculated using the PDP. The time to descend from 1500 m for Sky C.A.B. was calculated to be 11.65 minutes, and requires a fuel weight of 46.55 N. The range of descent for the aircraft is 38.4 km.

CRUISE:

A constant altitude cruise velocity for the beginning of level flight of 60 m/s was chosen for Sky C.A.B. The reason for this selection can be seen from Fig 2.4 and the following equation:

$$E = \int (n \times dw)/(Cp \times Preq)$$

E= the endurance

dw= small increment in weight

This equation shows that if n/(Cp x Preq) is a maximum, then the weight of the fuel required is a minimum. For n/(Cp x Preq) to be a maximum, (n/Cp) must be a maximum and Preq must be a minimum. (Note: n/Cp maximum corresponds to Cp/n minimum). But the problem here is Cp/n minimum and Preq minimum occur at different velocities which can be seen in Fig 2.2 and Fig 2.4. The minimum Cp/n occurs at a velocity of 60 m/s and the minimum Preq occurs at 50 m/s. Therefore we see a trade-off is needed. Before jumping into this, it should be noted that since Sky C.A.B. will be flying at constant altitude, a decrease in the velocity will occur during flight due to the loss of fuel weight. The final velocity for level flight was calculated to be 56.7 m/s. Because of this change in velocity, the most efficient range of velocities is needed instead of a single velocity. It was shown previously that 55 m/s is the most efficient velocity to fly at. The most efficient range can be determined by finding out if the efficiency is greater when the velocity is increased or decreased from this value.In the velocity range from 50 m/s to 55 m/s, the power required increases by 1% while Cp/n increases 3.5% . On the other hand, in the velocity range from 55 m/s to 60 m/s, the power required increases by 3% while Cp/n increases 1% . By observing these percentages it is apparent that the most efficient velocity range occurs between 55m/s and 60 m/s. For this reason, a velocity of 60 m/s was chosen for the beginning of level flight. It should be noted that this velocity does fall in the boundaries prescribed by the flight envelope since Vmin= 41 m/s and Vmax= 70 m/s for level flight at

1500 m.

The time required for cruise is simply the time to climb and the time to descend subtracted from the mandatory eight hour endurance. Thus, the time in cruise is 7.29 hrs The fuel used during cruise and the range for cruise were calculated with the assistance of the PDP. The weight of the fuel needed for an endurance of 7.29 hrs is 620 N and the range covered in this time is 1671.9 km.

SUMMARY:

To summarize, a complete mission profile for Sky C.A.B. will be looked at. For the entire mission profile, the design demand for an eight hour endurance has been met. During this eight hour flight , 722 N of fuel will be used and a total range of 1812.4 km will be obtained. The aircraft will begin the mission at a take-off velocity of 60 m/s. It will then decelerate to a velocity of 55 m/s at which speed it will climb at a rate of 0.862 m/s. This rate of climb chosen is also the maximum rate-of-climb of the aircraft. Sky C.A.B. will increase its speed as it enters its cruise segment to a velocity of 60 m/s where it will cruise at a constant altitude of 1500 m. The aircraft will end the cruise segment at a velocity of 56.7 m/s and decrease its speed to 55 m/s as it enters the descent segment. During this segment, Sky C.A.B. will descend at a rate of 2.24 m/s. At the end of descent, the aircraft will decrease its velocity to 41 m/s at which point it will safely land. Another succesful mission.

LEVEL FLIGHT ENVELOPE

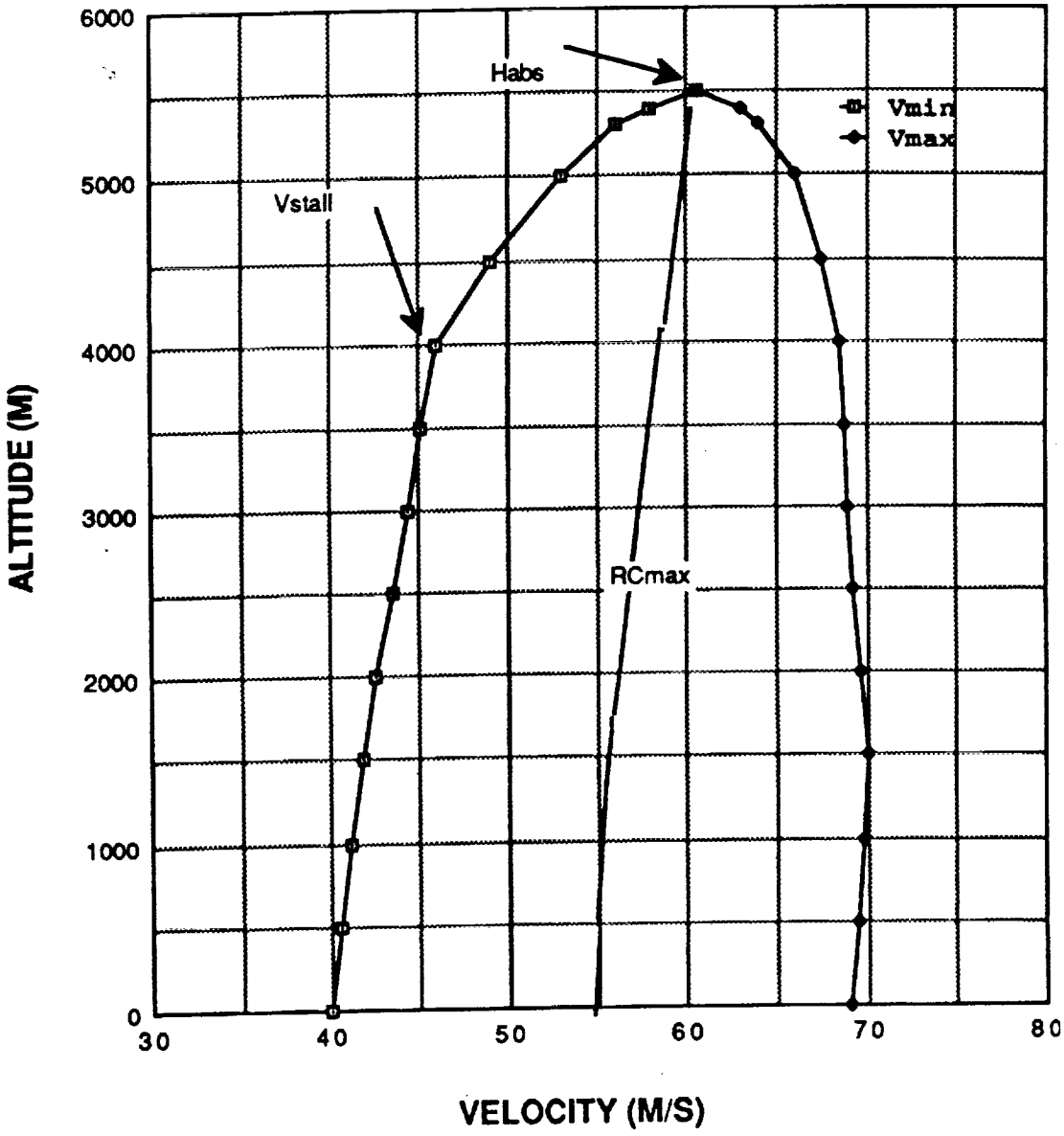

FIG 2.1

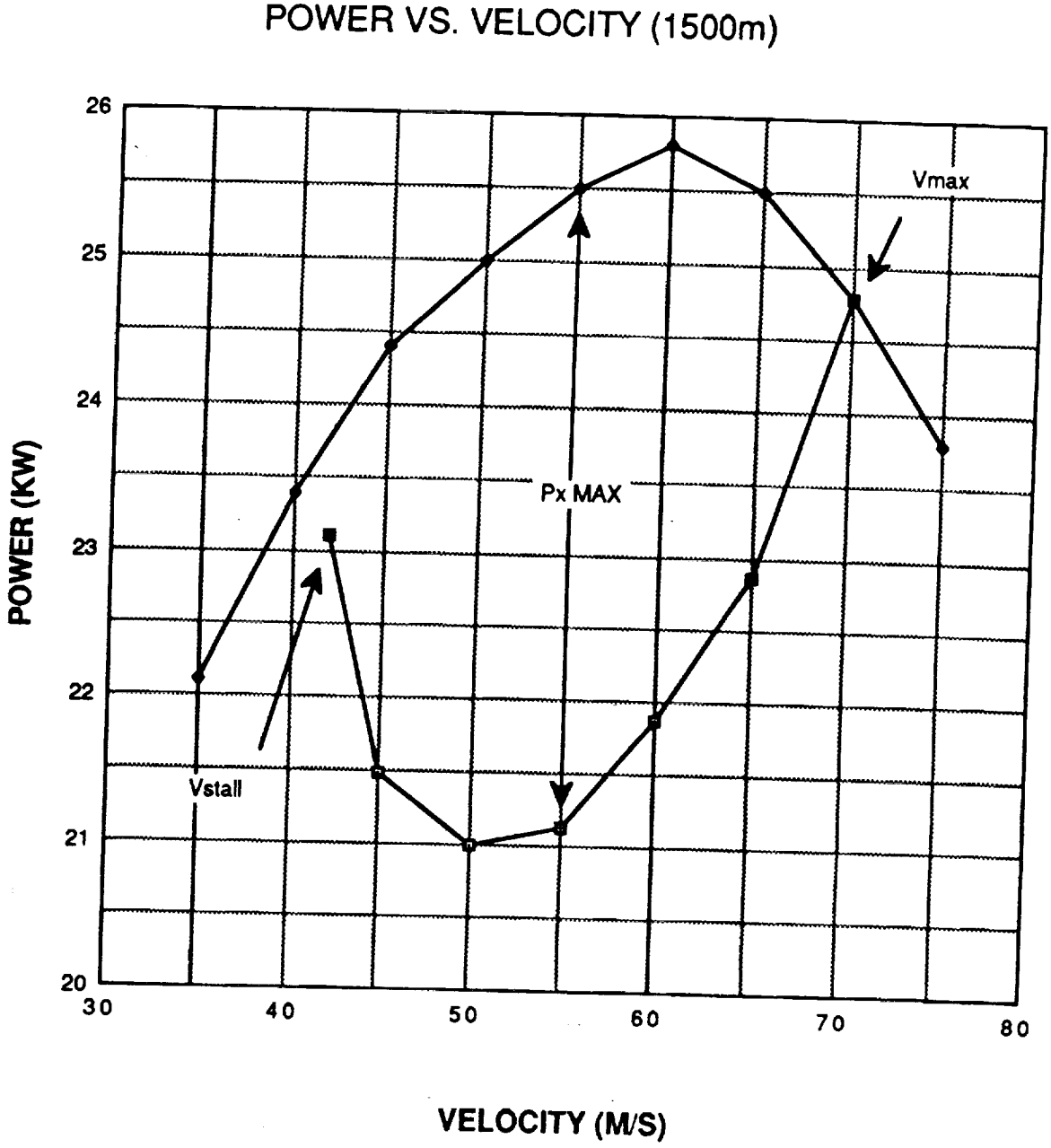
POWER VS. VELOCITY (1500m)
26
25
24
23
22
21
20
POWER (KW)
30
40
50
60
70
80
VELOCITY (M/S)
Vmax
Px MAX
Vstall

(FIG. 2.2)

POWER VS. VELOCITY (SEA LEVEL)

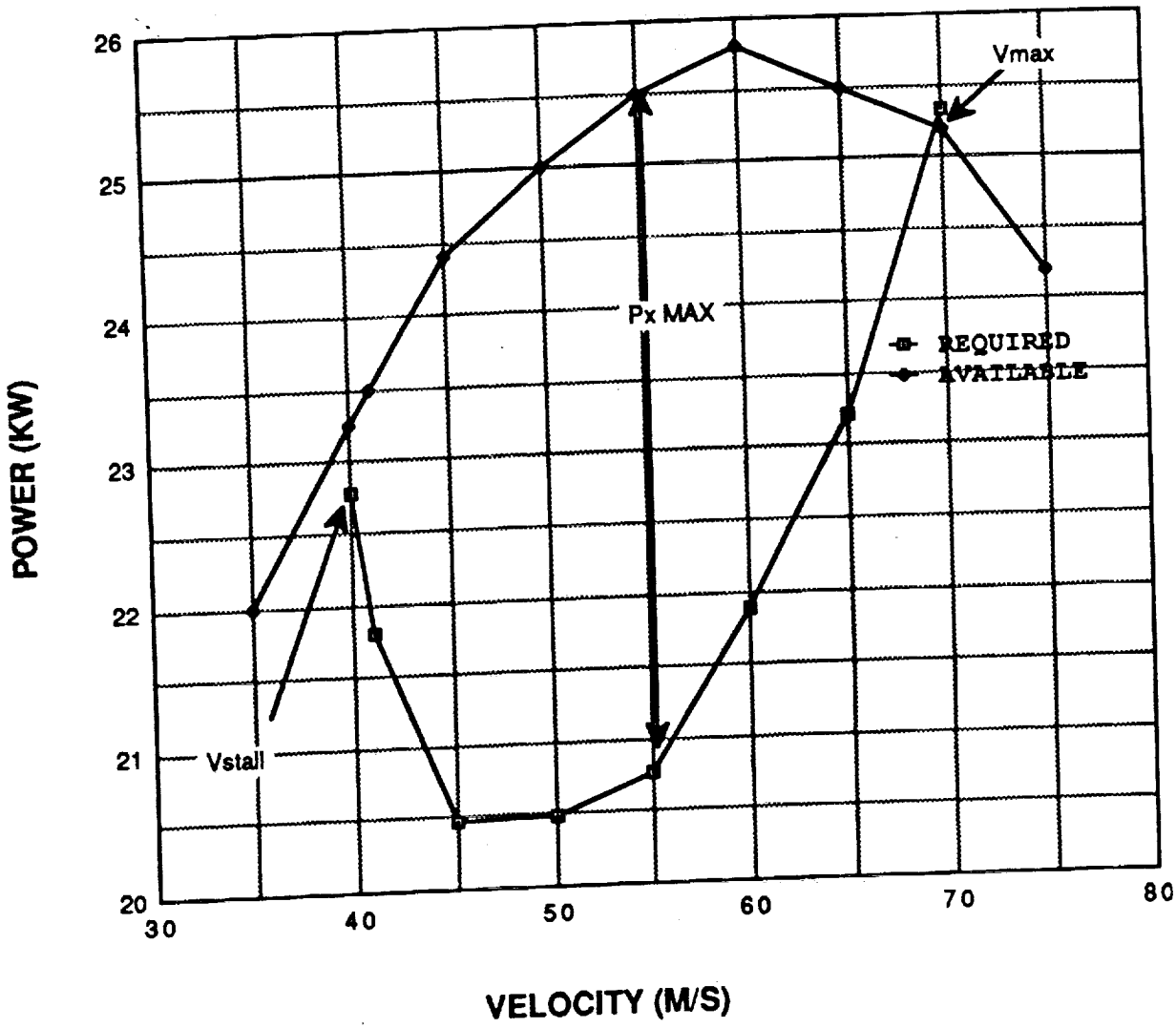

FIG 2.3

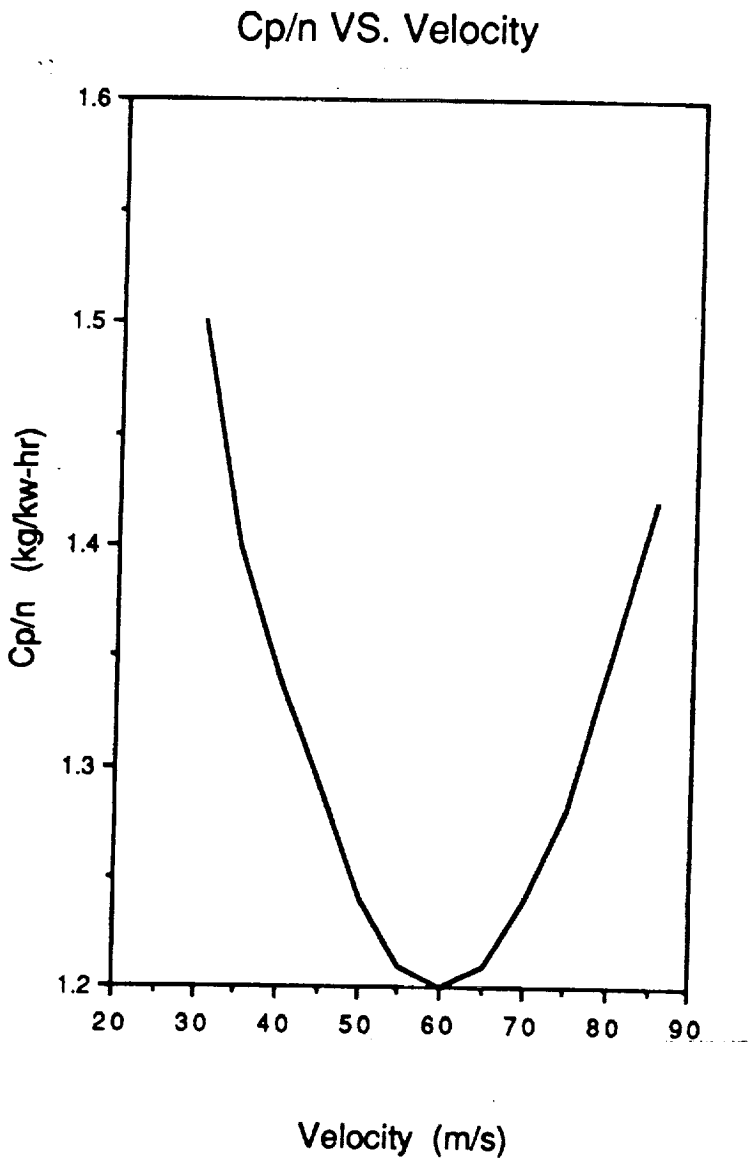
Cp/n VS. Velocity
1.6
1.5
1.4
1.3
1.2
Cp/n (kg/kw-hr)
20
30
40
50
60
70
80
90
Velocity (m/s)

FIG 2.4

POWER AND PROPULSION

James P. Goggin

DESIGN OBJECTIVE

The initial goal in the design of the Mars Airplane power and propulsion system was to deliver 22kW for the cruise condition of 1.5km at 60 m/s, and deliver up to 25kW for the climb condition at 50 m/s. Other considerations important in the design process were ability to run on fuels available in the martian environment, availability of components, mechanical simplicity and compatability with the aircraft structure. The system designed for the Mars Airplane, SKY C.A.B. fulfills these goals effectively.

SYSTEM SELECTION

The system selected for the Mars Airplane is technologically advanced, yet mechanically simple. The main components are either available today or are in the advanced development stage. The system will not require excessive maintenance and will run on fuels available in the martian environment.

The Mars Airplane power and propulsion system consists of:(fig. 1)

1. Free-piston Stirling heat-engine
2. Recirculating Combustor
3. Heat-pipe radiator
4. Cryogenic fuel storage
5. Samarium-Cobalt electric motor
6. Propeller

SYSTEM COMPONENTS

Stirling Engine

The Stirling Engine was selected because it is the most efficient thermodynamic engine cycle that exists.[1] The Stirling engine has the potential to be used with a variety of fuels[2], and has only two moving parts.

The Stirling Engine in principal is a simple device.(fig. 2) A cylinder is heated on one end and kept cool on the other. Oscillating in the cylinder is a displacer. This oscillatory motion is maintained by gas springs. These springs, which are actually the working fluid(He or H_2) get their spring effect by circulating back and forth between temperature extremes by way of the regenerator. The regenerator allows the oscillation of the working fluid, but at a frequency slightly out of phase with that of the displacer.

Attached to the displacer is the power piston. The power piston is really a magnet on the end of a push-rod. This Magnet moves through a coil, forming a linear alternator, at the same frequency and amplitude as the displacer,100 Hz and 1.0 cm.

The working fluid is also used to form gas bearings which eliminate the need for oil in the engine.

The engine selected is the Space Power Free-Piston Stirling Engine, now being developed under NASA's SP-100 program.(fig. 3) The engine will have a power density of 5 kg/kW and a thermal efficiency of greater than twenty percent.[3]

Recirculating Combustor

The Space Power Stirling Engine is designed to run on molten sodium which would be heated by solar or nuclear power. For test purposes the Na has been heated electrically. There seems to be no reason,however, which would prohibit the Na from being heated by combustion of CH_4 and LOX.

Methane has been chosen as the fuel for the mars airplane primarily because of availability on Mars, and experience with methane on Earth. Supplies of CO_2 and H_2O found in the martian environment should be able to be converted into methane and LOX with relative ease.

Direct combustion of LOX and hydrocarbon fuels results in an adiabatic flame temperature in the 4000°C range, this is much too high for existing materials. The Swedish Navy has developed a recirculating combustor for stirling engine use on submarines[4]. This combustor burns diesel fuel and LOX, recirculating the exhaust products back into the combustor. The flame temperature is lowered by this process to 1050°C, which also happens to be the design temperature for the Space Power Stirling engine. It will be a relatively simple matter to modify this combustor to burn CH_4 and LOX. This modification will also allow the combustor to heat the Na which will circulate between the combustor and the Stirling engine through heat pipes.(fig. 4)

Heat Pipe Radiator

The radiator selected for the Mars Airplane is a scaled down version of the SPAR Space Power System Radiator[5]. This radiator is designed to radiate heat at high temperatures with minimum surface area and weight. The radiator will operate at 550°C and radiate 96.75 kW of power. Cooling fluid(NaK) will circulate through the sodium/molybdenum heat pipes. The radiator will weigh 144N and be composed of two $3m^2$ panels mounted flush with the surface of the aircraft on both sides of the fuselage. This will reduce the drag associated with the radiator, but will require careful insulation of all parts of the aircraft structure which may come in contact with the radiator.

Fuel storage

The fuels for the Mars Airplane will be stored in lightweight insulated thermoplastic

tanks. The pressures will be kept low by cooling the fuels down to cryogenic temperatures with stirling cryocoolers. These cryocoolers work much like the Space Power Stirling Engine, but in reverse. Electric power is added and heat is removed from the cold reservoir. If the insulation on the tanks is sufficient, the power required to maintain the temperature of the fuels will be only a small portion of the 1kW allowed for onboard systems.

Samarium-Cobalt Electric Motor

This motor has been chosen because of it's low power density, 1.0 kg/kW [6]. The motor will be mounted on the tail of the aircraft receiving electric power from the stirling engine in the fuselage. This configuration has the advantage of placing minimal weight on the tip of the structurally vulnerable tail tip.

Propeller Design

The propeller design has proven to be the most troubling aspect of the propulsion system for the Mars Airplane, In the literature it has been found that at least two propellers have been designed for mars type environments[7,8], which have diameters of 2 to 4.5m and efficiencies from 78 to 85 percent. No specific data on such propellers has been made available. The decision was made to design a propeller with data available which will give unacceptable geometry but performance trends one may expect from a propeller more suited for the Mars environment.

The propeller selected is the 5868-9,Clark-Y section, two blades. Using available performance graphs for this propeller, a diameter of 8.265m, and a blade pitch angle of $\beta=15^{o}$ was selected. For most of the operating range efficiencies of greater than 80 percent were found, while maintaining subsonic blade tip Mach numbers, at the design speed of 50 m/s and 450 rpm.

In the event of a complete power failure, such that the propeller stops ratating, additional drag must be considered for such an off design condition. Fig. 5 allows one to find the added drag which must be accounted for an engine-out situation.

SYSTEM ASSEMBLY

Power requirements of 1.0 kW for onboard systems and 31.25 kW to be delivered to the propeller require an engine which will weigh 613 N. This engine will reject 96.85 kw heat and require a 144N radiator.

Two spherical fuel tanks are required to contain the 722N of fuel. One tank will be 0.54m in diameter, weigh 42N and hold 133.7N CH_4. The second tank will be 0.64. in diameter, weigh 58N and contain 588.3N LOX.

The fuel will be transported to a combustor which is estimated to weigh 50N.

Electric power from this system will drive a 100N electric motor on top of the tail which in turn drives a 110N propeller. This system is summarised in fig 6.

SYSTEM PERFORMANCE

The Stirling-engine in combination with the electric motor will operate at twenty percent thermal efficiency. Other engines operating at this efficiency on CH_4 require 0.18 kg/kWh CH_4. The combustor will require 110 percent stoicheometric mixture of oxygen for complete combustion, giving a total specific fuel consumption of approximately 1 kg fuel (LOX + CH_4) for every kW generated for the propeller and onboard systems. Taking into account the propeller efficiency and onboard power needs, the specific fuel consumption of the propulsion system was generated.(fig 7)

Given a constant power input of 31.25 kW from the Stirling engine, a graph of power available vs. velocity was generated.(fig. 8) It is encouraging to note that more than enough power is available to meet climb and cruise conditions. Takeoff thrust from this system, 450 N, is insufficient for the 1km field length and must be supplemented. Surface operations has designed a rocket-powered cart to assist take-off.

SUMMARY

The Propulsion system for the Mars Airplane SKY C.A.B. is a realistic solution to the problem of meeting power requirements in a restrictive environment such as Mars offers. The key components for this sytem are either available today or are projected to be available within a few years. The Stirling system does not require a disproportionate amount of weight or aircraft space, which is extremely limited. One of the most advantageous features of this system is that the power is generated at a structurally sound location in the fuselage, requiring only minimal weight to be place upon the tail.

REFERENCES

1. Jack G. Slaby and Donald L Algar, "1987 Overview of Free-Piston Stirling Technology for Space Power Application", NASA Technical Memorandum 89832.

2. G. Walker and R. Fauvel, "Yes Veronica, Stirling Engines are Good for Somethings", 1986 Intersociety Energy Conversion, Vol 1, pp 415.

3. Jack G. Slaby, "Overview of the 1986 Free-Piston Stirling SP-100 Activities at the NASA Lewis Research Center", 1986 Intersociety Energy Conversion, Vol 1, pp 420-421.

4. H. Nilsson and C. Bratt, "The V4-275 Stirling Engine in Underwater Application", 1986 Intersociety Energy Conversion, Vol 1, pp 623-626.

5. W. A. Ranken, "Heat-Pipe Development for SPAR Space Power System", Advances in Heat Pipe Technology, pp 561.

6. V. Clarke, A. Keram and R. Lewis, "A Mars Airplane?", Aeronautics & Astronautics,, January 1979, pp 50.

7. R. Dale Reed, "High-Flying Mini-Sniffer RPV: Mars Bound?", Aeronautics & Astronautics, June 1978, pp 33-34.

8. V. Clarke, A. Keram and R. Lewis, "A Mars Airplane?", Aeronautics & Astronautics, June 1978,pp 48.

9. Tim G. Adams, "The Development of Ford's Natural Gas Powered Ranger", SAE Paper 852277.

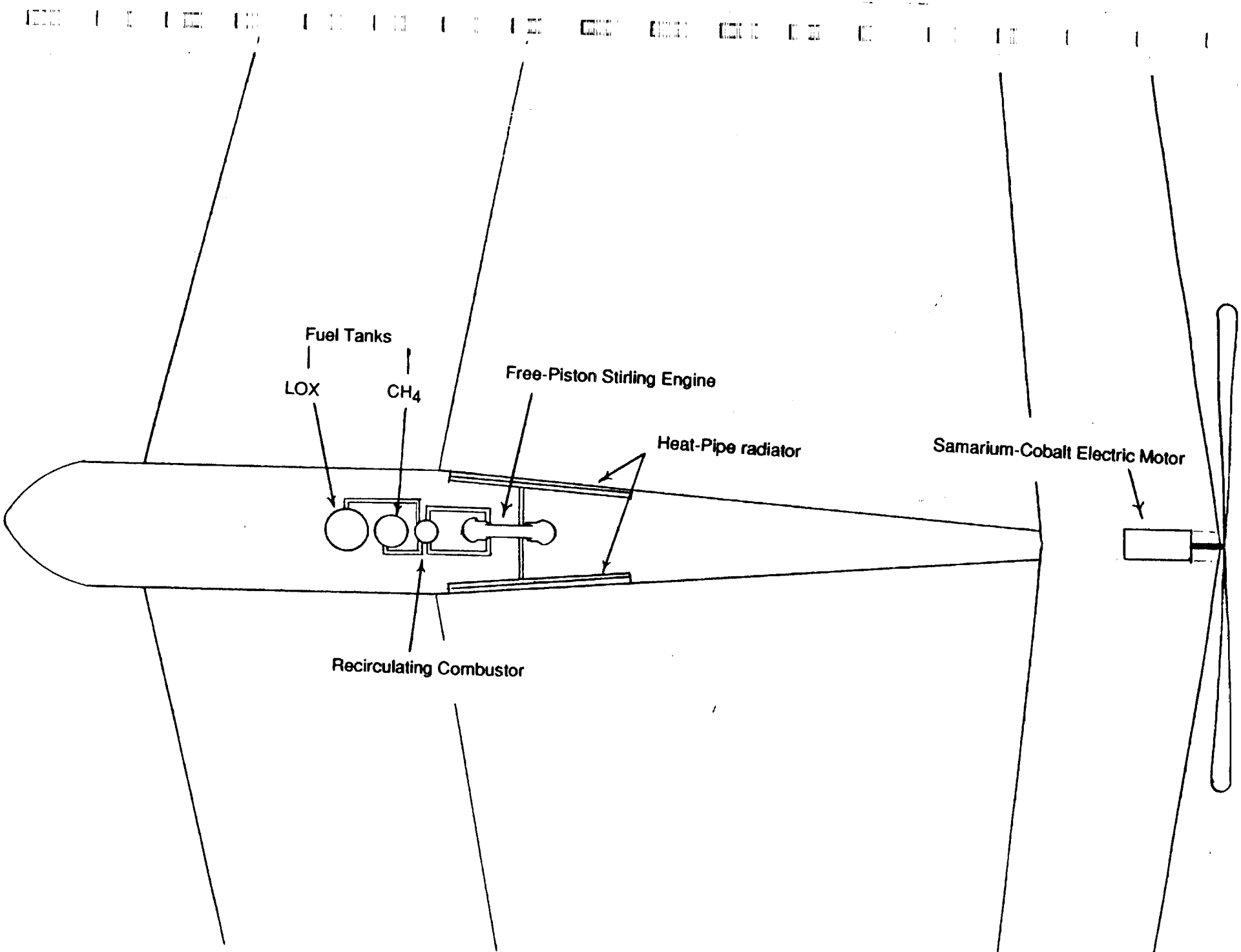

Fig. 1 SKY C.A.B. Power and Propulsion System

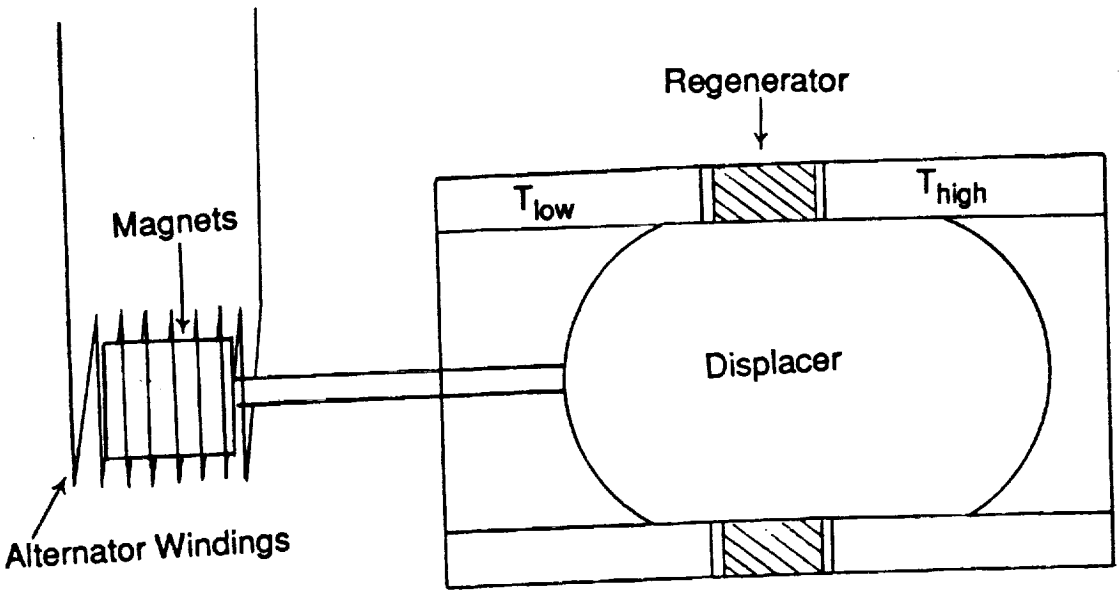

Fig. 2. Conceptual Stirling Engine

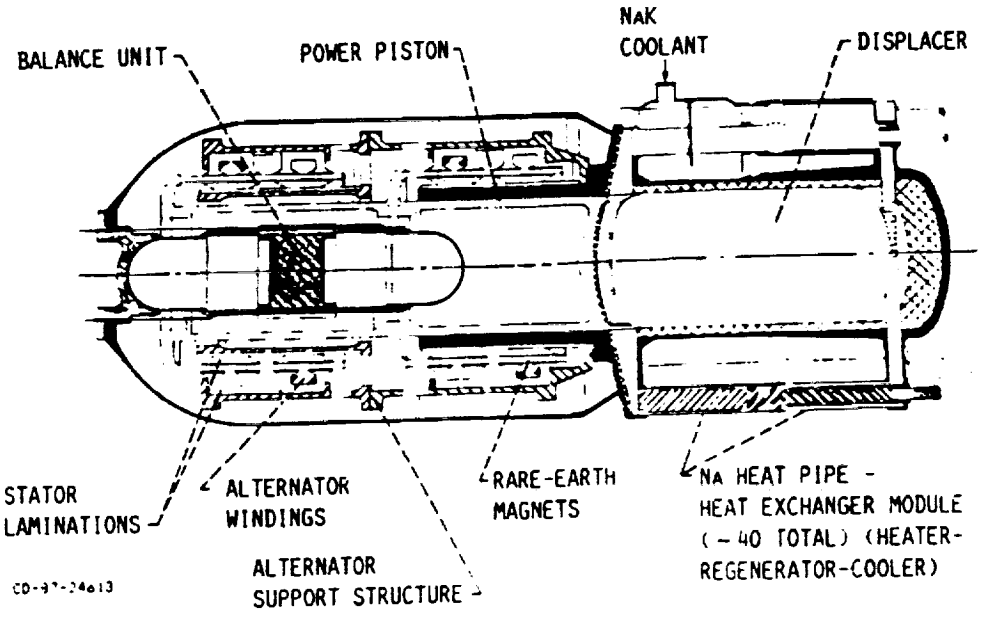

Fig. 3 Space Power Free-Piston Stirling Engine

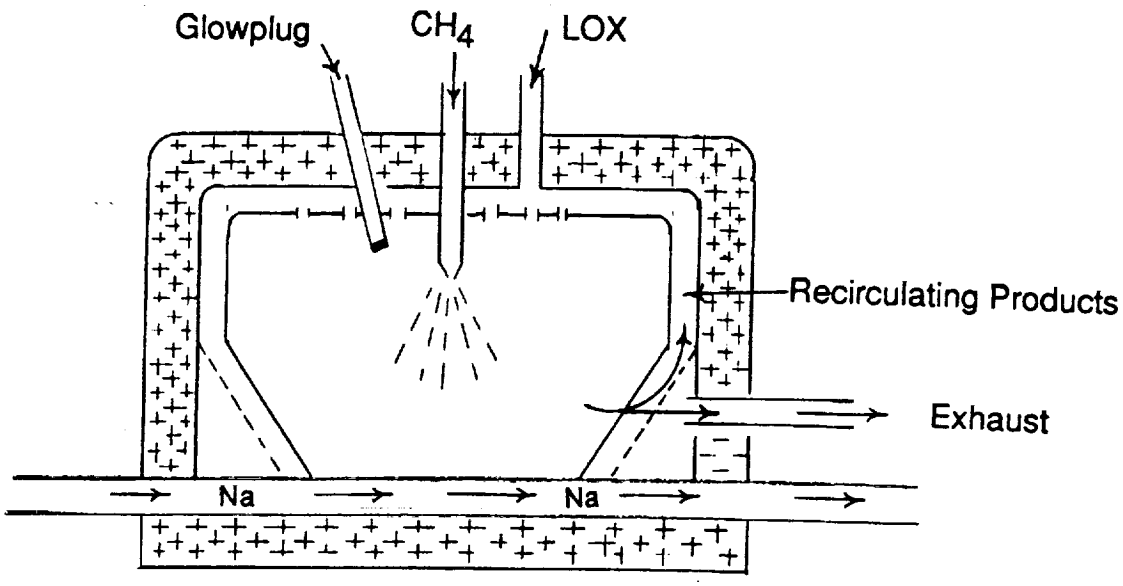

Fig. 4 Recirculating Combustor

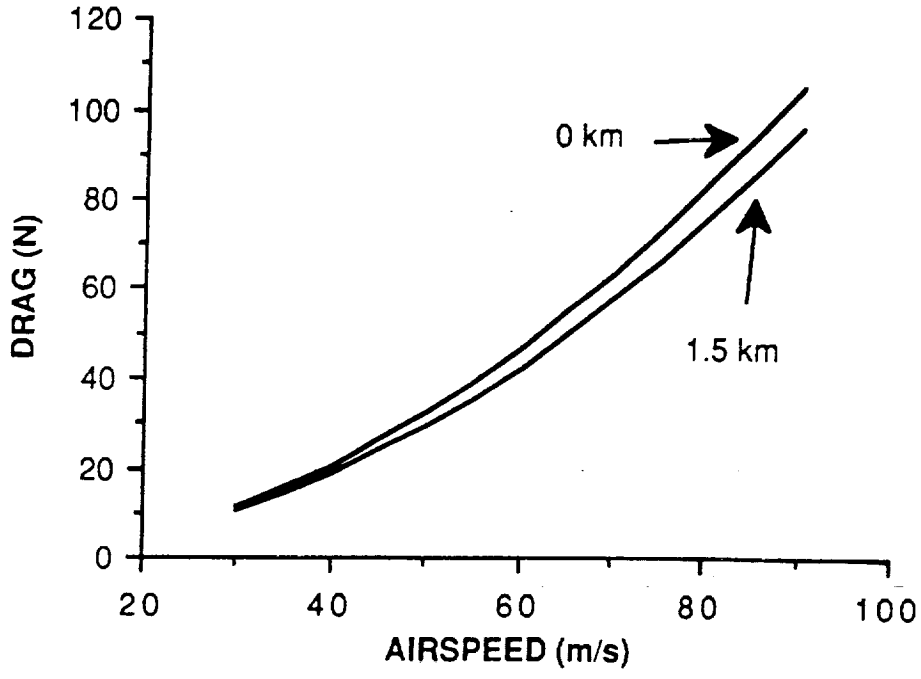

Fig. 5 Engine Inoperative Drag vs. Airspeed

COMPONENT	WEIGHT	DIMENSIONS
Stirling Engine	613.0 N	1.25m(l)x0.46m(Dia.)
Recirculating Combustor	50.0 N	0.30m(h)x0.46m(Dia.)
Heat-Pipe Radiator	144.0 N	1x3m(2 panels)
Fuel Tanks		
CH_4	42.0 N	0.54 m (Dia.)
LOX	58.0 N	.0.64 m (Dia)
Fuel		
CH_4	133.7 N	
Lox	588.3 N	
Samarium/Cobalt motor	100.0 N	1.0 m(l)x0.5 m (Dia.)
Propeller	110.0 N	8.265 m (Dia)
Total	1839.0 N	

Fig. 6 Power System Component Summary

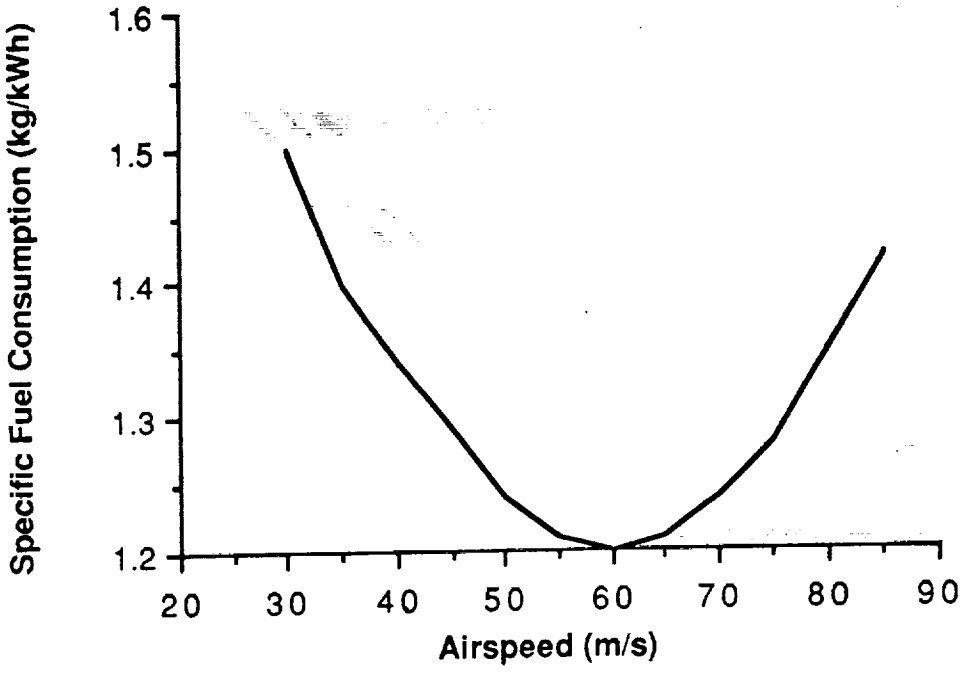

Fig. 7 Specific Fuel Consumption vs. Airspeed

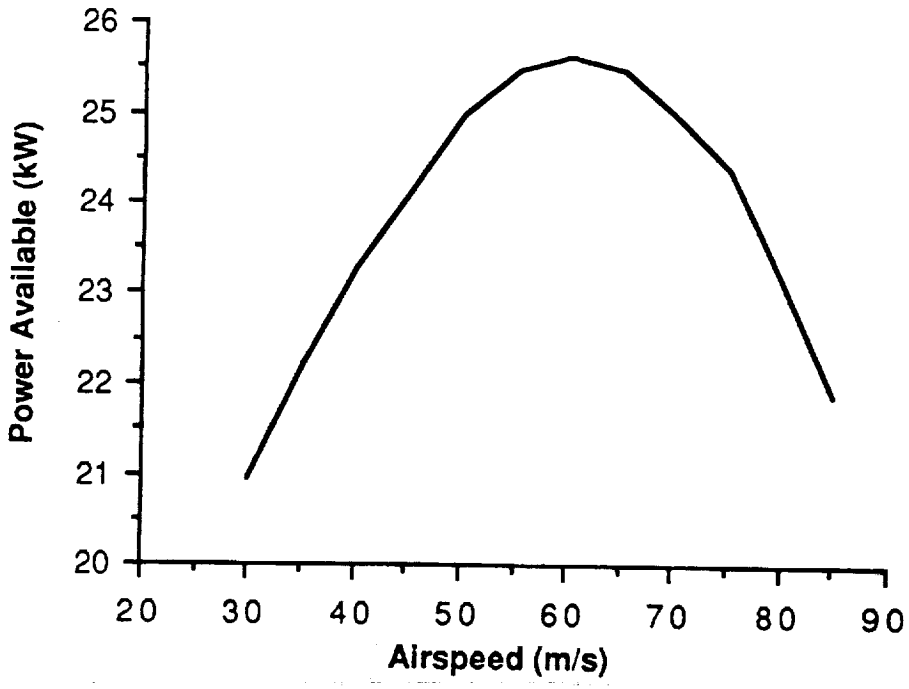

Fig. 8 Power Available vs. Airspeed

STABILITY AND CONTROL

Jamie Edgar

The Sky C.A.B. Mars aircraft is a two man joined wing aircraft designed for two passenger transport in the low density, low gravity Mars atmosphere. Sky C.A.B. employs four control surfaces, one on each of the four wing sections, to provide additional lift for takeoff and to provide control during takeoff, cruise, and landing conditions. While the large dihedral and sweep angles of the joined wing design complicate stability and control anaylisis, the large back wing allows larger control surfaces which provide better control than a conventional wing and tail configuration.

Sky C.A.B.'s Geometric Configuration

There were several reasons that a joined wing configuration was selected for Sky C.A.B. The main reason for selecting this configuration was to provide the highest amount of lift with the least amount of structural weight. The sizing requirements were a wing span of 86 meters and an aspect ratio of 8. Structures and wieghts chose an aft wing span which was 70 percent of the front wings because this would provide the lowest structural weight and still provide the desired lift. A 16 degree sweep angle was chosen for both wings (see three view diagram) to produce a reasonably sized fuslage.

Once these measurements were determined, chord lengths were chosen to provide the proper wing area. The front wing has a chord length of 5 meters at the fuselage and three meters at the tip. The aft wing has a chord length of three meters at the fuselage and two meters at the joint. The aft wing was make smaller in comparison to the front wing so that the pitching moments produced by the lift of the wings would be more balanced.

A vertical tail size was the next decision that had to be made. The height of the tail was chosen to provide ample distance between the front and rear wings. A height of 6.5 meters was chosen, which, when added to half of the two meter front fuslage diameter, provided a forward wing dihedral angle of 5 degrees above the horizontal and an aft wing dihedral angle of 15 degrees below the horizontal. Both of these angles are reasonable when compared with those of typical joined wing designs. The tail width was chosen to be 3 meters at the top and four meters at the bottom. The top number was chosen to match the aft wing chord at the top of the tail.

The joined wing design provides many options for control surface placement. Sky C.A.B. employs control surfaces which rotate both up and down on each of the four wings because this provides the greatest versatility. All four of the control surfaces extend from two to fifteen

meters from the plane of symmetry and take up 25 percent of the airfoils cross section (see three view diagram). Sky C.A.B. also has a rudder which is five meters high and one meter wide. All of the control surfaces are capable of rotating fourty degrees in either direction.

Longitudinal Stability

Sky C.A.B.'s geometry produces a neutral point nine meters behind the nose of the plane. The weights group has configurated the plane so that the center of gravity falls between 8 and 8.6 meters behind the nose, providing a static margin ranging from 10% to 25% (See Figure S+C 1). This range neglects the center of gravity with no pilot, but since Sky C.A.B. will not be flying without a pilot, this point does not need to be considered when studying flight capabilities. The empty center of gravity does fall in front of the rear landing gear so that the plane will be stable while on the ground. The static margin is effectively increased by 5% when the thrust of the propeller is added, giving a final static margin of between 15 and 30%. This static margin is comfortably above the minimum limit of 10% and the 30% maximum is the farthest point forward that the center of gravity can be at while still allowing the plane to be trimmed at C_{Lmax} using just the forward control surfaces.

Flying Qualities

The joined wing geometry provided difficulties in the calculations of the stability and control characteristics of Sky C.A.B. Many of the stability and control derivatives were calculated using Jan Roskam's paper (See References) and considering the aft wing to be the tail. Wolkovitch's paper suggested several corrections to these approximations, but was sometimes quite vague about the magnitude of the corrections. In addition to the derivative equations, actual moments and forces were checked to determine whether or not the results seemed reasonable and to assure that no mistakes had been made. In this way, the stability and control of Sky C.A.B. was determined with a reasonable amount of accuracy.

Many of the corrections suggested by Wolkovich were related to the control surfaces. Rudder effectiveness is decreased due to the enclosure of the vertical tail by the front and back wings (Wolkovitch, p. 46). To account for this, the moment created by the rudder is reduced by 10% in all stability and control calculations. The pitching moment due to the deflection of the front wing control surfaces is amplified in a joined wing. This is due to the change in the downwash on the aft wing when the control surface is moved. When the front wing control surfaces are deflected downward, the flow is turned more dramatically, and the downwash angle for the back

wing is increased. This produces less lift on the back wing when the front wing lift is increased by downward deflection, and therefore a stronger pitching moment is formed than if just the front lift had been increased. Decreaseing the lift on the front wing by raising the control surface has the opposite effect. This increases the lift on the back wing, also increaseing the total increment in the moment produced by the flap deflection. These effects are added in when computing the stability derivatives.

Downwash at the aft wing is another major correction that must be made. Downwash is affected both by the varying horizontal separation due to the large sweep angles and by the varying vertical separation due to the large dihedral angles. In calculating the longitudinal stability of a joined wing aircraft it is nescessary to use an averaged downwash parameter. This parameter is set equal to half of the downwash produced by a conventional aircraft's wing on a similar aspect ratio horizontal tail (Wolkovitch, p. 28).

Sky C.A.B. is designed for a cart assisted takeoff at a speed of 60 meters per second. Liftoff from the cart takes place at a five degree angle of attack. When the center of gravity is at its forward limit it is necessart to deflect the aft wing control surfaces upward the full fourty degrees and deflect the front wing control surfaces down five degrees to produce the proper amount of lift and allow for a slight nose up moment at liftoff. The aft wing deflection can be relaxed a bit if the front deflection is increased, but this also produces more lift and might cause the liftoff to be a little bit less smooth.

Sky C.A.B. is designed for a cruise speed of 60 meters per second at an altitude of 1.5 kilometers. Wing angles were selected so that no flap deflections are nescessary under these conditions. The four wing control surfaces provide many options for directional control. Each control surface produces both a lift and a sideforce due to the dihedral angles. Figure S+C 2 shows examples of sidforces produced in conjunction with additional lift on the front wing or decreased lift on the aft wing. The four control surfaces can be deflected to provide direct lift or they can be deflected so that the lift changes cancel and a direct sideforce is produced (see Figure S+C 3). Sky C.A.B. can also bank and turn in the normal manor, using either the front or back control surfaces. It is better to use the back control surfaces for roll because the front wing ailerons produce severe adverse yaw (Wolkovitch, p. 46). The front control surfaces can be used to provide the additional lift needed to keep the plane at a constant altitude. One aft control surface must be deflected up 26 degrees and the other down 26 degrees in order to develope a 30 degree banked turn in two seconds and the front flaps must be slowly deflected to nine degrees by the end of these two seconds to provide the additional lift nescessary to sustain the proper

altitude while the plane is banked. Electronic control of all of the control surfaces will be necessary for these maneuvers since the ratios of the deflections will depend on both airspeed and angle of attack.

Landing configuration for Sky C.A.B. requires the use of the front flaps rather than the back flaps as was done for takeoff. The reason for this is that by deflecting the front flaps downward and raising their lift coefficient the angle of attack for stall can be reduced. Front control surface deflection of 22 degrees is required to stall the plane at the approach speed of 41 meters per second. Roll control is a little more difficult at this speed, requiring 34 degrees of upward deflection on one aft control surface and 34 degrees of downward deflection of the other aft control surface to produce a 30 degree roll in the required two seconds. Landing in a crosswind requires 1.9 degrees of rudder deflection per degree of sideslip, easily allowing a 10 degree crosswind with a 19 degree rudder deflection. Full rudder sideslip without roll requires a 21 degree upward deflection of one aft control surface, and 21 degrees of downward control surface deflection on the other aft control surface. This deflection is well below the 75% maximum allowable deflection for this purpose.

Summary

Sky C.A.B. appears to fullfill all of the stability and control requirements. While a full deflection of the aft control surfaces is needed at takeoff, the remaining power in the front flaps is still available in case of unexpected problems. The stability and control group recomends that a model be built and tested in a wind tunnel if more accurate data is required.

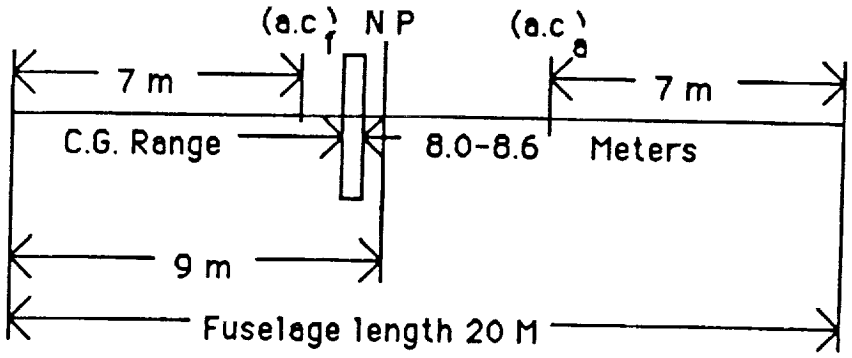

Figure S+C 1 Longitudinal Stability Points

References

Roskam, Jan, Methods for Estimating Stability and Control Derivatives of Conventional Subsonic Airplanes, University of Kansas, 1977.

Wolkovitch, Julian, Application of the Joined Wing to Turboprop Aircraft, Ames Research Center, 1984.

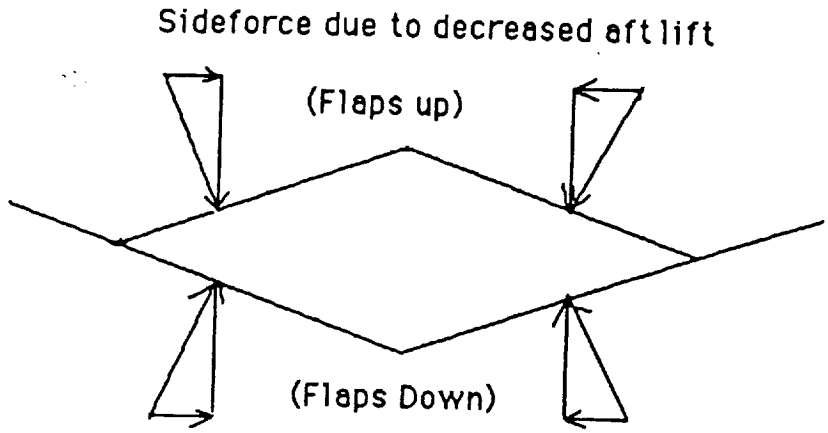

Figure S+C 2 Example of wing dihedral sideforce effects

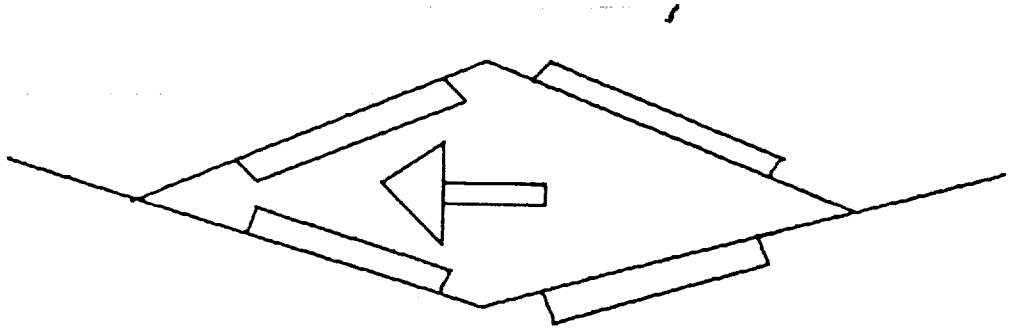

Figure S+C 3 Flap deflections for direct sideforce

STRUCTURES

Jami Munson

DESIGN OBJECTIVES

The design criteria that had to be met by the structures group when designing the Mars aircraft, SKY C.A.B., centered around three general constraints. The first was to design a wing configuration that would assist the aerodynamicist in obtaining the needed lift to fly through the thin atmosphere on Mars. The second objective was to make sure the wings would be strong enough to support the planes propulsion system, as well as withstanding a rocket-assisted take-off. The last structural consideration was to keep the weight and size of the aircraft at a minimum, allowing feasible transportation in a spacecraft to Mars. The structures group decided that a joined-wing configuration would best meet these requirements.

WING SELECTION

SKY C.A.B. will employ a new type of wing, known as the joined wing. NASA Langley Research Center[4], Rockwell International Corporation[6], and the U.S. Navy[4] have conducted various studies including wind tunnel testing on joined wing models. These tests provided a wide range of possible uses for joined wings. Two of the applications mentioned were for gliders and high-altitude reconnaissance aircraft.[4] Because the design team was faced with creating a plane that was a combination of these two aircrafts, joined wings were the wing configuration chosen.

Joined-wing aircraft have tandem wings arranged in such a way that in both the plan and front views they form a diamond shape. This diamond shape has the primary advantage of strength, in that each wing braces the other against lift loads.[2] The front and rear wings can be either tip joined or inboard-joined. Because of an increased weight savings and decrease in buckling constraints[5] when the joint location is inboard, a joint at 70% of the fore-wing span was selected for SKY C.A.B..

WING STRUCTURE SIZING

The internal structure of the joined wing is not conventional. This is mainly due to the chordwise tapering of wing thickness. The lift load acting upon any section of the wing must be resolved into two components, an "inplane" component acting parallel to the truss structure and an "out-of-plane" component acting normal to the truss structure. The determining angle for these two components is the tilt angle, shown on Fig. 5.[7]

The lift loads on the wing are resisted by a box beam extended from 5% to 75% of the chord. These are mostly concerned with resisting the out-of-plane components which tend to bend the wings about a tilted bending axis. The most effective positioning of the material is to concentrate it near the upper leading edge and the lower trailing edge.[4] This location also provides for the optimum weight advantage. The weight advantage is derived because the second moment of area about the tilted axis joining the centroid of the fore and aft wings at each section of span is maximized for this particular location of the material.[6]

For the inboard-joined wing configuration, the box structure discussed above provides the optimum design for all regions of the wings except the segment of the front wing that extends beyond the joint. This part of the wing can be treated as a conventional cantilever wing, thus the optimum box spar structure for it would extend from approximately 15% to 65% of the chord. The different box spar structures can be seen in Fig. 6. The overall airframe structural layout can be seen in Fig. 8.

Generating load diagrams for the joined wings could not be done in a conventional way. The first step in finding the wing weight distribution was to obtain chord as a function of semi-span. This was then multiplied by the cosine of the tilt angle, the wing weight, and divided by the wing area. This number was multiplied by the integral of the chord function from the fuselage to the tip of the front wing. The wings were considered as having an elliptical lift distribution. Both the front and rear wings provide lift. The percentage carried by each wing is 60% fore and 40% aft.[2] Only the total lift is shown on the graph in Fig.1. Once the loads are found, shear and moment diagrams can be calculated by taking the first and second integrals of the loading functions respectively. (see Fig. 2 and Fig.3). The torsional moment about the elastic axis (Fig.4) for the design determining flight condition is zero up to the joint location of the wings. The section of the front wing that extends beyond the joint can be treated as a cantilever wing. This is the only part of the joined wings that will exhibit torsional bending.

COMPOSITES

Advanced composite materials provide an attractive potential for reducing the structural mass of an aircraft. Composite materials are well suited for use on the chordwise tapering of wing thickness that is characteristic for joined wings.

Composite materials are material systems that are composed of a mixture or combination of two or more materials that are distinctly different in form and chemical composition. The combination produces a material which possesses properties that are superior to its own individual components.[3]

Carbon fibers used to reinforce some plastics are characterized by being light weight with high strengths and stiffness.[3] These properties make graphite epoxy the best choice for the aircraft's structural members, including spars, stiffners, flaps, and skins. Along with the weight savings and strength advantage, graphite epoxy is also more resistant to fatigue than other composites. Graphite panels will be used to cover SKY C.A.B. in all areas except those around the radiator. The radiator will have no covering on it and insulation will have to be used so that the heat emitted will not melt the surrounding structure.

SUMMARY

In conclusion, joined wings meet the necessary requirements of a wing configuration for a Martian aircraft. Joined wings have good lift capabilities that will assist in providing the lift necessary to fly through the Martian atmosphere. The unconventional structural design of the wing configuration will be able to withstand the forces exerted by the propulsion system during take-off. Finally, due to their light weight, joined wings in combination with the use of composites, will result in a lightweight plane that can be transported in a spacecraft to its destination on Mars. Overall, joined wings were the most feasible selection for SKY C.A.B.

BIBLIOGRAPHY

1. Lynch, Ted, Jerome Persh, Tony Wolf, and Nevin Rupert, "The Nation's Future Materials Needs", SAMPE Business Office, Covina, CA, 1987.
2. Samuels, Mary Fairchild, "Structural Weight Comparison of a Joined Wing and a Conventional Wing", Journal of Aircraft, June 1982, pp.485-491.
3. Smith, William F., "Principles of Materials Science and Engineering", McGraw-Hill Book Company, 1986, pp. 701-710.
4. Wolkovitch, Dr. Julian, "Principles of the Joined Wing", Engel Engineering Company Report No. 80-1, 1982.
5. Wolkovitch, Dr. Julian, "Parametric Weight Evaluation of Joined Wing by Structural Optimization", April 15-17, 1985. (AIAA-85-0642-CP)
6. Wolkovitch, Dr. J., "Joined-Wing Research Airplane Feasibility Study", SanDiego CA, Oct.31-Nov.2, 1984. (AIAA Paper 84-2471)
7. Wolkovitch, Dr. J., "The Joined Wing: An Overview", Reno, Nevada, Jan. 14-17, 1985. (AIAA Paper 85-0274)
8. Department of Transportation, "Airframe and Powerplant Mechanics Airframe Handbook" U.S. Government Printing Office, Washington D.C., 1972.
9. A Collection of Technical Papers AIAA/ASME 19th Structures, Structural Dynamics, and Materials Conference", Bethesda, Md, April 3-5, 1978.

Fig. 1 LOAD DIAGRAMS

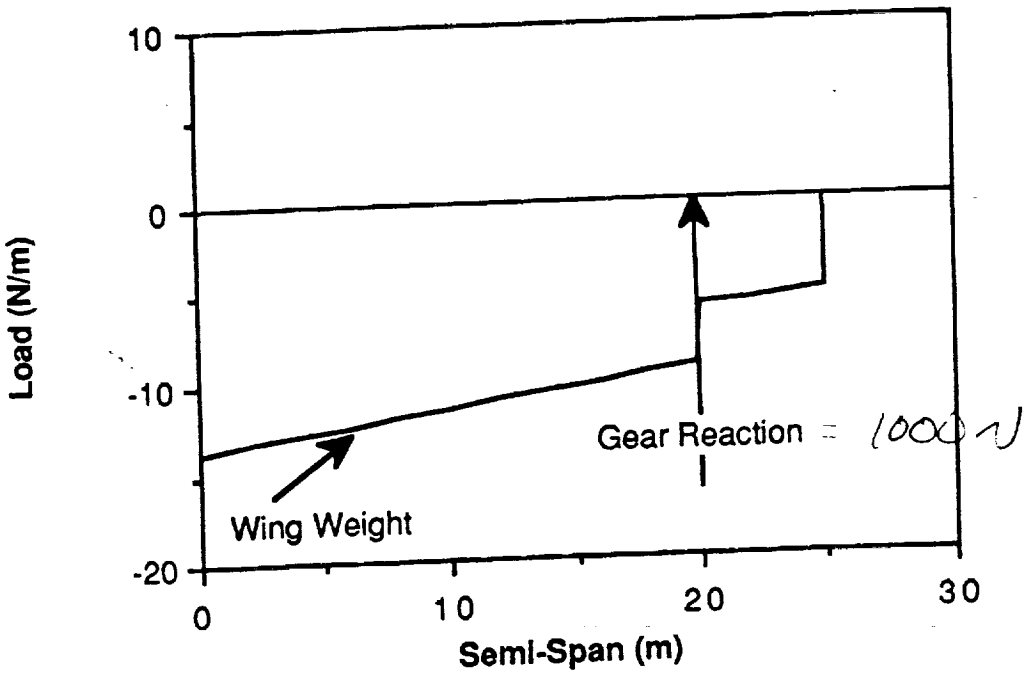

RAMP CONDITION

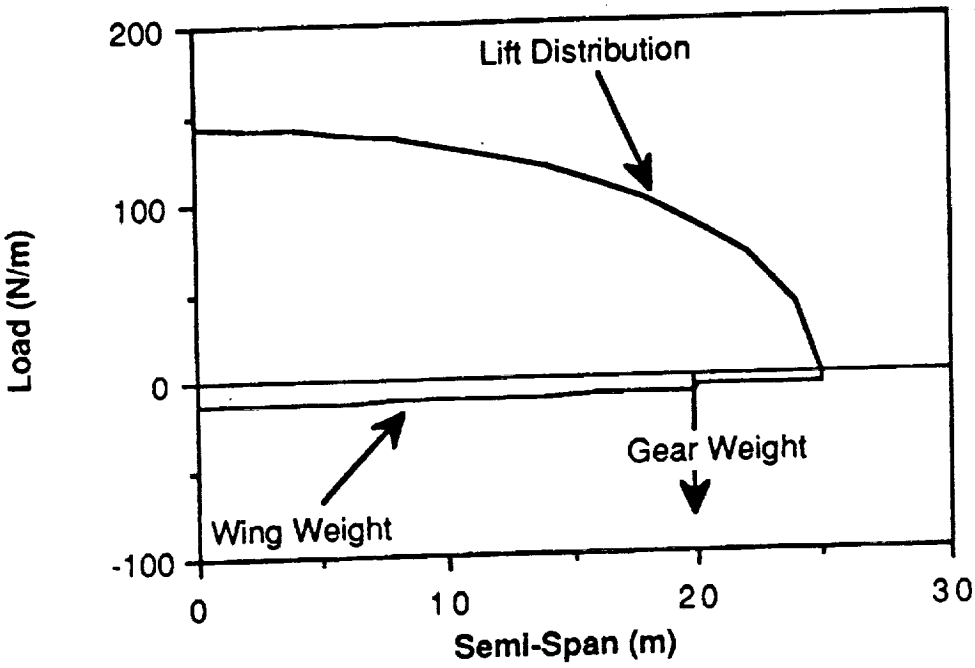

STEADY FLIGHT CONDITION

Fig. 2 SHEAR DIAGRAMS

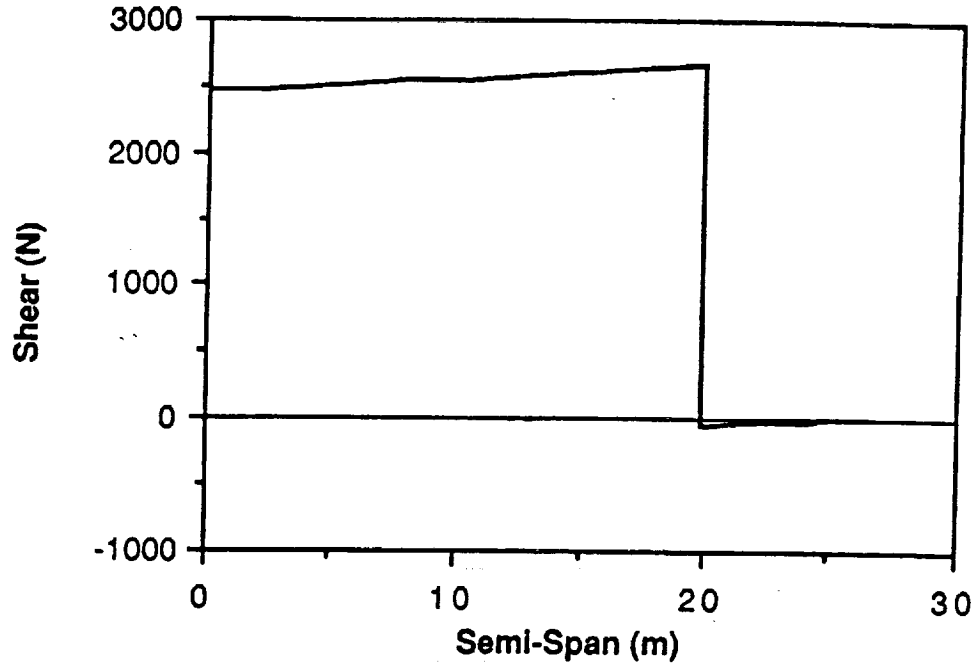

RAMP CONDITION

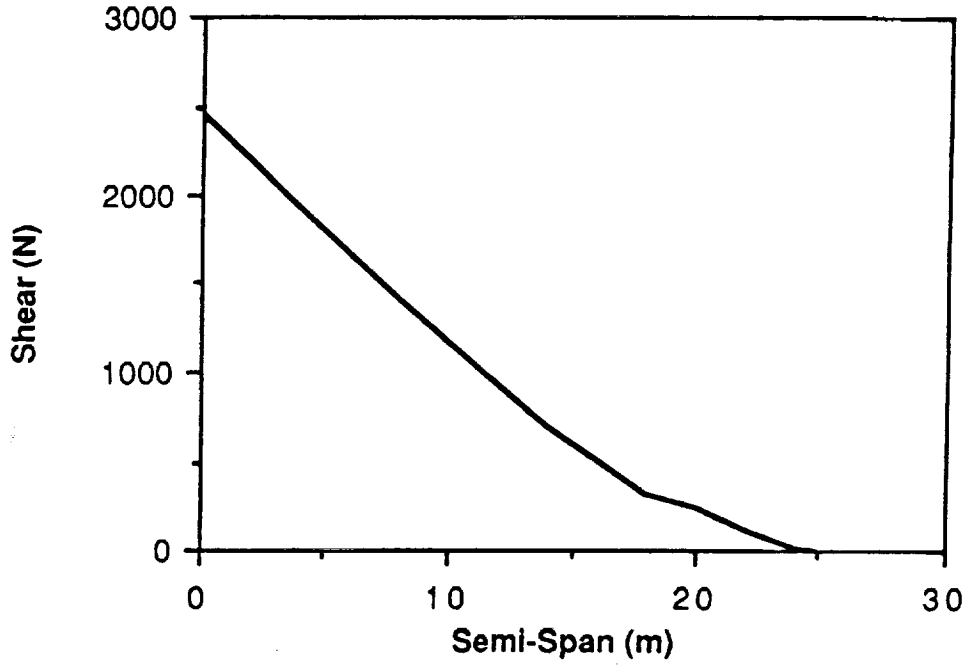

STEADY FLIGHT CONDITION

Fig. 3 MOMENT DIAGRAMS

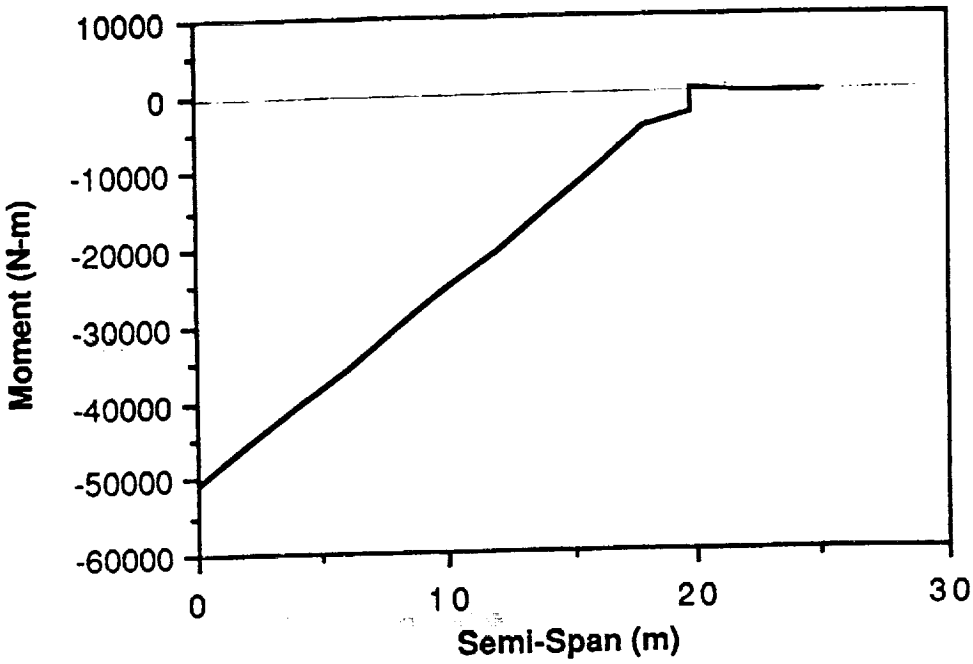

RAMP CONDITION

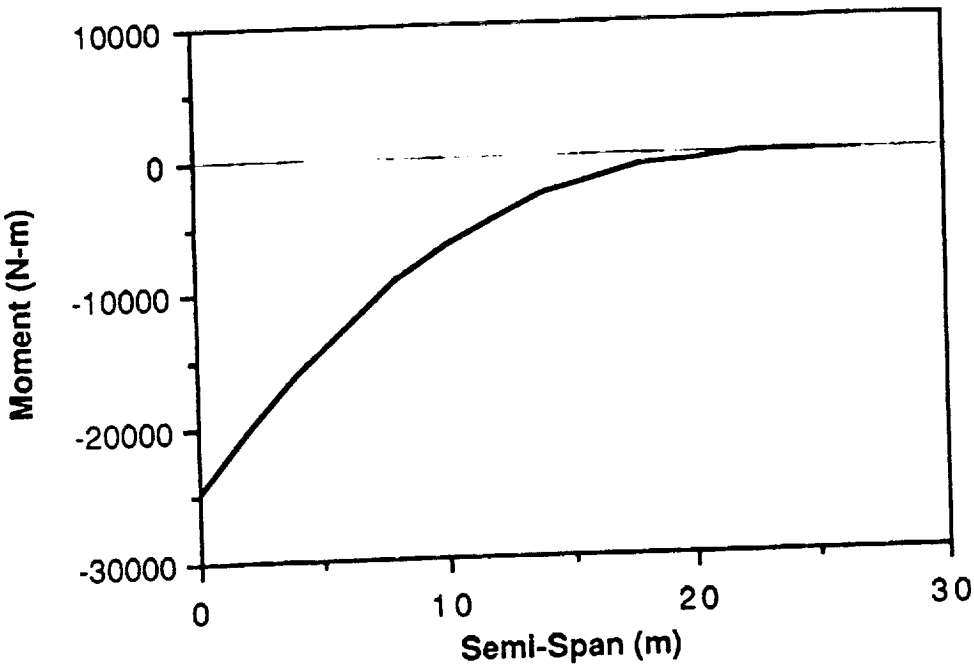

STEADY FLIGHT CONDITION

Fig. 4 TORSIONAL MOMENT

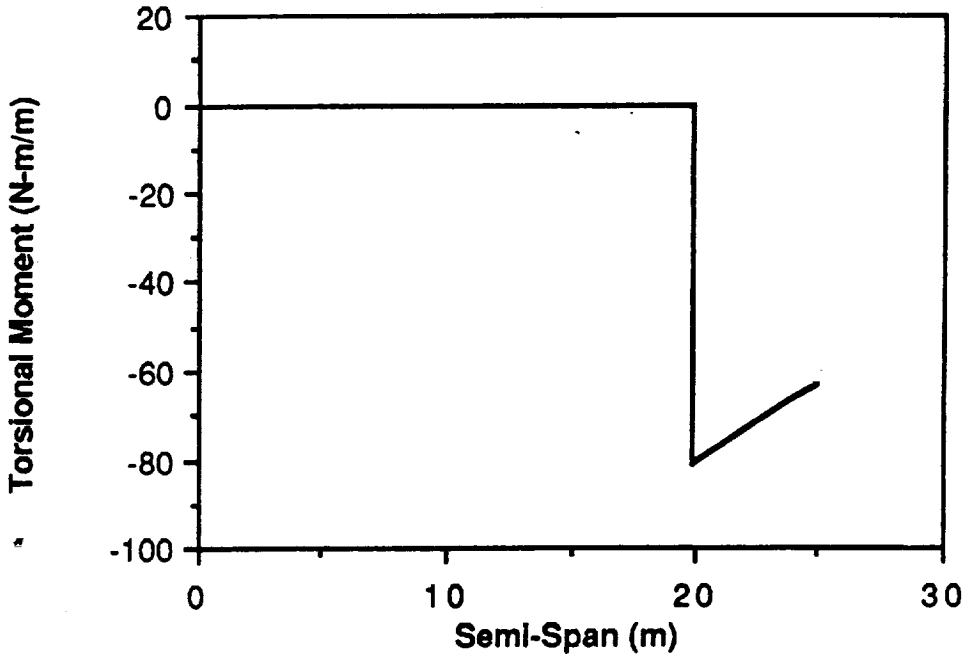

Fig. 5 LIFT COMPONENTS

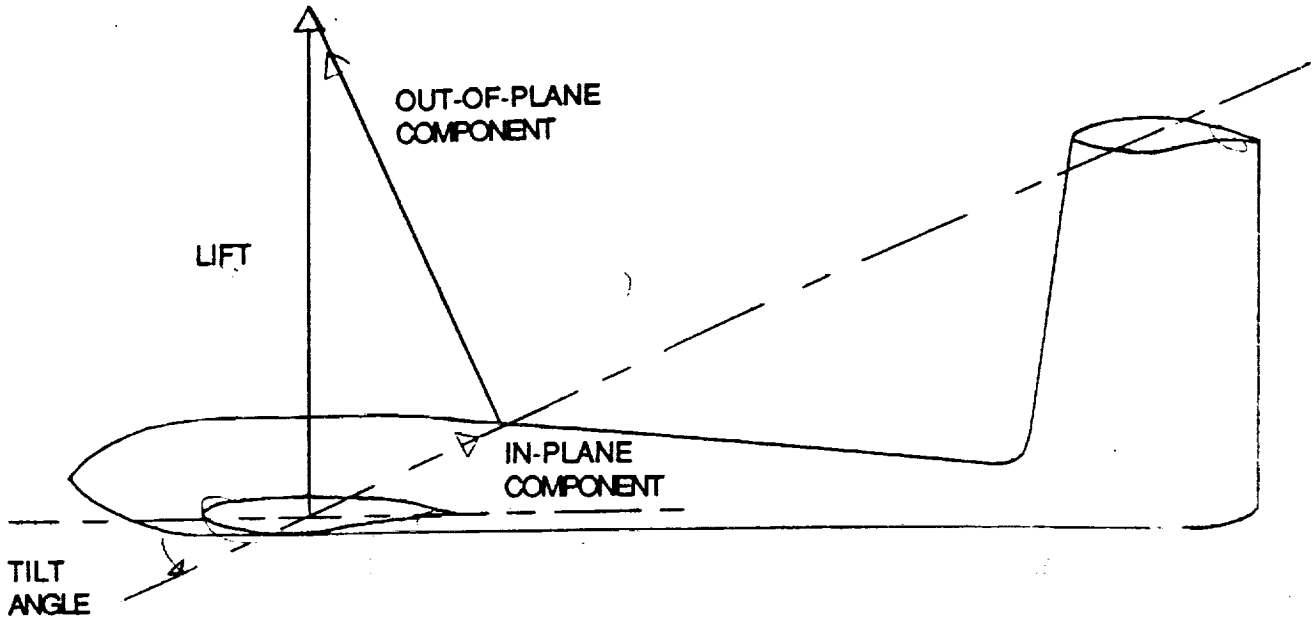

Fig. 6 OPTIMUM WING STRUCTURES

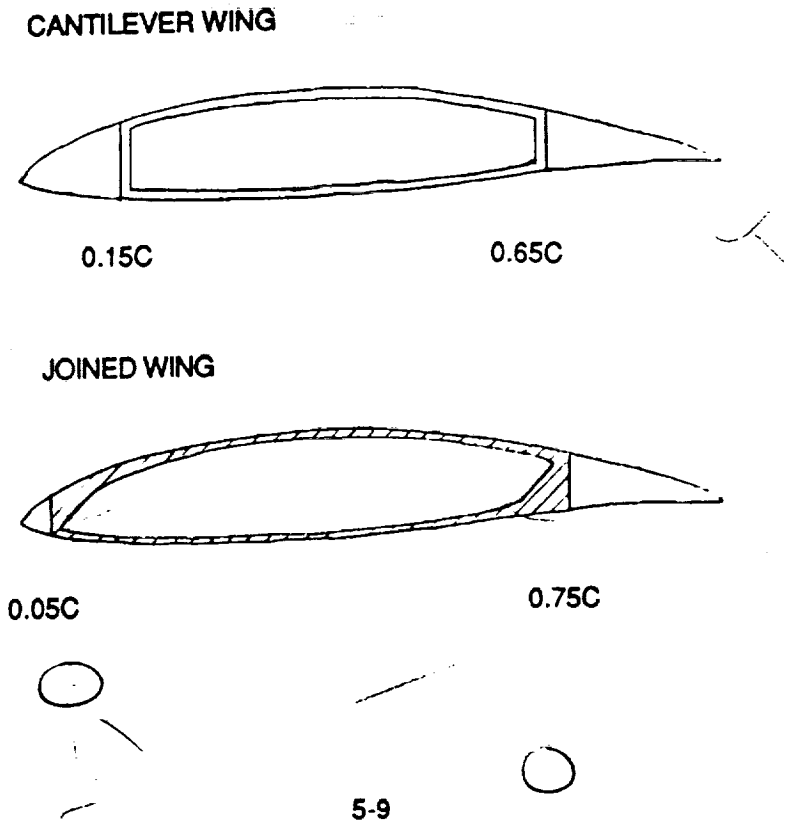

Fig. 7 AIRFRAME STRUCTURAL LAYOUT

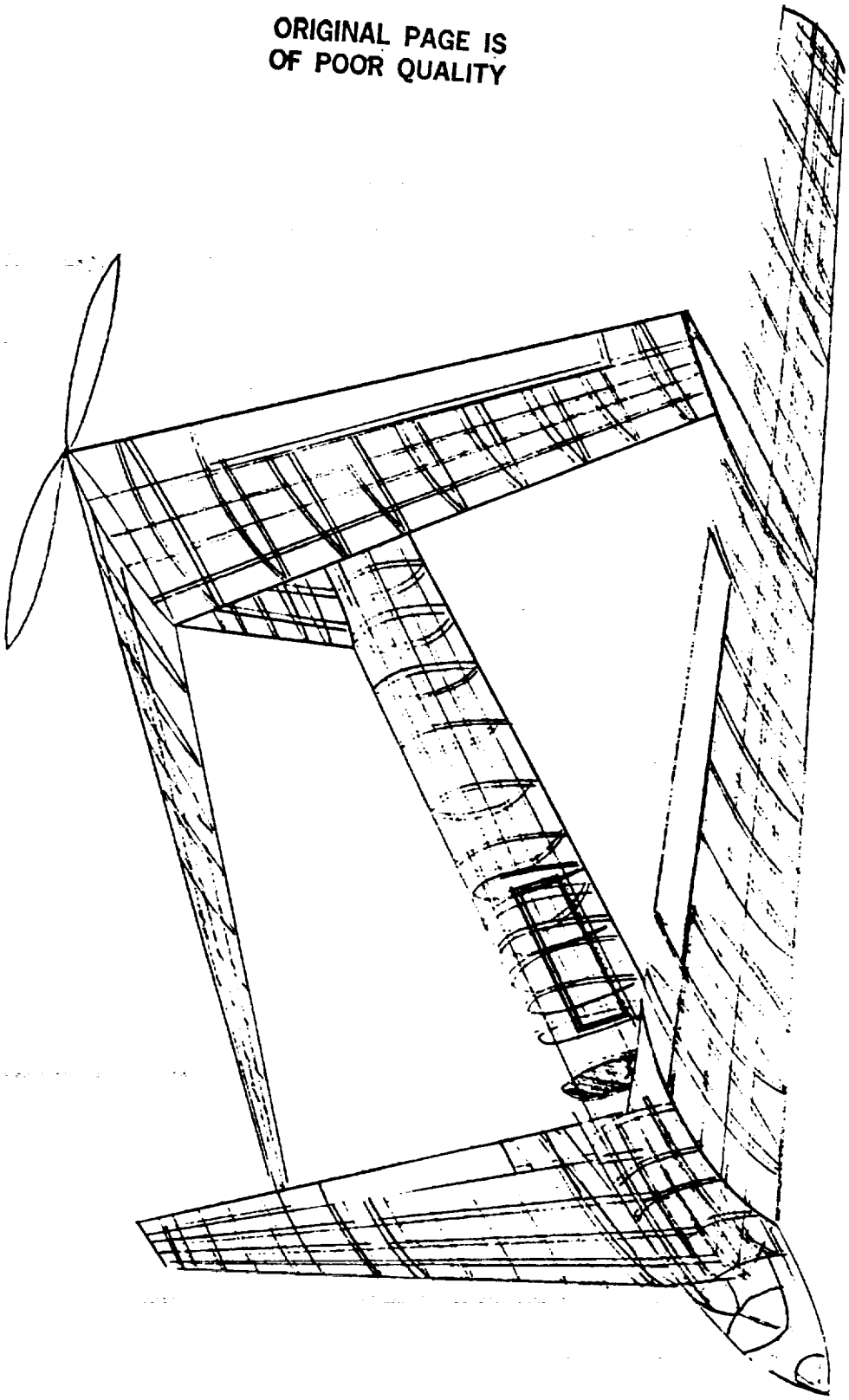

SURFACE OPERATIONS

By

Matt Miller

Abstract

The task of taking off and landing Sky C.A.B. within a required maximum distance proved to be quite difficult. A few factors such as obstacles, low densities, and surface conditions had to be taken into account. It was decided early in the design process to use a conventional take-off and landing configuration. To meet the take-off distance requirement, a cart assisted take-off will be utilized. The addition of the cart reduced the take-off distance below the maximum distance. The landing of Sky C.A.B. did not pose too many problems. The value calculated for landing distance turned out to be less than the maximum distance. A conventional braking system and plain flaps were utilized to decrease the distance.

Nomenclature

γ_A	Angle of Approach
γ_{cl}	Angle of Climb
S_A	Approach Distance
V_A	Approach Velocity
S	Area of Wings
a	Average Deceleration
μ_b	Braking Coefficient
c_f/c	Chord Ratio
S_{cl}	Climb Distance
ρ	Density at Sea Level
C_D	Drag Coefficient
δ_f	Flap Deflection (Plain Flaps)
S_F	Flare Distance
μ	Ground Friction Coefficient
S_G	Ground Roll Distance
C_L	Lift Coefficient
V_{LO}	Lift-off Velocity
h_{obs}	Obstacle Heighth
R	Radius of Flight Path
S_R	Rotation Distance
V_{stall}	Stall Velocity
S_{TO}	Total Distance
S_{TR}	Transition Distance
V_{TR}	Transition Velocity
W_{cart}	Weight of Cart
W_{fuel}	Weight of Fuel
W_g	Weight of Sky C.A.B.
P_r	Power Required

Data Summary

Conventional Take-off Analysis

W_G	= 5957 N	C_L	= 1.33
V_{stall}	= 38.35 m/s	C_D	= 0.0777
V_{tr}	= 49.85 m/s	S	= 312.5 m^2
V_{LO}	= 46.02 m/s	ρ	= 0.0150 kg/m^3
S_G	= 1477.8 m	R	= 744.8 m
S_R	= 138.1 m	γ_{cl}	= 5 °
S_{tr}	= 64.9 m	μ	= 0.04
S_{cl}	= 139.1 m	h_{obs}	= 15 m
S_{TO}	= 1820 m	c_f/c	= 0.25
P_r	= 28.0 kW	δ_f	= 30 °

Cart Assisted Take-off Analysis

V_{LO}	= 60 m/s	W_{cart}	= 300 N
R	= 1037.7 m	S_{cl}	= 126.3 m
μ	= 0.04	S_G	= 710.0 m
C_D	= 0.0286	S_{TO}	= 836.3 m
C_L	= 1.02	P_r	= 45.0 kW

Rocket Engine Data:

Type:	CH_4/LOX Gas Generator
Thrust	= 845.1 N per engine
Weight	= 43.6 N per engine
Total Thrust	= 4675.5 N (5 rocket engines + airplane engine)
Total Weight	= 218 N

Landing Analysis

W_{fuel}	= 720 N	γ_A	= 5 °
V_{stall}	= 36.36 m/s	R	= 1544.9 m
V_A	= 41.8 m/s	δ_f	= 20 °
S_A	= 171.5 m	a	= 1.43 m/s^2
S_F	= 67.4 m	C_D	= 0.0559
S_G	= 652.7 m	C_L	= 1.48
S_{TO}	= 891.6 m	μ_b	= 0.40

TAKE-OFF ANALYSIS

In the design of the take-off and landing configuration for the aircraft Sky C.A.B., a conventional take-off and landing (CTOL) design was chosen. The CTOL system was selected instead of a vertical take-off and landing (VTOL) system primarily because of the common uses of CTOL on lightweight aircraft in the United States. A conventional take-off involves the use of a propulsion system propelling an aircraft down a runway in order to obtain a minimum velocity required to get the aircraft airborne. For the take-off scenerio, a maximum distance of 1000 m was allotted for the length of the runway. Initially, calculations were made for the plane being propelled down the runway with the aircraft engine as the only means of propulsion. From the data summary, it can be seen that the ground roll distance (S_G) by itself exceeds the maximum runway length. With the rotation, transition, and climb distances added in, the total take-off distance is extremely high. The main cause for the excessive amount is the value of the required lift-off velocity (V_{LO}). To obtain the specified lift-off velocity within the 1000m distance, the power output of Sky C.A.B.'s engine would have to increase by a substantial amount. Because this power increase is not possible, an auxiliary propulsion system had to be implemented into the design.

CART ASSISTED TAKE-OFF (CATO)

After a few alternative propulsion systems were researched, a cart assisted take-off was selected. The addition of the cart made it possible to shorten the take-off field length. The cart's guidance system is operated by a remote control. A member of the ground crew will guide the cart down the runway until lift-off. After release, the cart will decelerate to a stop by use of a disc braking system on the wheels. As can be seen from Figures 1 and 2, the aircraft will fasten onto the top of the cart. Sky C.A.B. will be fastened onto the cart at the center of gravity position of the aircraft and at a distance of 8 m from the fuselage along both wings. When the required lift-off velocity is obtained, the pilot will pull a lever in the cockpit which will release the aircraft from the cart. The aircraft will be placed on the cart at an angle of attack of 5°. This will enable the aircraft, at the moment of release, to begin to climb at an angle of 5°. Since the aircraft is already starting at the specified angle of attack, the transition distance (S_{tr}) parameter can be eliminated from the total take-off distance calculation.

One of the initial constraints of the design was the assumption that there is a 15 m obstacle at the end of the runway. After conferring with the performance specialist, it was determined that once the aircraft is above the obstacle heighth (h_{obs}), it will level out and assume the rate of climb necessary to reach the desired altitude. To reach the obstacle heighth, a higher lift-off velocity was calculated. With the added power from the cart's propulsion system, the total take-off length was reduced to an amount below the maximum length.

Cart Propulsion System

To acquire the desired lift-off velocity, five CH_4/LOX rocket engines will be mounted on the tail of the cart(Fig. 2). The data for the rockets can be seen on the data summary sheet.[1] The power output from the rocket engines added to the power output of the aircraft engine will provide the required power to obtain lift-off velocity. The choice of the CH_4/LOX engine was mainly due to the ability to manufacture methane on the Mar's surface. This engine also generated a favorable power output which was important in the selection process. As one can see, the addition of an auxiliary propulsion system was essential. Due to the engines, the CATO system seems to work quite well.

LANDING ANALYSIS

Because a CTOL design was selected for the aircraft, a landing field distance had to be calculated. A conventional landing involves the aircraft descending towards the runway at a specified angle of attack. After the aircraft has landed, it decelerates until it has stopped. Initial constraints were also specified in the landing analysis. A maximum landing field length of 1000 m and an obstacle heighth of 15 m were designated. In the landing analysis, it was assumed that the runway consisted of firm and dry dirt.

During the landing procedure, some important parameters have to be taken into account. The total landing distance (S_{TO}) is divided into an approach distance (S_A), which is related to the approach angle, the flare distance, which is related to the radius of flight path (R), and a ground roll (S_G). The most important aspect of the landing procedure is the approach velocity (V_A). This variable has a direct relationship on all of the distance parameters.

After the initial calculations were made for ground roll, it was determined that a braking system needed to be included in the design. A braking coefficient (μ_b) was used to calculate the average deceleration rate (a) needed for the aircraft. The addition of brakes to Sky C.A.B. reduced the landing field distance to a safe amount below the maximum length. After the aircraft has completed the landing procedure, it will be taxied back to the hangar for maintenance and servicing.

LANDING GEAR

The use of high-quality landing gear on an aircraft is of the utmost importance. A major disaster could come about if the gear failed to carry out it's function. The primary test of the gear is to see if it can withstand the impact force at the instant of touch down. To compensate for the impact force, shock absorbers are included in the design of the landing gear. The most important component of the gear is the tire. In the case of the aircraft Sky C.A.B., which has a single wheel configuration at all three gear locations, it can not afford a tire to deflate or blow out under high pressures. This possible disaster causes the designer to select a reliable, sturdy tire to do the job. The following discussion will relate these design constraints to both the main and nose landing gear.

Nose Gear

The selection of the nose gear characteristics did not prove to be a big challenge. The location of the nose gear is approximately identical on most aircraft. Sky C.A.B.'s nose gear is located 1 m from the nose tip of the aircraft. Since the impact force on the nose gear is less than that of the main gear, a smaller tire size was selected for the nose gear. As can be seen in Figure 3, the nose gear contains a device on it known as the steering jack.[2] When the plane is being towed to and from the runway, the vehicle pulling the plane will latch onto this jack. The shock absorber chosen for both the nose and main gear, shown in Figure 4, had the highest efficiency among the choices. One problem related to the shock absorber is the possibility of the fluid inside the casing becoming to viscous. The answer for this problem is to combine the fluid with an anti-viscous (e.g. anti-freeze) solution. This will enable the shock absorbers to perform at a high efficiency at all times.

Another aspect of the nose gear is the forward retraction system. Retractable landing gear was selected in order to improve performance by reducing the drag. A forward retraction system was used so that in case of equipment malfunctions, gravity will take effect on the gear and retraction will occur.

Main Gear

The main gear characteristics, which can be seen in Figure 5, are much more important than the nose gear. The shock absorption system for the main gear is identical to the nose gear. The only difference in the tire selection is that the main gear tires sustain much larger impact forces than the nose tires. Therefore, the size of the tire is almost twice as large as the nose gear tires. The location of the gear is extremely important in terms of weights and stability and control. It is essential that the main landing gear be located aft of the center of gravity. It is obvious that if this requirement is not met, the aircraft will not be stable while sitting on the ground. The gear is located at the intersection of the front and rear wing. This position was determined to be the most structurally sound. To reduce the drag even more, the main gear will also be retractable. As shown in Figure 5, the gear will retract inward toward the fuselage. Due to the specified location of the gear (11.6 m back from the nose tip), it will retract diagonally toward the front wing at an angle approximately equal to the sweepback angle($\Lambda=16^{o}$). This position will also be beneficial because retraction will still occur in case of an equipment failure.

Due to the maximum landing field length of 1000 m, a braking system was required for the aircraft. Only the main landing gear will require a braking design. The system consists of an anti-skid, disc brake configuration. The anti-skid analysis is extremely important in aiding the pilot to keep Sky C.A.B. under control during the ground roll. As can be seen from the data summary, an average deceleration (a=1.43) was obtained through calculations. This reduced the total landing distance to an amount below the maximum length.

HIGH LIFT SYSTEM

A high lift system is essential for most conventional aircraft. In the design of Sky C.A.B., plain flaps were selected for a system.[3] From Figure 6, the diagram shows that all four wings are accompanied by flaps. The range of 2 m to 15 m was used for all of the wings. The use of flaps gives aid to the take-off procedure in that it increases the lift coefficient. A flap deflection is also favorable in a landing procedure because it increases the drag coefficient. Stability and control also benefits from the deflection of flaps while the aircraft is in flight.

SUMMARY

The design of the take-off and landing procedures can become much more complicated. In this design report, only the basic components were evaluated. After laboring through the necessary calculations, the design of the take-off and landing scenerio for Sky C.A.B. was quite favorable.

REFERENCES

[1] W.A. Visek, "LOX/Hydrocarbon Booster Engine Concepts," AIAA Paper No. 86-1687, AIAA/ASME/SAE/ASEE 22nd Joint Propulsion Conference Huntsville, Alabama, June 16-18, 1986.

[2] Norman S. Curry, "Landing Gear Design Handbook," January 1982

[3] AAE 241 Datcom Material on High Lift Wing System Revised January 1974.

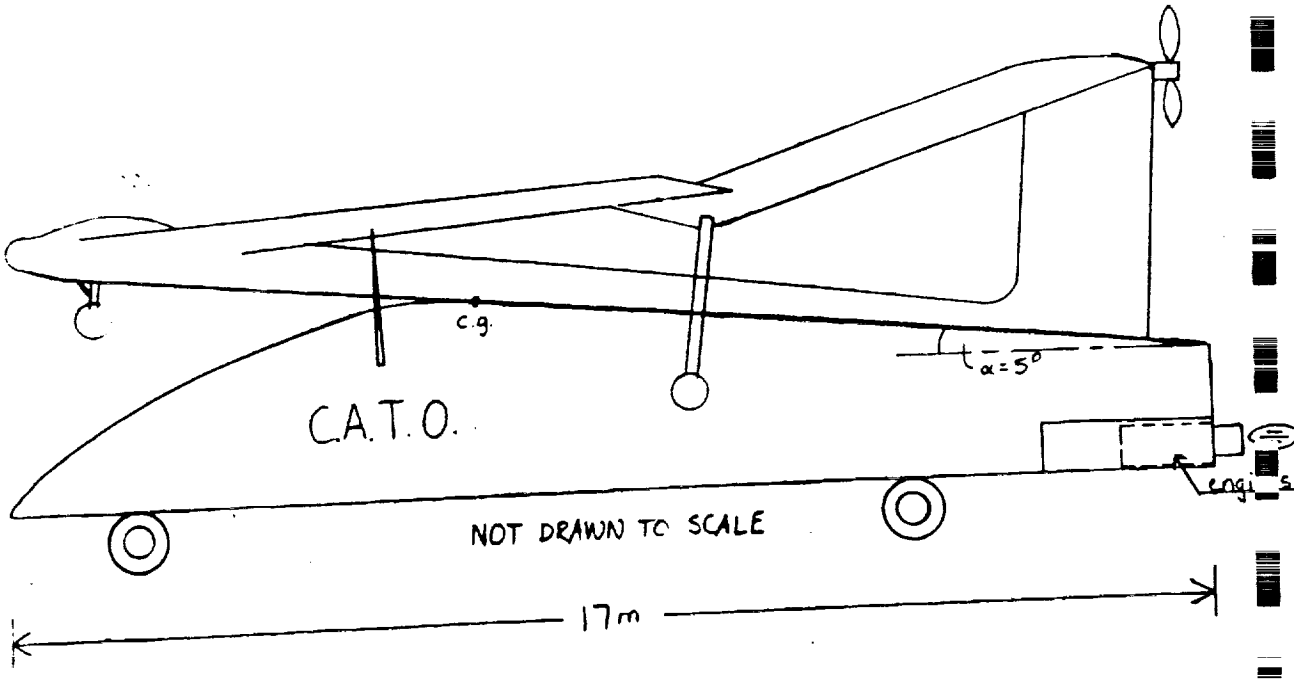

FIG. 1

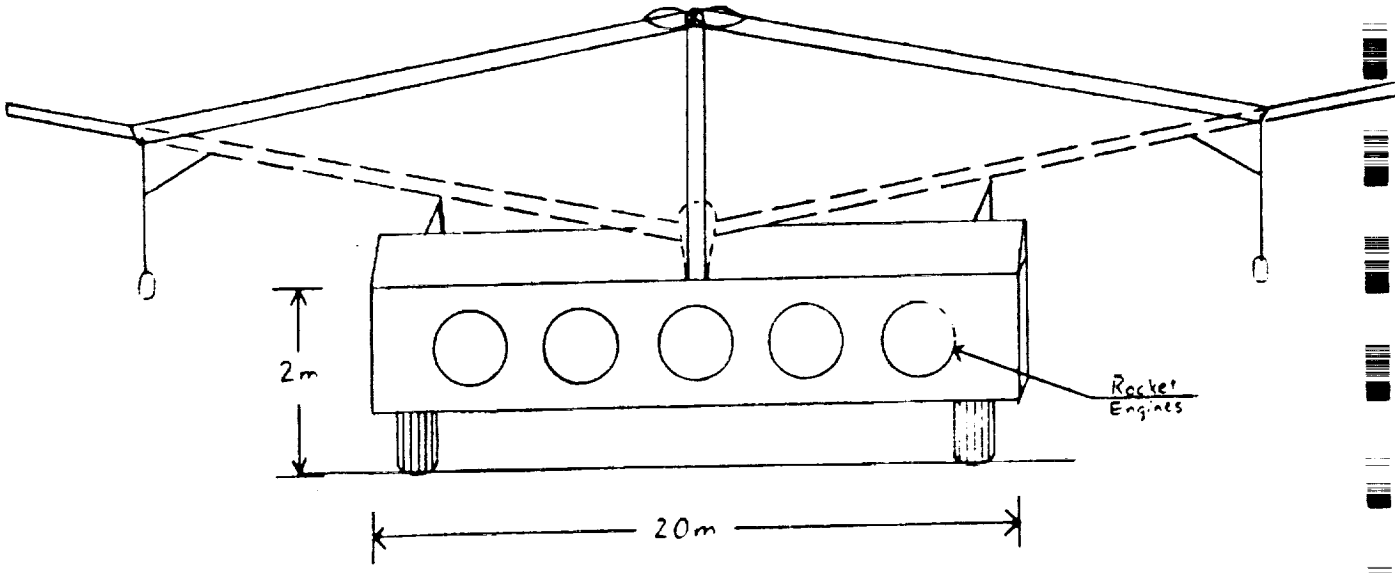

FIG. 2

ORIGINAL PAGE IS
OF POOR QUALITY

OLEO PNEUMATIC SHOCK ABSORBER

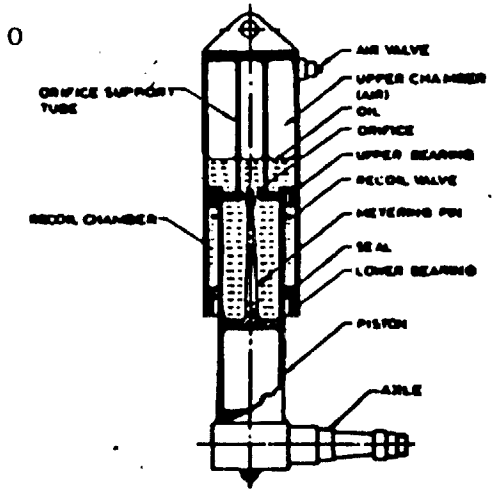

FIG. 4

NOSE GEAR

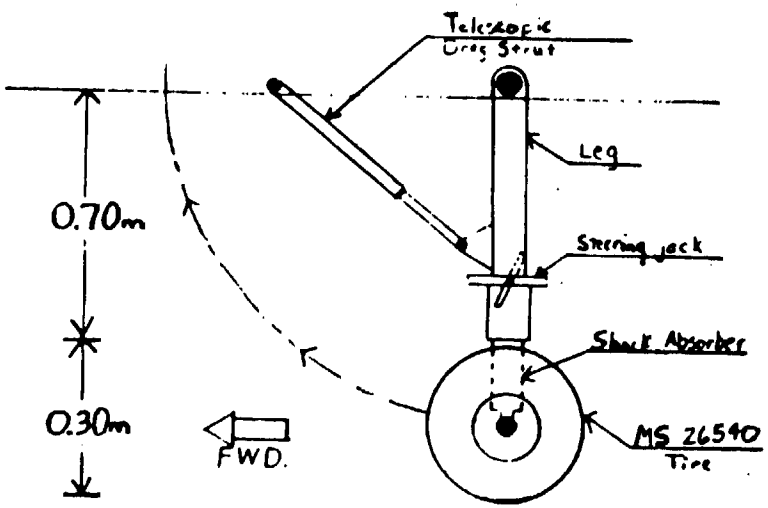

FIG 3

MAIN GEAR

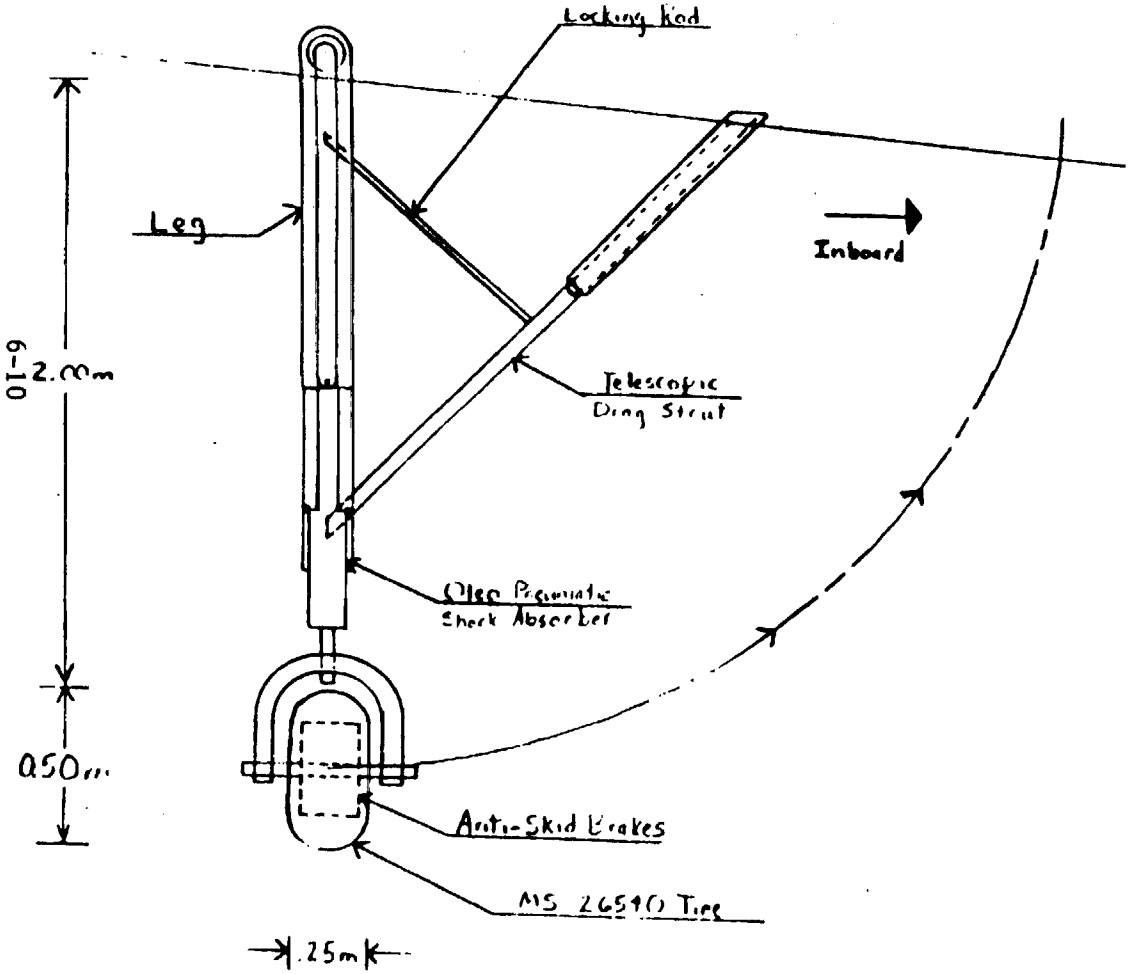

FIG 5

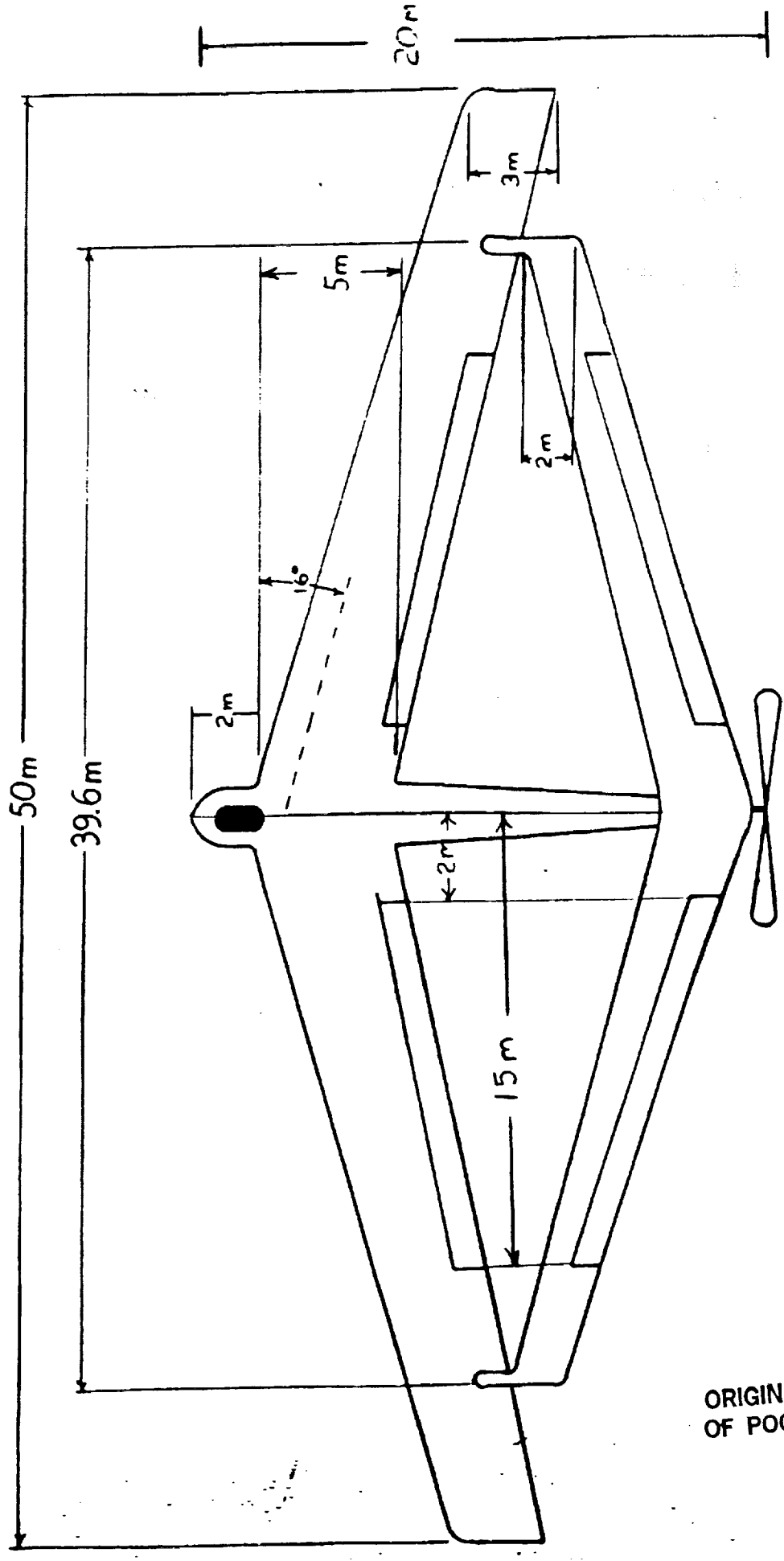

FIG 6

ORIGINAL PAGE IS
OF POOR QUALITY

WEIGHTS AND BALANCE

by
Angie Kostopoulos

The objective of the weights group was to compute a gross takeoff weight for the Mars Aircraft that would come close to the design goal weight of 5940 Nm which was computed from the initial sizing of the aircraft.

The Mars Aircraft structural system for the preliminary design consisted of :

1. Inboard joined wings.
2. A fuselage 40 m in length and a maximum parameter of 2 m in width and height.
3. A wing area of 742.50 m^2
4. A wingspan of 86 m.
5. An aspect ratio of 10.
6. A fin 10 m in height with a maximum width of 8 m.

As shown in table 7-1 the takeoff weight for this design exceeded the design goal weight of 5940 Nm by 2906 Nm . This excess weight was due to the size of the fuselage . It provided a lot of space and weight that was not needed. In order to compensate for this weight difference the size of the aircraft was reduced . The outcome of this reduction was the final design of the aircraft.

The Mars Aircraft structural system for the final design consisted of :

1. Inboard joined wings.
2. A fuselage 20 m in lenght with a maximum parameter of 2m in width for the first 14 m measured back from the nose , a width of 1 m for the other 6 m of the fuselage and a maximum height of 1 m.
3. A wingspan of 312.50 m^2
4. An aspect ratio of 8.
6. A fin 6.5 m in height and a maximum width of 4 m.

Wing weight computation

The wing weight for the final design was computed by computing the wing-plus-tail weight for a conventional cantilever wing by standard methods (Ref 1) . According to J. Wolkovitch (Ref2) the inboard joined wing provides a lighter wing system than joining the wings at their tips. However due to the nebulous savings of an inboard joind wing the weights group reduced the weight only by 30% which is the weight savings that a tip joined wing provides compared to a cantilever wing.
The wing weight was also reduced due to the weight savings of graphite apoxy which was the material used to construct the wings.

Fuselage weight computation.

The joined wing also provided reductions in the fuselage weight by reducing the bending moments on the fuselage. The bending moments were reduced due to the fact that the front and rear wing of a joined wing pair both lift upwards. Thus the fuselage is supported at both ends as opposed to the conventional wing-plus-tail system which supports the fuselage near it's middle with the tail applying a trimming download. The weight's group was able to reduce the overall weight of the fuselage by 15% (Ref 3) and was able to reduce the weight further due to weight savings of graphite apoxy.

Gross takeoff weight computation.

The gross takeoff weight of the final design was computed by summing the structural system weight , the power and propulsion system weight and the fixed equipment weight . The gross takeoff weight was kept as a variable in the fuselage , wing and vertical tail weight equations.The following equation was obtained :

source ?

$$W_{TO} = 0.70[33.63(W_{TO})^{0.397} + 0.0726(W_{TO})^{0.887}] + 59.1[[6(W_{TO})/10^5]3.066]^{0.458} + 205(W_{TO})^{0.144} + 2133$$

By iterating the above equation the weights group obtained a gross take- off weight of 5957Nm. Table 7-2A shows part of the iteration process. Table -3 shows a final detailed weight breakdown of the final design. When the gross takeoff weight was obtained a computation of the maximum takeoff weight,operational emty weight, maximum landing weight, useful load fraction and maximum fuel fraction was done. A tabulation of these values is shown in table 7-2B.

Center of gravity

A center of gravity range of 8 m to 8.6 m was given by the stability and control group. A center of gravity was calculated for five different travel conditions. AS shown in Fig 1 the center of gravity of each condition fell within the range of the forward and limit except for the operational empty weight condition . The center of gravity of this condition was located at 9.4 m from the nose of the aircraft . This condition violated the stability and control limits but since the wing landing gears were located 12m back from the nose of the aircraft , the landing gear conditions were not violated therefore stability was maintained even for this condition.

Conclusion.

By making the computations and weight reductions stated above as table 7-3 shows a gross takeoff weight of 5957 Nm was obtained which was only 17 Nm over the design goal weight.

Refrences

1. Roskam Jan, ' Airplane design V : component weight estimation'
   Roskam aviation and engineering corp.

2. Wolkovitch , J . ' The Joined Wing : An Overview '
   AIAA paper 85- 0274.
   January 14 - 17 ,1985 /Reno , Nevada.

3. Wolkovitch , J. and David w. Lund 'Application of the joined wing to
   Turboprop Transport aircraft'
   ACA Industries Inc.
   Torrence California.

GROUP WEIGHT BREAKDOWN
Preliminary Design
Table 7 -1

AIRPLANE TYPE: Sky C A B
ENGINE TYPE : SP-100 Free piston engine

GROUP INDICATION	WEIGHT (Nmars)	DISTANCE (meters)	MOMENT
AIRFRAME STRUCTURE:	5852		
FORWARD WING	816	12	9792
REAR WING	544	32.6	17734
TAIL GROUP	257	38	9766
FUSELAGE	2625	20	52500
NOSE GEAR	70	6	420
WING GEAR	180	22	3960
PROPULSION GROUP	1085		
ENGINE	765	33	25245
MOTOR	163	38	6194
OIL SYSTEM	23	33	759
FUEL SYSTEM	34	38	1292
PROPELLER	100	40.5	4050
AIRFRAME SERVICES.	213		
AVIONICS	52	3.5	182
FLIGHT CONTROLS	75	30	2250
FRONT SEAT	43	4	172
REAR SEAT	43	6	258
OPERATIONAL EMPTY WEIGHT: 7150			
PAYLOAD	1200		
FRONT PASSENGER	600	4	2400
REAR PASSENGER	600	6	3600
FUEL	496	38	18848
GROSS WEIGHT	8846		

ITERATION

Table 7-2A

INPUT(LBS)	OUTPUT(LBS)
3518	3523.7
3523.7	3524.39
3524.39	3524.47

Table 7 -2B

MAXIMUM ZERO FUEL WEIGHT	5235Nm
OPERATIONAL EMTY WEIGHT	4035Nm
MAXIMUM LANDING WEIGHT	5957Nm
USEFUL LOAD FRACTION	.322
MAXIMUM FUEL FRACTION	.121

GROUP WEIGHT BREAKDOWN
Table 7-3

FINAL DESIGN

AIRPLANE TYPE: Sky C A B.
ENGINE TYPE: SP-100 Free piston engine.

GROUP INDICATION	WEIGHT (Nmars) *	DISTANCE (meters) *	%	MOMENT
AIRFRAME STRUCTURE:	2532			
FORWARD WING	683.40	7	11.4	4783
REAR WING	455.60	17	7.6	7745
VERTICAL TAIL	90	17	1.5	1530
FUSELAGE	1123	8.5	18.8	9546
NOSE GEAR	40	1.5	.67	60
WING GEAR	140	12	2.35	1680
PROPULSION GROUP:	1117			
ENGINE	613	9	10.29	5517
MOTOR	100	17	1.60	1700
RADIATOR	144	9	2.42	1296
COMBUSTOR	50	7.8	.84	390
FUEL TANK 1	42	6	.71	252
FUEL TANK 2	58	7	.97	406
PROPELLER	110	21	.18	2310
AVIONICS AND EQP:	386			
AVIONICS	70	1	1.18	70
FLIGHT CONTROLS	100	4.5	1.68	450
ELECTRONICS	136	3	2.28	108
FRONT SEAT	40	2	.67	80
REAR SEAT	40	5.5	.67	220
BASIC (EMPTY) WEIGHT:	4035			
PAYLOAD:	1200			
FRONT PASSENGER	600	2	10.07	1200
REAR PASSENGER	600	5.5	10.07	3300
FUEL:	722			
OXYGEN	133.7	6	2.24	802
METHANE	588.3	7	9.88	4118
GROSS WEIGHT:	5957			

* All weights are in Nmars.
* All parameters are in meters.

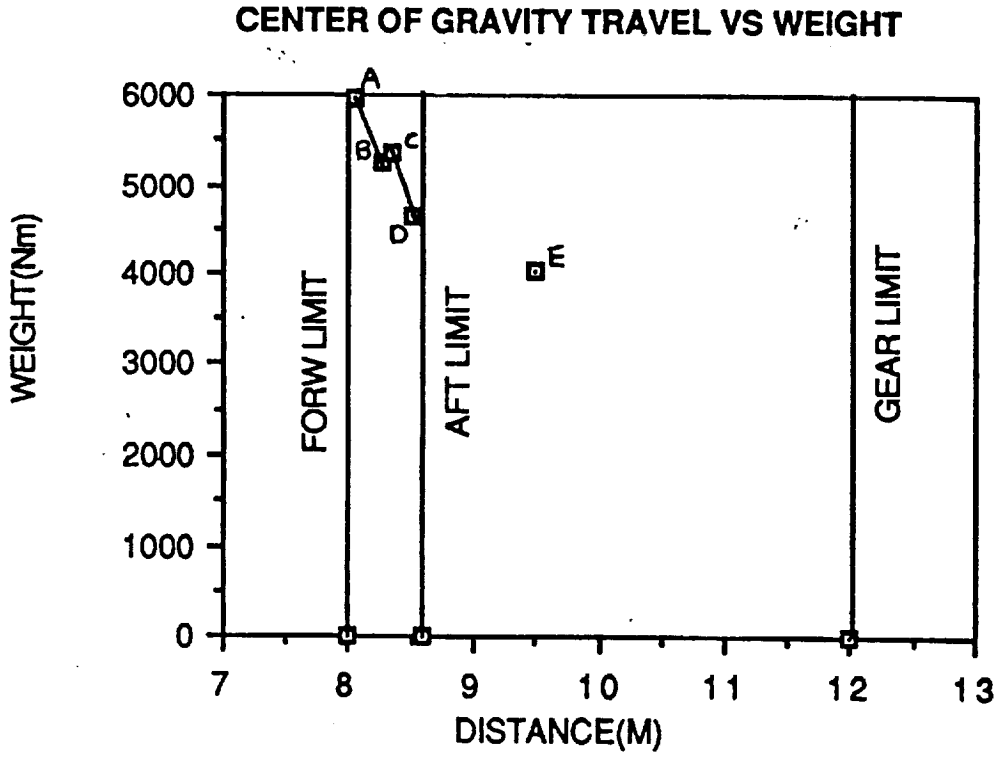

FIG -1

TRAVEL CONDITIONS

A	5957 Nm	Two passengers and fuel.
B	5235 Nm	Two passengers no fuel.
C	5357 Nm	One passenger and fuel.
D	4635 Nm	One passenger no fuel.
E	4035 Nm	No passengers no fuel.

Assembly and Deployment on Mars Surface

One of the first jobs for the Mar's ground crew is to assemble Sky C.A.B. after it is removed from the spacecraft. The assembling and deployment of Sky C.A.B. will take place in an all purpose airplane hangar. The major task for this job is the attaching and detaching of the wings. Once the plane is assembled, it is ready to be taxied out to the runway in preparation for its next flight.

COST ANALYSIS

Jami Munson

When designing an aircraft like SKY C.A.B., one of the major design constraints should be that of cost. However, our design group decided that for this particular design, cost would be of no object.

A cost analysis computer program was used to find a rough estimate of the cost of the aircraft. The computer program was written for the purpose of a spacecraft cost analysis, therefore discrepancies occurred.

SKY C.A.B.'s total cost, as calculated by the program, came out to be approximately 419 million dollars. The breakdown of this cost can be seen in Table 1. The costs listed in the table will be lower than the actual cost estimate due to a number of factors.

One of the problems with the program is that it does not take the use of composites into account. Composites are very expensive and since the entire plane is basically composed of these materials, the total cost increase will be large. The research and development that will be involved with the design of joined wings will also increase cost.

Overall, the programs main purpose was to show that cost is a function of the mass of the structure being built.

Fig. 1 COST ANALYSIS

COST ANALYSIS

	DDT & E	FHA	TOTAL
Structures	$M 46.0	$M 13.8	$M 59.8
Thermal	4.8	9.9	14.7
Attitude Control & Determination	42.2	9.6	51.9
Reaction Controls	0.0	0.0	0.0
Communication & Data Handling	14.3	2.4	16.7
Electrical Power	7.8	0.2	7.9
Propulsion	0.4	0.0	0.4
SUBTOTAL	115.5	35.9	151.4
System Test Hardware	64.5	0.0	64.5
System Test Operations	23.6	0.0	0.0
Software	0.0	0.0	0.0
GSE	19.5	0.0	0.0
SE&I	25.7	6.7	32.4
Program Management	15.8	3.8	19.6
SUBTOTAL	264.8	46.4	311.1
Contingency	53.0	9.3	62.2
FEE	31.8	5.6	37.3
Program Support	7.0	1.2	8.2
TOTAL	$356.5M	$62.4M	$418.9M

INBOARD PROFILE

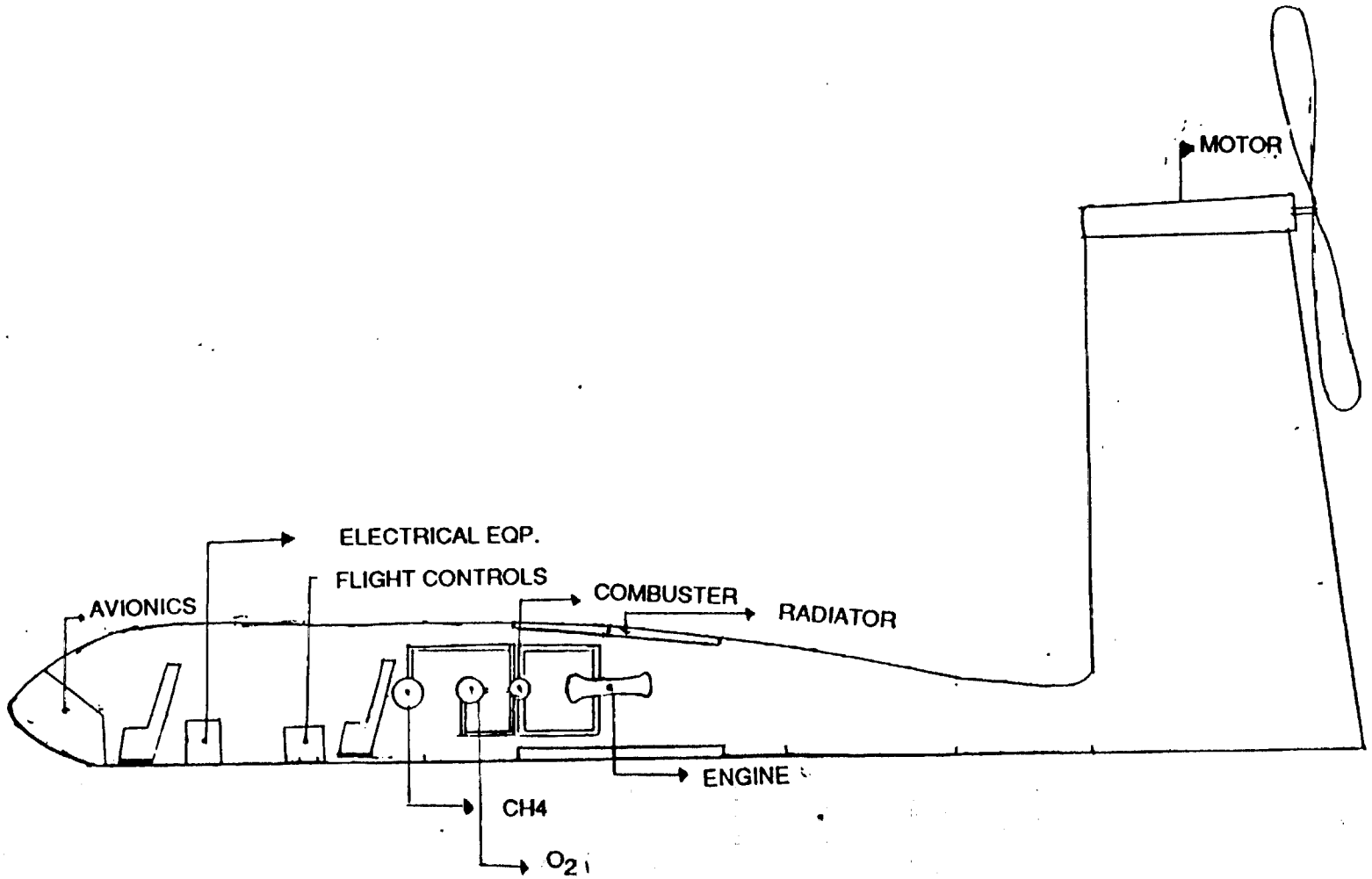

INBOARD PROFILE

The internal components of the aircraft were placed in a location such that stability would be maintained for all travel conditions . Most of the components of the aircraft were placed in the forward section of the aircraft . The engine and radiator were place at the center of gravity. The fuel tanks were placed near the center of gravity to avoid large fluctuations of the c.g location. The motor and propeller were placed at the top of the tail to avoid problems due to the diameter of the propeller. The payload was positioned at 2 m and 5.5 m measured from the nose of the aircraft.

Maintenance and Servicing on Mars

The maintenance and servicing of Sky C.A.B. may be the most important factor of the ground operations. It is extremely important that the plane be in top condition in order to ensure a successful flight. Before every scheduled flight, a full equipment check will be carried out between the pilot and the ground crew.

After Sky C.A.B. has completed a successful mission, the ground crew will administer a post-flight equipment evaluation. The plane will be taxied from the runway into a fully equipped airplane hangar. While in the hangar, Sky C.A.B. will be completely disassembled in order to perform the evaluation. The ground crew has to be certain that this aircraft will perform to its greatest ability.

PACKAGING FOR DEPLOYMENT

Designing and building the Mars airplane were not the only concerns of this project. The packaging for transport of the aircraft also had to be considered. It was determined that due to its size the plane would have to be partially disassembled. The decision was made to detatch the front wing one meter from the fuselage, and have a break just past the flap system. The rear wing wing would be detatched from the joint and be cut one meter from the tail and also past the flap system. This would result in eight partial wing section that could be more easily packed and transported.

It was found from the Space division of this project that the aircraft would have to be packed into an ellyptical cone with a protective heat shield for entry through the Martian atmosphere. It was decided that it would be advantageous to pre-package it on Earth in the cone and transported to a space station via a rocket or heavy-lift launcher. From there it could be deployed through the atmosphere. Two conceptual view are shown for the packaging in Figures P-1 and P-2.

FIGURE P-1.

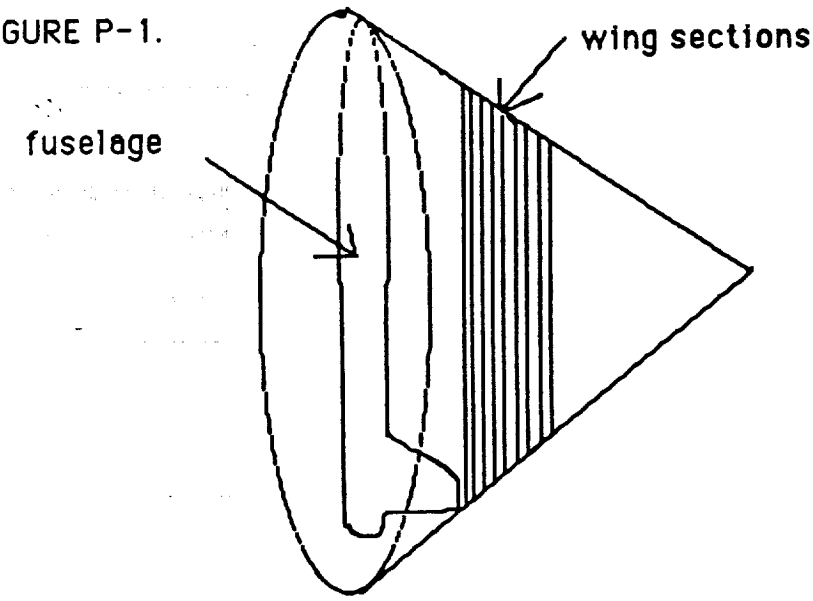

FIGURE P-2.

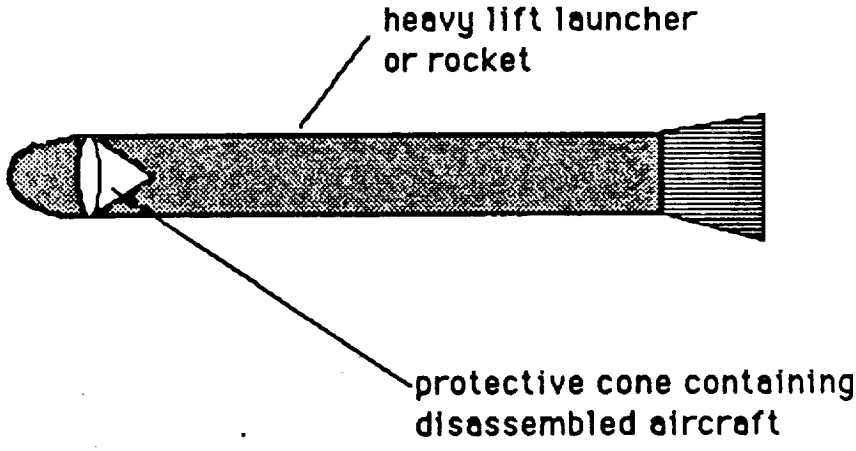

Rescue Scenario

Jamie Edgar

Sky C.A.B. was designed to take off from and land on a one kilometer runway, and because of this its use in a rescue mission is limited. All Sky C.A.B. pilots are provided with radios and homing devices in their flight suits so that when problems arise people at the base will immediately be informed of them. In the event of a downed pilot, another Sky C.A.B. is immediately sent out to drop supplies to the downed pilot. While these supplies are being delivered, a rescue team is assembled and sent out in a land rover to retrieve the pilot. This team will carry ample food and oxygen supplies plus climbing gear to aid in reaching the pilot in places that the rover can not go. The second Sky C.A.B. will serve as a guide to the rescue team, providing them with information on the best route to the pilot which crosses the least amount of difficult obstacles. The second plane can also be used to provide additional supplies as is necessary.